NOVEL APPROACHES TO ANTIMICROBIAL THERAPY OF PNEUMONIA USING ANTIBIOTICS AND THERAPEUTIC ANTIBODIES

Dissertation

zur Erlangung des naturwissenschaftlichen Doktorgrades der

Julius-Maximilians-Universität Würzburg

vorgelegt von

Marika Kutscher

aus Alzenau, Deutschland.

Würzburg 2016

Eingereicht bei der Fakultät für Chemie und Pharmazie am

28. April 2016

Gutachter der schriftlichen Arbeit

1. Gutachter: Prof. Dr. Dr. Lorenz Meinel

2. Gutachter: Prof. Dr. Oliver Germershaus

Prüfer des öffentlichen Promotionskolloquiums

1. Prüfer: Prof. Dr. Dr. Lorenz Meinel

2. Prüfer: Prof. Dr. Oliver Germershaus

3. Prüfer: Dr. Knut Ohlsen

Datum des öffentlichen Promotionskolloquiums

13. Juni 2016

Doktorurkunde ausgehändigt am

Für meine Eltern

TABLE OF CONTENTS

CHAPTER IV
NEBULIZATION OF THE HUMANIZED MONOCLONAL ANTIBODY UK-66 – PHYSICOCHEMICAL STABILITY AND *IN VIVO* EFFICACY 105

SUMMARY

The treatment of infections caused by methicillin-resistant *Staphylococcus aureus* (MRSA) still represents a formidable global challenge. Particularly nosocomial pneumonia caused by MRSA is linked to increased morbidity and mortality, prolonged hospitalization, and longer periods of mechanical ventilation. Current treatment recommendations for MRSA pneumonia and inherent problems are discussed in **chapter I** of this thesis. Within this review it is shown that systemic use of antibiotics alone is occasionally insufficient for the therapy of MRSA pneumonia owing to the associated risk of toxic side effects and the problem of rising antibiotic concentrations which are required to combat multi-drug resistant pathogens. The increasing emergence of bacterial resistance against established antibiotics fuels the demand for new antimicrobial agents and innovative delivery strategies. Since the industrial development of novel antibiotics has declined throughout the last years, a promising alternative is presented by antibody-based immunotherapeutic approaches. In addition, local delivery of the drugs to the lung is supposed to favor pneumonia treatment since it is associated with enhanced drug concentration at the site of infection and low systemic drug exposure, both potentially reducing the risk of resistance development. Nebulization is a straightforward method to administer drugs to the site of infection in intubated patients and is well studied for both, antibiotic and antibody pulmonary delivery. Further advances in device technology and drug delivery have been made for nebulization of antibiotics and antibodies but are hardly transferred to MRSA pneumonia treatment so far. Therefore, chapter I focuses on reviewing the advances in local drug delivery which are potentially applicable for treatment of MRSA pneumonia by antibiotics and antibodies.

Chapter II is dealing with nano-sized drug delivery systems for antibiotics circumventing solubility issues of poorly-water soluble drugs. Furthermore, the improved mucus penetration of nanoparticles can increase local drug concentrations at the site of action, thereby reducing the incidence of bacterial resistance. Nanoparticle complexes (nanoplexes) prepared by self-assembly of a drug and an oppositely charged polyelectrolyte allow higher drug loading than ordinary nanoparticles. Chapter II describes the evaluation of an analytical setup to identify optimal preparation conditions for nanoplex formation using ciprofloxacin (CIP) and dextran sulfate (DS) as model compounds. The suitability of isothermal titration calorimetry (ITC) as a screening tool for rational formulation optimization was assessed along with other analytical methods by analyzing the influence of different salt types and ionic strengths on CIP/DS nanoplex formation. The presence of low amounts of salt led to smaller and more numerous

particles of higher uniformity but had no influence on the release of CIP from nanoplexes. Importantly, binding affinity correlated with particle shape and morphology, potentially enabling optimization of critical quality attributes based on ITC data. Altogether, ITC along with supplemental methods proved to be a versatile screening tool for the evaluation of nanoplex formulation conditions regarding mixing ratio, salt type, and ionic strength.

In **chapter III,** the scope of treatment options for MRSA infections is extended to antibody-based immunotherapy. A promising approach to promote bacterial killing presents the targeting of bacterial cell surface components with immunogenic characteristics by hUK-66, a humanized monoclonal antibody. However, during production and shelf life, therapeutic proteins are facing a multitude of external stress, compromising conformational stability. To enable efficacious drug application and prevent unwanted immune responses due to aggregation of the protein molecule, this study aims at a formulation for hUK-66 preserving its chemical and physical stability. Based on the results from characterization of this antibody, optimal formulation pH was evaluated in a short-term stability study. Subsequently, combinations of excipients and dosage forms were analyzed for their suitability in preserving antibody stability by comparing different liquid and lyophilized formulations in a long-term stability study at different storage temperatures. Lyophilization of hUK-66 in histidine buffer, pH 6, containing the stabilizers sucrose and polysorbate 20 proved to preserve the stability of this antibody throughout formulation process and long-term storage at 2-8°C.

To deliver therapeutic proteins via the lung, generation of an inhalable aerosol is required. However, during the process of nebulization the air-liquid interface is substantially increased exposing biomolecules to interfacial stress. Therefore, in **chapter IV**, the previously developed hUK-66 formulations were studied for their suitability in stabilizing the antibody during air-jet nebulization. Considering the large sample volumes needed for nebulization, an *in vitro* surrogate method simulating the nebulization stress was initially developed to reduce drug substance consumption. The formulation of hUK-66 comprising sucrose and polysorbate proved to preserve the protein stability during the preliminary study as well as the actual nebulization process. Furthermore, it was shown that nebulization had no adverse effect on the chemical stability of the antibody. Finally, the immunotherapeutic efficacy of hUK-66 formulation administered via inhalation was proven by prolonged survival of mice infected intranasally with *S. aureus*. For this *in vivo* study a special set up to enable aerosol delivery to mice being awake and breathing normally had been developed successfully. An additional advantage of this set up was nose-only exposure which reduced the disadvantages of whole body exposure like adsorption over the skin and large amount of aerosol needed.

Altogether, multiple nebulization and intense recirculation of the protein formulation within the reservoir marginally impacted conformational stability of the antibody. Hence, stability of this hUK-66 formulation during nebulization and its immunotherapeutic potential in treating *S. aureus* infections effectively when administered pulmonary were demonstrated in this study.

A further important aspect for effective and rapid therapy of pneumonia is the immediate detection and identification of the pathogens which are causing the infection. The ensuing proper choice of medical treatment is crucial to avoid systemic spreading and persistence of the infection as well as emergence of antibiotic resistance. Therefore, efficient detection methods for pathogens and other biological specimens are in great demand in the field of clinical diagnostics. In **chapter V**, biosensors are investigated as promising alternative to improve pathogen detection since they permit sensitive, specific, and rapid analysis of diverse specimens. Selective detection of *S. aureus* was achieved by immobilizing target-specific hUK-66 antibodies on the surface of an optical planar Bragg grating sensor. Furthermore, to improve sensor reusability and reduce installation time, costs, as well as preparatory work we evaluated a sensor surface functionalization allowing the repetitive use of a sensing device for antibody-based detection of living bacteria. The immobilization of hUK-66, a capture antibody specific for *Staphylococcus aureus,* on the sensor surface by a cleavable linker as well as specific binding of *S. aureus* was monitored in real-time, highlighting the applicability of optical sensors for a specific and quick detection of large biological structures. Reusability of bacteria saturated sensors was successfully demonstrated by cleaving the antibody along with bound bacteria through reduction of disulfide bonds and subsequent re-functionalization with activated antibody, resulting in comparable sensitivity towards *S. aureus*.

ZUSAMMENFASSUNG

Die Behandlung von Infektionen, die durch Methicillin-resistente *Staphylococcus aureus* (MRSA)-Bakterien hervorgerufen wurden, stellt weltweit noch immer eine schwierige Herausforderung dar. Besonders durch MRSA ausgelöste nosokomiale Pneumonien stehen in direktem Zusammenhang mit erhöhter Morbidität und Mortalität sowie einer Verlängerung des Krankenhausaufenthaltes und der Beatmungsdauer. In **Kapitel I** dieser Dissertation werden die aktuellen Behandlungsempfehlungen für MRSA-Pneumonien und deren Nachteile diskutiert. Dabei wird in diesem Review aufgezeigt, dass aufgrund der drohenden Gefahr von schweren Nebenwirkungen und des Problems der steigenden Antibiotikakonzentrationen, die zur Bekämpfung von multiresistenten Krankheitserregern nötig sind, die alleinige systemische Anwendung von Antibiotika für eine Therapie der MRSA-Pneumonie mitunter nicht mehr ausreicht. Angesichts des vermehrten Auftretens von Resistenzen gegen die gängigen Antibiotika ist der Bedarf an neuen antimikrobiellen Mitteln sowie innovativen Strategien zur Wirkstoffapplikation hoch. Da die Entwicklung neuer Antibiotika in den letzten Jahrzehnten deutlich nachlässt, stellen Antikörper-basierte immuntherapeutische Ansätze eine vielversprechende Alternative dar. Darüber hinaus soll eine lokale Wirkstoffverabreichung in die Lunge die Pneumonie-Behandlung infolge erhöhter Wirkstoffkonzentration am Ort der Infektion und gleichzeitiger geringer systemischer Wirkstoffbelastung begünstigen, was das Risiko einer Resistenzentwicklung verringern kann. Verneblung ist hierbei ein direkter und einfacher Weg, Wirkstoffe bei intubierten Patienten an ihren Wirkort zu bringen und ist für die pulmonale Verabreichung von Antibiotika sowie Antikörpern gut erforscht. Zwar wurden weitere Fortschritte in der Weiterentwicklung der Gerätetechnologie und Wirkstoff-verabreichung für die Verneblung von Antibiotika und Antikörpern gemacht, diese wurden aber bisher kaum in der Behandlung von MRSA-Pneumonien umgesetzt. Deshalb konzentriert sich das erste Kapitel auf eine Übersicht über die Fortschritte in der lokalen Wirkstoffapplikation, welche potentiell auf die Behandlung von MRSA-Pneumonie mittels Antikörpern und Antibiotika übertragbar wären.

Kapitel II beschäftigt sich mit „Drug Delivery"-Systemen für Antibiotika in Nanometergröße, welche eine Umgehung des Löslichkeitsproblems von schwer wasserlöslichen Wirkstoffen ermöglichen. Außerdem kann eine durch Nanopartikel verbesserte Mucuspenetration die Wirkstoffkonzentrationen am Wirkort erhöhen, was als Möglichkeit angesehen wird, das Auftreten von Antibiotikaresistenz zu vermindern. Nanopartikel-Komplexe (Nanoplexe), welche durch Selbst-Zusammenlagerung eines Wirkstoffs und eines entgegengesetzt

geladenen Polyelektrolyts hergestellt werden, erlauben eine noch höhere Wirkstoffbeladung als herkömmliche Nanopartikel. In diesem Kapitel wurde unter Verwendung von Ciprofloxacin (CIP) und Dextransulfat (DS) als Modellkomponenten ein analytisches Setup evaluiert, das geeignet sein soll, optimale Herstellungsbedingungen für die Bildung von Nanoplexen zu identifizieren. Hierbei wurde die Eignung von Isothermaler Titrationskalorimetrie (ITC) zusammen mit anderen analytischen Methoden als Selektions-Hilfsmittel für eine rationale Formulierungsoptimierung bewertet, indem der Einfluss von unterschiedlichen Salzen und verschiedenen ionischen Stärken auf die CIP/DS-Nanoplexbildung untersucht wurde. Die Anwesenheit von Salz führte hierbei zu kleineren und zahlreicheren Partikeln mit größerer Einheitlichkeit, hatte aber keinen Einfluss auf die Freisetzung von CIP aus den Nanoplexen. Bedeutsam ist auch, dass die Bindungsaffinität mit Partikelform und Morphologie korrelierte, was möglicherweise eine Optimierung entscheidender Qualitätseigenschaften basierend auf ITC-Daten ermöglicht. Insgesamt erwies sich ITC zusammen mit den ergänzenden Methoden als nützliches Instrument für die Evaluierung von Bedingungen für Mischungsverhältnis, Art des Salzes und ionische Stärke für die Bildung von Nanoplexen.

In **Kapitel III** wird der Rahmen der Behandlungsmöglichkeiten für MRSA-Infektionen auf Antikörper-basierte Immuntherapien erweitert. Einen vielversprechenden Ansatz, die Abtötung der Bakterien zu fördern, stellt der zielgerichtete Angriff auf Komponenten der Bakterienoberfläche mit immunogenen Eigenschaften durch den humanisierten monoklonalen Antikörper hUK-66 dar. Allerdings werden therapeutische Proteine während ihrer Herstellung und bis zum Ende ihrer Aufbrauchsfrist mit einer Vielzahl von externen Einflüssen konfrontiert, die ihre Konformation und somit Stabilität beeinträchtigen können. Um eine wirksame Wirkstoffverabreichung zu ermöglichen und ungewollte Reaktionen des Immunsystems aufgrund Aggregation des Proteinmoleküls zu vermeiden, erstrebt dieses Kapitel die Identifizierung einer Formulierung für hUK-66, welche dessen physikalische und chemische Proteinstabilität bewahrt. Mit Hilfe von Ergebnissen der Charakterisierung des Antikörpers wurde ein optimaler pH-Wert für die Formulierung in einer Stabilitätsstudie mit kurzer Laufzeit evaluiert. In direktem Anschluss wurden verschiedene Kombinationen von Hilfsstoffen und Darreichungsformen hinsichtlich ihrer Fähigkeit, die Antikörperstabilität zu bewahren, analysiert, indem unterschiedliche flüssige und gefriergetrocknete Formulierungen in einer Langzeitstabilitätsstudie bei verschiedenen Lagerungstemperaturen untersucht wurden. Eine Lyophilisierung von hUK-66 in Histidinpuffer, pH 6, zusammen mit den Stabilisatoren Saccharose und Polysorbat 20 konnte die Stabilität dieses Antikörpers während

des gesamten Formulierungsprozesses und einer Langzeit-Einlagerung bei 2-8°C nachweislich bewahren.

Um therapeutische Proteine über die Lunge zu applizieren, ist es nötig, ein inhalierbares Aerosol zu erzeugen. Da sich jedoch während des Verneblungsprozesses die Luft-Flüssigkeitsgrenzfläche erheblich vergrößert, werden die Biomoleküle einem Grenzflächenstress ausgesetzt. Deshalb werden in **Kapitel IV** die zuvor entwickelten hUK-66-Formulierungen hinsichtlich ihrer Eignung untersucht, den Antikörper während der Verneblung durch einen Düsenvernebler zu stabilisieren. Da zum Vernebeln eine sehr große Probenmenge benötigt wird, wurde zuerst ein *In-vitro*-Ersatzverfahren entwickelt, welches den Verneblungsstress simuliert, um den Wirkstoffverbrauch zu reduzieren. Die hUK-66-Formulierung mit Saccharose und Polysorbat 20 bewies, dass sie die Stabilität dieses Proteins sowohl im Vorversuch als auch bei der eigentlichen Verneblung bewahren konnte. Es konnte weiterhin gezeigt werden, dass eine Verneblung keinen nachteiligen Effekt auf die chemische Stabilität des Antikörpers ausgeübt hat. Zuletzt konnte die immuntherapeutische Wirksamkeit der vernebelten hUK-66-Formulierung bewiesen werden, da die Überlebensrate von Mäusen, die intranasal mit *S. aureus* infiziert worden waren, durch Inhalation der Antikörperformulierung verlängert werden konnte. Für diese *In-vivo*-Studie wurde ein spezieller Aufbau erfolgreich entwickelt, der die Applikation des Aerosols an wache und normal atmende Mäuse ermöglicht. Ein zusätzlicher Vorteil dieses Aufbaus war, dass die Mäuse dem Aerosol nur mit der Nase ausgesetzt waren, was die Nachteile einer Ganzkörperverneblung, wie Absorption über die Haut und Bedarf an großen Mengen an Aerosol, verringerte. Insgesamt gefährdeten die vielfache Verneblung und Rezirkulation der Proteinlösung innerhalb des Reservoirs die Konformation des formulierten Antikörpers unwesentlich. Somit konnte in dieser Arbeit die Stabilität von hUK-66 in einer optimierten Formulierung während einer Verneblung bewiesen sowie sein immuntherapeutisches Potential für eine effektive Behandlung von *S. aureus* Infektionen bei pulmonaler Verabreichung gezeigt werden.

Ein weiterer wichtiger Punkt für eine effektive und schnelle Behandlung von Pneumonien ist die umgehende Detektion und Identifikation derjenigen Krankheitserreger, welche die Infektion auslösen. Eine anschließende geeignete Wahl der Medikation ist entscheidend, um eine systemische Verbreitung und Fortdauer der Infektion genauso wie das Auftreten von Antibiotikaresistenzen zu vermeiden. Deshalb sind effiziente Detektionsmethoden für Pathogene im Bereich der klinischen Diagnostik sehr gefragt. In **Kapitel V** wurden Biosensoren als vielversprechende Alternative zur Verbesserung der Pathogendetektion untersucht, da sie eine sensitive, spezifische und schnelle Analyse diverser Proben erlauben.

Durch Immobilisierung von hUK-66-Antikörpern auf der Oberfläche eines optischen planaren Bragg-Gitter-Sensors konnte eine selektive Detektion von *S. aureus* erreicht werden. Um weiterhin die Wiederverwendbarkeit der Sensoren zu verbessern sowie Installationszeit, Kosten und Vorbereitungsaufwand zu reduzieren, wurde eine Sensoroberflächen-funktionalisierung dahingehend evaluiert, ob sie eine wiederholte Verwendung des Sensors für die Antikörper-basierte Detektion von lebenden Bakterien ermöglicht. Die Anbindung von hUK-66, einem Fänger-Antikörper spezifisch für *S. aureus*, auf der Sensoroberfläche mit Hilfe eines spaltbaren Linkers sowie die anschließende spezifische Bindung von *S. aureus* konnten in Echtzeit nachverfolgt werden, was die Anwendbarkeit von optischen Sensoren für eine spezifische und schnelle Detektion von großen biologischen Strukturen hervorhebt. Die Wiederverwendbarkeit der mit Bakterien gesättigten Sensoren konnte erfolgreich durch eine Abspaltung des Antikörpers zusammen mit den angebundenen Bakterien mittels Reduktion der Disulfidbindungen und anschließender Refunktionalisierung mit aktiviertem Antikörper gezeigt werden und führte zu einer vergleichbaren Sensitivität gegenüber *S. aureus*.

CHAPTER I

LOCAL DRUG DELIVERY OPTIONS FOR TREATMENT OF NOSOCOMIAL PNEUMONIA DUE TO METHICILLIN-RESISTANT *STAPHYLOCOCCUS AUREUS* BY ANTIBIOTICS AND THERAPEUTIC ANTIBODIES

Unpublished manuscript.

Abstract

The treatment of infections caused by methicillin-resistant *Staphylococcus aureus* (MRSA) still represents a sophisticated challenge worldwide. Particularly nosocomial pneumonia due to MRSA is linked to increased morbidity and mortality, prolonged hospitalization and longer periods of mechanical ventilation. Current treatment guidelines recommend the systemic use of the antibiotics vancomycin and linezolid for therapy of MRSA pneumonia. However, standard systemic dosing of vancomycin seems no longer sufficient due to its poor lung penetration and increasing concentration of antibiotic that is required to treat MRSA due to resistance development. In addition, the required higher concentrations are associated with risk of toxic side effects. Likewise, linezolid is facing the problem of drug interactions and increased risk of resistance. Due to this increasing issue of bacterial resistance, the demand for new antimicrobial agents is high. Since the development of novel antibiotics has declined throughout the last decades, a promising alternative is emerging through antibody-based immunotherapeutics. In addition, local delivery of drugs to the lung is supposed to favor pneumonia treatment since it is associated with enhanced drug concentration at the site of infection and low systemic drug exposure reducing the risk of resistance development. Nebulization is a straightforward method to administer drugs to the site of infection in intubated patients and is well studied for both antibiotic and antibody pulmonary delivery. Further advances in device technology and drug delivery have been made for nebulization of antibiotics and antibodies but are hardly transferred to MRSA pneumonia treatment so far. Therefore, this review focuses on advances in local drug delivery potentially applicable for the treatment of MRSA pneumonia using antibiotics and antibodies.

1. Introduction

1.1. Clinical relevance of nosocomial pneumonia due to MRSA and corresponding problems

Nosocomial infections with multi-resistant pathogens represent a global and everyday problem in hospitals. Besides *Enterococcus feacium, Klebsiella pneumoniae, Acinetobacter baumannii, Pseudomonas aeruginosa,* and *Enterobacter* species, *Staphylococcus aureus* is one of the most problematic bacteria today (called ESKAPE pathogens according to their first letters) [1]. Its methicillin-resistant form (MRSA) is responsible for most antimicrobial-resistant healthcare-associated infections. In Europe, on average 18% of *S. aureus* isolates in hospitals were methicillin-resistant in 2013 [2]. Although this percentage of resistance generally decreased compared to 2010, the decreasing trend was less distinct compared to the preceding four-year period. Large variations between countries were observed across Europe. 0% MRSA incidence are reported in Iceland compared to 64.5% in Romania reflecting a general north-to-south divide (**Figure 1**) [2]. Both facts underline that MRSA is still a problematic issue to be solved in Europe. However, other nations such as the USA and Japan are affected as well [3–5].

Bacterial infection can originate from hospital environment or the own flora of the patient. Additional suppression of natural defense mechanism such as cough, mucociliary clearance, and immune responses by intubation of patients e.g. in the intensive care units favors respiratory infections [6]. When the natural barriers are challenged by intubation, the gram-positive bacterium that usually colonizes the nasal region as well as the skin can enter the respiratory tract easily [7]. Due to its virulence and efficiency as respiratory pathogen, MRSA is a major cause of hospital-acquired pneumonia and is associated with a high morbidity and a mortality rate of 33% [8,9]. For patients colonized within 24 h of intubation, a risk of 30% to develop an early ventilator-associated pneumonia was reported in Spain [9,10]. Besides increased morbidity and mortality, MRSA pneumonia is linked to prolonged hospitalization particularly with extended temporal stay in the intensive care unit and longer periods of mechanical ventilation [7].

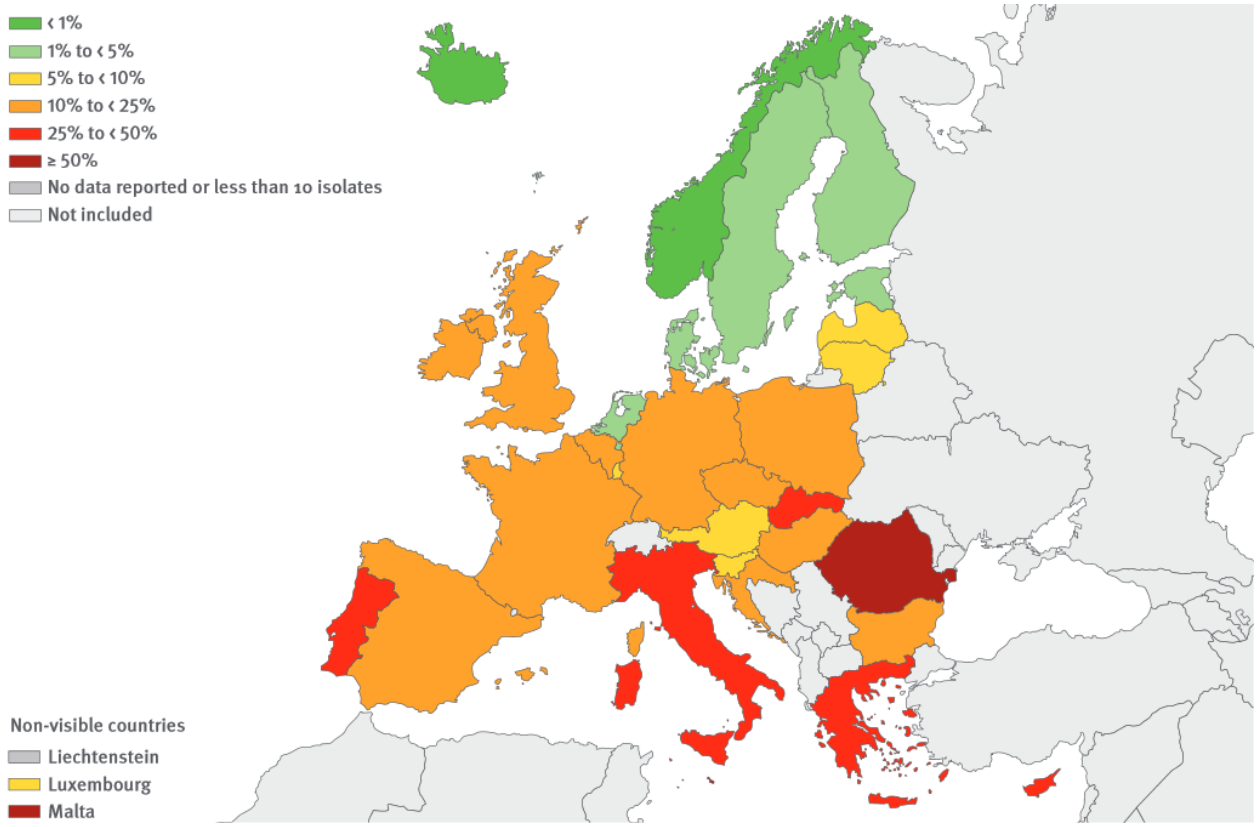

Figure 1: Occurrence of MRSA bacteria strains over Europe in 2013 in percentage of invasive isolates resistant to methicillin per country. Reproduced from [2].

1.2. Current treatment options for nosocomial pneumonia due to MRSA

1.2.1. Preventive strategies

Preventing the spread of infections and MRSA colonization is an important starting point for controlling the increasing resistance. As transmission of the bacteria often occurs by the hands of healthcare personnel [9], hygiene regulations such as hand disinfection are a mainstay for prevention of nosocomial infection [6,11]. With colonized inpatients being the prevalent reservoir of MRSA, carrier screening and appropriate isolation of patients proved to be effective [9,12]. Technical strategies to prevent ventilator-associated pneumonia include coating of the endotracheal tube with antimicrobial silver and aspiration of subglottic secretions to reduce oropharyngeal colonization as well as lung absorption of colonized secretions. Whenever possible, tracheal intubation and mechanical ventilation should be avoided, for example by using noninvasive ventilation instead. Furthermore, a slightly upright position (30 to 40 degree) of intubated patients is recommended and oral hygiene by rinsing with antiseptics such as chlorhexidine appeared to be effective [6,13].

1.2.2. Systemic treatment approaches

If an onset of pneumonia is suspected, guidelines recommend the collection of lower respiratory tract samples for culture and concomitant start of empiric antimicrobial therapy until the microbiologic results are available and therapy can be specified. Whereas methicillin-sensitive *S. aureus* strains are susceptible to a large number of antibiotics such as penicillinase-resistant betalactam antibiotics, macrolides, clindamycin, and fluoroquinolones (resistance rate < 10%), MRSA exhibits a resistance rate of above 80% against these antimicrobials [14]. For the treatment of MRSA pneumonia, the glycopeptide vancomycin and the oxazolidinone linezolid are recommend by international guidelines [13–15]. Whether one of these two alternatives is more effective than the other is still a matter of intensive debate [1,6,7,16–24]. In a recent randomized clinical trial, linezolid led to higher clinical efficacy in patients with MRSA nosocomial pneumonia whereas vancomycin showed more frequent nephrotoxicity. However, mortality rates as well as incidence of adverse events were comparable [16]. The inclusion criteria of this study were criticized by several other reviews as the vancomycin group involved more patients with MRSA bacteremia, diabetes, kidney, and cardiac diseases or being mechanically ventilated, potentially biasing the results. Additionally, the used vancomycin dosing regime was considered insufficient as too low levels of vancomycin in patients had been noted [1,17,21]. Nevertheless, summarizing the new insights into this discussion, linezolid seems to be an appropriate choice especially for patients with renal impairments even if superiority could not be evidenced completely and gastro-intestinal adverse events might be more frequent [6,7,23–27]. However, the seldom but severe adverse effect of myelosuppression needs to be considered since applying linezolid over periods longer than two weeks increases the probability of occurrence [21,28].

When alternatives are not suitable, a further treatment option for hospital-acquired pneumonia (HAP) caused by MRSA is the glycopeptide telavancin, which was brought on market in 2011. However, it must be used with caution due to potential nephrotoxicity and QT prolongation [1,26]. Another common antibiotic effective against MRSA, daptomycin, is not applicable for treatment of pneumonia since it is inactivated by pulmonary surfactant [1,29]. Novel pharmaceutical agents with activity against MRSA include the cephalosporins ceftobiprole and ceftaroline. Ceftobiprole was approved in 2013 for treatment of community- (CAP) and hospital-acquired pneumonia (HAP) but not for ventilator-associated pneumonia (VAP) [1]. In contrast, ceftaroline so far is approved for CAP only [18,21]. A promising retrospective review of data on ceftaroline treatment of patients with MRSA pneumonia was already published by Carreno et al [30]. Nevertheless, clinical trials studying the efficacy in

treating MRSA pneumonia are still required for both cephalosporins [26]. A new basis for hope offered the discovery of teixobactin in 2015 which showed excellent activity against MRSA in an animal model [31–33]. However, human clinical trials still have to prove its safety and efficacy.

1.2.3. Local treatment strategies

Local treatment of respiratory infection is regarded effective and advantageous since it enables high levels of drug in the lung and reduced side effects as well as toxicity compared to systemic application [18,34,35]. Enhanced drug levels at the site of infection are assumed to shorten antibiotic exposure and in turn to lower the likelihood of development of microbial resistance [36]. Nevertheless, so far only limited research has been done in the field of local treatment of MRSA nosocomial pneumonia using nebulized antibiotics. For cystic fibrosis already several antibiotics were approved, particularly formulated for inhalation [35,37–39], but for nosocomial pneumonia mostly off-label use of aerosolized antibiotics was reported [37,40]. Larger randomized clinical trials are required to affirm the benefit of aerosolized antibiotics as adjunctive therapy in pneumonia [18,41,42]. However, if intravenous antibiotic treatment of VAP caused by multi-drug resistant pathogens alone is ineffective, the use of inhaled antibiotics is already recommend by the guideline of the American Thoracic Society from 2005 [13].

In the last years multiple successful studies on treatment of pneumonia caused by gram-negative bacteria using aerosolized antibodies have been performed [34,38,41,43,44], providing a promising basis for gram-positive pathogens like MRSA. However, so far data about aerosolized antibiotics against pneumonia caused by gram-positive pathogens are sparse [38,45,46]. In a recent clinical trial by Palmer et al. aerosolized vancomycin was studied amongst several other antibiotics for its efficacy in treating VAP caused by diverse multi-drug resistant pathogens in combination with systemic antibiotics [47]. The inhaled antibiotics proved to eradicate resistant organisms in tracheal secretions of critically ill intubated patients, did not result in resistance to the aerosolized antibiotics, and reduced the formation of new resistance to systemic agents [47]. In conjunction with proceeding encouraging studies [48–50] these results affirm the potential of aerosolized vancomycin to treat MRSA pneumonia.

During investigation of the efficacy of nebulized fosfomycin and amikacin/tobramycin combinations for treatment of *Pseudomonas aeruginosa* infections in cystic fibrosis patients, a potentially positive effect was observed for patients co-infected with MRSA [51]. Based on these promising results, a phase 2 randomized clinical trial is planned by Cardeas Pharma to demonstrate the safety and efficacy of an adjunctive therapy with an Amikacin Fosfomycin

Inhalation System (AFIS) versus aerosolized placebo in mechanically ventilated patients with gram-negative and/or gram-positive bacterial colonization (including MRSA) [52]. Another phase 2 clinical trial investigates AeroVanc™, an inhaled dry powder form of vancomycin in a capsule-based device, for the treatment of persistent methicillin-resistant *Staphylococcus aureus* lung infection in cystic fibrosis patients [40,53].

1.2.4. Challenges and problems

There are some concerns evolving in the standard treatment of MRSA pneumonia by vancomycin and linezolid. High clinical failure rates in treatment of MRSA pneumonia are reported for standard systemic doses of vancomycin [25]. This is presumably caused by the poor lung penetration of this molecule resulting in low concentrations in epithelial lining fluid (ELF) and alveolar macrophages, the sites of bacterial infection [8,21]. Higher dosages are required to increase plasma and hence ELF concentrations but are associated with enhanced incidence of nephrotoxicity [54]. The minimum inhibitory concentration (MIC) of vancomycin required to treat MRSA was observed to increase, diminishing the bactericidal activity of vancomycin against MRSA [8,25]. Even though linezolid in contrast achieves high lung ELF concentrations, it is associated with drug interaction issues causing adverse events such as serotonin syndrome and increased risk for development of resistance [17,21].

1.3. Need for new therapeutic options

Due to the increasing emergence of bacterial resistance against the conventional antimicrobial agents, the demand for new agents is enormous. However, the research and development on new antibiotics is diminishing despite availability of advanced techniques to screen new entities [32,33,55]. Among others, reasons for this dilemma are the high drug development costs for new entities as well as tedious approval procedures but low chance for profit, making antibiotics a disliked field of investment for the pharmaceutical industry. Furthermore, sales of novel antibiotics will not be that high compared to drugs for chronic diseases since they are only needed for short term therapies due to acute infections while being additionally restricted in their use in general to avoid development of resistance [8,32,56]. Particularly to circumvent this danger of emergence of resistant bacteria strains, the development of new antimicrobial treatment methods is of increasing interest.

Owing to major achievements in biotechnology during the last four decades, monoclonal antibodies (mAbs) developed into efficient human therapeutics for several indications with 30 mAbs on the market achieving revenues of approximately 18.5 billion US Dollar in 2010 [57,58]. Antibodies offer several advantages for the treatment of infectious diseases. They are

not only suitable for treatment of immunocompromised patients where other antimicrobials are relatively inefficient but also feature low toxicity. Based on their high specificity, the patients' flora remains mostly intact while only the harmful disease triggering microorganisms are targeted [58]. Furthermore, versatile effects beneficial for bacteria treatment can be initiated by antibodies such as toxin neutralization, direct antimicrobial activity, or immune system activation, among others (**Figure 2**) [58,59]. Several antibody-based immunotherapy approaches have been followed to combat MRSA in the last decade with *S. aureus* virulence factors or surface components providing a valuable target for the development of therapeutic antibodies [59,60]. For example, tefibazumab (Aurexis™), a humanized mAb against the clumping factor A which is said to be one of the major microbial surface components recognizing adhesive matrix molecules (MSCRAMM®) facilitating bacterial attachment to host tissues during colonization. By targeting this virulence factor the antibody is reported to prevent adherence and hence infection as well as endorsing rapid clearance through opsonophagocytosis [61,62]. Combining this mAb with vancomycin significantly enhanced clearing of MRSA in an animal model and reduced its seeding compared to applying the antibiotic only [63]. However, tefibazumab could not prove a significant benefit in a phase 2 clinical trial so far [64]. Another promising approach presents the targeting of bacterial cell wall components with immunogenic characteristics such as the immunodominant staphylococcal antigen A (IsaA) which features a high molecular density on the surface of the bacteria, is a highly conserved protein and is expressed in all *S. aureus* strains during the whole growth phase [60,65]. The anti-IsaA murine antibody UK-66P already proved to activate phagocytes and to promote killing of bacteria *ex vivo* and lead to lower bacterial burden *in vivo* in an intravenous animal infection and therapy model [60]. The humanized mAb hUK-66 demonstrated similar binding specificity as well as biological activity to that of UK-66P *in vitro* and induced significant killing activity in blood sample tests [66].

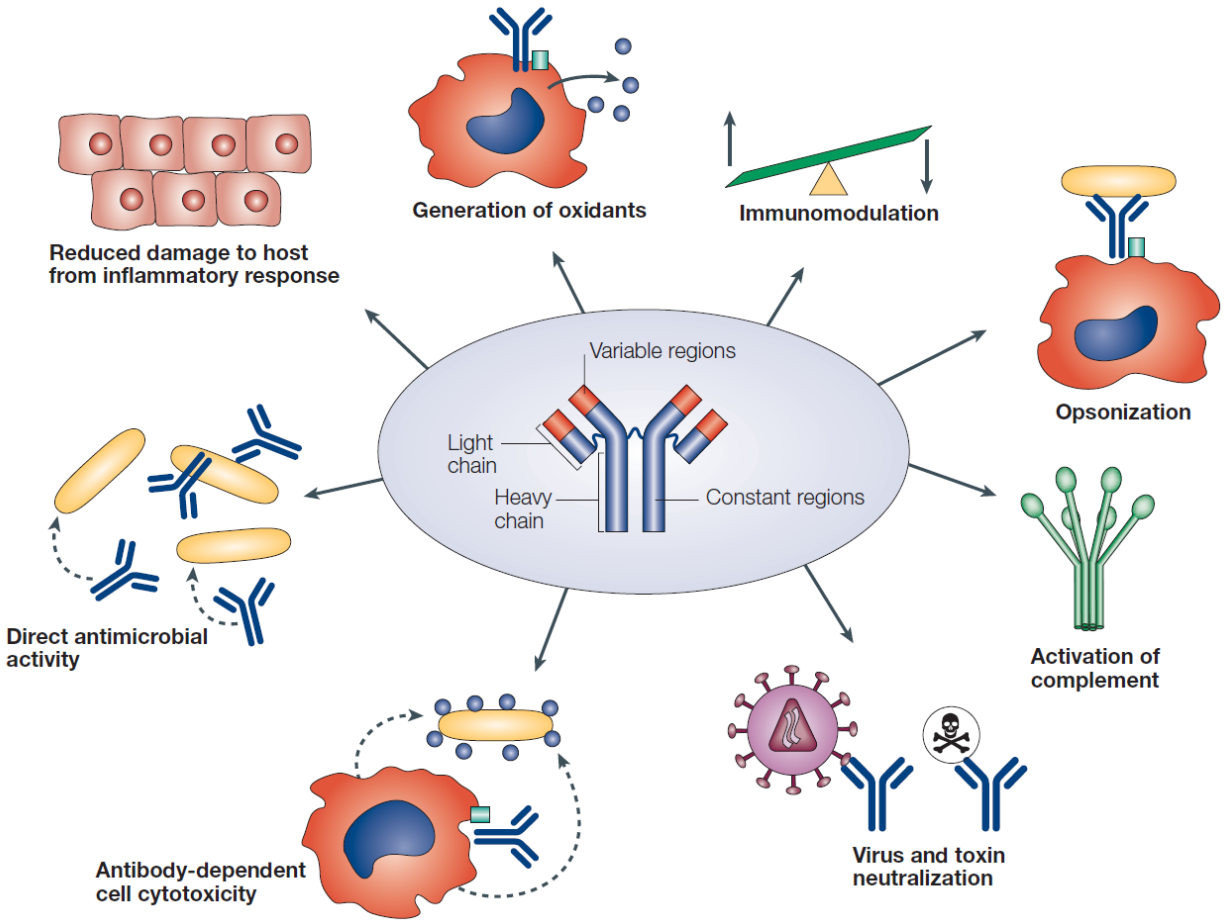

Figure 2: Versatility of potential biological effects of antibodies in treatment of infectious diseases. Antibody-dependent cellular cytotoxicity and opsonization involve contribution of other host cells and mediators of the immune system while the rest of effects functions independently. Reprinted from [58] with permission from Macmillan Publishers Ltd.

2. Pharmacokinetic and pharmacodynamic aspects

2.1. General situation

2.1.1. Infection pathogenesis

The pathogenesis of pulmonary infections with *Staphylococcus aureus* in general is characterized by complex interactions of the host immune system and virulence factors of *S. aureus*. Surface adhesins enable its colonization, adherence and persistence in the lung, whereas leukocidins and α-toxin facilitate invasion and damage of host tissue cells by lysis [8,67–69]. As soon as the bacteria invade the respiratory tract, they are confronted with phagocytes such as alveolar macrophages which intend to clear the intruders immediately from the lung [8,70]. The most challenging characteristic of this pathogen is its ability to evade the immune response. *S. aureus* can produce capsular polysaccharides and biofilms to shelter from detection by the immune system [69,71]. Furthermore, opsonization and phagocytosis may be additionally alleviated through other *S. aureus* effectors including the surface component protein A. Although *S. aureus* is considered to be an extracellular pathogen, some of the bacteria can reside within a host cell including phagocytic cells such as macrophages and neutrophils, which in turn actually try to clear the pathogen. Hence, the bacteria are protected from antimicrobial drugs inside this reservoir and can spread away from the infection site [72]. After several days within the reservoir, viable pathogens have been reported to escape by host cell lysis [73,74].

2.1.2. Requirements for effective treatment of MRSA

S. aureus can be found extracellularly, trying to evade opsonization and phagocytosis, as well as intracellularly, sheltering from the immune response [75]. For treating extracellular pathogens causing lung diseases, sufficient drug concentration in the epithelial lining fluid (ELF) is important whereas alveolar macrophages representing the intracellular infection site and need to be targeted to combat intracellular bacteria [25,76]. To reach the ELF from the blood-site, drugs need to pass through the alveolar capillary wall, interstitial fluid, and alveolar epithelial cells. Protein binding was reported to influence the crossing to the interstitial fluid as only unbound antibiotics can penetrate through the endothelial membrane [8,76]. Additionally, lipophilicity, diffusibility, and charge of the drugs have an impact on their transport route through the epithelial barriers. However, during bacterial infection and inflammation the permeability is enhanced [8,76].

2.2. Lung penetration of aerosolized antibiotics

Until today, few contributions on lung tissue concentrations of aerosolized antibiotics especially in the field of gram-positive nosocomial pneumonia are available [35,40,46]. Pharmacokinetic/pharmacodynamic studies are complicated by the debate whether the concentration of the antibiotic in the ELF or in the sputum can be predictive for therapeutic outcome. Since ELF needs invasive bronchioalveolar lavage (BAL) for extraction, the easier obtainable sputum is a common way to access drug concentration near the site of infection in clinical trials. However, it may not represent the concentration at the site of infection properly due to different patient-related variable factors as well as binding of the drug to several biomolecules of the sputum [40,77]. Another possibility is to access the whole lung parenchyma, which is only possible in animal studies or lung resection. An overall high variability has been detected in lung concentration of antibiotics presumably caused by individual patient-related factors like breathing pattern, non-homogenous distribution in lung or dissolution in sputum, as well as bioanalytical variations [78]. By studying ventilated pigs with *E. coli* pneumonia, Goldstein et al. demonstrated in 2002 that nebulized amikacin resulted in several-fold higher lung tissue deposition with more effective bactericidal activity than intravenous amikacin [79]. However, in healthy lungs the aerosolized antibiotic showed a more homogenously distributed pulmonary deposition and less systemic diffusion than in infected lungs. Massively infected lung segments exhibited lower amikacin concentrations compared to less infected areas [42,79,80]. In mechanically ventilated human patients with gram-negative VAP, Luyt et al. reported that administration of nebulized amikacin combined with intravenous therapy resulted in high concentrations in the lower respiratory tract with ELF concentrations of the aminoglycoside being much higher than the corresponding MIC [81].

In general, inhalation of antibiotics is capable of achieving highly targeted drug deposition within central and peripheral lung areas exceeding the minimum inhibitory concentrations of the most common respiratory bacteria compared to systemic administration. Reaching deeper areas of the lung, the antibiotics can be absorbed through the bronchial epithelium and spread via the lung by a network of sub-mucosal capillaries. However, systemic diffusion is relatively low enabling the application of antibiotics with high systemic toxicity such as colistin [38,77,82,83].

2.3. Lung penetration of monoclonal antibodies

Antibodies are molecules with special pharmacokinetic and pharmacodynamic characteristics [84]. In infectious diseases, a rapid invasion of the drug to the site of infection is of significant importance for fast inactivation of the bacteria and impeding tissue damage [85]. However, monoclonal antibodies (mAbs) typically are administered parenterally which leads to high immediate systemic bioavailability but only low and delayed concentrations in the targeted lung tissue [84–88]. To some extent this might be due to the large size of the macromolecules and their hydrophilicity which impair passive diffusion across the endothelium [84]. In the transport of the mAbs from the bloodstream to the lung tissue the neonatal Fc receptor (FcRn) is believed to be involved as well as transvascular transport processes such as convection and/or diffusion [89,90]. However, the precise mechanism has not been clarified with certainty since most studies so far only examined the transport of mAb by FcRn from the lung into the bloodstream [91–93]. Nevertheless, after intravenous administration, concentrations of mepolizumab, an antibody specific for IL-5 and used for treatment of asthma, were reported to be 500-fold lower in the BAL fluid obtained from the lung than in plasma [94]. Therefore, for an adequate concentration in the lung essentially higher drug doses are required when administered intravenously not only exposing the body to potential toxicity and adverse effects such as anaphylactic reactions but also causing high treatment expenses [84,95]. Local delivery of antibodies to the lungs by aerosolization represents a preferred, well-tolerated, non-invasive route of administration for treatment of lung diseases which increases drug concentration at the site of action and decreases systemic drug exposure [84–86,88,89,96]. For cetuximab, an anti-EGFR antibody for treatment of lung cancer, twice the concentration than those after intravenous administration were reported to have rapidly accumulated in the lung tissue by aerosolized delivery at early time points (2 h to 1 day). Furthermore, it was shown that this antibody also reached the fringe of the lungs due to the large dose achieved by local delivery unlike systemically administered cetuximab [85]. The plasma concentration of cetuximab was reported to be 9 times lower when applied directly to the lungs compared to parenteral administration reducing the probability of unwanted side effect (bioavailability of 11%). Since the maximal plasma concentration was measured after 48 h, Maillet et al. concluded that pulmonary delivery proved to offer a long availability of cetuximab at the site of action [89].

3. Galenic achievements in local pulmonary drug delivery

3.1. Antibiotics

3.1.1. Galenic hurdles

General requirements for an ideal inhalable formulation are absence of preservatives, neutral pH value, adequate osmolarity of about 300 mosmol/l while comprising some anions preventing cough or bronchospasm [36,43]. These criteria rule out the option to nebulize the available intravenous formulations but point out the need for development of special inhalable formulations of antibiotics [36]. For delivering drugs to the relevant lower lung regions an adequate size of the aerosol droplets is needed. Only particles with an aerodynamic diameter of 1 to 5 µm feature a suitable fine particle fraction for deposition in peripheral lung, while larger particles are depositing in mouth or throat, and smaller particles probably are exhaled [70,96,97]. There are three main mechanisms by which particles can deposit in the lungs: impaction, sedimentation, and diffusion. The irregular movement of sufficiently small particles (< 0.5 µm) due to collisions with gas molecules (Brownian motion) can cause particles to hit the airway wall and hence deposit in the lung. According to the *Stokes-Einstein* equation, the diffusion is correlated to the particle size:

$$D = \frac{k_B \cdot T}{3\pi \cdot \eta \cdot d} \tag{1}$$

Where D is the diffusion coefficient, k_B is the Boltzmann's constant, T is the absolute temperature, η is the viscosity and d the diameter of the particle. Therefore, the deposition by diffusion is inversely related to the particle size and hence decreasing particle size increases the probability to deposit due to Brownian motion [98,99]. Particles of medium size (0.5-3 µm) prevalently settle by sedimentation due to the influence of gravity. Sedimentation is time dependent and the settling velocity v is given by *Stokes' law*:

$$v = \frac{(\rho_p - \rho_a) \cdot d^2 \cdot g}{18 \cdot \eta} \tag{2}$$

where g is the acceleration due to gravity and ρ_p the density of the particle being higher than the density of air ρ_a [98,99]. In contrast, particles > 3 µm display inertia and hence deposit in the branched respiratory tract due to collision with the walls (impaction). Deposition due to impaction increases with enhanced particle diameter and enhanced airflow velocity whereas breath-holding prolongs time for particle sedimentation [99].

Hence, using the appropriate device for targeted pulmonary delivery of antibiotics is indispensable [18,100]. During treatment of mechanically ventilated patients, loss of drug due to adsorption to ventilator tubes must be considered and humidification of the ventilated air should be reduced since it is influencing the particle size negatively [43].

3.1.2. Recent developments in local pulmonary antibiotic delivery

Improvements in the administration of aerosolized antibiotics have been made by development of new delivery devices during the last years. The new generation of vibrating mesh nebulizers demonstrated enhanced pharmacokinetic and application features such as minor residual volume and rapid output [101]. Shorter application time and a trend to higher sputum concentrations of tobramycin were detected using a PARI eFlow® rapid vibrating mesh nebulizer compared to a jet nebulizer when administered to cystic fibrosis patients in a two-period crossover study [78].

Another approach to enhance pharmacokinetic/pharmacodynamic properties of antibiotics and decrease toxic side effects is based on liposomal drug delivery systems [102]. Advantages are a decrease of dosing intervals due to sustained drug release as well as prolonged presence at infection site and targeted delivery [101]. It could be shown that encapsulation of vancomycin into liposomes enhanced uptake into macrophages and increased subsequent intracellular killing of "hiding" MRSA bacteria *in vitro* [8,103,104]. Furthermore, PEGylation of vancomycin liposomes prolonged plasma circulation time and increased lung tissue concentrations after systemic application [105]. After nebulization of vancomycin liposomes modified with chitosan as well as of conventional liposomes in a recent animal study, higher available drug amount and pulmonary tissue concentration were detected compared to nebulized vancomycin solution [106].

In addition, nanoparticles as well as microparticles present further promising alternatives. Encapsulation of antibiotics into nanoparticles enables higher local drug concentrations, may improve mucus penetration, and circumvent solubility problems [107–109]. Nanoplexes prepared by polyelectrolyte-drug self-assembly showed a high drug loading and may enhance the bioavailability of poorly soluble drugs such as ciprofloxacin, an effective antibiotic against the respiratory pathogen *Pseudomonas aeruginosa* [110,111]. Complexes of the poorly soluble rifampicin with cyclodextrins were shown *in vitro* to represent a further potential drug delivery system for pulmonary nebulization which increases local delivery of active antibiotics [112]. In an animal study nebulization of antibiotics encapsulated in alginate nanoparticles enhanced relative bioavailability and prolonged the presence of drug over MIC

in the lung compared to the free drug representing a feasible controlled drug release system [113].

3.2. Antibodies

3.2.1. Challenges in pulmonary delivery of antibodies

Effective pulmonary delivery of antibodies is far more demanding than aerosolization of small molecules. The therapeutic activity of proteins depends on the individual conformational structure, which is endangered by a multitude of external influences. The pH value, mechanical stress, and temperature represent the most important factors to consider [70,114,115]. Therefore, preserving the stability and hence bioactivity of proteins during manufacture, shelf life, and application is the most important challenge in formulation development.

Since nebulizers are the devices of choice to deliver aerosolized drugs to intubated patients, nebulization is a promising way of treating pneumonia. Furthermore, nebulization enables direct application of drugs in solutions. This is beneficial since liquid protein formulations are easier, cheaper, and faster to develop than dry powder formulations since no further potentially detrimental process steps like drying are needed [84,116]. However, during dispersion of the drug solution into numerous small liquid droplets, the antibody is exposed to an enormous air-liquid interface which can lead to protein adsorption at the interface, partial unfolding, and aggregation [84,117]. Protein aggregation in turn impairs bioactivity and can lead to unwanted immunogenicity [118–120]. Ultrasonic and jet-nebulizers cause additional stress onto the biomolecule due to recirculation of protein molecules inside the devices until droplets of appropriate sizes are generated. Furthermore, ultrasonic as well as vibrating mesh devices endanger protein stability by warming during the nebulization process [84,117,121]. Nevertheless, cooling of the vibrating mesh device during nebulization as well as addition of formulation excipients can reduce detrimental effects and preserve protein stability [87,116,121–126]. Surfactants are the most feasible excipient for protection against interfacial stress [127–129]. Further potential stabilizing excipients compatible for pulmonary delivery are polyols like PEG [125,126], sugars such as cyclodextrins [121], and small amino acids [84,96]. However, no general rule for stabilization can be applied to all proteins but individual formulation development combined with choosing the most suitable nebulization device is required for every single protein [87].

3.2.2. Recent developments in delivery of antibodies to the lung

Recently, research is focusing on overcoming the drawbacks of protein delivery to the airways considering their sensitive conformational stability as well as fast clearance by macrophages, the mucociliary escalator, and proteolysis [130].

For the nebulization of antibodies the development of a novel promising device was reported. Surface acoustic waves generate an aerosol while preserving the proteins stability and bioactivity. Advantages of the Respite™ system are its small size, low costs, battery operation, and portability [131].

Koussoropolis et al. reported that the therapeutic efficacy of inhaled biopharmaceuticals may be increased by PEGylation. The pulmonary presence of the otherwise rapidly cleared antibody fragments could be prolonged through mucoadhesion and escape from alveolar macrophages by PEGylation [132].

Furthermore, nebulization of proteins or peptides encapsulated into liposomes presents a promising alternative for local pulmonary delivery by enabling longer residence time while lowering unwanted side effects in the lungs [133]. Cyclosporine, a peptide drug for treatment of transplant rejection, could be aerosolized as liposomal formulation overcoming its poor water solubility and led to high and prolonged concentrations at the site of action while reducing the risk of drug related site effects [134]. Hajor et al. reported that the short half-life of vasoactive intestinal peptides (VIP), which is due to enzymatic degradation in the lung, could be sustained by unilamellar VIP-loaded liposomes in an *ex vivo* vasorelaxation model. These liposomes also proved to be stable during nebulization [135].

In a very recent study, antibodies were used as a drug delivery system for antibiotics to defeat intracellular hiding bacteria which is of particular interest with regard to treatment of MRSA pneumonia. An antibody directed against specific sugar modifications on wall-teichoic acids produced by all *S. aureus* strains which is engineered to contain unpaired cysteine residues (THIOMAB) was covalently linked to an antibiotic able to kill intracellular bacteria (rifalogue). By the help of these specialized antibody-drug conjugates the antibiotics were attached to the bacteria and taken up inside the respective cells. Intracellular proteases activated the antibiotic by cleavage of the linkage to the antibody. This antibody-antibiotic conjugate was demonstrated to be more efficient in treating bacteremia in mice than vancomycin [72]. Similar antibody drug conjugates have also been applied to deliver cytotoxic drugs to tumors or virus-synthesizing cells to increase their potency [57,58,84].

4. Conclusion

The challenge of antibiotic resistance is gaining increasing importance in treatment of infectious diseases. Even the up to now reliable antibiotic vancomycin appears to reach its limits in treating infections caused by MRSA. Development of new antibiotics alone cannot handle this serious problem. Instead, innovative and efficient delivery strategies for the available drugs as well as application of appropriate immunotherapeutic options are a promising approach. Especially, local delivery of the drugs to the site of infection proved to be a valuable tool for therapeutic improvement. Inhalation of aerosolized antibiotics or antibodies seems to enable increased local drug levels and shorter application times. Furthermore, pulmonary delivery appears to improve clinical efficacy especially when combined with systemic antimicrobial therapy. Numerous different drug delivery possibilities for aerosol inhalation to the lungs have been successfully studied so far reaching from advances in device technology over encapsulation into nanoparticles or particularly liposomes to drug targeting.

This research progress opens a very promising future for the development of more effective treatment options for MRSA pneumonia by local drug delivery of antibiotics, immunotherapeutic drugs or combinations of both. Yet, further studies particularly directed to combat MRSA pneumonia are desperately needed.

References

[1] N.E. Holmes, S.Y.C. Tong, J.S. Davis, S.J. van Hal, Treatment of methicillin-resistant Staphylococcus aureus: vancomycin and beyond., Semin. Respir. Crit. Care Med. 36 (2015) 17–30. doi:10.1055/s-0034-1397040.

[2] European Centre for Disease Prevention and Control, Antimicrobial resistance surveillance in Europe 2013. Annual Report of the European Antimicrobial Resistance Surveillance Network (EARS-Net), ECDC, Stockholm, 2014. doi:10.2900/39777.

[3] K. Yanagihara, N. Araki, S. Watanabe, T. Kinebuchi, M. Kaku, S. Maesaki, et al., Antimicrobial susceptibility and molecular characteristics of 857 methicillin-resistant Staphylococcus aureus isolates from 16 medical centers in Japan (2008-2009): nationwide survey of community-acquired and nosocomial MRSA., Diagn. Microbiol. Infect. Dis. 72 (2012) 253–7. doi:10.1016/j.diagmicrobio.2011.11.010.

[4] H.-J. Linde, N. Lehn, Methicillin-resistenter Staphylococcus aureus (MRSA), Der Hautarzt. 53 (2002) 690–701. doi:10.1007/s00105-002-0424-y.

[5] F.C. Tenover, L.K. McDougal, R. V Goering, G. Killgore, S.J. Projan, J.B. Patel, et al., Characterization of a strain of community-associated methicillin-resistant Staphylococcus aureus widely disseminated in the United States., J. Clin. Microbiol. 44 (2006) 108–18. doi:10.1128/JCM.44.1.108-118.2006.

[6] G.L. Bassi, M. Ferrer, J.D. Marti, T. Comaru, A. Torres, Ventilator-associated pneumonia., Semin. Respir. Crit. Care Med. 35 (2014) 469–81. doi:10.1055/s-0034-1384752.

[7] J. Chastre, F. Blasi, R.G. Masterton, J. Rello, A. Torres, T. Welte, European perspective and update on the management of nosocomial pneumonia due to methicillin-resistant Staphylococcus aureus after more than 10 years of experience with linezolid., Clin. Microbiol. Infect. 20 Suppl 4 (2014) 19–36. doi:10.1111/1469-0691.12450.

[8] A.S. Pumerantz, PEGylated liposomal vancomycin: a glimmer of hope for improving treatment outcomes in MRSA pneumonia., Recent Pat. Antiinfect. Drug Discov. 7 (2012) 205–12. doi:10.2174/157489112803521904.

[9] A.S. Haddadin, S.A. Fappiano, P.A. Lipsett, Methicillin resistant Staphylococcus aureus (MRSA) in the intensive care unit., Postgrad. Med. J. 78 (2002) 385–92.

[10] J.M. Sirvent, A. Torres, L. Vidaur, J. Armengol, J. de Batlle, A. Bonet, Tracheal colonisation within 24 h of intubation in patients with head trauma: risk factor for developing early-onset ventilator-associated pneumonia., Intensive Care Med. 26 (2000) 1369–72. doi:10.1007/s001340000611.

[11] I.K. Murni, T. Duke, S. Kinney, A.J. Daley, Y. Soenarto, Reducing hospital-acquired infections and improving the rational use of antibiotics in a developing country: an effectiveness study., Arch. Dis. Child. 100 (2015) 454–9. doi:10.1136/archdischild-2014-307297.

[12] C. Chaix, I. Durand-Zaleski, C. Alberti, C. Brun-Buisson, Control of endemic methicillin-resistant Staphylococcus aureus: a cost-benefit analysis in an intensive care unit., JAMA. 282 (1999) 1745–51. doi:10.1001/jama.282.18.1745.

[13] American Thoracic Society, Infectious Diseases Society of America, Guidelines for the management of adults with hospital-acquired, ventilator-associated, and healthcare-associated pneumonia., Am. J. Respir. Crit. Care Med. 171 (2005) 388–416. doi:10.1164/rccm.200405-644ST.

[14] K. Dalhoff, M. Abele-Horn, S. Andreas, T. Bauer, H. von Baum, M. Deja, et al., Epidemiology, diagnosis and treatment of adult patients with nosocomial pneumonia. S-3 Guideline of the German Society for Anaesthesiology and Intensive Care Medicine, the German Society for Infectious Diseases, the German Society for Hygiene and Microbi, Pneumologie. 66 (2012) 707–65. doi:10.1055/s-0032-1325924.

[15] K. Dalhoff, S. Ewig, Gideline Development Group, M. Abele-Horn, S. Andreas, T.T. Bauer, et al., Adult patients with nosocomial pneumonia: epidemiology, diagnosis, and treatment., Dtsch. Ärzteblatt Int. 110 (2013) 634–40. doi:10.3238/arztebl.2013.0634.

[16] R.G. Wunderink, M.S. Niederman, M.H. Kollef, A.F. Shorr, M.J. Kunkel, A. Baruch, et al., Linezolid in methicillin-resistant Staphylococcus aureus nosocomial pneumonia: a randomized, controlled study., Clin. Infect. Dis. 54 (2012) 621–9. doi:10.1093/cid/cir895.

[17] A.C. Kalil, M. Klompas, G. Haynatzki, M.E. Rupp, Treatment of hospital-acquired pneumonia with linezolid or vancomycin: a systematic review and meta-analysis., BMJ Open. 3 (2013) e003912. doi:10.1136/bmjopen-2013-003912.

[18] J. Garnacho-Montero, Y. Corcia-Palomo, R. Amaya-Villar, L. Martin-Villen, How to treat VAP due to MDR pathogens in ICU patients., BMC Infect. Dis. 14 (2014) 135. doi:10.1186/1471-2334-14-135.

[19] P. Peyrani, T.L. Wiemken, R. Kelley, M.J. Zervos, D.H. Kett, T.M. File, et al., Higher clinical success in patients with ventilator-associated pneumonia due to methicillin-resistant Staphylococcus aureus treated with linezolid compared with vancomycin: results from the IMPACT-HAP study., Crit. Care. 18 (2014) R118. doi:10.1186/cc13914.

[20] M.W. Pletz, O. Burkhardt, T. Welte, Nosocomial methicillin-resistant Staphylococcus aureus (MRSA) pneumonia: linezolid or vancomycin? - Comparison of pharmacology and clinical efficacy., Eur. J. Med. Res. 15 (2010) 507–13. doi:10.1186/2047-783X-15-12-507.

[21] M. Segarra-Newnham, T.J. Church, Pharmacotherapy for methicillin-resistant Staphylococcus aureus nosocomial pneumonia., Ann. Pharmacother. 46 (2012) 1678–87. doi:10.1345/aph.1R370.

[22] M.M. An, H. Shen, J.D. Zhang, G.T. Xu, Y.Y. Jiang, Linezolid versus vancomycin for meticillin-resistant Staphylococcus aureus infection: a meta-analysis of randomised controlled trials., Int. J. Antimicrob. Agents. 41 (2013) 426–33. doi:10.1016/j.ijantimicag.2012.12.012.

[23] H. Jiang, R.-N. Tang, J. Wang, Linezolid versus vancomycin or teicoplanin for nosocomial pneumonia: meta-analysis of randomised controlled trials., Eur. J. Clin. Microbiol. Infect. Dis. 32 (2013) 1121–8. doi:10.1007/s10096-013-1867-z.

[24] Y. Wang, Y. Zou, J. Xie, T. Wang, X. Zheng, H. He, et al., Linezolid versus vancomycin for the treatment of suspected methicillin-resistant Staphylococcus aureus nosocomial pneumonia: a systematic review employing meta-analysis., Eur. J. Clin. Pharmacol. 71 (2015) 107–15. doi:10.1007/s00228-014-1775-x.

[25] G.E. Stein, E.M. Wells, The importance of tissue penetration in achieving successful antimicrobial treatment of nosocomial pneumonia and complicated skin and soft-tissue infections caused by methicillin-resistant Staphylococcus aureus: vancomycin and linezolid., Curr. Med. Res. Opin. 26 (2010) 571–88. doi:10.1185/03007990903512057.

[26] P. Peyrani, J. Ramirez, What is the best therapeutic approach to methicillin-resistant Staphylococcus aureus pneumonia?, Curr. Opin. Infect. Dis. 28 (2015) 164–70. doi:10.1097/QCO.0000000000000149.

[27] A.R. Caffrey, H.J. Morrill, L.A. Puzniak, K.L. Laplante, Comparative effectiveness of linezolid and vancomycin among a national veterans affairs cohort with methicillin-resistant Staphylococcus aureus pneumonia., Pharmacotherapy. 34 (2014) 473–80. doi:10.1002/phar.1390.

[28] S.L. Gerson, S.L. Kaplan, J.B. Bruss, V. Le, F.M. Arellano, B. Hafkin, et al., Hematologic effects of linezolid: summary of clinical experience., Antimicrob. Agents Chemother. 46 (2002) 2723–6. doi:10.1128/AAC.46.8.2723-2726.2002.

[29] P.E. Grgurich, J. Hudcova, Y. Lei, A. Sarwar, D.E. Craven, Management and prevention of ventilator-associated pneumonia caused by multidrug-resistant pathogens., Expert Rev. Respir. Med. 6 (2012) 533–55. doi:10.1586/ers.12.45.

[30] J.J. Carreno, T.P. Lodise, Ceftaroline Fosamil for the Treatment of Community-Acquired Pneumonia: from FOCUS to CAPTURE., Infect. Dis. Ther. 3 (2014) 123–32. doi:10.1007/s40121-014-0036-8.

[31] L.L. Ling, T. Schneider, A.J. Peoples, A.L. Spoering, I. Engels, B.P. Conlon, et al., A new antibiotic kills pathogens without detectable resistance., Nature. 517 (2015) 455–9. doi:10.1038/nature14098.

[32] G. Wright, Antibiotics: An irresistible newcomer., Nature. 517 (2015) 442–4. doi:10.1038/nature14193.

[33] A. Kali, Teixobactin: a novel antibiotic in treatment of gram positive bacterial infections., J. Clin. Diagn. Res. 9 (2015) DL01. doi:10.7860/JCDR/2015/13033.5720.

[34] F.G. Zampieri, A.P. Nassar, D. Gusmao-Flores, L.U. Taniguchi, A. Torres, O.T. Ranzani, Nebulized antibiotics for ventilator-associated pneumonia: a systematic review and meta-analysis., Crit. Care. 19 (2015) 150. doi:10.1186/s13054-015-0868-y.

[35] J.K. Hagerman, K.E. Hancock, M.E. Klepser, Aerosolised antibiotics: a critical appraisal of their use., Expert Opin. Drug Deliv. 3 (2006) 71–86. doi:10.1517/17425247.3.1.71.

[36] M.H. Kollef, C.W. Hamilton, A.B. Montgomery, Aerosolized antibiotics: do they add to the treatment of pneumonia?, Curr. Opin. Infect. Dis. 26 (2013) 538–44. doi:10.1097/QCO.0000000000000004.

[37] L.B. Palmer, Aerosolized antibiotics in the intensive care unit., Clin. Chest Med. 32 (2011) 559–74. doi:10.1016/j.ccm.2011.05.012.

[38] T. Abu-Salah, R. Dhand, Inhaled antibiotic therapy for ventilator-associated tracheobronchitis and ventilator-associated pneumonia: an update., Adv. Ther. 28 (2011) 728–47. doi:10.1007/s12325-011-0051-z.

[39] P.A. Flume, D.R. VanDevanter, Clinical applications of pulmonary delivery of antibiotics., Adv. Drug Deliv. Rev. 85 (2015) 1–6. doi:10.1016/j.addr.2014.10.009.

[40] T. Velkov, N. Abdul Rahim, Q.T. Zhou, H.-K. Chan, J. Li, Inhaled anti-infective chemotherapy for respiratory tract infections: successes, challenges and the road ahead., Adv. Drug Deliv. Rev. 85 (2015) 65–82. doi:10.1016/j.addr.2014.11.004.

[41] G.C. Wood, Aerosolized antibiotics for treating hospital-acquired and ventilator-associated pneumonia., Expert Rev. Anti. Infect. Ther. 9 (2011) 993–1000. doi:10.1586/eri.11.126.

[42] E. Lesho, Role of inhaled antibacterials in hospital-acquired and ventilator-associated pneumonia., Expert Rev. Anti. Infect. Ther. 3 (2005) 445–51. doi:10.1586/14787210.3.3.445.

[43] G.T. Dimopoulos, M. Kollef, D.K. Matthaiou, B. Montgomery, Aerolized antibiotics for the treatment of Ventilator Associated Pneumonia: A new era!, PNEUMON Number 1. 27 (2014) 87–93.

[44] H.M. Arnold, A.M. Sawyer, M.H. Kollef, Use of adjunctive aerosolized antimicrobial therapy in the treatment of Pseudomonas aeruginosa and Acinetobacter baumannii ventilator-associated pneumonia., Respir. Care. 57 (2012) 1226–33. doi:10.4187/respcare.01556.

[45] C.-E. Luyt, A. Combes, A. Nieszkowska, J.-L. Trouillet, J. Chastre, Aerosolized antibiotics to treat ventilator-associated pneumonia., Curr. Opin. Infect. Dis. 22 (2009) 154–8. doi:10.1097/QCO.0b013e328322a006.

[46] J. Chastre, C.-E. Luyt, Other therapeutic modalities and practices: implications for clinical trials of hospital-acquired or ventilator-associated pneumonia., Clin. Infect. Dis. 51 Suppl 1 (2010) S54–8. doi:10.1086/653050.

[47] L.B. Palmer, G.C. Smaldone, Reduction of bacterial resistance with inhaled antibiotics in the intensive care unit., Am. J. Respir. Crit. Care Med. 189 (2014) 1225–33. doi:10.1164/rccm.201312-2161OC.

[48] L.B. Palmer, G.C. Smaldone, J.J. Chen, D. Baram, T. Duan, M. Monteforte, et al., Aerosolized antibiotics and ventilator-associated tracheobronchitis in the intensive care unit., Crit. Care Med. 36 (2008) 2008–13. doi:10.1097/CCM.0b013e31817c0f9e.

[49] L. Máiz, R. Cantón, N. Mir, F. Baquero, H. Escobar, Aerosolized vancomycin for the treatment of methicillin-resistant Staphylococcus aureus infection in cystic fibrosis., Pediatr. Pulmonol. 26 (1998) 287–9.

[50] D. Hayes, B.S. Murphy, T.W. Mullett, D.J. Feola, Aerosolized vancomycin for the treatment of MRSA after lung transplantation., Respirology. 15 (2010) 184–6. doi:10.1111/j.1440-1843.2009.01647.x.

[51] B.C. Trapnell, S.A. McColley, D.G. Kissner, M.W. Rolfe, J.M. Rosen, M. McKevitt, et al., Fosfomycin/tobramycin for inhalation in patients with cystic fibrosis with pseudomonas airway infection., Am. J. Respir. Crit. Care Med. 185 (2012) 171–8. doi:10.1164/rccm.201105-0924OC.

[52] NCT02218359, Aerosolized Amikacin and Fosfomycin in Mechanically Ventilated Patients With Gram-negative and/or Gram-positive Bacterial Colonization, Clinicaltrials.gov. (2015). https://clinicaltrials.gov/ct2/show/NCT02218359 (accessed November 11, 2015).

[53] NCT01746095, Efficacy and Safety Study of AeroVanc for the Treatment of Persistent MRSA Lung Infection in Cystic Fibrosis Patients, Clinicaltrials.gov. (2014). https://clinicaltrials.gov/ct2/show/NCT01746095 (accessed November 24, 2015).

[54] T.P. Lodise, B. Lomaestro, J. Graves, G.L. Drusano, Larger vancomycin doses (at least four grams per day) are associated with an increased incidence of nephrotoxicity., Antimicrob. Agents Chemother. 52 (2008) 1330–6. doi:10.1128/AAC.01602-07.

[55] B. Spellberg, R. Guidos, D. Gilbert, J. Bradley, H.W. Boucher, W.M. Scheld, et al., The epidemic of antibiotic-resistant infections: a call to action for the medical community from the Infectious Diseases Society of America., Clin. Infect. Dis. 46 (2008) 155–64. doi:10.1086/524891.

[56] S.J. Projan, Why is big Pharma getting out of antibacterial drug discovery?, Curr. Opin. Microbiol. 6 (2003) 427–30. doi:10.1016/j.mib.2003.08.003.

[57] N.A.P.S. Buss, S.J. Henderson, M. McFarlane, J.M. Shenton, L. de Haan, Monoclonal antibody therapeutics: history and future., Curr. Opin. Pharmacol. 12 (2012) 615–22. doi:10.1016/j.coph.2012.08.001.

[58] A. Casadevall, E. Dadachova, L. Pirofski, Passive antibody therapy for infectious diseases., Nat. Rev. Microbiol. 2 (2004) 695–703. doi:10.1038/nrmicro974.

[59] K. Ohlsen, U. Lorenz, Immunotherapeutic strategies to combat staphylococcal infections., Int. J. Med. Microbiol. 300 (2010) 402–10. doi:10.1016/j.ijmm.2010.04.015.

[60] U. Lorenz, B. Lorenz, T. Schmitter, K. Streker, C. Erck, J. Wehland, et al., Functional antibodies targeting IsaA of Staphylococcus aureus augment host immune response and open new perspectives for antibacterial therapy., Antimicrob. Agents Chemother. 55 (2011) 165–73. doi:10.1128/AAC.01144-10.

[61] A.E. Hall, P.J. Domanski, P.R. Patel, J.H. Vernachio, P.J. Syribeys, E.L. Gorovits, et al., Characterization of a protective monoclonal antibody recognizing Staphylococcus aureus MSCRAMM protein clumping factor A., Infect. Immun. 71 (2003) 6864–70. doi:10.1128/IAI.71.12.6864-6870.2003.

[62] J.M. Patti, A humanized monoclonal antibody targeting Staphylococcus aureus., Vaccine. 22 Suppl 1 (2004) S39–43. doi:10.1016/j.vaccine.2004.08.015.

[63] P.J. Domanski, P.R. Patel, A.S. Bayer, L. Zhang, A.E. Hall, P.J. Syribeys, et al., Characterization of a humanized monoclonal antibody recognizing clumping factor A expressed by Staphylococcus aureus., Infect. Immun. 73 (2005) 5229–32. doi:10.1128/IAI.73.8.5229-5232.2005.

[64] V.G. Fowler, R.A. Proctor, Where does a Staphylococcus aureus vaccine stand?, Clin. Microbiol. Infect. 20 Suppl 5 (2014) 66–75. doi:10.1111/1469-0691.12570.

[65] U. Lorenz, K. Ohlsen, H. Karch, M. Hecker, A. Thiede, Jã¶. Hacker, Human antibody response during sepsis against targets expressed by methicillin resistant Staphylococcus aureus., FEMS Immunol. Med. Microbiol. 29 (2000) 145–53. doi:10.1111/j.1574-695X.2000.tb01517.x.

[66] B. Oesterreich, B. Lorenz, T. Schmitter, R. Kontermann, M. Zenn, B. Zimmermann, et al., Characterization of the biological anti-staphylococcal functionality of hUK-66 IgG1, a humanized monoclonal antibody as substantial component for an immunotherapeutic approach., Hum. Vaccin. Immunother. 10 (2014) 926–37.

[67] S. Defres, C. Marwick, D. Nathwani, MRSA as a cause of lung infection including airway infection, community-acquired pneumonia and hospital-acquired pneumonia., Eur. Respir. J. 34 (2009) 1470–6. doi:10.1183/09031936.00122309.

[68] D. Parker, A. Prince, Immunopathogenesis of Staphylococcus aureus pulmonary infection., Semin. Immunopathol. 34 (2012) 281–97. doi:10.1007/s00281-011-0291-7.

[69] R.J. Gordon, F.D. Lowy, Pathogenesis of methicillin-resistant Staphylococcus aureus infection., Clin. Infect. Dis. 46 Suppl 5 (2008) S350–9. doi:10.1086/533591.

[70] S.-J. Koussoroplis, R. Vanbever, Peptides and Proteins: Pulmonary Absorption, in: Encycl. Pharm. Sci. Technol. Vol. IV, 4th ed., Taylor & Francis Group, LLC, 2013: pp. 2607–2618. doi:10.1081/E-EPT4-120050324.

[71] F.R. DeLeo, B.A. Diep, M. Otto, Host defense and pathogenesis in Staphylococcus aureus infections., Infect. Dis. Clin. North Am. 23 (2009) 17–34. doi:10.1016/j.idc.2008.10.003.

[72] S.M. Lehar, T. Pillow, M. Xu, L. Staben, K.K. Kajihara, R. Vandlen, et al., Novel antibody-antibiotic conjugate eliminates intracellular S. aureus., Nature. 527 (2015) 323–8. doi:10.1038/nature16057.

[73] J.M. Voyich, K.R. Braughton, D.E. Sturdevant, A.R. Whitney, B. Saïd-Salim, S.F. Porcella, et al., Insights into mechanisms used by Staphylococcus aureus to avoid destruction by human neutrophils., J. Immunol. 175 (2005) 3907–19. doi:10.4049/jimmunol.175.6.3907.

[74] M. Kubica, K. Guzik, J. Koziel, M. Zarebski, W. Richter, B. Gajkowska, et al., A potential new pathway for Staphylococcus aureus dissemination: the silent survival of S. aureus phagocytosed by human monocyte-derived macrophages., PLoS One. 3 (2008) e1409. doi:10.1371/journal.pone.0001409.

[75] G.Y. Liu, Molecular pathogenesis of Staphylococcus aureus infection., Pediatr. Res. 65 (2009) 71R–77R. doi:10.1203/PDR.0b013e31819dc44d.

[76] S. Kiem, J.J. Schentag, Interpretation of antibiotic concentration ratios measured in epithelial lining fluid., Antimicrob. Agents Chemother. 52 (2008) 24–36. doi:10.1128/AAC.00133-06.

[77] J.K. Mukker, R.S.P. Singh, H. Derendorf, Pharmacokinetic and pharmacodynamic implications in inhalable antimicrobial therapy., Adv. Drug Deliv. Rev. 85 (2015) 57–64. doi:10.1016/j.addr.2015.03.002.

[78] M. Govoni, G. Poli, D. Acerbi, D. Santoro, H. Cicirello, O. Annoni, et al., Pharmacokinetic and tolerability profiles of tobramycin nebuliser solution 300 mg/4 ml administered by PARI eFlow(®) rapid and PARI LC Plus(®) nebulisers in cystic fibrosis patients., Pulm. Pharmacol. Ther. 26 (2013) 249–55. doi:10.1016/j.pupt.2012.12.002.

[79] I. Goldstein, F. Wallet, A. Nicolas-Robin, F. Ferrari, C.-H. Marquette, J.-J. Rouby, Lung deposition and efficiency of nebulized amikacin during Escherichia coli pneumonia in ventilated piglets., Am. J. Respir. Crit. Care Med. 166 (2002) 1375–81. doi:10.1164/rccm.200204-363OC.

[80] I. Goldstein, F. Wallet, J. Robert, M.-H. Becquemin, C.-H. Marquette, J.-J. Rouby, Lung tissue concentrations of nebulized amikacin during mechanical ventilation in piglets with healthy lungs., Am. J. Respir. Crit. Care Med. 165 (2002) 171–5. doi:10.1164/ajrccm.165.2.2107025.

[81] C.-E. Luyt, M. Clavel, K. Guntupalli, J. Johannigman, J.I. Kennedy, C. Wood, et al., Pharmacokinetics and lung delivery of PDDS-aerosolized amikacin (NKTR-061) in intubated and mechanically ventilated patients with nosocomial pneumonia., Crit. Care. 13 (2009) R200. doi:10.1186/cc8206.

[82] R. Dhand, The role of aerosolized antimicrobials in the treatment of ventilator-associated pneumonia., Respir. Care. 52 (2007) 866–84.

[83] S.W.S. Yapa, J. Li, K. Patel, J.W. Wilson, M.J. Dooley, J. George, et al., Pulmonary and systemic pharmacokinetics of inhaled and intravenous colistin methanesulfonate in cystic fibrosis patients: targeting advantage of inhalational administration., Antimicrob. Agents Chemother. 58 (2014) 2570–9. doi:10.1128/AAC.01705-13.

[84] R. Respaud, L. Vecellio, P. Diot, N. Heuzé-Vourc'h, Nebulization as a delivery method for mAbs in respiratory diseases., Expert Opin. Drug Deliv. 12 (2015) 1027–39. doi:10.1517/17425247.2015.999039.

[85] L. Guilleminault, N. Azzopardi, C. Arnoult, J. Sobilo, V. Hervé, J. Montharu, et al., Fate of inhaled monoclonal antibodies after the deposition of aerosolized particles in the respiratory system., J. Control. Release. 196 (2014) 344–54. doi:10.1016/j.jconrel.2014.10.003.

[86] V. Hervé, N. Rabbe, L. Guilleminault, F. Paul, L. Schlick, N. Azzopardi, et al., VEGF neutralizing aerosol therapy in primary pulmonary adenocarcinoma with K-ras activating-mutations., MAbs. 6 (2014) 1638–48. doi:10.4161/mabs.34454.

[87] R. Respaud, D. Marchand, C. Parent, T. Pelat, P. Thullier, J.-F. Tournamille, et al., Effect of formulation on the stability and aerosol performance of a nebulized antibody., MAbs. 6 (2014) 1347–55. doi:10.4161/mabs.29938.

[88] J.L. Cleland, A. Daugherty, R. Mrsny, Emerging protein delivery methods., Curr. Opin. Biotechnol. 12 (2001) 212–9. doi:10.1016/S0958-1669(00)00202-0.

[89] A. Maillet, L. Guilleminault, E. Lemarié, S. Lerondel, N. Azzopardi, J. Montharu, et al., The airways, a novel route for delivering monoclonal antibodies to treat lung tumors., Pharm. Res. 28 (2011) 2147–56. doi:10.1007/s11095-011-0442-5.

[90] M. Tabrizi, G.G. Bornstein, H. Suria, Biodistribution mechanisms of therapeutic monoclonal antibodies in health and disease., AAPS J. 12 (2010) 33–43. doi:10.1208/s12248-009-9157-5.

[91] D.C. Roopenian, S. Akilesh, FcRn: the neonatal Fc receptor comes of age., Nat. Rev. Immunol. 7 (2007) 715–25. doi:10.1038/nri2155.

[92] A.J. Bitonti, J.A. Dumont, Pulmonary administration of therapeutic proteins using an immunoglobulin transport pathway., Adv. Drug Deliv. Rev. 58 (2006) 1106–18. doi:10.1016/j.addr.2006.07.015.

[93] J.A. Dumont, A.J. Bitonti, D. Clark, S. Evans, M. Pickford, S.P. Newman, Delivery of an erythropoietin-Fc fusion protein by inhalation in humans through an immunoglobulin transport pathway., J. Aerosol Med. 18 (2005) 294–303. doi:10.1089/jam.2005.18.294.

[94] T.K. Hart, R.M. Cook, P. Zia-Amirhosseini, E. Minthorn, T.S. Sellers, B.E. Maleeff, et al., Preclinical efficacy and safety of mepolizumab (SB-240563), a humanized monoclonal antibody to IL-5, in cynomolgus monkeys., J. Allergy Clin. Immunol. 108 (2001) 250–7. doi:10.1067/mai.2001.116576.

[95] T.T. Hansel, H. Kropshofer, T. Singer, J. a Mitchell, A.J.T. George, The safety and side effects of monoclonal antibodies., Nat. Rev. Drug Discov. 9 (2010) 325–38. doi:10.1038/nrd3003.

[96] F. Depreter, G. Pilcer, K. Amighi, Inhaled proteins: challenges and perspectives., Int. J. Pharm. 447 (2013) 251–80. doi:10.1016/j.ijpharm.2013.02.031.

[97] F. Andrade, D. Rafael, M. Videira, D. Ferreira, A. Sosnik, B. Sarmento, Nanotechnology and pulmonary delivery to overcome resistance in infectious diseases., Adv. Drug Deliv. Rev. 65 (2013) 1816–27. doi:10.1016/j.addr.2013.07.020.

[98] G. Scheuch, M.J. Kohlhaeufl, P. Brand, R. Siekmeier, Clinical perspectives on pulmonary systemic and macromolecular delivery., Adv. Drug Deliv. Rev. 58 (2006) 996–1008. doi:10.1016/j.addr.2006.07.009.

[99] T.C. Carvalho, J.I. Peters, R.O. Williams, Influence of particle size on regional lung deposition--what evidence is there?, Int. J. Pharm. 406 (2011) 1–10. doi:10.1016/j.ijpharm.2010.12.040.

[100] H. Heijerman, E. Westerman, S. Conway, D. Touw, G. Döring, consensus working group, Inhaled medication and inhalation devices for lung disease in patients with cystic fibrosis: A European consensus., J. Cyst. Fibros. 8 (2009) 295–315. doi:10.1016/j.jcf.2009.04.005.

[101] Q.T. Zhou, S.S.Y. Leung, P. Tang, T. Parumasivam, Z.H. Loh, H.-K. Chan, Inhaled formulations and pulmonary drug delivery systems for respiratory infections., Adv. Drug Deliv. Rev. 85 (2015) 83–99. doi:10.1016/j.addr.2014.10.022.

[102] Z. Drulis-Kawa, A. Dorotkiewicz-Jach, Liposomes as delivery systems for antibiotics., Int. J. Pharm. 387 (2010) 187–98. doi:10.1016/j.ijpharm.2009.11.033.

[103] C.O. Onyeji, C.H. Nightingale, M.N. Marangos, Enhanced killing of methicillin-resistant Staphylococcus aureus in human macrophages by liposome-entrapped vancomycin and teicoplanin., Infection. 22 (1994) 338–42. doi:10.1007/BF01715542.

[104] A. Pumerantz, K. Muppidi, S. Agnihotri, C. Guerra, V. Venketaraman, J. Wang, et al., Preparation of liposomal vancomycin and intracellular killing of meticillin-resistant Staphylococcus aureus (MRSA)., Int. J. Antimicrob. Agents. 37 (2011) 140–4. doi:10.1016/j.ijantimicag.2010.10.011.

[105] K. Muppidi, J. Wang, G. Betageri, A.S. Pumerantz, PEGylated liposome encapsulation increases the lung tissue concentration of vancomycin., Antimicrob. Agents Chemother. 55 (2011) 4537–42. doi:10.1128/AAC.00713-11.

[106] M.J. de Jesús Valle, J.G. González, F.G. López, A.S. Navarro, Pulmonary disposition of vancomycin nebulized as lipid vesicles in rats., J. Antibiot. (Tokyo). 66 (2013) 447–51. doi:10.1038/ja.2013.32.

[107] J.S. Suk, S.K. Lai, Y.-Y. Wang, L.M. Ensign, P.L. Zeitlin, M.P. Boyle, et al., The penetration of fresh undiluted sputum expectorated by cystic fibrosis patients by non-adhesive polymer nanoparticles., Biomaterials. 30 (2009) 2591–7. doi:10.1016/j.biomaterials.2008.12.076.

[108] W.S. Cheow, K. Hadinoto, Green preparation of antibiotic nanoparticle complex as potential anti-biofilm therapeutics via self-assembly amphiphile-polyelectrolyte complexation with dextran sulfate., Colloids Surf. B. Biointerfaces. 92 (2012) 55–63. doi:10.1016/j.colsurfb.2011.11.024.

[109] M. Kutscher, W.S. Cheow, V. Werner, U. Lorenz, K. Ohlsen, L. Meinel, et al., Influence of salt type and ionic strength on self-assembly of dextran sulfate-ciprofloxacin nanoplexes., Int. J. Pharm. 486 (2015) 21–9. doi:10.1016/j.ijpharm.2015.03.022.

[110] W.S. Cheow, K. Hadinoto, Self-assembled amorphous drug-polyelectrolyte nanoparticle complex with enhanced dissolution rate and saturation solubility., J. Colloid Interface Sci. 367 (2012) 518–26. doi:10.1016/j.jcis.2011.10.011.

[111] W.S. Cheow, K. Hadinoto, Green amorphous nanoplex as a new supersaturating drug delivery system., Langmuir. 28 (2012) 6265–75. doi:10.1021/la204782x.

[112] F. Tewes, J. Brillault, W. Couet, J.-C. Olivier, Formulation of rifampicin-cyclodextrin complexes for lung nebulization., J. Control. Release. 129 (2008) 93–9. doi:10.1016/j.jconrel.2008.04.007.

[113] Z. Ahmad, S. Sharma, G.K. Khuller, Inhalable alginate nanoparticles as antitubercular drug carriers against experimental tuberculosis., Int. J. Antimicrob. Agents. 26 (2005) 298–303. doi:10.1016/j.ijantimicag.2005.07.012.

[114] S. Frokjaer, D.E. Otzen, Protein drug stability: a formulation challenge., Nat. Rev. Drug Discov. 4 (2005) 298–306. doi:10.1038/nrd1695.

[115] E.Y. Chi, S. Krishnan, T.W. Randolph, J.F. Carpenter, Physical stability of proteins in aqueous solution: mechanism and driving forces in nonnative protein aggregation., Pharm. Res. 20 (2003) 1325–36. doi:10.1023/A:1025771421906.

[116] S. Hertel, T. Pohl, W. Friess, G. Winter, That's cool! – Nebulization of thermolabile proteins with a cooled vibrating mesh nebulizer., Eur. J. Pharm. Biopharm. 87 (2014) 357–365. doi:10.1016/j.ejpb.2014.03.001.

[117] S.P. Hertel, G. Winter, W. Friess, Protein stability in pulmonary drug delivery via nebulization., Adv. Drug Deliv. Rev. 93 (2015) 79–94. doi:10.1016/j.addr.2014.10.003.

[118] V. Filipe, A. Hawe, H. Schellenkens, W. Jiskoot, Aggregation and Immunogenicity of Therapeutic Proteins, in: W. Wang, C.J. Roberts (Eds.), Aggregation of Therapeutic Proteins, John Wiley & Sons, Inc., Hoboken, NJ, USA, 2010. doi:10.1002/9780470769829.

[119] A.S. Rosenberg, Effects of protein aggregates: an immunologic perspective., AAPS J. 8 (2006) E501–7. doi:10.1208/aapsj080359.

[120] V. Filipe, W. Jiskoot, A.H. Basmeleh, A. Halim, H. Schellekens, V. Brinks, Immunogenicity of different stressed IgG monoclonal antibody formulations in immune tolerant transgenic mice., MAbs. 4 (2012) 740–52. doi:10.4161/mabs.22066.

[121] S. Hertel, T. Pohl, W. Friess, G. Winter, Prediction of protein degradation during vibrating mesh nebulization via a high throughput screening method., Eur. J. Pharm. Biopharm. 87 (2014) 386–394. doi:10.1016/j.ejpb.2014.03.020.

[122] Y.Y. Albasarah, S. Somavarapu, K.M.G. Taylor, Stabilizing protein formulations during air-jet nebulization., Int. J. Pharm. 402 (2010) 140–5. doi:10.1016/j.ijpharm.2010.09.042.

[123] H. Steckel, F. Eskandar, K. Witthohn, Effect of cryoprotectants on the stability and aerosol performance of nebulized aviscumine, a 57-kDa protein., Eur. J. Pharm. Biopharm. 56 (2003) 11–21. doi:10.1016/S0939-6411(03)00044-4.

[124] H. Steckel, F. Eskandar, K. Witthohn, The effect of formulation variables on the stability of nebulized aviscumine., Int. J. Pharm. 257 (2003) 181–94. doi:10.1016/S0378-5173(03)00126-1.

[125] R.W. Niven, A.Y. Ip, S.D. Mittelman, C. Farrar, T. Arakawa, S.J. Prestrelski, Protein nebulization: I. Stability of lactate dehydrogenase and recombinant granulocyte-colony stimulating factor to air-jet nebulization., Int. J. Pharm. 109 (1994) 17–26. doi:10.1016/0378-5173(94)90117-1.

[126] R.W. Niven, Protein nebulization II. Stabilization of G-CSF to air-jet nebulization and the role of protectants., Int. J. Pharm. 127 (1996) 191–201. doi:10.1016/0378-5173(95)04209-1.

[127] J.S. Bee, T.W. Randolph, J.F. Carpenter, S.M. Bishop, M.N. Dimitrova, Effects of surfaces and leachables on the stability of biopharmaceuticals., J. Pharm. Sci. 100 (2011) 4158–70. doi:10.1002/jps.22597.

[128] M.C. Manning, D.K. Chou, B.M. Murphy, R.W. Payne, D.S. Katayama, Stability of protein pharmaceuticals: an update., Pharm. Res. 27 (2010) 544–75. doi:10.1007/s11095-009-0045-6.

[129] W. Wang, Instability, stabilization, and formulation of liquid protein pharmaceuticals., Int. J. Pharm. 185 (1999) 129–88. doi:10.1016/S0378-5173(99)00152-0.

[130] C.Y. Dombu, D. Betbeder, Airway delivery of peptides and proteins using nanoparticles., Biomaterials. 34 (2013) 516–25. doi:10.1016/j.biomaterials.2012.08.070.

[131] C. Cortez-Jugo, A. Qi, A. Rajapaksa, J.R. Friend, L.Y. Yeo, Pulmonary monoclonal antibody delivery via a portable microfluidic nebulization platform., Biomicrofluidics. 9 (2015) 052603. doi:10.1063/1.4917181.

[132] S.J. Koussoroplis, G. Paulissen, D. Tyteca, H. Goldansaz, J. Todoroff, C. Barilly, et al., PEGylation of antibody fragments greatly increases their local residence time following delivery to the respiratory tract, J. Control. Release. 187 (2014) 91–100. doi:10.1016/j.jconrel.2014.05.021.

[133] S. Cryan, Carrier-based strategies for targeting protein and peptide drugs to the lungs., AAPS J. 7 (2005) E20–41. doi:10.1208/aapsj070104.

[134] J. Behr, G. Zimmermann, R. Baumgartner, H. Leuchte, C. Neurohr, P. Brand, et al., Lung deposition of a liposomal cyclosporine A inhalation solution in patients after lung transplantation., J. Aerosol Med. Pulm. Drug Deliv. 22 (2009) 121–30. doi:10.1089/jamp.2008.0714.

[135] F. Hajos, B. Stark, S. Hensler, R. Prassl, W. Mosgoeller, Inhalable liposomal formulation for vasoactive intestinal peptide., Int. J. Pharm. 357 (2008) 286–94. doi:10.1016/j.ijpharm.2008.01.046.

CHAPTER II

INFLUENCE OF SALT TYPE AND IONIC STRENGTH ON SELF-ASSEMBLY OF DEXTRAN SULFATE-CIPROFLOXACIN NANOPLEXES

This chapter was published in the International Journal of Pharmaceutics and appears in this thesis with permission from Elsevier:

M. Kutscher, W.S. Cheow, V. Werner, U. Lorenz, K. Ohlsen, L. Meinel, K. Hadinoto, O. Germershaus, Influence of salt type and ionic strength on self-assembly of dextran sulfate-ciprofloxacin nanoplexes., Int. J. Pharm. 486 (2015) 21–29. doi:10.1016/j.ijpharm.2015.03.022.

Abstract

We evaluated an analytical setup to identify optimal preparation conditions for nanoplex formation of small molecule drugs and polyelectrolytes using Ciprofloxacin (CIP) and dextran sulfate (DS) as model compounds. The suitability of isothermal titration calorimetry (ITC) as a screening tool for rational formulation optimization was assessed. Besides ITC, static and dynamic light scattering, zeta potential measurements, and scanning electron microscopy were applied to analyze the influence of different salt types and ionic strengths on CIP/DS nanoplex formation. The addition of low amounts of salt, especially 0.1 M NaCl, improved the formation of CIP/DS nanoplexes. The presence of low amounts of salt led to smaller and more numerous particles of higher uniformity but had no influence on the release of CIP from nanoplexes. Furthermore, the molar range, within which efficient complexation was achieved, was broader in the presence of 0.1 M NaCl than in the absence of salt with overall comparable complexation efficiency. Importantly, binding affinity correlated with particle shape and morphology, potentially enabling optimization of critical quality attributes based on ITC data. Altogether, ITC along with supplemental methods is a versatile screening tool for the evaluation of nanoplex formulation conditions regarding mixing ratio, salt type, and ionic strength.

1. Introduction

Ciprofloxacin (CIP) is one of the few potent antibiotics against *Pseudomonas aeruginosa*, a bacterial pathogen common in severe respiratory diseases like chronic obstructive pulmonary disease (COPD) [1–3]. A major obstacle to efficient treatment of *P. aeruginosa* infections is its ability to form biofilms in which bacteria are protected from defensive attacks by the immune system as well as xenobiotics. Moreover, biofilm colonies are entrapped in the pulmonal mucus layer, which most free drugs cannot penetrate readily due to interactions with anionic and hydrophobic mucus components [4,5]. Another major drawback in the treatment of lung infections is ciprofloxacin's poor solubility in aqueous media at physiological conditions [6,7]. Hence, the main therapeutic challenge is to reach sufficient CIP concentration at the site of action.

An approach to overcome these problems is encapsulation of the antibiotic into nanoparticles enabling higher local concentrations of CIP and circumventing solubility issues [8]. Further advantages of this drug delivery system could be improved mucus penetration to the site of action as well as slower and less effective clearance from the lung by phagocytosis through alveolar macrophages due to its small size [4,9]. Enhanced delivery to the site of action increases the therapeutic efficacy and is even considered to reduce occurrence of bacterial resistance against antibiotics [4,10]. However, common nano-carriers often suffer from low drug loading, limiting their use for pulmonary delivery of antibiotics [11]. In contrast, nanoparticle complexes (nanoplexes) prepared by self-assembly of a drug and an oppositely charged polyelectrolyte allow higher drug loading [11,12]. Self-assembly of complexes has already been used in diverse pharmaceutical applications such as cancer therapy and to improve bioavailability of drugs with adverse biopharmaceutical properties [12–14]. Polymer-drug complexes may also increase the solubility of poorly water-soluble drugs and stabilize the drug in the amorphous state [6,15,16]. Since CIP is well soluble at a pH of about 6 as a cation, it can be used herein for complex formation [6,7]. Dextran sulfate (DS), a natural biodegradable polyanion, readily forms complexes by ionic interactions when mixed with CIP at low pH [17]. Additionally, hydrophobic interactions of the drug molecules presumably contribute to nanoplex formation and stabilization [6]. The presence of salt is thought to be a key parameter [18], as it may increase flexibility of the polyanion DS through reduction of intramolecular repulsion, in turn increasing complexation efficiency [6,19]. Consequently, the type of cation, its valency, and ionic strength were varied during formulation optimization in this study to analyze their influence on nanoplex formation.

The overall aim of this study was the evaluation of an analytical setup to identify optimal preparation conditions for nanoplexes using CIP and DS as model compounds. Isothermal titration calorimetry (ITC) is a convenient method for the investigation of interactions during complex formation [20,21] and may serve as a tool for rational formulation optimization [22]. Furthermore, complex stability in the presence of salt [21] and the origin of polyelectrolyte interactions may be analyzed by ITC [23]. However, if calorimetric methods are applied to complex systems often complicated thermograms are obtained, which are difficult to interpret in isolation. Therefore, ITC data was supplemented by additional analytical methods such as static and dynamic light scattering (SLS and DLS), zeta potential measurements, and scanning electron microscopy (SEM) helping to clarify the cause and the way of interaction of molecules [24,25].

2. Materials and methods

2.1. Materials

Sodium dextran sulfate (DS) with an average molecular weight of 5 kDa was purchased from Wako Pure Chemical Industries Ltd. (Osaka, Japan). Ciprofloxacin (CIP) (≥ 98% (HPLC)) was obtained from Sigma-Aldrich Chemie GmbH (Steinheim, Germany). All other chemicals were at least of analytical grade. Purified water was used in all experiments (Milli-Q Synthesis Ultrapure Water Purification System, EMD Millipore Corporation, Billerica, USA).

2.2. Preparation of polyelectrolyte-drug nanoplexes

The nanoplexes were prepared as described before [6] with slight modifications. CIP was dissolved in a 2% (V/V) aqueous acetic acid solution and subsequently diluted tenfold with water to a final concentration of 18.29 µM. The CIP solution was added to an aqueous DS solution of 0.1 µM at varying molar ratios of CIP to DS in absence or presence of salt. To identify optimal conditions for complex formation, the salt type and ionic strength were varied. Hence, nanoplexes were prepared in absence (0 M) and presence of NaCl, KCl, or $CaCl_2$ each at an ionic strength of 0.1, 0.3, and 1 M. Immediately upon addition of CIP to DS, the solution turned cloudy and/or formed white precipitates depending on the amount of CIP used. Therefore, the prepared nanoplex suspensions were centrifuged at 13 000 *g* and the pellet was resuspended in water three times to remove non-complexed CIP, DS, and salt.

2.3. Characterization of polyelectrolyte-drug nanoplexes

2.3.1. Determination of CIP complexation efficiency (CE)

The optimal CIP/DS molar ratio for nanoplex preparation at the different ionic strengths was evaluated with regards to CIP complexation efficiency (CE) by addition of increasing volumes of CIP (18.29 µM) to 2 ml of aqueous DS solution (0.1 µM) in presence of NaCl at 0, 0.1, 0.3, and 1 M ionic strength. CE was also determined in the presence of different salt types and ionic strengths. CE was calculated based on the amount of non-complexed CIP after preparation of the CIP/DS nanoplexes and the amount of CIP initially added. The amount of non-complexed CIP was determined after the first centrifugation step by UV absorption measurement of the supernatant at λ = 277 nm (Genesys 10s UV-Vis spectrophotometer, Thermo Fisher Scientific Corporation, Waltham, USA). The amount of CIP complexed within the nanoplexes represented the absolute CE whereas the relative CE was calculated by

dividing the amount of complexed CIP by the total amount of CIP initially used for preparation.

2.3.2. Static light scattering (SLS)

The time-averaged intensity of scattered light was used to analyze the extent of nanoplex formation depending on CIP/DS mixing ratio, salt type, and ionic strength. Dependence of scattering intensity on mixing ratio during the actual nanoplex formation process was analyzed in 0.1 M NaCl prior to centrifugation. In addition, SLS intensity was determined at a fixed CIP/DS molar ratio of 31 depending on ionic strength and salt type after washing of the nanoplexes. Light scattering was measured using a LS 50B luminescence spectrometer (Perkin Elmer, Waltham, USA) at a fixed angle of 90° for 60 s using a data interval of 1.2 s, an integration time of 0.1 s at λ = 638 nm and slit width of 2.5 nm.

2.3.3. Dynamic light scattering (DLS)

The particle size distributions of the CIP/DS nanoplexes were measured using a Delsa Nano HC Particle Analyzer (Beckman Coulter, Inc., Fullerton, CA, USA) at 25°C. To prevent disturbance from larger agglomerates, the samples were left to settle down overnight before analyzing the supernatant. Each run consisted of three individual measurements comprising 70 accumulations each, and size distribution by intensity, average hydrodynamic diameter, and polydispersity index (PdI) were determined.

2.3.4. Electrophoretic light scattering (ELS)

Zeta potential measurements were performed by ELS using a Delsa Nano HC Particle Analyzer (Beckman Coulter, Inc., Fullerton, CA, USA) using laser light at λ = 658 nm and a scattering angle of 15° at a temperature of 25°C. Each measurement consisted of 10 accumulations and 3 repetitions. The applied voltage was set to 60 V. System performance was checked using polystyrene latex particles (Otsuka Electronics Co., Ltd., Osaka, Japan, P/N A50695).

2.3.5. Scanning electron microscopy (SEM)

For SEM, nanoplex suspensions prepared using different salt types and ionic strengths were lyophilized (primary drying: -10°C, 0.16 mbar; secondary drying: 5°C and later 30°C, 0.06 mbar) in a laboratory freeze-dryer alpha 1-4 (Martin Christ GmbH, Osterode, Germany) without addition of additional excipients. Subsequently, samples were sputter-coated with

gold-palladium (SSCD 005, Bal-Tec AG, Liechtenstein) and examined using a JSM-7500F field emission scanning electron microscope (Jeol, Tokyo, Japan) at an acceleration voltage of 5 kV by secondary electron imaging (SEI). Obtained nanoplex images were analyzed using ImageJ 1.44p (National Institutes of Health, USA). The size of 20-30 particles per image was manually determined and mean size as well as standard deviations were calculated for each sample.

2.4. Isothermal titration calorimetry (ITC)

ITC was performed using a MicroCal iTC200 (GE Healthcare, Buckinghamshire, GB). ITC monitors the electrical power (µcal/sec) required to maintain a constant temperature in a sample cell filled with the substrate (DS) when the titrant (CIP) is added gradually over time. To analyze the influence of salt during nanoplex formation, DS solution was supplemented with NaCl, KCl, or $CaCl_2$ at an ionic strength of 0, 0.1, 0.3, and 1 M, respectively. The cell was filled with 200 µl 0.1 mM DS or DS/salt solution (polyelectrolyte) and 38.2 µl of 18.29 mM CIP in 0.2% (V/V) aqueous acetic acid (counterion) were injected into the cell in steps of 2 µl, each lasting 4 s with a spacing of 150 s between injections at 25°C under stirring at 400 rpm. The first injection consisted of 0.2 µl, lasted 0.4 s and was omitted to minimize the impact of equilibration artifacts, according to the manufacturer's recommendations. Positive peaks indicated endothermic reactions and vice versa. All titrations were corrected by a blank titration, performed by titrating CIP solution into salt solutions at the respective ionic strengths without DS.

2.5. Release study

Nanoplex suspension was added into a quartz cuvette containing 2 mL PBS (pH 7.4, ionic strength 150 mM) to give a suspension concentration of 0.1 mg/mL. The concentration of free CIP was obtained by continuously monitoring absorbance at λ = 324 nm and was calculated using a standard curve (UV-mini 1240, Shimadzu, Kyoto, Japan). The contribution from suspension turbidity to absorbance measurements was corrected by determining absorbance at λ = 600 nm and deducting the absorbance value from the absorbance at λ = 324 nm. The development of free CIP concentration is reported for up to 15 minutes of incubation, beyond this time point no significant change of concentration was observed for up to 24 hours after start of the experiment.

2.6. Statistical analysis

Data were analyzed for statistically significant differences in size, polydispersity indices, and zeta potential between the different salt types or between varying ionic strength, respectively, by one-way analysis of variance (ANOVA) using multiple comparisons versus control by the Holm−Sidak method for comparison of multiple groups. The Brown-Forsyth method was used to test for equal variances. Overall significance level of 0.05 was applied (OriginPro 9, OriginLab Corporation, Northampton, MA, USA and Prism 6, GraphPad Software, La Jolla, CA, USA).

3. Results

3.1. Evaluation of optimal CIP/DS molar ratio for nanoplex preparation

The first step towards optimized preparation conditions of drug-polyelectrolyte nanoplexes was the identification of the optimal molar ratio of CIP to DS at which maximum drug loading could be achieved at various ionic strengths. CE was evaluated depending on molar ratio of CIP to DS and ionic strength of NaCl in terms of both, relative CE in relation to CIP amount used to prepare the nanoplexes (amount of CIP complexed divided by total amount of CIP used for preparation) and absolute CE of CIP (amount of CIP in mg complexed within the nanoplexes) (**Figure 1**).

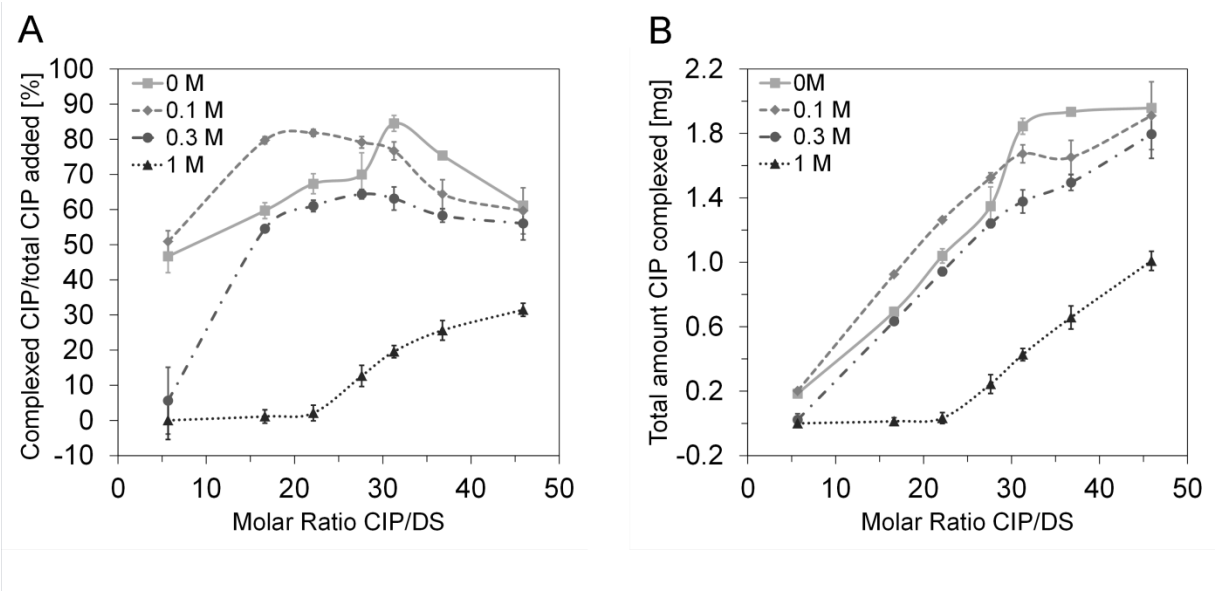

Figure 1: Relative [A] and absolute [B] CIP complexation efficiency (CE) at increasing CIP/DS molar ratios and at different ionic strength from NaCl as assessed photometrically (n=3, ± S.D.).

Overall, maximum relative CE of 84.5% ± 2.3% was achieved at a molar ratio of approximately 31 in the absence of salt whereas in the presence of 0.1 M NaCl the maximal CE was shifted to lower molar ratios, reaching a plateau at about 80% relative CE at a molar ratio of 17 with a drop of CE above a molar ratio of 30 (**Figure 1A**). These results corroborate earlier findings for the relative CE at 0.1 M ionic strength [1]. Regarding absolute CE (**Figure 1B**), the incorporated mass of CIP is increasing with the mass of CIP introduced during nanoplex formation, reaching saturation at approximately 1.9 mg encapsulated CIP in the absence of salt at a molar ratio of 31.

Analysis of both, relative and absolute CE revealed that at molar ratios up to approximately 29 presence of NaCl at a low ionic strength of 0.1 M enhanced the quantity of incorporated CIP compared to nanoplexes prepared in the absence of salt. However, at higher ionic strength of

0.3 and 1 M complexation efficiency was decreased. As a compromise between high relative and absolute CE at various ionic strengths, a molar ratio of 31 was selected for further experiments.

3.2. Influence of different salts on nanoplex formation at optimal CIP/DS molar ratio

3.2.1. Analysis of CIP complexation efficiency and extent of nanoplex formation

After definition of the optimal molar ratio for preparation of drug–polyelectrolyte complexes, the influence of varying salt types at increasing ionic strengths on nanoplex formation was examined in terms of relative CE and extent of particle formation determined by static light scattering, at a fixed molar ratio of 31. While increasing ionic strength resulted in decreasing CE **(Figure 2A)** for all salt types, the magnitude of nanoplex formation as detected by static light scattering intensity was significantly increased at 0.1 M NaCl compared to the condition without salt (**Figure 2B**). Among the several salt types, the neutral salt NaCl and kosmotropic $CaCl_2$ showed only slightly differing results. In contrast, both, CE and extent of particle formation were significantly reduced in the presence of the chaotropic salt KCl compared to NaCl and $CaCl_2$ at ionic strength above 0.1 M. At an ionic strength of 1 M KCl nanoplex formation was completely suppressed.

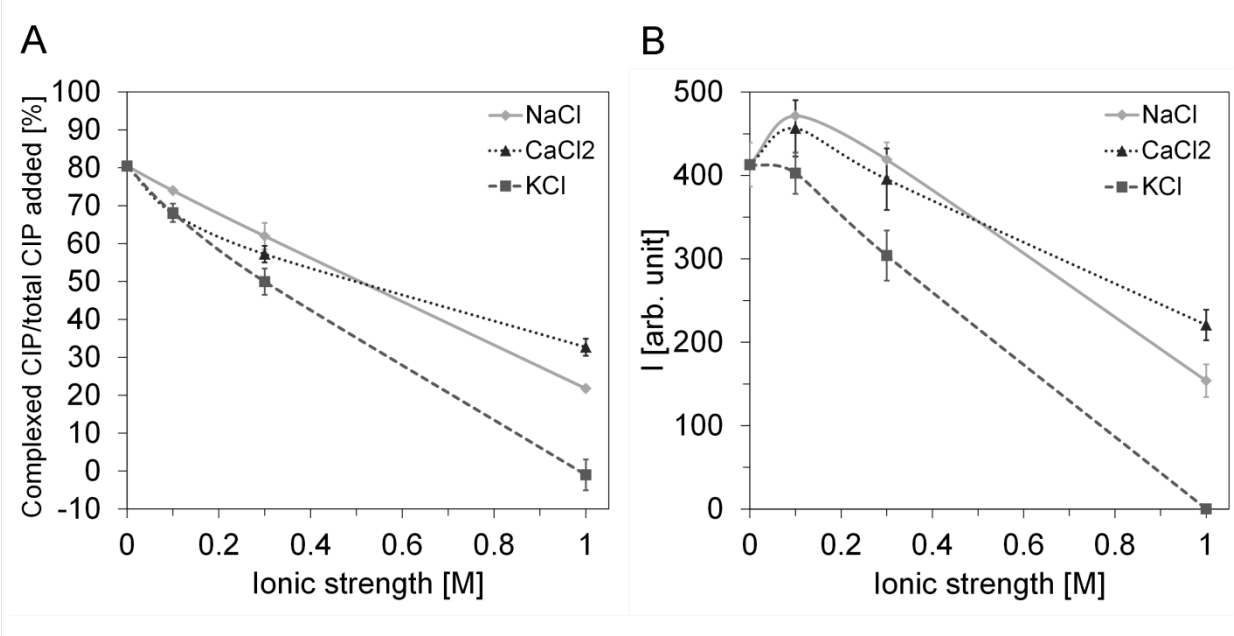

Figure 2: Effect of salt type and ionic strength on relative complexation efficiency [A] and static light scattering intensity [B] of CIP/DS nanoplexes prepared at a CIP/DS molar ratio of 31 (n=3, ± S.D.).

3.2.2. Determination of nanoplex size and surface charge

In the absence of salt, addition of CIP to DS resulted in drug-polyelectrolyte particles with hydrodynamic diameters of 629 ± 130 nm (**Figure 3A**). The addition of NaCl and KCl at low ionic strength of 0.1 and 0.3 M during nanoplex preparation resulted in a significant particle size reduction compared to particles in the absence of salt. In addition, particle size distributions appeared to be more uniform at higher ionic strength based on both reduced standard deviations as well as lower PdIs (**Figure 3A**). The smallest and most uniform particles were obtained using 0.1 M (403 ± 27 nm) and 0.3 M NaCl (383 ± 19 nm). Despite the fact that nanoplex formation was abolished at 1 M KCl (see **Figure 2**), addition of KCl had a similar impact like NaCl on the nanoplex size at lower ionic strength (420 ± 44 nm at 0.1 M and 458 ± 36 nm at 0.3 M, respectively). In contrast, hydrodynamic diameters of approximately 550 nm were observed in the presence of 0.1 and 0.3 M $CaCl_2$ being similar to particle size at 0 M ionic strength. All samples exhibited polydispersity indices in the range of 0.2-0.25 indicating fairly monodisperse size distribution of the samples (**Figure 3A**).

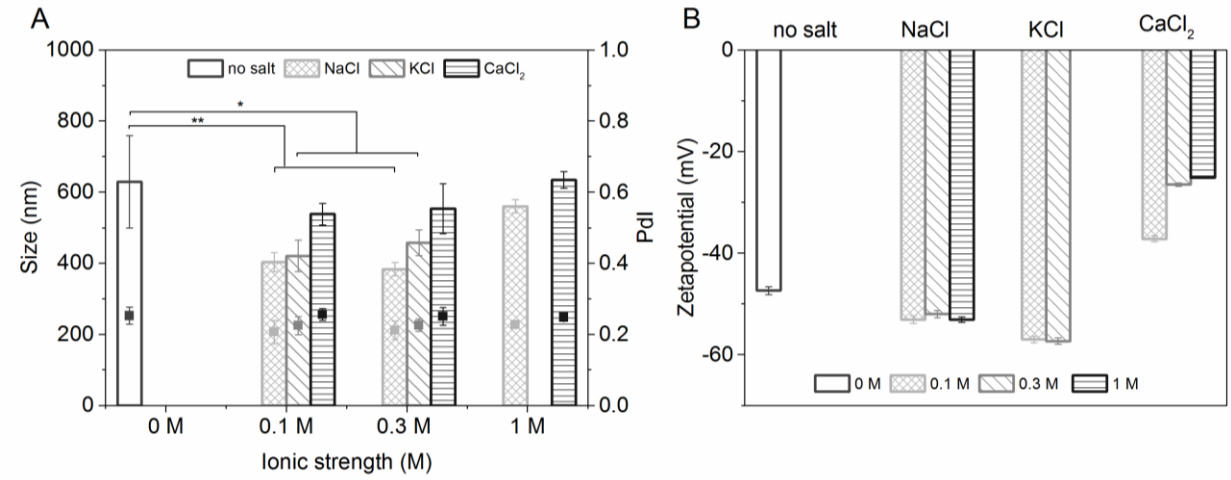

Figure 3: Effect of salt type and ionic strength on hydrodynamic diameter (bars, left y-axis) as well as polydispersity index (PdI, squares, right y-axis) [A] and zeta potential [B] of CIP/DS nanoplexes prepared at molar ratio of 31 (asterisks indicate significance level: * $p < 0.05$; ** $p < 0.01$).

All nanoplexes had a negative surface charge (**Figure 3B**). In salt-free conditions, drug-polyelectrolyte complexes exhibited a surface charge of - 47 mV whereas significantly higher surface charge of - 50 to - 55 mV was observed in the presence of NaCl and KCl. In contrast, particles prepared in the presence of $CaCl_2$ showed significantly lower surface charge between approximately - 25 and - 35 mV compared to the other salt types and salt-free conditions.

3.2.3. Characterization of morphology by SEM

CIP/DS nanoplexes exhibited an almost spherical shape and smooth surface in absence of salt and in the presence of 0.1 M NaCl (**Figure 4**). No significant differences in size were observed for the nanoplexes prepared without salt and with 0.1 M and 0.3 M NaCl or KCl, all having diameters of approximately 100 nm. An increase of particle size of nanoplexes was observed in presence of $CaCl_2$ with 118 ± 31 nm at 0.1 M and 121 ± 35 nm at 0.3 M ionic strength, the latter being significantly larger than diameters of nanoplexes prepared with NaCl, KCl, or in the absence of salt. In the presence of KCl, elliptical, plate-like, and curl-shaped particles where observed in addition to spherical particles. For all salt types the percentage of spherical particles appeared to decrease with increasing ionic strength and no spherical particles were observed at 1 M ionic strength. Overall, 0.1 M NaCl showed the most homogenous distribution with regards to particle shape and size.

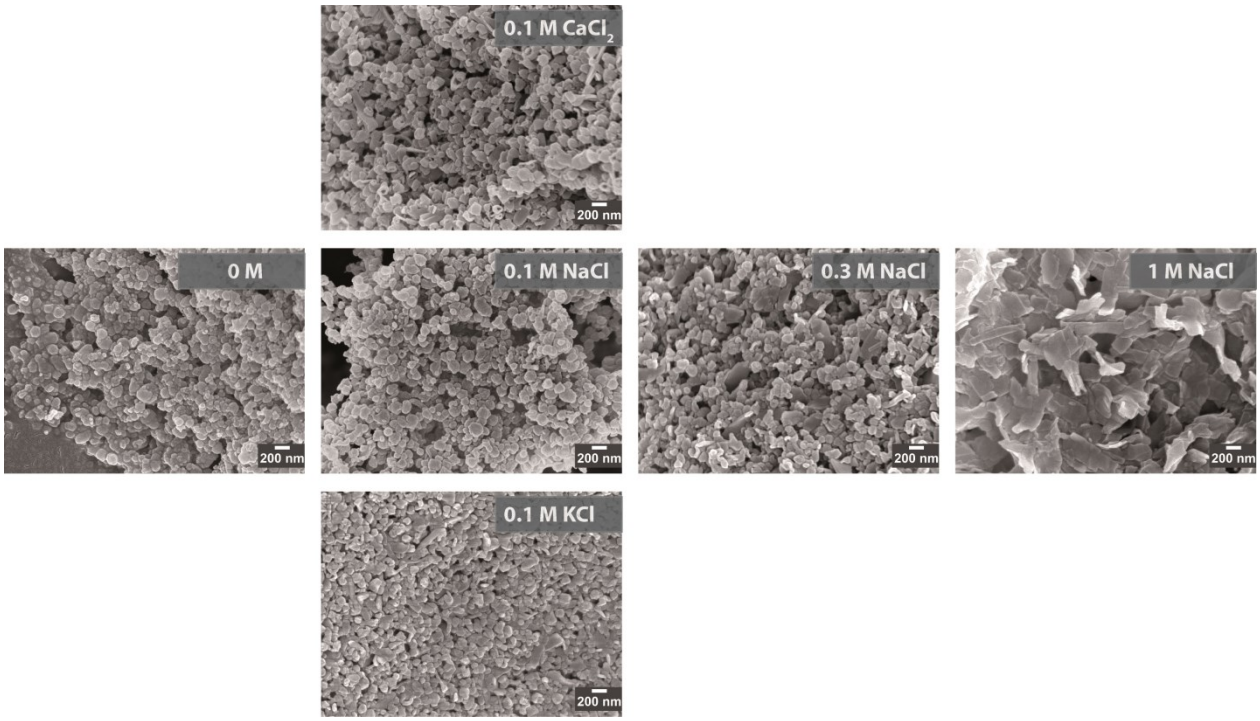

Figure 4: Scanning electron micrographs of CIP/DS nanoplexes shown as function of salt type (vertical) and ionic strength (horizontal). For clarity of presentation, only particles prepared in the presence of NaCl are shown at all ionic strengths whereas nanoplexes prepared with KCl and $CaCl_2$ were compared to NaCl at the ionic strength of 0.1 M.

3.3. Characterization of interactions of CIP and DS during nanoplex formation

The interactions of the oppositely charged drug and polyelectrolyte during formation of the complexes were analyzed using isothermal titration calorimetry (ITC). The electrical power (µcal/sec) required to maintain a constant temperature in a sample cell filled with the substrate (DS) was monitored when the titrant (CIP) was added gradually over time. (**Figure 5**, upper graphs) [20].

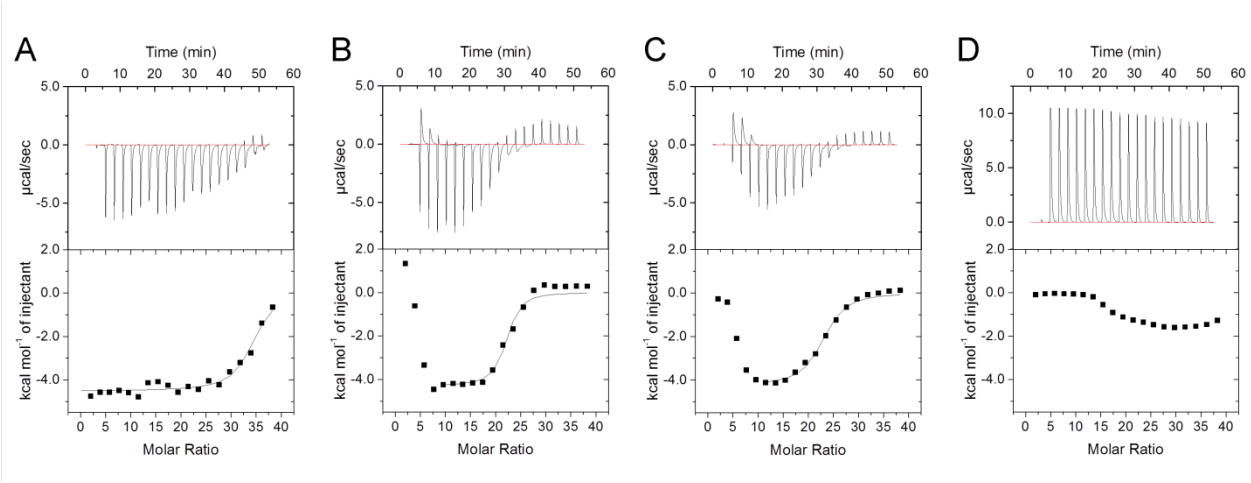

Figure 5: ITC titration data of the binding reaction of CIP to DS in presence of NaCl at 0 M (A), 0.1 M (B), 0.3 M (C), and 1 M (D) ionic strength. Raw data of electrical power is depicted in the upper graphs and lower graphs show the corresponding enthalpy curves. The heats evolving for the references (dilution of injectant in salt solutions) are corrected for in the enthalpy curves but not in the thermograms.

To obtain the corresponding thermodynamic parameters, several fitting models may be applied to the enthalpy curves. However, the suitability of the common models for the analysis of polyelectrolyte complexes is discussed intensively [20,23,26]. Priftis et al. as well as Feng et al. [20,23] point out that the one set of sites model cannot properly describe the complicated curves obtained during interaction of macromolecules. Therefore, fitting was solely used to compare the sigmoidal parts of the binding enthalpy curve. Hence, the calculated entropy and enthalpy values were omitted but the binding affinities and the stoichiometry obtained for nanoplexes prepared under varying conditions were compared, as these are calculated from the slope and the inflexion point of the sigmoidal curves. All enthalpy curves except the ITC data of 1 M ionic strength could be fitted using this model. In the case of 1 M ionic strength no sigmoidal curve shape was found, preventing application of the model (**Figure 5D**). The highest binding affinity constant *K* was achieved in presence of 0.1 M NaCl, with similar *K* values for 0 M and 0.1 M $CaCl_2$ and 0.1 M KCl (**Table 1**).

Regarding the stoichiometry, the analysis revealed CIP to DS mole ratios of approximately 20 to 27 in presence of salt and approximately 34 in the absence of salt **(Table 1)**.

Table 1: Binding affinity and stoichiometry of representative samples of the different formulations ordered by binding affinity value.

Formulation	**Binding affinity *K* [M^{-1}]**	**Stoichiometry *N***
0.1 M NaCl	$1.2 \cdot 10^5 \pm 5.6 \cdot 10^4$	21.4
0 M salt	$7.7 \cdot 10^4 \pm 2.1 \cdot 10^4$	33.6
0.1 M $CaCl_2$	$6.3 \cdot 10^4 \pm 1.9 \cdot 10^4$	20.4
0.1 M KCl	$6.0 \cdot 10^4 \pm 2.8 \cdot 10^4$	20.0
0.3 M NaCl	$4.7 \cdot 10^4 \pm 9.7 \cdot 10^3$	22.3
0.3 M $CaCl_2$	$3.1 \cdot 10^4 \pm 5.7 \cdot 10^3$	22.3
0.3 M KCl	$2.0 \cdot 10^4 \pm 3.4 \cdot 10^3$	26.9

ITC data of the binding reaction of CIP to DS at constant ionic strength but with variation of salt type resembled each other closely (**Figure 6**). Altogether, the extent of the enthalpy signal of the nanoplex formation was quite small in presence of all salt types and ionic strengths which is already known for polyelectrolyte complex formation [23].

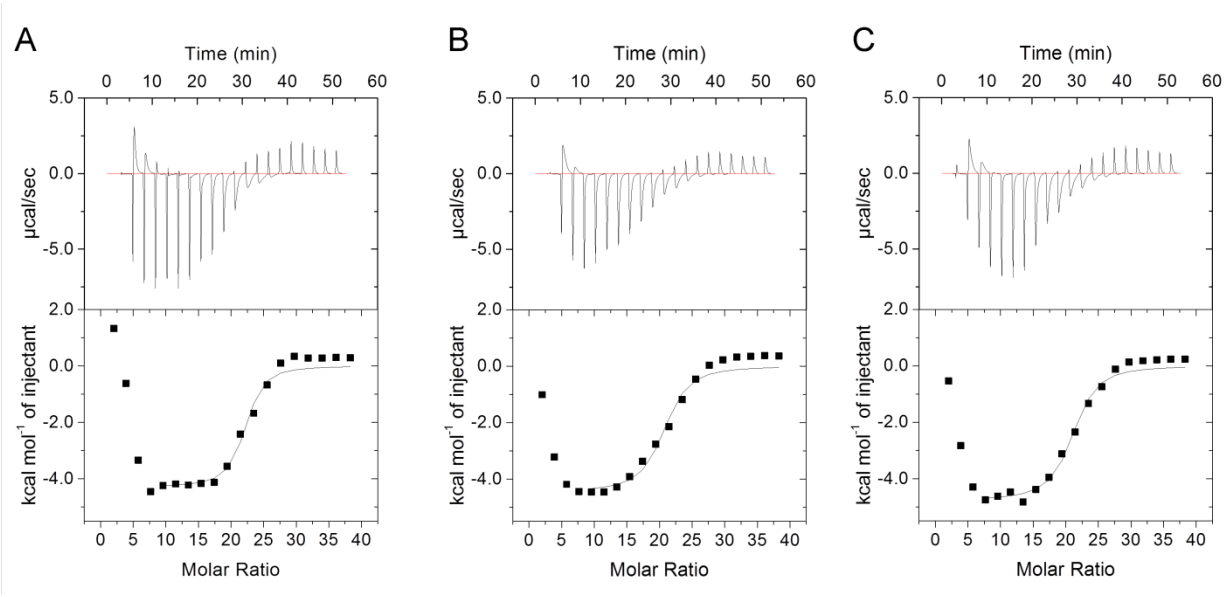

Figure 6: ITC titration data of the binding reaction of CIP to DS at 0.1 M ionic strength of NaCl (A), KCl (B), and $CaCl_2$ (C).

To characterize the nanoplex formation process in more detail, ITC data was supplemented with results from static light scattering as well as complexation efficiency for nanoplex preparation in presence of 0.1 M NaCl (**Figure 7**). Up to a molar ratio of approximately 2.5,

the reaction was found to be endothermic by ITC. Above a molar ratio of 2.5, the reaction became exothermic and heat signal decreased to a value of approximately -4 kcal/mol of injectant and stayed constant until molar ratio of 17. Afterwards, exothermicity of the reaction decreased until a plateau at an enthalpy value of 0 was reached at a ratio of 30 and above. Light scattering intensity steadily increased starting at a molar ratio above 2 and leveling off above molar ratio of approximately 35. The complexation efficiency in presence of 0.1 M NaCl increased up to a molar ratio of approximately 17, followed by a plateau up to a molar ratio of approximately 30, and decreased at higher molar ratios.

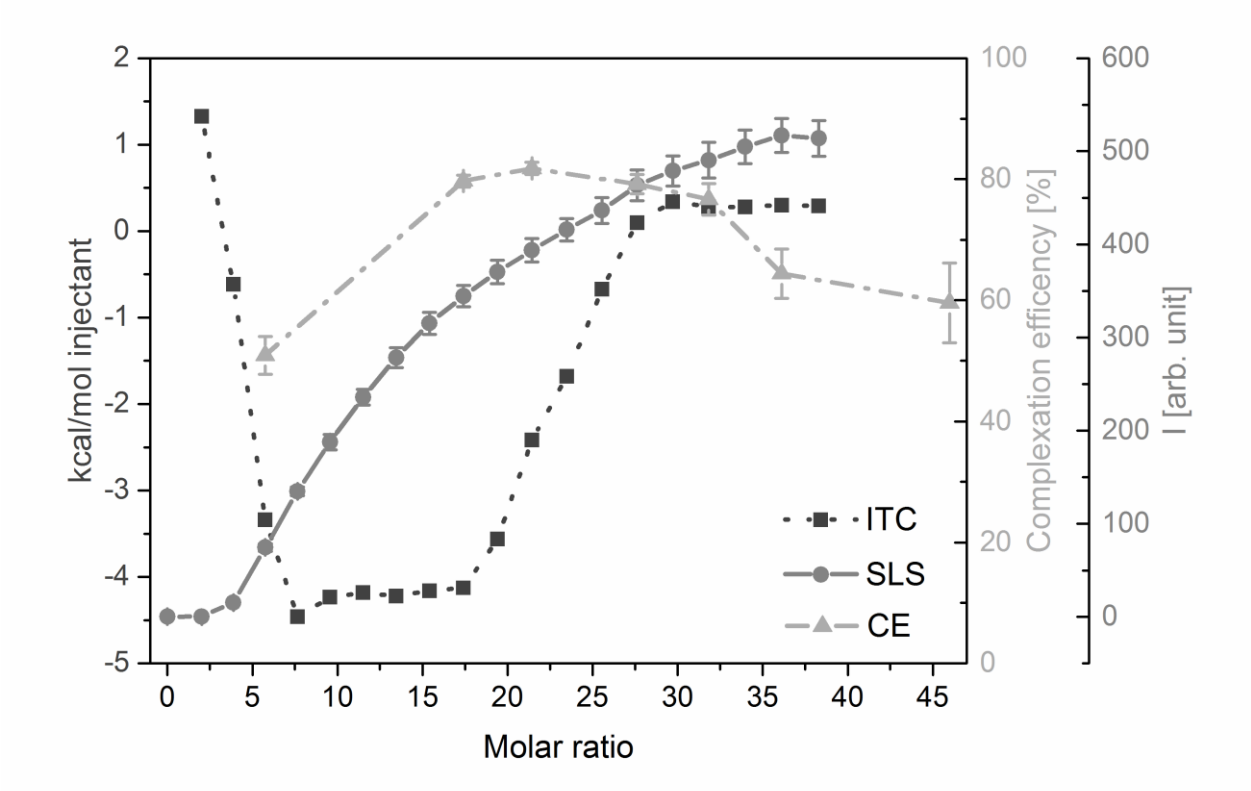

Figure 7: Light scattering intensity (circles) and heat of reaction (kcal/mol of injectant, squares) during titration of CIP into DS in 0.1 M NaCl at increasing molar ratios. Complexation efficiency (triangles) at respective molar ratios was determined after complex formation and washing of nanoplexes.

3.4. Release study

The nanoplexes prepared using the different salt types were compared with regard to their release behavior at ionic strength of 0.1 M as this ionic strength was regarded most relevant with regards to CIP release from nanoplexes prepared with and without salt.

After 15 min almost all CIP was released from all nanoplexes and only negligible additional release of approximately 2% was observed between 15 min and 24 h. In terms of absolute release of CIP, nanoplexes prepared in presence of NaCl and $CaCl_2$ showed a significantly higher release of 0.09 mg/ml and 0.08 mg/ml after 15 minutes, respectively than particles prepared without salt or in presence of KCl (0.05 mg/ml) (**Figure 8A**). In terms of relative release, no significant differences were observed between the different preparations (**Figure 8B**).

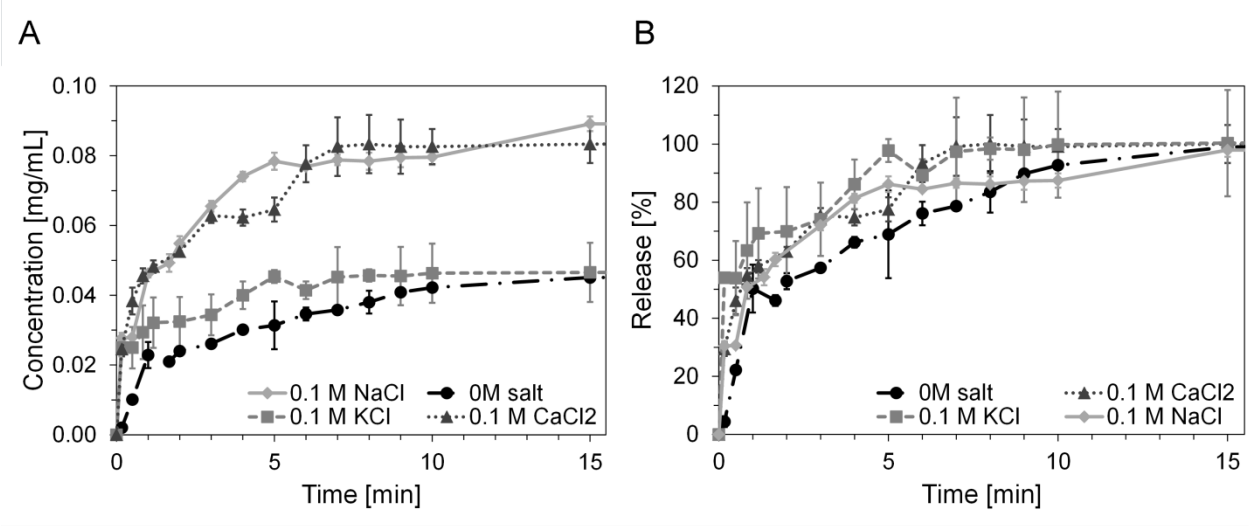

Figure 8: Release of CIP from nanoplexes over time in PBS buffer plotted as absolute concentration of CIP (A) and amount of released CIP relative to released amount of CIP after 24 h (B).

4. Discussion

Nanoplex formation between small molecule drugs and polyionic polymers is an emerging method to improve solubility and to overcome delivery challenges associated with numerous drugs. However, the effect of excipients such as salts of different type and varying ionic strength has not been studied in detail. Furthermore, formulation development of drug/polyelectrolyte complexes is complicated due to a lack of predictive screening methods allowing to assess the effect of excipients on nanoplex formation. Herein, CIP and DS were employed as model drug and polyanionic polymer, respectively, to study nanoplex formation using a panel of analytical methods. ITC enthalograms obtained for the titration of CIP into DS were correlated with static light scattering intensity and complexation efficiency and allowed interpretation of the process with regards to events leading to and affecting particle formation. Interaction of negatively charged polyelectrolyte and positively charged drug was reflected in a steep increase of the exothermic signal above a molar ratio of 2.5 accompanied by increasing light scattering intensity at an ionic strength of 0.1 M NaCl pointing to colloidal complex formation (**Figure 7**) [27]. The subsequent plateau from molar ratio 8 to 17 at negative enthalpy (exothermic reaction) as well as the concurrent further increase of light scattering intensity indicated further progress of the complexation reaction with binding of additional CIP to DS [22,27]. From molar ratio 17 onwards, the exothermic signal decreased and finally, at a molar ratio of 30, resulted in a plateau at enthalpy values of approximately 0 suggesting a saturation of binding sites up to an equilibrium state where the addition of CIP did not result in interaction with DS. However, the light scattering intensity increased above a molar ratio of 30 indicating aggregation of the primary nanoplexes to form precipitates, which were visually observed when removing the sample after the measurement. The onset of the saturation of the DS binding sites at a molar ratio of about 17 as observed by ITC correlated with the start of the plateau of maximum complexation efficiency in presence of 0.1 M NaCl (**Figure 7**). Above this molar ratio not all added CIP could bind to DS resulting in decreasing CE. In summary, by combining ITC, SLS, and CE determination it was shown that addition of CIP to DS in presence of 0.1 M NaCl resulted in nanoplex formation above a molar ratio of 2.5 and up to a molar ratio of approximately 30, whereas further addition of CIP resulted in aggregation and precipitation. However, the beginning of aggregation could not be determined exactly and most likely paralleled complex formation.

ITC, CE, and SLS data obtained at 0.1 M ionic strength allowed interpretation of enthalpy curves generated in absence of salt and in the presence of alternative salt types at varying ionic strength (**Figure 5** and **Figure 6**). Variation of the salt type at constant ionic strength did

not substantially affect the binding reaction, signified by similar curve shape and maximal exothermic signal value (**Figure 6**). The plateau at negative enthalpy which marked the very strong binding was more pronounced with regards to molar ratio range and uniformity of enthalpy values for NaCl compared to the other salt types (**Figure 6A**). Similarly, binding affinity was higher in the presence of NaCl than KCl or $CaCl_2$ (**Table 1**). In the absence of salt, binding of CIP to DS occurred from the very beginning of the titration and resulted in higher stoichiometry value of approximately 34 (**Figure 5A and Table 1**). This finding correlated with the fact that the maximal complexation efficiency in absence of salt was reached at a molar ratio of approximately 30 (**Figure 1**). Moreover, the calculation of the stoichiometry revealed that considerably more CIP molecules could bind to DS in a salt-free system (**Table 1**). Furthermore, applying the same experimental conditions as used for the titrations in presence of salt no equilibrium was achieved at the highest molar ratio tested (**Figure 5A**).

In contrast, at high ionic strength (e.g. 1 M NaCl; **Figure 5D**), the binding reaction was attenuated, requiring higher molar ratios to initiate interaction between CIP and DS. Huang and Lapitsky noticed that at higher NaCl concentrations the time required to reach the equilibrium increased and hence the binding becomes too slow to cause significant enthalpic signals [27,28]. Suppressed binding at high ionic strength as observed by ITC correlated well with very low complexation efficiency of 20% at 1 M NaCl (**Figure 1 and Figure 2**). We hypothesize that charge screening at high ionic strength inhibited complex formation [29]. However, some large particles were detected in presence of 1 M NaCl and $CaCl_2$ (**Figure 3A and Figure 4**), presumably representing self-aggregates of either DS and/or CIP. At high ionic strength, DS can form inter-chain aggregates due to the preponderance of hydrophobic interactions when ionic interactions were effectively screened by salt [30]. CIP may aggregate in a similar fashion at sufficiently high ionic strength [24].

Interestingly, in other studies maximum enthalpy observed during titration decreased in the presence of low amount of salt [21,26]. However, this effect was not pronounced for CIP/DS nanoplex formation. Almost the same maximum enthalpy was observed in the absence and presence of 0.1 M salt, suggesting that in addition to electrostatic interactions alternative forces, e.g. hydrophobic interaction of the amphiphilic CIP, contribute to complex formation [11]. Only a slight trend of decreasing maximum enthalpy with increasing ionic strength was observed but the presence of salt in excess (1 M ionic strength) resulted in a distinct reduction of the enthalpy signal (**Figure 5D**). Additionally, high ionic strength was associated with loss of spherical shape of particles (**Figure 4**; 1 M NaCl). In contrast, 0.1 M NaCl as well as no

salt led to spherical particles and featured high binding affinities (**Figure 4** and **Table 1**). We observed that within the dataset some correlation existed between particle shape and binding affinity, with high binding affinities leading to highly spherical particles whereas low binding affinities were related to irregular particles or suppressed particle formation. Therefore, optimization of binding affinity as determined by ITC through variation of the formulation may allow optimization of critical particle quality attributes.

At all tested conditions CIP/DS nanoplexes revealed smaller sizes in SEM than in DLS measurements which is attributed to shrinking of nanoplexes during lyophilization prior to SEM imaging [11,12]. For both DLS and SEM, addition of $CaCl_2$ during preparation yielded the largest nanoplexes whereas the use of NaCl and KCl led to smaller nanoplex sizes. In contrast, comparing the preparation without salt and with 0.1 M NaCl, particles formed in presence of 0.1 M NaCl were significantly smaller than under salt free conditions by DLS, but after freeze-drying no size difference was observed by SEM (**Figure 3A** and **Figure 4**). This effect was most likely caused by a reduction of the electrostatic repulsion within the nanoplexes themselves due to shielding of surplus charges of DS in the presence of salt at low ionic strength [31–33]. Hence, particles could coil more densely whereas in salt free surroundings the polyelectrolyte chains were less flexible due to intra- and inter-chain repulsion resulting in larger nanoplexes [33]. In addition, the nanoplexes appeared to be more uniform in terms of particle size as well as shape distribution when 0.1 M NaCl was added relative to salt-free systems (**Figure 3A** and **Figure 4**). The improved particle size uniformity hypothetically was an effect of deceleration of the particle formation process by addition of low amounts of salt which allowed the added drug to homogenously mix with the polyelectrolyte and form nanoplexes by ionic interactions before aggregation could occur [34].

Another important aspect were the deviating results in size and zeta potential observed in presence of $CaCl_2$ compared to the other salt types. The larger particle sizes could be explained by cross-linking by $CaCl_2$ (**Figure 3 and Figure 4**). Unlike monovalent Na^+ and K^+, Ca^{2+}, as a bivalent ion, could physically cross-link the oppositely charged DS chains [35] but did not feature the hydrophobic interactions which were exhibited by CIP, further stabilizing the particle. Furthermore, the presence of $CaCl_2$ led to a diminished surface charge of the nanoplexes compared to particles prepared in presence of NaCl and KCl (**Figure 3B**) as the bivalent ion could probably shield the surface charges of the negatively charged particles more effectively than monovalent ions [36]. However, all nanoplexes revealed a highly negative surface charge which could be attributed to the negatively charged polyelectrolyte

DS and supported the hypothesis that DS acts as colloidal stabilizer of the complex [11]. Although the particles were prepared at a molar ratio of 31 CIP to DS, DS can be regarded as major component of the complexes due to the higher molecular weight and the numerous charge bearing groups in DS compared to CIP. Hence, DS potentially formed a stabilizing shell around the complexes [18].

Comparing the different applied salt types regarding their influence on the release behavior of the CIP/DS-nanoplexes revealed that nanoplexes prepared in presence of NaCl and $CaCl_2$ released more CIP than using KCl or salt free conditions (**Figure 8A**). However, nanoplexes prepared without salt featured the highest loading followed by nanoplexes prepared with NaCl (**Figure 2**). Relative release from CIP/DS nanoplexes were not influenced by the type of salt (**Figure 8B**), which might be explained by the presence of PBS being used as release buffer, significantly changing the environment with regards to ionic strength.

Overall, applying ITC in combination with other analytical methods enabled the definition of the formulation conditions at which the complexation of CIP and DS was most efficient for example regarding mixing ratio and salt type amongst other things. Moreover, with the help of other analytical methods like SEM, SLS, and DLS it could be shown that ITC may even be suitable to predict shape and morphology of the complexes.

5. Conclusion

Isothermal titration calorimetry proved to be a versatile screening tool for the evaluation of nanoplex formulation conditions. Results of additional physicochemical characterization methods correlated well with the ITC measurements and revealed that the addition of salt in low amounts improved the formulation of CIP/DS nanoplexes by causing more coordinated particle formation, especially in the presence of 0.1 M NaCl. Furthermore, the presence of salt at 0.1 M was favorable compared to salt-free systems with regards to the molar ratio range within which efficient complexation could be achieved.

References

[1] W.S. Cheow, K. Hadinoto, Lipid-polymer hybrid nanoparticles with rhamnolipid-triggered release capabilities as anti-biofilm drug delivery vehicles., Particuology. 10 (2012) 327–333. doi:10.1016/j.partic.2011.08.007.

[2] G.G. Zhanel, K. Ennis, L. Vercaigne, A. Walkty, A.S. Gin, J. Embil, et al., A critical review of the fluoroquinolones: focus on respiratory infections., Drugs. 62 (2002) 13–59.

[3] J.M. Blondeau, A review of the comparative in-vitro activities of 12 antimicrobial agents, with a focus on five new "respiratory quinolones"., J. Antimicrob. Chemother. 43 Suppl B (1999) 1–11.

[4] W.S. Cheow, K. Hadinoto, Green preparation of antibiotic nanoparticle complex as potential anti-biofilm therapeutics via self-assembly amphiphile-polyelectrolyte complexation with dextran sulfate., Colloids Surf. B. Biointerfaces. 92 (2012) 55–63. doi:10.1016/j.colsurfb.2011.11.024.

[5] L.M. Ensign, C. Schneider, J.S. Suk, R. Cone, J. Hanes, Mucus penetrating nanoparticles: biophysical tool and method of drug and gene delivery., Adv. Mater. 24 (2012) 3887–94. doi:10.1002/adma.201201800.

[6] W.S. Cheow, K. Hadinoto, Self-assembled amorphous drug-polyelectrolyte nanoparticle complex with enhanced dissolution rate and saturation solubility., J. Colloid Interface Sci. 367 (2012) 518–26. doi:10.1016/j.jcis.2011.10.011.

[7] S.A. Breda, A.F. Jimenez-Kairuz, R.H. Manzo, M.E. Olivera, Solubility behavior and biopharmaceutical classification of novel high-solubility ciprofloxacin and norfloxacin pharmaceutical derivatives., Int. J. Pharm. 371 (2009) 106–13. doi:10.1016/j.ijpharm.2008.12.026.

[8] M. V Ramírez-Rigo, M.E. Olivera, M. Rubio, R.H. Manzo, Enhanced intestinal permeability and oral bioavailability of enalapril maleate upon complexation with the cationic polymethacrylate Eudragit E100., Eur. J. Pharm. Sci. 55 (2014) 1–11. doi:10.1016/j.ejps.2014.01.001.

[9] P.G. Rogueda, D. Traini, The nanoscale in pulmonary delivery. Part 1: deposition, fate, toxicology and effects, Expert Opin. Drug Deliv. 4 (2007) 595–606. doi:10.1517/17425247.4.6.595.

[10] K. Hadinoto, A. Sundaresan, W.S. Cheow, Lipid–polymer hybrid nanoparticles as a new generation therapeutic delivery platform: A review., Eur. J. Pharm. Biopharm. 85 (2013) 427–443. doi:10.1016/j.ejpb.2013.07.002.

[11] W.S. Cheow, K. Hadinoto, Green amorphous nanoplex as a new supersaturating drug delivery system., Langmuir. 28 (2012) 6265–75. doi:10.1021/la204782x.

[12] L. Meng, B. Ji, W. Huang, D. Wang, G. Tong, Y. Su, et al., Preparation of pixantrone/poly(γ-glutamic acid) nanoparticles through complex self-assembly for oral chemotherapy., Macromol. Biosci. 12 (2012) 1524–33. doi:10.1002/mabi.201200137.

[13] N.E. Ceschan, V. Bucalá, M.V. Ramírez-Rigo, New alginic acid-atenolol microparticles for inhalatory drug targeting., Mater. Sci. Eng. C. Mater. Biol. Appl. 41 (2014) 255–66. doi:10.1016/j.msec.2014.04.040.

[14] K.T. Al-Jamal, W.T. Al-Jamal, J.T.-W. Wang, N. Rubio, J. Buddle, D. Gathercole, et al., Cationic poly-L-lysine dendrimer complexes doxorubicin and delays tumor growth in vitro and in vivo., ACS Nano. 7 (2013) 1905–17. doi:10.1021/nn305860k.

[15] Y. Baena A., R.H. Manzo, L.F. Ponce D'Leon Q., Preparation and physicochemical characterization of some polyelectrolyte-diclofenac complexes., Vitae. 18 (2011) 305–311.

[16] W.-G. Dai, L.C. Dong, Y.-Q. Song, Nanosizing of a drug/carrageenan complex to increase solubility and dissolution rate., Int. J. Pharm. 342 (2007) 201–7. doi:10.1016/j.ijpharm.2007.04.032.

[17] Z. Liu, Y. Jiao, Y. Wang, C. Zhou, Z. Zhang, Polysaccharides-based nanoparticles as drug delivery systems., Adv. Drug Deliv. Rev. 60 (2008) 1650–62. doi:10.1016/j.addr.2008.09.001.

[18] H. Dautzenberg, Polyelectrolyte complex formation in highly aggregating systems. 1. Effect of salt: Polyelectrolyte complex formation in the presence of NaCl., Macromolecules. 30 (1997) 7810–7815. doi:10.1021/ma970803f.

[19] A. Bertin, Polyelectrolyte Complexes of DNA and Polycations as Gene Delivery Vectors, in: Adv. Polym. Sci., Springer-Verlag Berlin Heidelberg, 2013: pp. 103–195. doi:10.1007/12_2013_218.

[20] D. Priftis, N. Laugel, M. Tirrell, Thermodynamic characterization of polypeptide complex coacervation., Langmuir. 28 (2012) 15947–57. doi:10.1021/la302729r.

[21] Y. Tian, L. Bromberg, S.N. Lin, T.A. Hatton, K.C. Tam, Complexation and release of doxorubicin from its complexes with pluronic P85-b-poly(acrylic acid) block copolymers., J. Control. Release. 121 (2007) 137–45. doi:10.1016/j.jconrel.2007.05.010.

[22] H.A. Santos, J.A. Manzanares, L. Murtomäki, K. Kontturi, Thermodynamic analysis of binding between drugs and glycosaminoglycans by isothermal titration calorimetry and fluorescence spectroscopy., Eur. J. Pharm. Sci. 32 (2007) 105–14. doi:10.1016/j.ejps.2007.06.003.

[23] X. Feng, M. Leduc, R. Pelton, Polyelectrolyte complex characterization with isothermal titration calorimetry and colloid titration., Colloids Surfaces A Physicochem. Eng. Asp. 317 (2008) 535–542. doi:10.1016/j.colsurfa.2007.11.053.

[24] K. Bouchemal, New challenges for pharmaceutical formulations and drug delivery systems characterization using isothermal titration calorimetry., Drug Discov. Today. 13 (2008) 960–72. doi:10.1016/j.drudis.2008.06.004.

[25] O. Germershaus, V. Werner, M. Kutscher, L. Meinel, Deciphering the mechanism of protein interaction with silk fibroin for drug delivery systems., Biomaterials. 35 (2014) 3427–34. doi:10.1016/j.biomaterials.2013.12.083.

[26] B.B. Raju, F.M. Winnik, Y. Morishima, A look at the thermodynamics of the association of amphiphilic polyelectrolytes in aqueous solutions: Strengths and limitations of isothermal titration calorimetry., Langmuir. 17 (2001) 4416–4421. doi:10.1021/la001554i.

[27] Y. Huang, Y. Lapitsky, Determining the colloidal behavior of ionically cross-linked polyelectrolytes with isothermal titration calorimetry., J. Phys. Chem. B. 117 (2013) 9548–57. doi:10.1021/jp405384b.

[28] Y. Huang, Y. Lapitsky, Salt-assisted mechanistic analysis of chitosan/tripolyphosphate micro- and nanogel formation., Biomacromolecules. 13 (2012) 3868–76. doi:10.1021/bm3014236.

[29] R. Chollakup, W. Smitthipong, C.D. Eisenbach, M. Tirrell, Phase behavior and coacervation of aqueous poly(acrylic acid)−poly(allylamine) solutions., Macromolecules. 43 (2010) 2518–2528. doi:10.1021/ma902144k.

[30] Z. Luo, X. Wang, G. Zhang, Ion-specific effect on dynamics of polyelectrolyte chains., Phys. Chem. Chem. Phys. 14 (2012) 6812–6. doi:10.1039/c2cp40077d.

[31] R. Chollakup, J.B. Beck, K. Dirnberger, M. Tirrell, C.D. Eisenbach, Polyelectrolyte molecular weight and salt effects on the phase behavior and coacervation of aqueous solutions of poly(acrylic acid) sodium salt and poly(allylamine) hydrochloride., Macromolecules. 46 (2013) 2376–2390. doi:10.1021/ma202172q.

[32] H. Dautzenberg, N. Karibyants, Polyelectrolyte complex formation in highly aggregating systems. Effect of salt: response to subsequent addition of NaCl., Macromol. Chem. Phys. 200 (1999) 118–125. doi:10.1002/(SICI)1521-3935(19990101)200:1<118::AID-MACP118>3.0.CO;2-K.

[33] C. Schatz, J.-M. Lucas, C. Viton, A. Domard, C. Pichot, T. Delair, Formation and properties of positively charged colloids based on polyelectrolyte complexes of biopolymers., Langmuir. 20 (2004) 7766–78. doi:10.1021/la049460m.

[34] Y. Lapitsky, Ionically crosslinked polyelectrolyte nanocarriers: Recent advances and open problems., Curr. Opin. Colloid Interface Sci. 19 (2014) 122–130. doi:10.1016/j.cocis.2014.03.014.

[35] J.D. Kosmala, D.B. Henthorn, L. Brannon-Peppas, Preparation of interpenetrating networks of gelatin and dextran as degradable biomaterials., Biomaterials. 21 (2000) 2019–23. doi:10.1016/S0142-9612(00)00057-0.

[36] M. Chorom, P. Rengasamy, Dispersion and zeta potential of pure clays as related to net particle charge under varying pH, electrolyte concentration and cation type., Eur. J. Soil Sci. 46 (1995) 657–665. doi:10.1111/j.1365-2389.1995.tb01362.x.

CHAPTER III

DEVELOPMENT OF A STABLE FORMULATION FOR THE HUMANIZED MONOCLONAL ANTIBODY UK-66

Unpublished manuscript.

Abstract

During production and shelf life, therapeutic proteins are facing a multitude of external stress factors potentially compromising their conformational stability. To enable efficacious drug application and prevent unwanted immune responses due to aggregation of the protein molecule, the development of tailor made protein formulations preserving protein's chemical and physical stability is required. Therefore, this study aimed at the development of a stabilizing formulation for hUK-66, a humanized monoclonal antibody directed against *S. aureus*. Based on the results of antibody characterization, optimal formulation pH was evaluated in a short-term stability study. Subsequently, combinations of excipients and dosage forms were analyzed for their suitability in preserving antibody stability by comparing different liquid and lyophilized formulations in a long-term stability study at different storage temperatures. Lyophilization of hUK-66 in histidine buffer, pH 6, containing the stabilizers sucrose and polysorbate 20 proved to preserve stability of this antibody throughout formulation process and long-term storage at 2-8°C.

1. Introduction

Maintaining protein stability of therapeutic antibodies during manufacture and throughout shelf life of a biopharmaceutical product is a significant challenge in formulation development since changes in protein structure can cause loss of therapeutic activity as well as unwanted immune responses [1,2]. The conformation of a protein is sensitive to external stress factors. However, during manufacturing and distribution, therapeutic proteins experience numerous production steps such as fermentation, purification, formulation, filtration, filling, shipment, and storage where they are exposed to a variety of stresses. In addition, during all these steps the protein gets into contact with a multitude of materials and surfaces, i.e., glass, steel, various plastics, silicone, or rubbers which may affect protein stability [3–8].

A successful formulation of therapeutic proteins depends on knowledge about their physico-chemical characteristics, chemical and physical stability, and immunogenicity [1,5]. Physical and chemical protein instability can result from a multitude of factors such as pH, ionic strength, temperature, protein concentration, purity, surface adsorption, mechanical stress, excipients, freezing, thawing, drying, etc. and manifest as unfolding, precipitation, adsorption, and aggregation of the protein. Aggregates can be distinguished by their size (soluble and insoluble), their type of bond (covalent and noncovalent), their conformation (native or nonnative structure) and reversibility (reversible and irreversible) [3–5,7,9]. Compared to the native protein, aggregates have no or reduced activity, are less soluble and have greater immunogenicity potential [2,5,7,10–12]. Major chemical protein degradation reactions include deamidation, isomerization, oxidation, hydrolysis, succinimidation, disulfide bond shuffling as well as deglycosylation which may compromise conformation and biologic activity [5,13,14].

Since every protein has unique physical and chemical stabilization requirements, the final dosage form and formulation strongly depends on the respective protein as well as indication and the target patient population [15].

Liquid formulations are advantageous regarding easy manufacturing, handling and application but lyophilized protein formulations are often found to be more stable. Lyophilized products are also less sensitive to mechanical stress and chemical degradation due to reduced reaction rates, restricted protein mobility and decreased conformational flexibility in a dried state. However, the process of freeze-drying can impair protein stability, requires additional expensive equipment and reconstitution is needed before application generating a potential source of errors but also enabling an elegant way to increase protein concentration [5,9,15–20].

Especially in case of lyophilized formulations, excipients protecting the protein against the stresses that emerge during freezing and dehydration are required. In the field of freeze-drying cryoprotectants (stabilization during freezing only) or lyoprotectants (stabilization during both, freezing and drying) are commonly employed [15,21]. In the case of liquid formulations excipients are essential for protein stabilization against stresses occurring during processing, transportation, and storage.

Surfactants are frequently used for liquid and lyophilized formulations. Since protein molecules are surface-active, they tend to accumulate at interfaces like water/air and to adsorb to solid/water interfaces like the storage container, often leading to unfolding and subsequent aggregation during all process steps, transportation, and storage. Surfactants are able to prevent these unwanted adsorption and aggregation by replacing the protein molecules at the interfaces and blocking hydrophobic sites on the protein surface susceptible to aggregation [4,8,17,22,23]. Particularly nonionic surfactants such as polysorbate (Tween®) are important excipients to formulate a protein for lyophilization since they are capable of inhibiting unfolding during the freezing step and subsequent aggregation during rehydration. They are supposed to accelerate the reconstitution of the lyophilizates as wetting agents and protect proteins from unfolding by replacing protein molecules at the air-ice interface. Polysorbate 20 is considered as one of the most effective surfactants and only low concentrations are needed [5,6,10,15,21,24]. However, it has to be considered that surfactants can also induce oxidation and aggregation of the therapeutic protein during storage due to contamination by residual peroxides [25,26].

Furthermore, sugars or polyols are frequently used as stabilizers in protein formulations. These stabilizers are known to be preferentially excluded from the surface of the protein molecule in liquid formulations and to be substituted by water molecules resulting in hydration of the protein molecule. However, preferential exclusion usually causes an increase in chemical potential of the protein which is thermodynamically unfavorable. Since the extent of this increase presumably depends on the surface area of the protein, unfolded protein molecules result in a larger change in free energy compared to the natural compact state. Therefore, addition of sugars to protein solution lead to stabilization of the more compact folded form and hence mitigation of aggregation [5,9,22,27–30]. Among these, non-reducing disaccharides like sucrose and trehalose are the most efficient stabilizers during lyophilization since they protect the native state of the protein during freezing and inhibit unfolding as well as aggregation during the drying step by forming an amorphous phase with the protein. These lyoprotectants are able to compensate the loss of the hydration shell surrounding the protein

during dehydration by hydrogen-bonding interaction with the protein (water replacement/substitution) [17,21,31]. Furthermore, disaccharides like trehalose are said to immobilize protein molecules in a glassy matrix (vitrification) and hereby prevent protein unfolding and aggregation [17,32–34].

In addition, glycine and mannitol are commonly used crystallizing bulking agents in lyophilized formulations to improve cake appearance [10,15,21].

The overall goal of this study was the development of a pharmaceutical formulation for the humanized monoclonal antibody hUK-66 ensuring stability and bioactivity of the protein during processing, storage, and transportation. Initially, formulation pH was optimized. An adequate pH-value as starting point for the pH screening was chosen based on analysis of isoelectric point (pI) and pH-dependent unfolding temperatures. The stability of hUK-66 in relation to pH and elevated temperature was evaluated using different analytical methods for structural characterization in a short-term storage stability study under accelerated and stressed conditions.

For the selected optimal formulation pH, a long-term stability study was conducted evaluating the impact of different excipients (polysorbate, sucrose, mannitol, trehalose, and glycine) on the formation of aggregates and degradation products. In this context, the influence of the dosage form on stability of hUK-66 was assessed, as well.

2. Materials and methods

2.1. Materials

hUK-66, a humanized monoclonal antibody (mAb) of the IgG1 subclass, targeting the immunodominant staphylococcal antigen A (IsaA) on the surface of *Staphylococcus aureus* [35], was provided at a concentration of 2.8 mg/ml or 9.81 mg/ml in PBS buffer, pH 7.4, by the Institute for Molecular Infection Biology (University of Wurzburg, Germany). It was diafiltrated using an Amicon® stirred ultrafiltration cell 8010 (EMD Millipore Corporation, Billerica, MA, USA) equipped with a 50 kDa ultrafiltration membrane disk filter (25 mm, PALL® Life Sciences Corporation, Ann Arbor, MI, USA) against the buffer needed for respective experiments.

L-Histidine Reagent Plus® ≥ 99% (TLC) and bovine serum albumin were purchased from Sigma-Aldrich Co. (St. Louis, USA). Sucrose, D-mannitol, trehalose, and polysorbate 20 from Sigma-Aldrich (Steinheim, Germany) were employed as formulation excipients. 0.01 M HCl and 0.01 M KOH were used to adjust the pH of protein samples. The fluorescent dye SYPRO® Orange (SYPRO® Orange Protein gel stain, Sigma-Aldrich, Steinheim, Germany) was provided in a 5000x concentrated stock solution in DMSO and diluted to a stock solution 1:10 with DMSO. Ultrapure water was used throughout the study (Milli-Q Synthesis Ultrapure Water Purification System, EMD Millipore Corporation, Billerica, USA).

2.2. Sample preparation for formulation screening

2.2.1. Short-term storage stability study of minimally formulated drug substance

The drug substance hUK-66 was formulated in PBS buffer at pH 7.4. It was stored at refrigerated conditions (2-8°C) at a concentration of approximately 1.35 mg/ml over a period of 4 months to analyze the storage stability of the bulk solution of this humanized antibody. After defined intervals, samples were stored at -80°C and analyzed regarding aggregation and formation of degradation products using size exclusion chromatography. Additionally, the concentration was monitored using UV-Vis spectroscopy. To prove that freezing at -80°C did not lead to structural changes, the drug substance was analyzed regarding stability after one freeze-thaw cycle.

2.2.2. pH screening under accelerated and stressed storage conditions

hUK-66 was dialyzed against a 50 mM histidine buffer, pH 6, and diluted to a concentration of approximately 1 mg/ml. Subsequently, the samples were sterile filtered using sterile syringe filter units (0.2 µm, PES membrane, 13 mm diameter, Nalge Nunc International Corporation, Rochester, USA) and divided into aliquots of 550 µl each under laminar air flow (LAF). The aliquots were adjusted to one of the five chosen pH-values (5, 5.5, 6, 6.5, and 7) each and incubated at 25°C (accelerated conditions) as well as 40°C (stressed conditions) for 4 and 8 weeks (**Table 1**) in a climate chamber KBF 115 and a heating oven ED 115 (Binder GmbH, Tuttlingen, Germany). After these defined time periods, the samples were stored at -80°C and analyzed side-by-side using the described analytical methods after thawing and gentle mixing. Due to limited availability of mAb material, for this pre-study no triplicates were manufactured.

Table 1: Overview of storage periods and conditions for the accelerated pH screening study of hUK-66.

Period	**initial**	**4 weeks**										**8 weeks**									
Condition		25°C					40°C					25°C					40°C				
pH	6	5	5.5	6	6.5	7	5	5.5	6	6.5	7	5	5.5	6	6.5	7	5	5.5	6	6.5	7

2.2.3. Formulation screening for liquid and lyophilized dosage forms under long-term storage conditions

To evaluate the best stabilizer and dosage form for formulation of hUK-66, a formulation screening was conducted in liquid and lyophilized state.

2.2.3.1. Preparation of liquid formulations

For the liquid dosage form, hUK-66 was dialyzed against a 50 mM histidine buffer, pH 6, and concentrated to approximately 50 mg/ml using an Amicon® stirred ultrafiltration cell 8010 (EMD Millipore Corporation, Billerica, MA, USA). Three formulations were prepared varying the type of polyol (mannitol, sucrose, or trehalose) each containing 34 mg/ml hUK-66 along with 0.04% polysorbate 20 (PS 20) and 270 mM polyol. For this purpose, 1% PS 20 and 1 M sugar stock solutions in 50 mM histidine were prepared in advance. The formulations were sterile filtered using sterile syringe filter units (0.2 µm, PES membrane, 13 mm diameter, Nalge Nunc International Corporation, Rochester, USA) and divided into aliquots of approximately 100 µl each under LAF. The liquid formulations were incubated in autoclaved

2R glass vials at 2-8°C as well as 25°C for 3, 6, and 9 months (**Table 2**). After the defined time periods, the samples were stored at -80°C. For side-by-side analysis using the described analytical methods the samples were thawed in a water bath at 37°C and gently mixed. Only single samples were prepared due to limited availability of hUK-66.

Table 2: Overview of the liquid formulations of hUK-66, their storage conditions, and periods for the long-term stability study.

Formulation	**Mannitol**							**Trehalose**							**Sucrose**						
Composition	hUK-66, PS 20, mannitol							hUK-66, PS 20, trehalose							hUK-66, PS 20, sucrose						
Condition	initial	2-8°C			25°C			initial	2-8°C			25°C			initial	2-8°C			25°C		
Incubated months	0	3	6	9	3	6	9	0	3	6	9	3	6	9	0	3	6	9	3	6	9

2.2.3.2. Preparation of lyophilized formulations

For the lyophilized formulations, hUK-66 was diafiltrated into a 10 mM histidine buffer and concentrated to approximately 13 mg/ml. Using stock solutions of 1% PS 20, 1 M sucrose, glycine, or mannitol in histidine buffer, formulations were prepared yielding 0.01% PS 20 and 90 mM sucrose, respectively. To analyze the stabilization effect of glycine and mannitol, both were added supplementary to sucrose resulting in three formulations: (1) sucrose only, (2) 20 mM glycine, and (3) 60 mM mannitol (**Table 3**). An additional sample without protein was prepared as a reference for the temperature measurement during lyophilization. The samples were sterile filtered into autoclaved 2R vials in aliquots of 200 µl and frozen at -80°C. Lyophilization was performed using a VirTis adVantage Plus freeze-drier (SP scientific, Gardiner, NY, USA) starting with equilibrating the samples at -5°C for 10 min and freezing to -40°C with a temperature ramp of 0.7°C/min at 0.53 mbar. After 3 h at -40°C, the samples were annealed at -20°C for 30 min before the temperature was reduced to -40°C for another 30 min. Subsequently, the pressure was reduced to 0.20 mbar and the shelf temperature increased to -20°C for 3 h. After primary drying, the temperature was increased to -10°C for 2 h, before secondary drying was conducted at 10°C for 6 h. The pressure was reduced to 0.13 mbar for the last 4 h. The vials were stoppered and tightly sealed before incubation at 2-8°C for 3, 6, and 9 months. At the defined time points, the samples were stored at -80°C and analyzed after reconstitution with purified water to result in a volume of 50 µl. The amount of water which had to be added for reconstitution was identified by analyzing the density of a surrogate formulation containing bovine serum albumin (BSA) instead of hUK-66 and

subtracting the mass of protein and excipients from the calculated mass for the formulations. Only single samples were prepared due to limited availability of hUK-66.

Table 3: Composition, storage conditions, and periods of the lyophilized hUK-66 formulations.

Formulation	**Sucrose only**				**Glycine**				**Mannitol**			
Composition	hUK-66, PS 20, sucrose				hUK-66, PS 20, sucrose, glycine				hUK-66, PS 20, sucrose, mannitol			
Condition	initial	2-8°C			initial	2-8°C			initial	2-8°C		
Incubated months	0	3	6	9	0	3	6	9	0	3	6	9

2.3. Analytical methods

2.3.1. UV-Vis spectroscopy

UV-visible absorbance spectroscopy was performed using a Genesys 10s UV-Vis spectrophotometer (Thermo Fisher Scientific Corporation, Waltham, USA). Volumes of 200-400 µl of each sample were analyzed in a 0.5 ml disposable cuvette (UVette®, Eppendorf AG, Hamburg, Germany) with a path length of 10 mm at 25°C. UV-visible absorbance spectra were recorded from 200 to 800 nm using intervals of 1 nm. To determine the antibody concentration of the samples, an extinction coefficient of 1.475 $ml \cdot mg^{-1} \cdot cm^{-1}$ for absorption at 280 nm was used which was calculated based on the amino acid sequence using ExPASy [36]. If necessary, the samples were diluted to a concentration which guaranteed a measurement in the linear range.

2.3.2. Electrophoretic mobility assay

For the determination of the isoelectric point (pI) of the antibody, zeta potential measurements were performed by electrophoretic light scattering (ELS) using a Delsa™ Nano HC Particle Analyzer (Beckman Coulter®, Inc., Fullerton, CA, USA). Each measurement consisted of 3 repetitions with 10 accumulations each. The applied voltage was set to 60 V and temperature was held at 25°C. The system was calibrated using an aqueous suspension of polystyrene latex as mobility control (Otsuka Electronics Co., Ltd., Osaka, Japan, P/N A50695).

To analyze the zeta potential of hUK-66 at different pH values, the mAb was dialyzed against a 5 mM Britton-Robinson buffer (H_3BO_3, H_3PO_4, CH_3COOH) and adjusted to the defined pH values of 6, 7, and 8 using 0.1 M NaOH [37]. In this process, the mAb concentrations were set to a final concentration of 0.5 mg/ml.

A 10 mM Britton-Robinson buffer was prepared by dissolution of 0.62 g boric acid, 0.61 g acetic acid, and 1.15 g phosphoric acid (85%) in 1 l of water and diluted 1:2 to obtain a 5 mM Britton-Robinson buffer.

2.3.3. Dynamic scanning fluorimetry (DSF)

The unfolding temperatures of the two domains of hUK-66 at different pH values were analyzed by dynamic scanning fluorimetry (DSF) using a 7900HT Fast Real-Time PCR System (Applied Biosystems, life technologies, Thermo Fisher Scientific, Darmstadt, Germany). Thermal unfolding of proteins can be detected by an increase of fluorescence of a non-covalent extrinsic dye that binds to the hydrophobic regions of a protein exposed during unfolding [38,39]. Samples were prepared by diluting hUK-66 with 5 mM Britton-Robinson buffer of different pH values to a final concentration of 0.2 mg/ml protein and a final volume of 100 µl. The buffer was adjusted to pH values from 5 to 9 in 0.5 steps using 0.1 M NaOH. The samples were filled into a 96 well plate and 0.5 µl of the fluorescent dye Sypro Orange diluted 1:10 in DMSO was added to each well resulting in a final dye dilution of 1:2000.
Subsequently, the well plate was heated starting from 25°C which was held stable for 15 seconds to 95°C using a heating slope of 4%. Fluorescence excitation was performed at 488 nm and emission was detected from 625 to 710 nm during the measurement.
After analysis, the emission of each sample was plotted against the respective temperature and the first derivative of this function was calculated. The maxima of this derivation can be assigned to the unfolding temperatures of the antigen binding fragment and the hinge-C_H-region [38,40].

2.3.4. pH measurement

The pH values of the samples were adjusted and measured using a pH meter Lab phenomenal pH 1000 L (VWR International GmbH, Darmstadt, Germany) equipped with an InLab Micro pH electrode (Mettler-Toledo GmbH, Giessen, Germany) before and after incubation. For the adjustment of the buffer's pH value, a glass pH-electrode pHenomenal® 221 (VWR International GmbH, Darmstadt, Germany) was used. The electrodes were calibrated weekly by a two point calibration using technical buffer pH 4 and pH 7 (VWR International GmbH, Darmstadt, Germany).

2.3.5. Dynamic light scattering (DLS)

Particle size distributions of the protein samples were measured using a Delsa™ Nano HC Particle Analyzer (Beckman Coulter®, Inc., Fullerton, CA, USA) at 25°C. Every measurement consisted of three individual runs comprising 200 accumulations each. 60 µl of the different samples were analyzed in a glass micro-cuvette (Beckman Coulter®, Inc., Fullerton, CA, USA). The intensity size distribution, the hydrodynamic diameter and the polydispersity index (PdI) were obtained and compared with regard to potential aggregates in nanometer size range formed during incubation.

2.3.6. High performance size exclusion chromatography (SEC)

To analyze the stability and purity of the protein samples by SEC, the samples were diluted to a final concentration of approximately 1 mg/ml and centrifuged at 4400 x g for 30 min at 5°C (Eppendorf Centrifuge 5804 R, Rotor A-4-44, Eppendorf AG, Hamburg, Germany).
The supernatants were transferred into 1.5 ml vials with 100 µl glass vial inserts and analyzed using a VWR Hitachi LaChromUltra™ HPLC system equipped with a diode array detector and a 7.8 mm x 300 mm TSK-Gel® G3000SWXL column as well as a TSK-Gel® SWXL Guard column (both Tosoh Bioscience, Stuttgart, Germany).
A 150 mM potassium phosphate buffer, pH 6.5, was used as mobile phase. 20 µl of each sample were injected and separated at a flow rate of 0.4 ml/min for 40 min at room temperature. The chromatographic data were recorded at 210 nm using a UV-Vis diode array detector and evaluated using the Agilent EZChrom Elite software (Agilent Technologies, Inc., Pleasanton, CA, USA).

2.3.7. Cation exchange chromatography (CEX)

Immediately after SEC, mAb samples were analyzed for their charge heterogeneity using a VWR Hitachi LaChromUltra™ HPLC system equipped with a diode array detector and a 4 mm x 250 mm PROPAC® WCX-10 analytical column (P/N 054993) as well as a 4 x 50 mm PROPAC® WCX-10G guard column (both Dionex® Corporation, Thermo Fisher Scientific, Inc., Sunnyvale, CA, USA). 10 µl of each sample were injected and separated at a flow rate of 1.0 ml/min for 52 min at room temperature. A gradient of mobile phases A (20 mM sodium acetate, pH 5.6) and B (20 mM sodium acetate, 240 mM sodium chloride, pH 5.6) was used. The percentage of B increased from 20% (0 min) to 40% (2 min) to 80% (52 min). The column was regenerated after each run by 100% mobile phase B for 4.9 min and re-equilibrated using 80% A and 20% B for another 20 min prior to analysis of the next sample [41]. The data were recorded at 280 nm and 214 nm, respectively, using a UV-Vis diode array

detector and evaluated using the Agilent EZChrom Elite software (Agilent Technologies, Inc., Pleasanton, CA, USA).

To define variants of hUK-66 which possess a C-terminal lysine charge heterogeneity, 150 µl of the anti-Isa A antibody at a concentration of 1 mg/ml were treated with 1 µl carboxypeptidase B at a concentration of 5 mg/ml (Sigma-Aldrich Chemie GmbH, Steinheim, Germany), incubated for 15 min, and analyzed as described above.

Deamidation of hUK-66 was achieved by addition of 10% ammonium carbonate and incubation at 37°C for 48 h. After 24 h, an aliquot of 75 µl was removed and stored at -80°C. The final concentrations of mAb and ammonium carbonate were 1 mg/ml and 1%, respectively [42].

3. Results and discussion

3.1. Characterization of hUK-66

3.1.1. Determination of the isoelectric point of hUK-66

For the determination of the isoelectric point (pI) of hUK-66, the net charges of the protein at different pH values have been assessed to identify the pH value at which the net charge was zero. The net charge of a protein in solution can be estimated by measuring the zeta potential, which is defined as the potential difference between the medium and the stationary layer of fluid surrounding the particle and containing the counter ions of the buffer [43].

Although the analyzed pH range was relatively narrow, the zeta potentials differed significantly. hUK-66 was positively charged in the acidic pH range (pH 6.25) and negatively charged in basic regions (pH 8) (**Figure 1**).

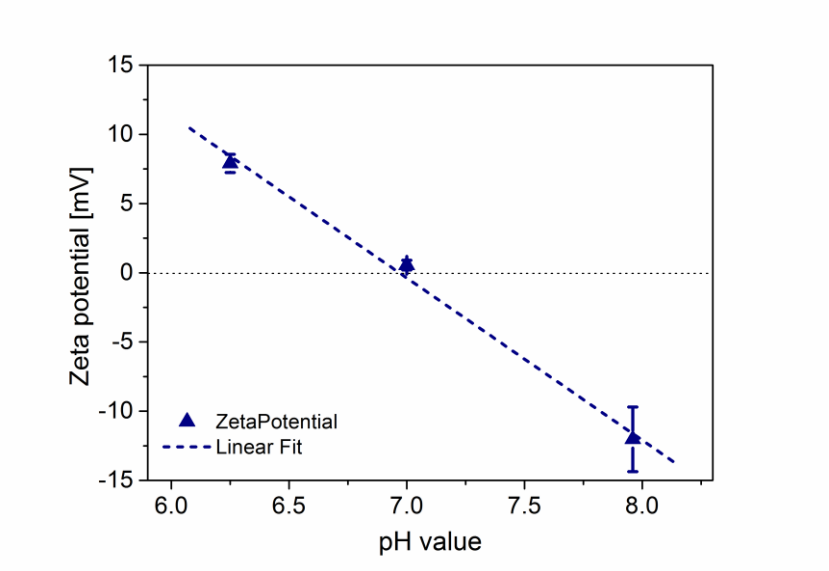

Figure 1: Measured zeta potentials of hUK-66 at different pH values. The intersection with the x-axis determines the pI of this protein.

At pH 7, the intersection point with the x-axis, the net charge of the protein was zero representing the isoelectric point of hUK-66. At this pH value, the aggregation propensity of hUK-66 is assumed to be highest due to reduced charge repulsion [4,22,44]. Therefore, pH 7.0 was avoided for the formulation of hUK-66. However, at pH values far away from the protein's pI the protein molecules not only are characterized by reduced thermodynamic stability but also are prone to undergo chemical degradation [4,5,13,22]. Hence, optimal formulation stability is frequently achieved at pH values about one unit above or below the

protein's pI [18]. Accordingly, pH 6 or pH 8 could be chosen as formulation pH. However, under basic conditions susceptibility to deamidation is higher than at pH 6 [13].

3.1.2. Determination of the unfolding temperature of hUK-66 at different pH values

Thermal unfolding was analyzed at a broad pH range since the unfolding temperature is increased when a formulation condition thermodynamically stabilizes the protein [5,39]. Monoclonal antibodies can unfold at two different domains. Regarding an IgG molecule, Vermeer et al. found that the F_{ab} region starts to unfold at lower temperatures than the F_c region [40,45]. For detection of the unfolding, non-covalent extrinsic dyes like SYPRO Orange are convenient tools. These dyes show minor fluorescence in a hydrophilic environment but high fluorescence upon interaction with hydrophobic regions, such as the surface of proteins after unfolding or aggregation [38,46]. As the fluorescence intensity of the dye sample mixtures was analyzed over a broad temperature range, the unfolding temperature could be determined as maximum of the first derivative of the emission intensity-temperature curve. Both domains showed the lowest unfolding temperature at pH 7.5 with approximately 80°C for unfolding of the hinge-C_H and approximately 70°C for F_{ab} unfolding (**Figure 2**). Additionally, at pH 5 the antibody started to unfold at a low temperature, as well. Hence, these pH values represented the conditions where hUK-66 was thermodynamically most instable. In contrast, at pH 5.5 and pH 6 hUK-66 featured highest unfolding temperatures of both domains (82°C for hinge-C_H and 72°C for F_{ab} region).

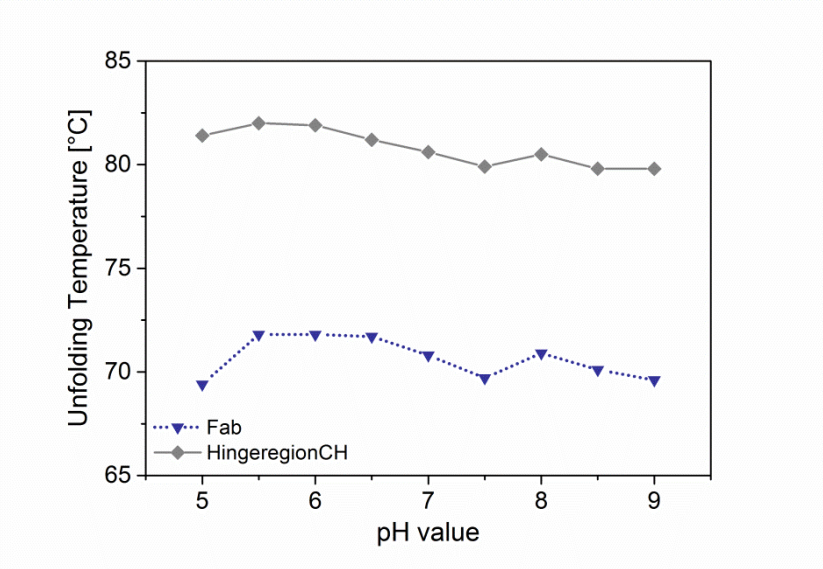

Figure 2: Unfolding temperature of two domains of hUK-66 at different pH values. The pH with the highest unfolding temperature indicates the pH value at which the protein is thermodynamically most stable.

3.1.3. Identification of lysine variants of hUK-66

Monoclonal antibodies often exhibit charge heterogeneity which can be caused by variations in C-terminal lysine content [47–49]. To identify potential lysine variants of hUK-66, the antibody sample was treated with carboxypeptidase B, an exopeptidase, which specifically cleaves C-terminal lysine residues. Comparing the CEX chromatograms of hUK-66 before and after enzyme treatment, the peaks at 27 min and 29 min have disappeared (**Figure 3**). It was, therefore, concluded that these peaks represented variants containing one (27 min) or two (29 min) terminal lysine residues on their heavy chains, respectively. In addition, the area under the major peak increased correspondingly indicating that this peak could be assigned to the variant with no terminal lysine [42,47–50].

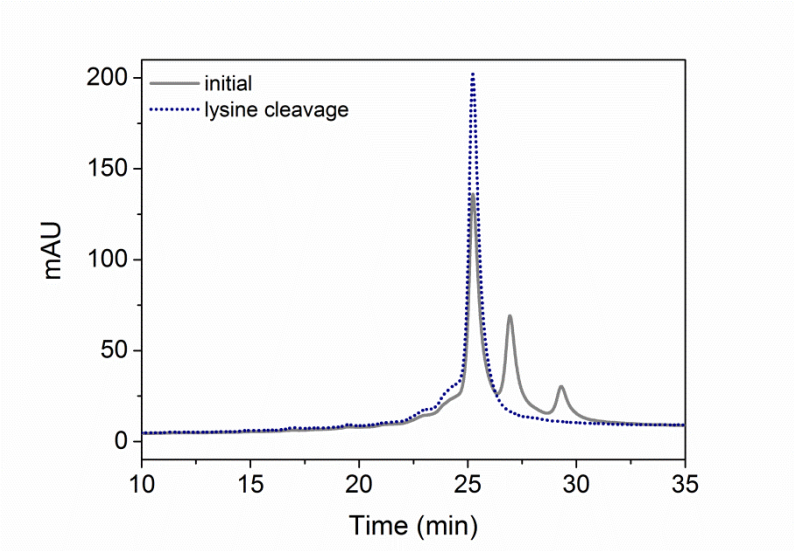

Figure 3: Chromatographic profile of hUK-66 before (solid grey line) and after (dotted blue line) treatment with carboxypeptidase (lysine cleavage).

3.1.4. Forced degradation under basic conditions

Degradation was forced by the addition of ammonium carbonate to identify changes in the chromatographic profile of hUK-66 associated to deamidation, a prevalent protein degradation mechanism [5,10]. Thus, asparagine residues (neutral amino acid) were converted to aspartic acid residues (acidic amino acid). This resulted in an increase of acidic variants compared to the CEX-chromatogram of the mAb without treatment while the main peak area decreased (**Figure 4**), indicating chemical degradation by deamidation [10,49].

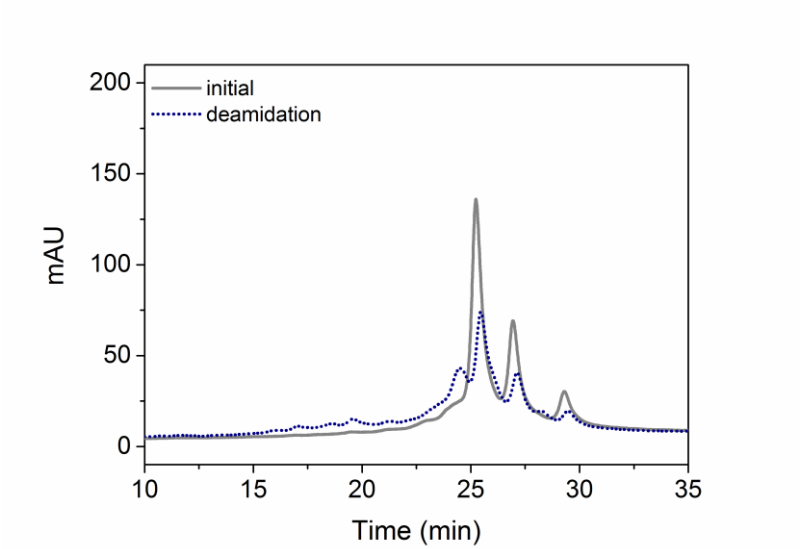

Figure 4: Chromatographic profile of hUK-66 before (solid grey line) and after (dotted blue line) treatment with ammonium carbonate (deamidation).

3.2. Purity and storage stability of the drug substance

Bulk drug substance of hUK-66 was analyzed by SEC, resulting in 91% monomer content, 1.5% aggregates and 7% degradation products (**Figure 5A**). Freezing at -80°C and thawing at room temperature did not result in a significant change of mAb purity underlining its stability (**Figure 5B**). Hence, storage of samples at -80°C was not expected to result in aggregation of the antibody enabling collection of stability samples and storage at -80°C until side-by-side analysis of the entire sample set.

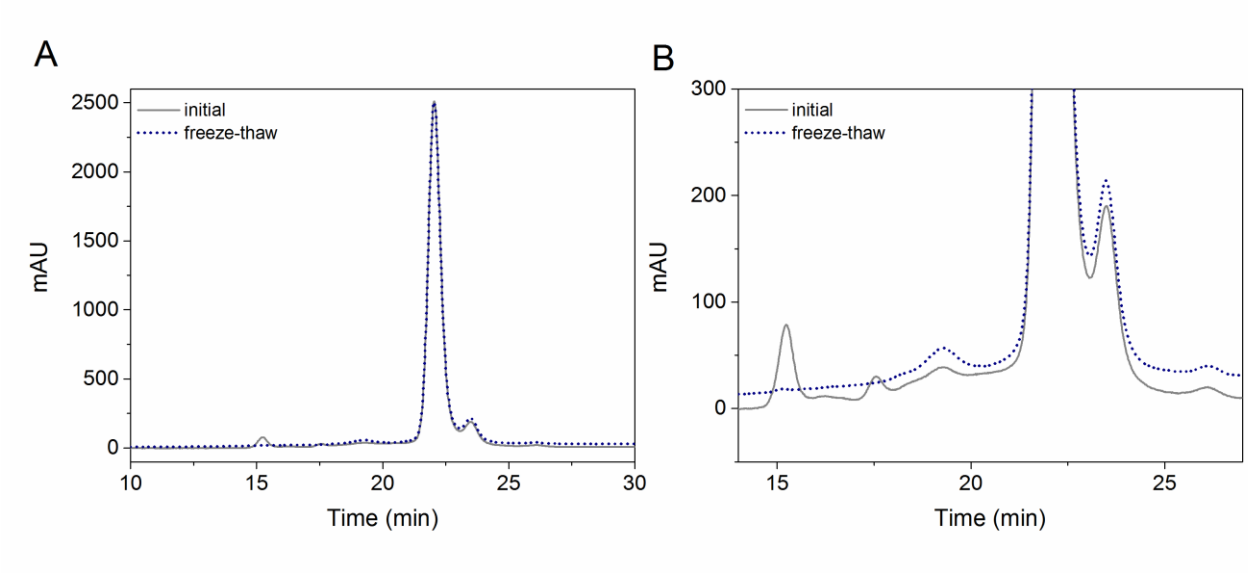

Figure 5: SEC-Chromatogram of hUK-66 in PBS before (solid grey line) and after (dotted blue line) one freeze-thaw cycle (A). The main peak depicts the percentage of monomer in the sample. Subsequent peaks can be assigned to degradation products whereas prior eluted peaks represent aggregates as recognizable in the magnification of the chromatogram (B).

For characterization of the drug substance stability, hUK-66 was stored at 2-8°C over 4 months in PBS and analyzed with regard to formation of aggregates or degradation products using SEC. After 4 months of incubation at 2-8°C in PBS, the protein content of the drug substance was preserved well since the total peak area showed only small variation from $4.45 \cdot 10^8$ to $4.67 \cdot 10^8$ A.U.·min. Hence, no considerable loss due to insoluble aggregates removed by centrifugation before analysis or adsorption to containers during storage was detected (**Figure 6A**). A decrease of 0.7 percentage points of soluble aggregates was observed during storage at 2-8°C in PBS which led to the conclusion that no substantial aggregation occurred during storage (**Figure 6D**).

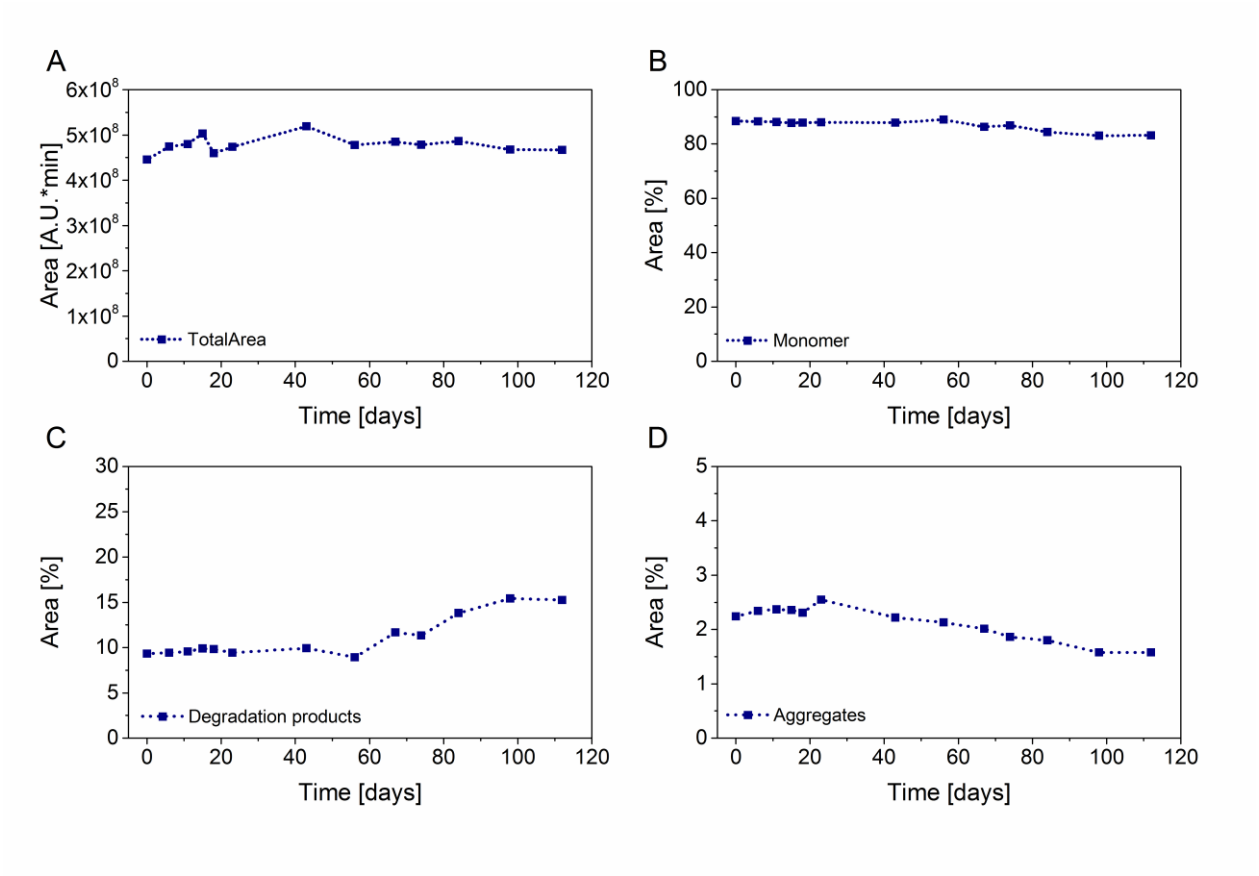

Figure 6: Stability of hUK-66 drug substance in PBS at 2-8°C over 4 months. Total peak area (A), relative percentage of monomer (B), degradation products (C), and soluble aggregates (D) are shown over incubation time.

However, the percentage of monomer decreased by approximately 5 percentage points (**Figure 6B**) from 88% to 83% accompanied by an increase of degradation products of approximately 6 percentage points (**Figure 6C** and **Figure 7**) after 4 months. Hence, degradation was more pronounced than aggregation when hUK-66 was stored in PBS at 2-8°C. Altogether, the drug substance showed good stability in PBS providing a valuable basis for further development of a stabilizing formulation for hUK-66 while simultaneously leaving space for optimization regarding protection against degradation and aggregation during processing, transportation and storage.

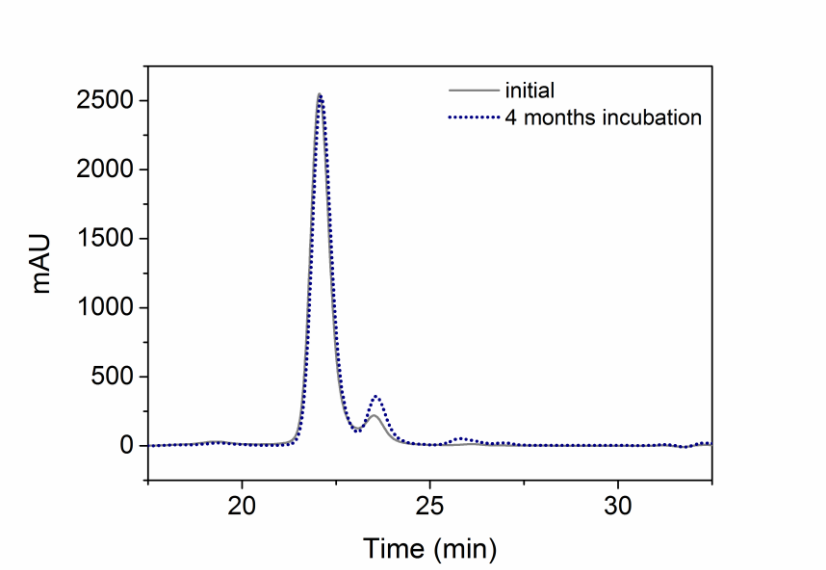

Figure 7: SEC-Chromatogram of hUK-66 drug substance in PBS before (solid grey line) and after (dotted blue line) incubation at 2-8°C over 4 months.

3.3. pH screening study

Besides the definition of the protein concentration and the dosage form (e.g. liquid or freeze-dried), the selection of the pH value is one of the most relevant parameters for defining a formulation [18]. Thus, formulation development is frequently started with determination of the optimal formulation pH value [10] based on detailed characterization of the protein. The formulation pH should be adjusted not only in a range preserving the antibody from chemical degradation, e.g. due to deamidation (basic/acid pH) and oxidation (acidic pH), but also should be as close as possible to the physiological pH of 7.2 to guarantee local tolerability and reduce injection pain [10,18]. Based on analyzed pI and unfolding temperatures, pH 6 appeared to be the most appropriate center-point for a pH stability study. For confirmation of this expected optimal formulation pH, the stability of hUK-66 was evaluated at different pH values centered around pH 6. For this purpose, the mAb was incubated at pH 5, 5.5, 6, 6.5, and 7 at 25°C and 40°C for 4 and 8 weeks, respectively and analyzed afterwards.

Another important aspect is the choice of a suitable buffering agent. Citrate buffer is suspected to cause injection pain when applied subcutaneously [18,51], while phosphate as well as succinate buffer are supposed to lead to a pH shift by selective crystallization of buffer components upon freezing [10,15,18]. Furthermore, acetate buffers are not recommended for lyophilization because of evaporation as acetic acid, resulting in pH shift or loss of excipient. Histidine buffer was chosen as formulation buffer for hUK-66 as it is commonly used for both liquid and freeze-dried IgG formulations [15,18,33]. Furthermore, histidine has a pK_a of 6.0 and hence allowed for sufficient buffer capacity at a pH of 6.0 ± 1.0 [10,33].

3.3.1. Stability of formulation pH during incubation

All pH values stayed constant over the whole period of 8 weeks (**Figure 8**). Small variations observed were probably due to measuring inaccuracies.

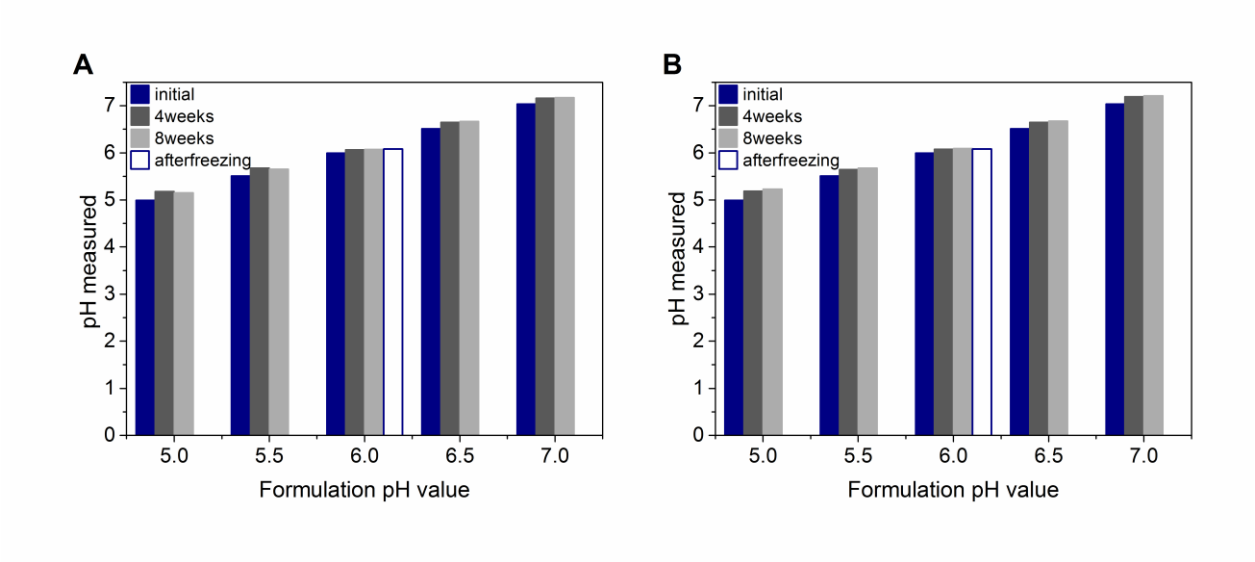

Figure 8: Change of pH after incubation at 25°C (A) and 40°C (B) for 4 (grey bars) and 8 (light grey bars) weeks compared to initial adjusted pH (dark blue bars) as well as after freezing/thawing (white bars).

3.3.2. Determination of hUK-66 concentration after incubation by UV-assay

To detect a potential loss of protein during storage, the concentrations of the pH screening samples were determined by UV-absorption at 280 nm (**Figure 9**). Protein concentrations were ranging between 0.96 and 1.20 mg/ml after incubation at 25°C or 40°C for up to 8 weeks at the different pH values. The slight variations to the initial concentrations of approximately 1.10 mg/ml were probably caused by measuring inaccuracies. Furthermore, protein concentrations might have been influenced by solvent evaporation and/or adsorption to glass vials and stoppers causing small deviations from the initial values. In conclusion, incubation at different pH values had no considerable effect on protein concentration.

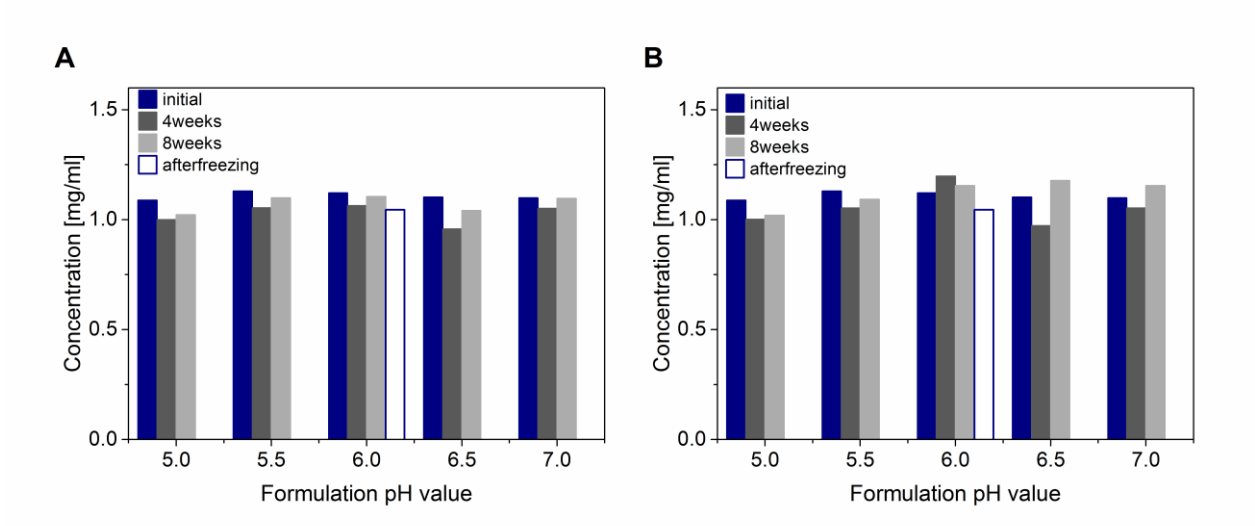

Figure 9: Change in concentration of hUK-66 at different pH values after incubation at 25°C (A) and 40°C (B) for 4 (grey bars) to 8 (light grey bars) weeks and after freezing/thawing (white bars) compared to initial adjusted pH (dark blue bars) determined by UV-absorption at $\lambda = 280$ nm.

3.3.3. Analysis of aggregates by DLS

The protein stability can be characterized by analyzing the formation of aggregates as protein aggregation is probably the most common manifestation of protein instability [25]. Improper formulation conditions can favor partial unfolding or refolding of the protein which may result in aggregation [1]. For analyzing the size of formed aggregates in the nanometer range, particle size distributions and polydispersity indices of hUK-66 were measured after incubation at different pH values for 8 weeks at 25°C and 40 °C (**Figure 10**).

The polydispersity index (PdI) is a parameter characterizing the size distribution width of the particle collective. Applying a scale from 0 to 1, low PdI values such as 0.1 represent narrow size distribution within the sample whereas higher PdIs are considered to indicate polydispersity [52]. The PdIs obtained for all analyzed samples were distinctly below 0.2, therefore a relative monodisperse distribution of hUK-66 and a lack of aggregates could be assumed for all pH conditions (**Figure 10**).

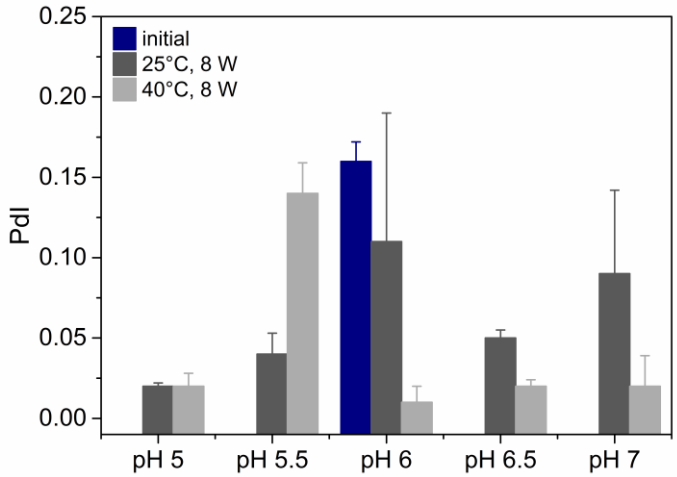

Figure 10: Polydispersity index (PdI) of hUK-66 at the different pH values after incubation for 8 weeks at 25°C (grey bars) and 40°C (light grey bars) in comparison to the initial sample (dark blue bar) analyzed by dynamic light scattering.

3.3.4. Analysis of aggregates, monomer and degradation products by SEC

Furthermore, the loss of monomer and hence the formation of soluble aggregates and degradation products during storage of the mAb at the different pHs was evaluated using size exclusion chromatography (SEC).

Based on the total peak area obtained by SEC analysis, hUK-66 content could be assessed for all storage conditions (**Figure 11**). Due to centrifugation prior to chromatography, insoluble precipitates and particles were removed. Therefore, the slight loss of protein that occurred after 4 and 8 weeks at pH 5 and 6.5 may be assigned to formation of insoluble aggregates.

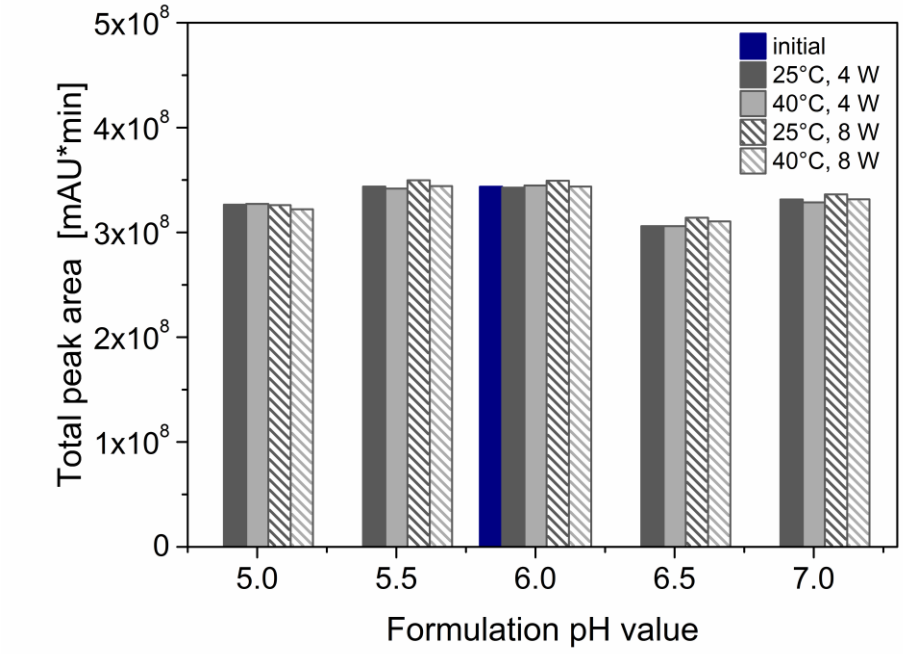

Figure 11: Total peak area of hUK-66 at the different pH values after incubation for 4 (filled bars) and 8 weeks (striped bars) at 25°C (grey) and 40°C (light grey) in comparison to the initial amount of hUK-66 (dark blue bar) analyzed by SEC.

On the other hand, at pH 5.5 and pH 6 the total peak area and therefore the concentration of anti-IsaA mAb stayed constant compared to the initial protein content. Following, no loss caused by formation of insoluble aggregates could be observed. Additionally, almost no formation of soluble aggregates was observed over the incubation period at both temperatures (**Figure 12**). This indicated a very good stability in the chosen histidine buffer and corroborated the DLS results. Nevertheless, the amount of degradation products increased at all pH values during incubation at 40°C. Especially at pH 5, substantial formation of degradation products was observed at elevated storage temperature.

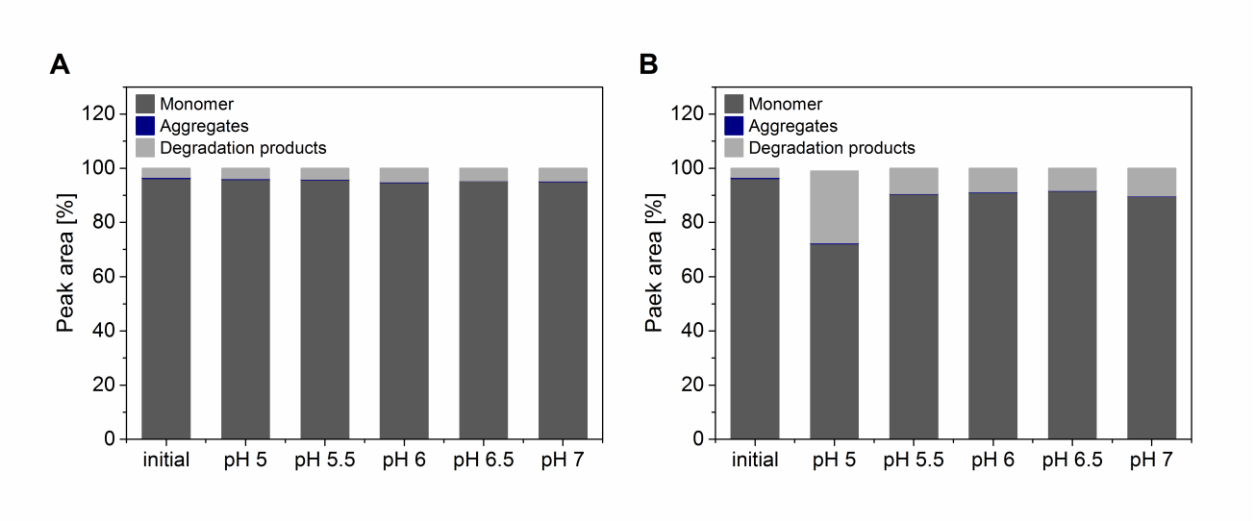

Figure 12: Relative percentage of monomer (grey), aggregates (dark blue) and degradation products (light grey) of hUK-66 after storage for 8 weeks at 25°C (A) and 40°C (B) at different pH values.

3.3.5. Analysis of protein variants using CEX

To monitor stability and heterogeneity of the mAb as well as protein deamidation and the variety of degradation products at the different pH values, cation exchange chromatography (CEX) was used. The protein was separated by charge using this chromatographic method, hence acidic variants were eluting before basic ones.

At 25°C storage temperature, the protein stability was preserved quite well as the area of the main peak remained relatively constant over 8 weeks (**Figure 13A**). Nevertheless, a clear formation of acidic variants at pH 7 accompanied with loss of main peak and basic variants could be noticed. In contrast, at 40°C significant degradation of the main peak and corresponding formation of acidic variants occurred for all pH values (**Figure 13B**). However, at pH 5.5 and pH 6 the extent of degradation was reduced compared to the other pH values whereas at pH 7 the main peak was almost fully degraded.

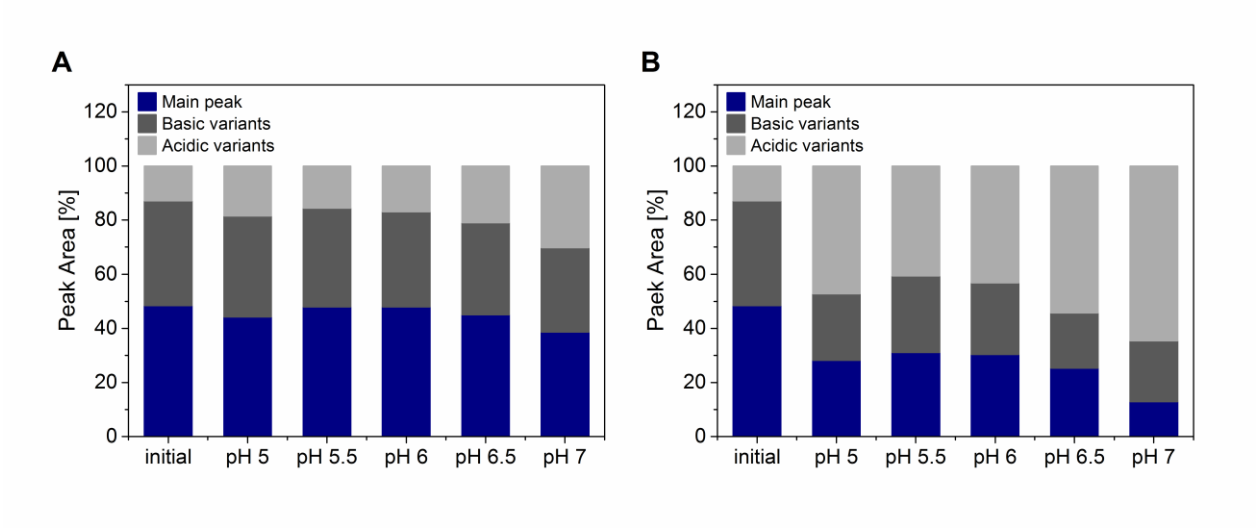

Figure 13: Relative percentage of main peak, basic, and acidic variants of hUK-66 at different pH-values after storage for 8 weeks at 25°C (A) and 40°C (B).

As observed in forced degradation under basic conditions during characterization of hUK-66 in chapter 3.1.4, increased peaks in the region of acidic variants according with decreased main peak may be due to deamidation. Especially for pH values above pH 6, deamidation is a likely cause for the development of acidic variants as seen before (**Figure 4**). Furthermore, for proteins in general deamidation is the most frequently occurring chemical degradation process [13].

Looking at the chromatographic profiles of the different hUK-66 formulations after 8 weeks at 40°C, particularly at pH 5 a clear peak in the area of acidic variants stood out correlating with the emergence of a specific degradation product as demonstrated by SEC results (**Figure 14**

and **Figure 12**). Additionally, the area of the main peak of hUK-66 was clearly decreased for all pH values compared to the mAb at pH 6 before incubation (**Figure 14**). Most notably, at pH 7, the determined pI of hUK-66, the main peak was almost completely degraded.

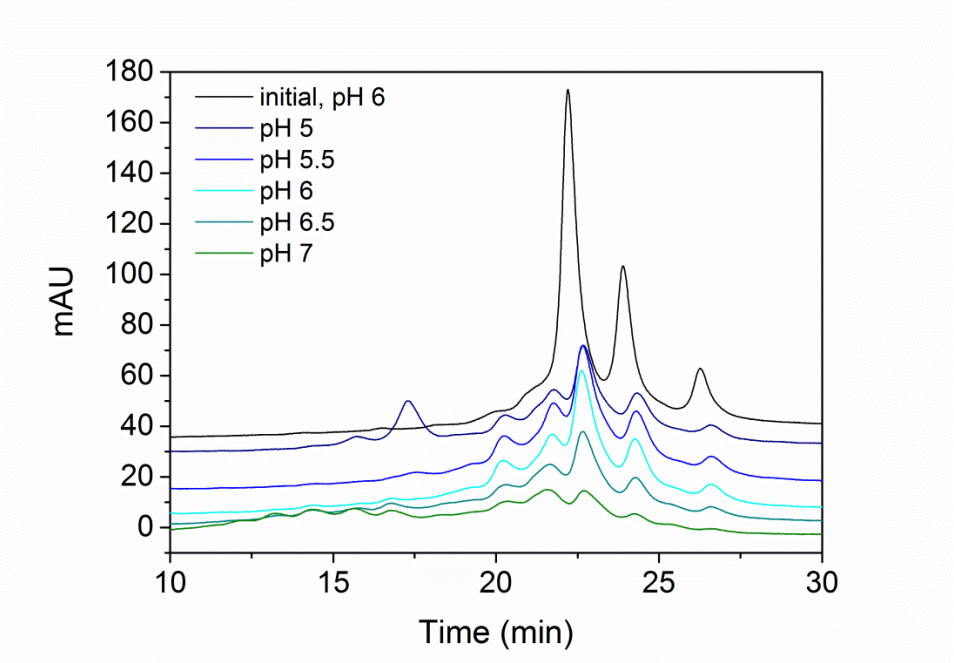

Figure 14: Chromatographic profiles of the different formulations of hUK-66 after 8 weeks at 40°C.

3.3.6. Conclusions from pH screening for the development of a stable hUK-66 formulation

Overall, considering that the storage temperature of the drug product most likely will be 2-8°C, hUK-66 showed good stability in 50 mM histidine buffer in the accelerated stability study as no major changes occurred at 25°C for up to 8 weeks for a formulation pH range from 5 to 7.

However, if the mAb was stored under elevated temperatures (40°C) stability was reduced at all pH values, though to different extents (**Table 4**). Summarizing the results from all analytical methods (**Table 4**), pH 6 proved to be a well applicable pH value for formulation of hUK-66, corresponding well with the results of the pI determination and the analysis of unfolding temperatures at different pH values.

Table 4: Summarized results of analytical characterization of hUK-66 at different formulation pH after incubation for 8 weeks at 40°C compared to the initial mAb before incubation. (+) denotes for results comparable to initial hUK-66 whereas impairments of the results are graded in (-) minor and (- -) major.

Formulation pH of hUK-66	**5.0**	**5.5**	**6.0**	**6.5**	**7.0**
pH stability	+	+	+	+	+
Concentration stability (UV)	+	+	+	+	+
Monodispersity of size distribution (DLS)	+	+	+	+	+
Aggregates (SEC)	+	+	+	+	+
Degradation products (SEC)	- -	-	-	-	-
Acidic variants (CEX)	- -	-	-	- -	- -
Insoluble aggregates (SEC, CEX)	-	+	+	-	-

In addition, also pH 5.5 seemed to be suitable for the development of a parenteral formulation for anti-IsaA monoclonal antibody to guarantee the stability of the protein during storage, corroborating the DSF results. At both pH values, degradation products and acidic variants as well as insoluble aggregates (detectable in loss of total peak area) did not form in the same extent as at other pH values. This is in accordance with the fact that for most antibodies weakly acidic conditions proved to be optimal [10]. However, a formulation pH close to the physiologic pH of 7.2 is considered favorable regarding local tolerability and injection pain. Furthermore, the risk of methionine residue oxidation increases with lower pH value. Therefore, pH 6 was defined as reasonable formulation pH value for hUK-66 [18]. Nevertheless, based on the results for evaluating optimal pH value, hUK-66 formulation required further improvement regarding stability against degradation but also against aggregation during processing, transportation, and storage.

3.4. Long-term stability of liquid and lyophilized hUK-66 formulations

After definition of the optimal formulation pH and buffer, further formulation development regarding dosage form and stabilizing excipients was necessary to define a pharmaceutically acceptable formulation.

To evaluate the influence of the dosage form on stability of hUK-66, liquid and lyophilized formulations were prepared in histidine buffer at pH 6, incubated at refrigerated conditions (2-8°C) for 9 months, and compared regarding their stabilizing potential based on analytical characterization. Stability of liquid formulations was additionally analyzed at accelerated conditions (25°C).

Simultaneously, variations of excipients within the respective formulations were included in the long-term formulation screening to find the overall optimal formulation for hUK-66. Regarding the choice of excipients, the nonionic surfactant polysorbate 20 was used for both liquid and lyophilized formulations as stabilizer against aggregation due to interfacial stresses. However, its potential to induce aggregates upon long-term storage needed to be observed [13,25,26]. Furthermore, polyols are frequently included as stabilizing excipients [5,9,13,22,27–30]. While for the liquid formulation, the best of the three different stabilizers mannitol, trehalose, and sucrose was evaluated for stabilization of hUK-66 in the formulation study, sucrose was chosen for lyophilization since it is a common starting point for formulation development in combination with polysorbate for freeze-drying [15,20]. However, the effect of additional mannitol or glycine on stability of hUK-66 during lyophilization and subsequent storage was analyzed in the long-term formulation study as both are known as bulking agents in diluted protein systems which crystallize during lyophilization and form a strong lyophilization cake [15,21].

For evaluation of hUK-66 stability, different analytical methods were applied. SEC and DLS were carried out to detect and characterize aggregates as well as fragments. UV-Vis spectroscopy was used to monitor changes in protein concentration and CEX was applied to monitor chemical degradation of the mAb due to change in charge heterogeneity.

3.4.1. Stability of formulation pH

Since changes in the pH can lead to aggregation or degradation and proteins are only stable over a narrow pH range, the pH values of the different formulations were measured after defined time points of the long-term formulation study [5]. For all liquid formulations, the adjusted pH value (pH 6) remained constant for 9 months incubation at accelerated (25°C) and real storage conditions (2-8°C) (**Figure 15A**). In addition, also freeze-drying and subsequent storage of the lyophilized formulations at 2-8°C for 9 months did not result in a change of the formulation pH (**Figure 15B**).

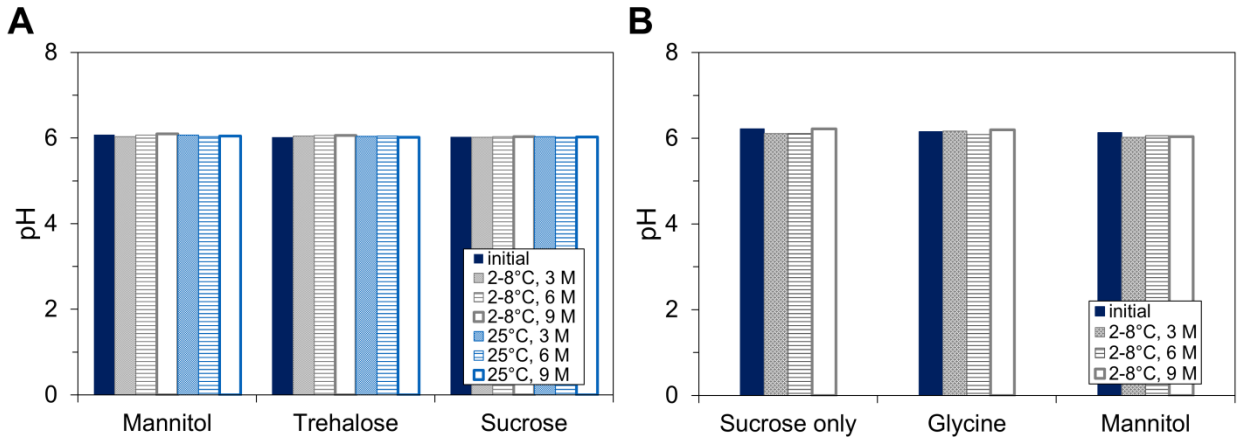

Figure 15: Change in pH of liquid (A) and lyophilized (B) hUK-66 formulations after incubation at 2-8°C (grey bars) or 25°C (light blue bars) for 3 months (patterned bars), 6 months (striped bars), and 9 months (empty bars) compared to the respective initial adjusted pH (dark blue bars).

3.4.2. Stability of hUK-66 concentration

After reconstitution of the lyophilized samples, the reduction of all initial protein concentrations in comparison to later time-points was prominent (**Figure 16B**). This was probably due to dilution of initial samples since the same reconstitution volumes as for later time-points of the respective formulation were added, although the cakes of all initial samples had already become liquid only during short term storage at room temperature after removing from the storage at -80°C. Supposedly, this was caused by presence of moisture, as Carpenter et al. already pointed towards the "unexpected danger" of moisture transfer from the stopper to the cake during storage of lyophilizates [15]. The variations among the concentrations of the lyophilized formulations and the discrepancy to the intended concentration of 40 mg/ml could be explained by inaccuracy during reconstitution with less than 50 µl water along with potential loss of protein due to adsorption at stoppers and vials.

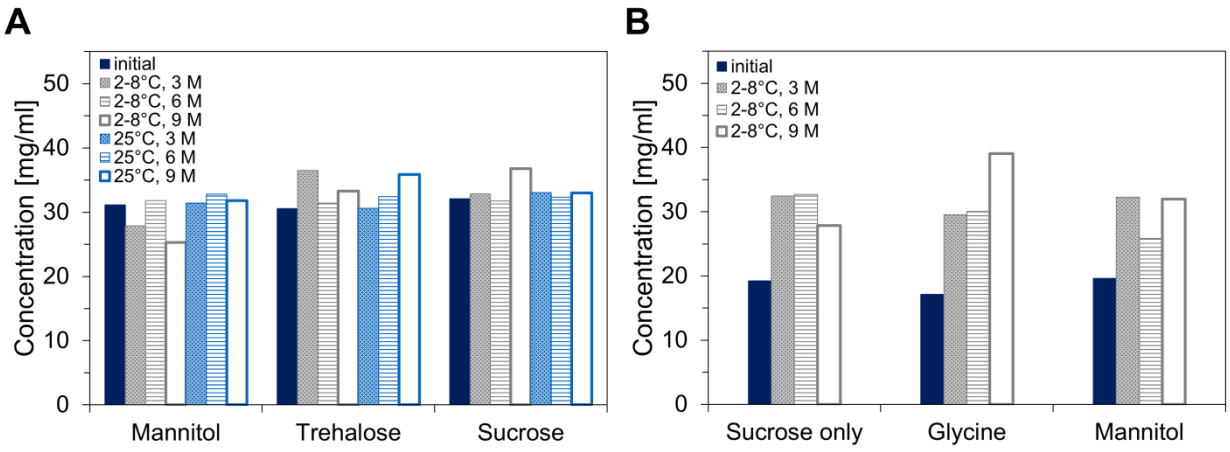

Figure 16: Change in concentration of hUK-66 in liquid (A) and lyophilized (B) formulations after incubation at 2-8°C (grey bars) or 25°C (light blue bars) for 3 (patterned bars), 6 (striped bars), and 9 (empty bars) months compared to initial formulation (dark blue bars) calculated based on absorption of the protein samples at $\lambda = 280$ nm.

Furthermore, no distinct trend within the concentrations of the liquid formulations was recognizable. Slightly more variation in concentration could be observed for liquid formulations stored at refrigerated conditions compared to ambient conditions (**Figure 16A**). Particularly mannitol revealed a distinct decrease in concentration after 9 months storage at 2-8°C. However, no statistical analysis could be performed since only single samples could be analyzed in this study due limited availability of material.

3.4.3. Stability of hUK-66 monomer

Using dynamic light scattering, not only the size of soluble protein aggregates can be analyzed but also the relative size distribution evaluated by monitoring the polydispersity index (PdI). Furthermore, the different formulations can be analyzed without requiring sample preparation like dilution as long as they are optically clear [3].

For liquid and lyophilized formulations of hUK-66, PdIs were below 0.3 over the entire storage time indicating almost monomodal distribution of particle sizes (**Figure 17A** and **B**). Hence, the measured hydrodynamic diameters represented the average sizes of hUK-66 in the respective formulations (**Figure 17C** and **D**). Whereas liquid formulations containing trehalose and sucrose exhibited initial particle sizes of approximately 13 nm, the addition of mannitol resulted in particles more than twice the size (**Figure 17C**). It can be assumed that the presence of mannitol either promoted dimer or oligomer formation of hUK-66 or led to changes in viscosity of the protein sample influencing size measurements by DLS [52]. Since the presence of small soluble aggregates regarding mannitol formulations could not be

confirmed by SEC, dilution of the samples required for UV and HPLC analysis as well as mechanical agitation during processing could have led to dissolution of the agglomerated monomer molecules as seen before [3]. Hence, the aggregates observed for fluid mannitol formulations would have been reversible. Otherwise, the fact that aggregation was not affirmed by SEC corroborated the assumption that mannitol changed the sample viscosity leading to deviations in size measurement by DLS. However, after lyophilization and incubation up to 6 months, DLS analysis of reconstituted mannitol samples displayed mean hydrodynamic diameters of 16 nm (**Figure 17D**) indicating no aggregation just like sucrose only and glycine formulations but contradicting the viscosity hypothesis. In contrast, after 9 months incubation increased particle size was detected. Hence, the only conclusion which can be drawn from these measurements is that mannitol seemed to produce slightly inferior results in size distribution analysis by DLS compared to sucrose only and glycine formulations.

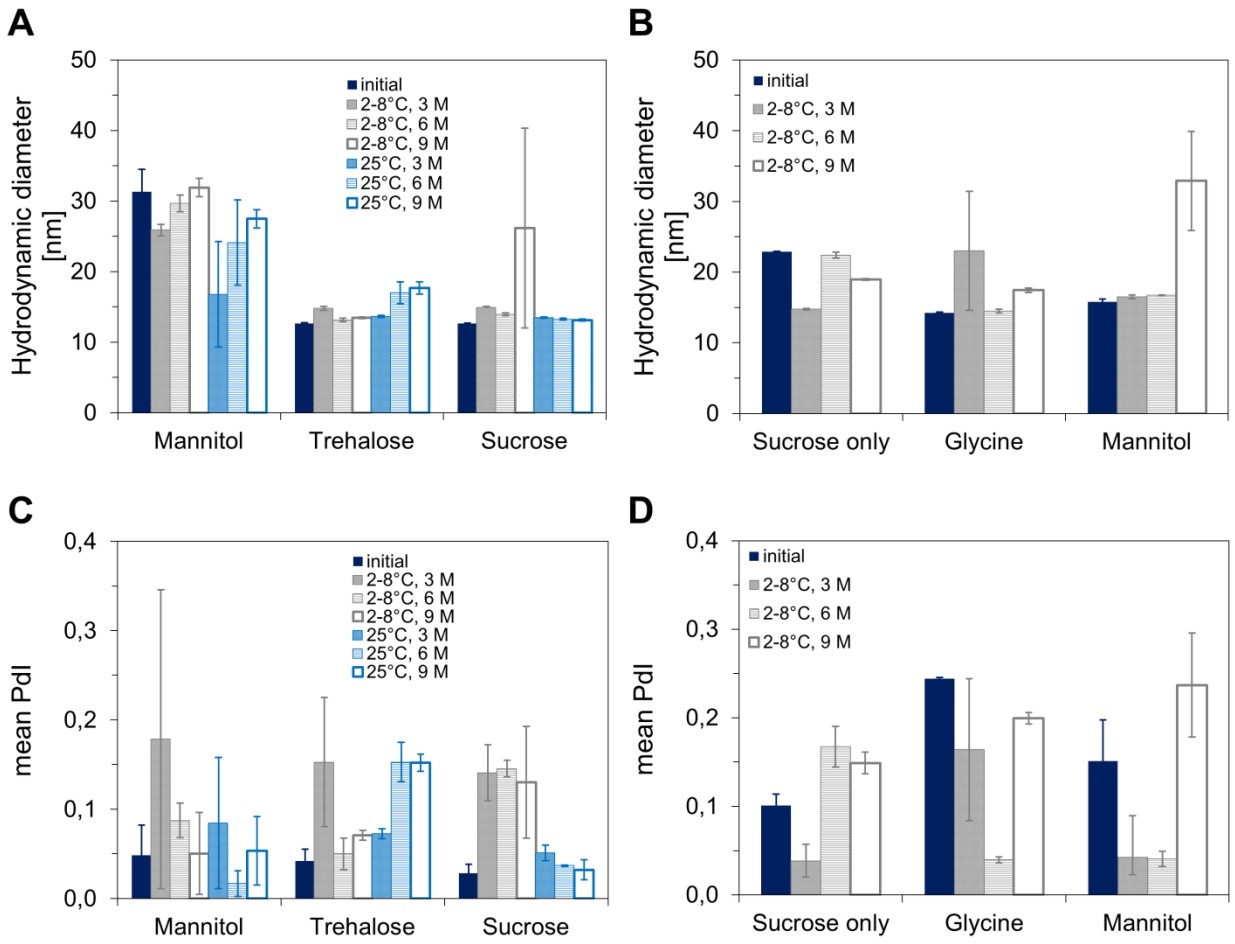

Figure 17: Polydispersity indices and hydrodynamic diameter of liquid (A, C) and lyophilized (B, D) formulations after incubation at 2-8°C (grey bars) or 25°C (light blue bars) for 3 (patterned bars), 6 (striped bars), and 9 months (empty bars) compared to initial formulation (dark blue bars) analyzed by dynamic light scattering.

Using size exclusion chromatography, quantification supplemental to detection of aggregates as well as degradation products and monomer content is enabled [3]. The total peak areas analyzed by SEC confirmed the results of the UV analysis regarding protein concentration of the formulations (**Figure 18A** and **B**). Almost no loss of monomer was observed for liquid and lyophilized formulations at 2-8°C (**Figure 18C**). Only trehalose led to slightly diminished monomer content after 9 months storage at 2-8°C.

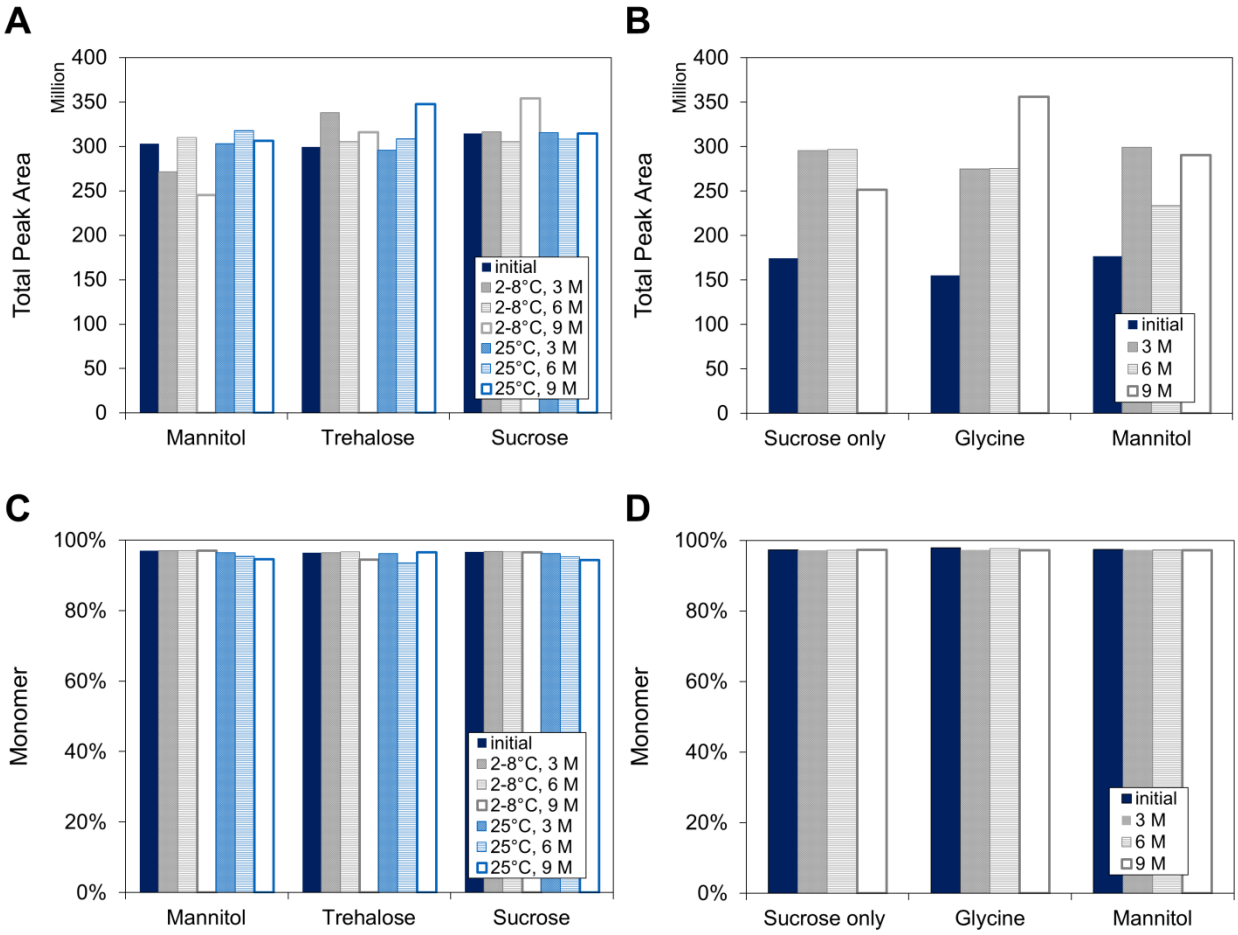

Figure 18: Total peak area and monomer content of liquid (A, C) and lyophilized (B, D) formulations after incubation at 2-8°C (grey bars) or 25°C (light blue bars) for 3 (patterned bars), 6 (striped bars), and 9 (empty bars) months compared to initial formulation (dark blue bars) analyzed by SEC.

Liquid formulations with mannitol and sucrose showed a decreasing trend of monomer proportion over incubation time accompanied by a correlating increase of degradation products particularly when stored at 25°C (**Figure 18C** and **Figure 19C**). In contrast, the addition of trehalose revealed very inconsistent results with already strong formation of degradation products after 9 months at 2-8°C. Lyophilization in presence of sucrose only and additional mannitol prevented the formation of degradation products slightly more efficiently than glycine (**Figure 19D**).

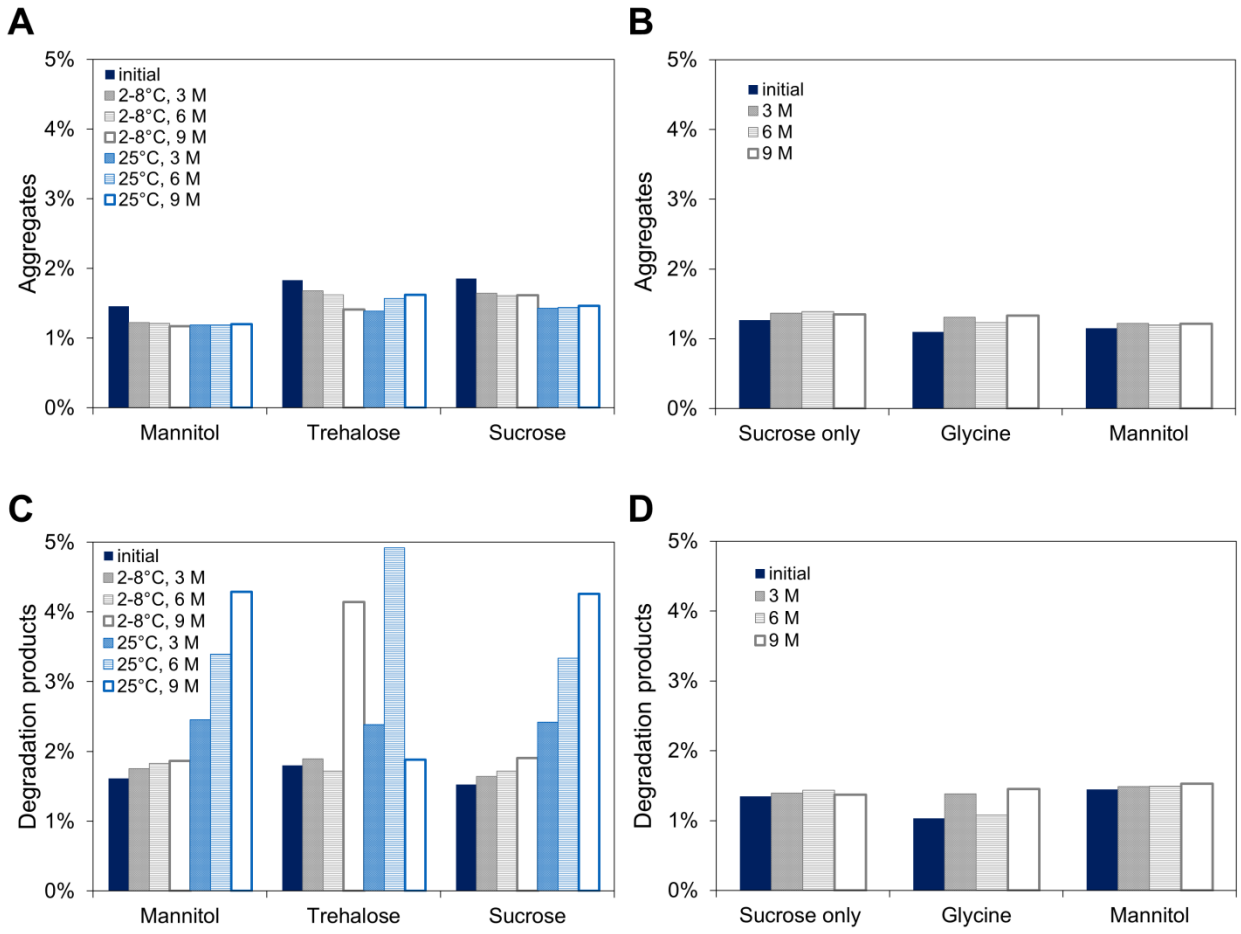

Figure 19: Relative percentage of aggregates and degradation products of liquid (A, C) and lyophilized (B, D) formulations after incubation at 2-8°C (grey bars) or 25°C (light blue bars) for 3 (patterned bars), 6 (striped bars), and 9 (empty bars) months compared to initial formulation (dark blue bars) analyzed by SEC.

Interestingly, fewer aggregates were detected after initial sample preparation for lyophilized formulations compared to liquid formulations (**Figure 19A** and **B**). This observation was attributed to different ultra-filtration processes of hUK-66 during sample preparation for both dosage forms which led to different extent of aggregation [8]. However, some of the aggregates initially contained in the liquid formulations dissociated during storage up to 3 months. While the content of aggregates stagnated during further incubation for mannitol and sucrose, storage in presence of trehalose lead to a further decrease of aggregates over time at refrigerated conditions and to an increase at ambient conditions. In contrast, for all lyophilized samples no distinct variation of the aggregation content was observed. Overall, hUK-66 manifested as more susceptible to degradation than to aggregation.

To get a better insight into the degradation of the different formulations and dosage forms, the samples were analyzed using CEX to monitor their charge heterogeneity during long-term

storage (see chapter 3.1.4) [53]. Changes in the main peak of the different formulations and both, acidic as well as basic, variants over time correlated with each other in aqueous conditions. The distinct decrease of the basic variants' summarized peak area during storage at 2-8°C over 9 months was accompanied by an increase of the main peak and the summarized peak area of acidic variants (**Figure 20A, C,** and **E**).

Particularly for trehalose, the correlation of basic and acidic variants was apparent. After an initial high content of basic variants of approximately 40% but only 10% acidic variants, 9 months incubation of the trehalose formulation at 2-8°C resulted in inversion of the proportions with 44% acidic variants and 0% basic variants. Accordingly, the main peak increased by 6 percentage points from 50% to 56%. Hence, for the fluid formulations conversion of hUK-66 basic variants occurred primarily into acidic variants along with incubation in aqueous environment.

Elevated storage temperatures of 25°C dramatically increased the formation of acidic variants in the liquid formulations and thus favored the chemical degradation of the protein potentially by deamidation. Whereas during incubation at 2-8°C the content of acidic variants increased only by up to 3 percentage points from 12% to 15% after 9 months for the liquid formulations of mannitol and sucrose, incubation at 25°C led to an substantially increased acidic variant content of 27% for mannitol and 47% for sucrose after 9 months. However, formation of acidic variants induced by high-temperature during accelerated stability studies need to be interpreted cautiously since deamidation can be preferentially accelerated with increasing temperature [10].

In contrast, lyophilization preserved the initial ratios of main peak, acidic and basic variants very well (**Figure 20B, D**, and **F**). No distinct changes of the main peak could be detected for the lyophilized samples over 9 months storage at 2-8°C for all formulations. After 9 months, the level of acidic variants increased in presence of glycine by 1.3 percentage points whereas the presence of mannitol or no additional excipient led to constant levels of chemical degradation products.

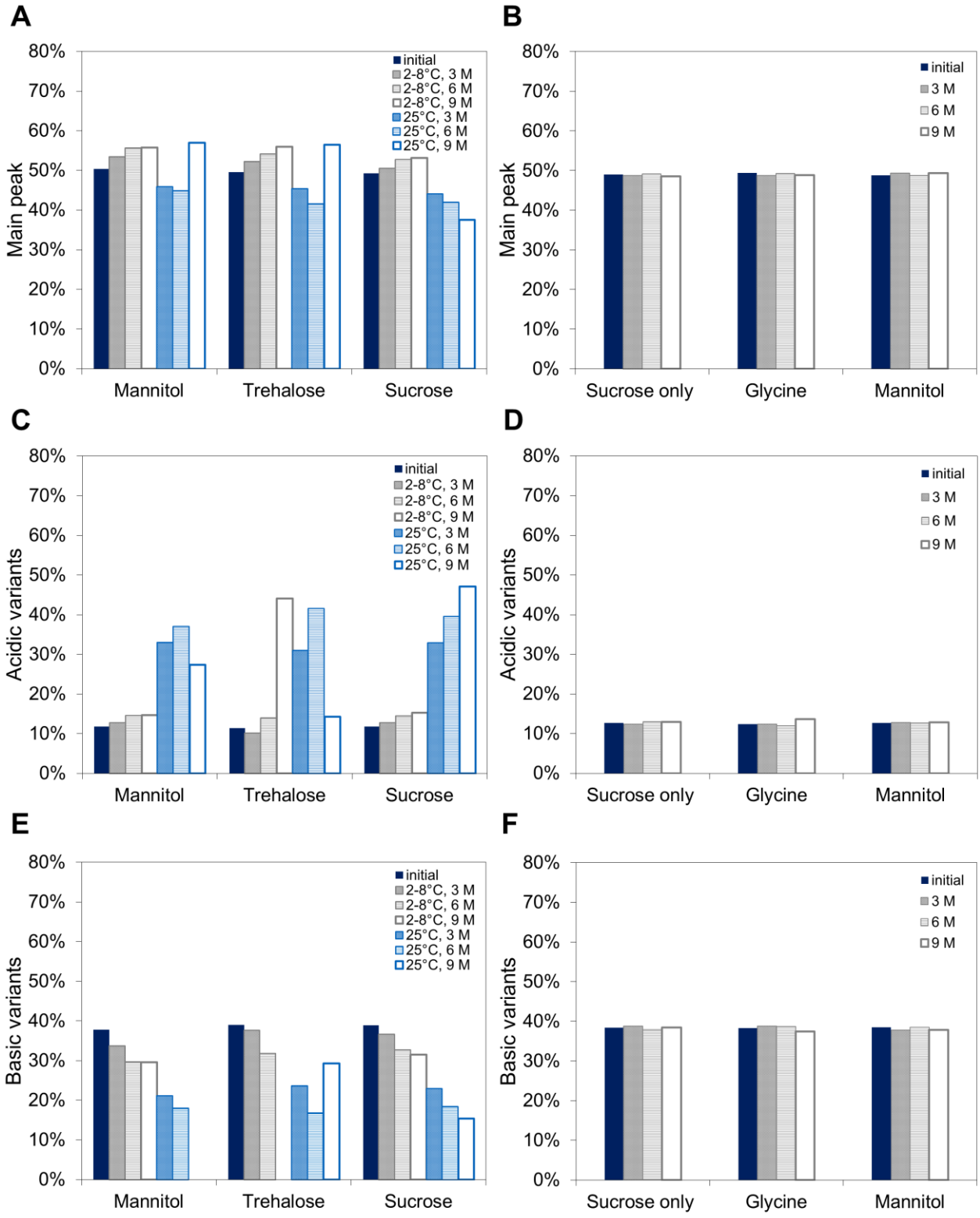

Figure 20: Relative percentage of main peak, acidic, and basic variants of liquid (A, C, E) and lyophilized (B, D, F) formulations after incubation at 2-8°C (grey bars) or 25°C (light blue bars) for 3 (patterned bars), 6 (striped bars), and 9 (empty bars) months compared to initial formulation (dark blue bars) analyzed by CEX.

3.4.4. Conclusions from long-term stability study for hUK-66 formulation development

Summarizing the results of the long-term formulation screening, hUK-66 proved to be relatively stable in a formulation consisting of polysorbate, polyol and histidine buffer at pH 6 in both dosage forms, liquid and lyophilized, for up to 9 months at the intended storage conditions of 2-8°C.

Physical instabilities due to aggregation during handling, freeze-drying, and storage could be minimized by addition of polysorbate (**Table 5**). However, it was concluded that hUK-66 is sensitive to chemical degradation particularly in aqueous environments. Storage at elevated temperatures exacerbated deamidation in liquid formulations. In contrast, lyophilization protected hUK-66 quite efficiently from chemical degradation by minimizing hydrolytic reactions due to removal of water [9].

With respect to these observations, the formulations can be ranked as follows: lyophilized formulations were superior to liquid formulations because of prevention of chemical degradation of the protein. Within the liquid formulations, the presence of trehalose was less successful regarding stabilization of hUK-66 against deamidation than mannitol or sucrose since immense formation of acidic variants was observed already at 2-8°C after 9 months. The content of acidic variants increased by 32 percentage points for the trehalose formulation compared to only 3 percentage points for mannitol and sucrose. Mannitol was slightly inferior to sucrose and trehalose regarding particle size after formulation preparation detected by dynamic light scattering in the concentrated samples. Within the lyophilized samples, the supplemental components mannitol and glycine could not improve the stability of hUK-66 in comparison to sucrose alone, which is in accordance with prior observations [10].

Since only as many excipients as necessary should be used for protein stabilization [15], the best formulation for the monoclonal antibody hUK-66 consisted of sucrose and polysorbate in histidine buffer at pH 6 and optimal dosage form stability was observed for lyophilizates.

Since the developed formulation for hUK-66 lead to vanishingly small aggregate formation over the long-term stability study of 9 months, the shelf life of hUK-66 cannot be estimated as the slope of the regression line revealed no statistically significant difference from zero. Incubation studies needed to be prolonged until a pronounced aggregation can be measured for the assessment of the shelf life of hUK-66.

Table 5: Overview of the results of the different formulations of hUK-66 after incubation for 3, 6, and 9 months compared to the initial mAb before incubation. (+) denotes for results comparable to initial hUK-66 whereas impairments of the results are graded in (-) minor and (- -) major.

Formulation of mAb	Liquid Mannitol	Liquid, Trehalose	Liquid, Sucrose	Lyo, Sucrose only	Lyo, Glycine	Lyo, Mannitol
pH stability	+	+	+	+	+	+
Concentration stability	+	+	+	+	+	+
Monodispersity (DLS)	-	+	+	+	+	-
Insoluble aggregates (SEC)	+	+	+	+	+	+
Aggregates (SEC)	+	-	+	+	+	+
Degradation products (SEC)	-	- -	-	+	-	+
Acidic variants (CEX)	-	- -	-	+	-	+
Basic variants (CEX)	-	- -	-	+	+	+

4. Summary and conclusion

The goal of this study was to develop a formulation for hUK-66 stabilizing its native protein conformation against numerous stresses occurring during final production steps, processing, shipping, and long-term storage of the biopharmaceutical product.

Since every protein has individual stabilization demands, detailed knowledge of its distinctive physicochemical properties is important for stabilization [15]. Hence, hUK-66 characterization regarding drug substance stability, possible degradation profiles, isoelectric point (pI), and thermal stability at different pH values paved the way for formulation development. High unfolding temperatures of the two antibody domains at pH 5.5 and pH 6 indicated stabilizing conditions for hUK-66. Considering these results and hUK's pI of pH 7, pH 6 was selected as an adequate pH-value for conducting a formulation pH screening. In a short-term storage stability study over 8 weeks, the pH for hUK-66 in histidine buffer was optimized in a range from pH 5 to 7 regarding mAb stability in relation to pH and elevated temperature under accelerated and stressed conditions. Under stressed conditions at 40°C the mAb turned out to be highly predisposed for deamidation in aqueous surroundings over the whole pH range. Particularly at both ends of the analyzed pH range (pH 5 and 7), the mAb was susceptible to degradation into acidic variants whereas at pH 5.5 and 6 chemical degradation was reduced compared to the other conditions.

As degradative reactions can be slowed in a dried state by restricting protein conformational mobility and reducing hydrolytic reactions due to removal of water [9,15], lyophilization of hUK-66 was assessed in terms of stabilizing capability in comparison to aqueous liquid formulation for the selected formulation pH of 6 in a long-term stability study over 9 months.

The evaluation of the influence of different excipients (polysorbate, sucrose, mannitol, trehalose, and glycine) on the formation of aggregates and degradation products dependent on the dosage form revealed that all analyzed formulations prevented formation of aggregates for both liquid and lyophilized formulations which was probably attributable to the presence of polysorbate. However, only freeze-drying and subsequent storage as dried solid at 2-8°C protected the antibody from chemical degradation. The addition of bulking agents like mannitol or glycine was not required to obtain a stable lyophilized formulation.

Thus, it was concluded that for stabilization of hUK-66, lyophilization in histidine buffer, pH 6, in combination with the two stabilizing excipients sucrose and polysorbate 20 is recommended to be applied to achieve a protection of the protein's native structure and hence its therapeutic activity throughout the formulation process as well as long-term storage at 2-8°C.

References

[1] S. Frokjaer, D.E. Otzen, Protein drug stability: a formulation challenge., Nat. Rev. Drug Discov. 4 (2005) 298–306. doi:10.1038/nrd1695.

[2] A.S. Rosenberg, Effects of protein aggregates: an immunologic perspective., AAPS J. 8 (2006) E501–7. doi:10.1208/aapsj080359.

[3] H. Mahler, W. Friess, U. Grauschopf, S. Kiese, Protein aggregation: pathways, induction factors and analysis., J. Pharm. Sci. 98 (2009) 2909–34. doi:10.1002/jps.21566.

[4] W. Wang, S. Nema, D. Teagarden, Protein aggregation-pathways and influencing factors., Int. J. Pharm. 390 (2010) 89–99. doi:10.1016/j.ijpharm.2010.02.025.

[5] W. Wang, Instability, stabilization, and formulation of liquid protein pharmaceuticals., Int. J. Pharm. 185 (1999) 129–88. doi:10.1016/S0378-5173(99)00152-0.

[6] S.J. Shire, Formulation and manufacturability of biologics., Curr. Opin. Biotechnol. 20 (2009) 708–14. doi:10.1016/j.copbio.2009.10.006.

[7] J. den Engelsman, P. Garidel, R. Smulders, H. Koll, B. Smith, S. Bassarab, et al., Strategies for the assessment of protein aggregates in pharmaceutical biotech product development., Pharm. Res. 28 (2011) 920–33. doi:10.1007/s11095-010-0297-1.

[8] J.S. Bee, T.W. Randolph, J.F. Carpenter, S.M. Bishop, M.N. Dimitrova, Effects of surfaces and leachables on the stability of biopharmaceuticals., J. Pharm. Sci. 100 (2011) 4158–70. doi:10.1002/jps.22597.

[9] S.J. Shire, Z. Shahrokh, J. Liu, Challenges in the development of high protein concentration formulations., J. Pharm. Sci. 93 (2004) 1390–402. doi:10.1002/jps.20079.

[10] W. Wang, S. Singh, D.L. Zeng, K. King, S. Nema, Antibody structure, instability, and formulation., J. Pharm. Sci. 96 (2007) 1–26. doi:10.1002/jps.20727.

[11] J.F. Carpenter, T.W. Randolph, W. Jiskoot, D.J.A. Crommelin, C.R. Middaugh, G. Winter, et al., Overlooking subvisible particles in therapeutic protein products: gaps that may compromise product quality., J. Pharm. Sci. 98 (2009) 1201–5. doi:10.1002/jps.21530.

[12] V. Filipe, A. Hawe, H. Schellenkens, W. Jiskoot, Aggregation and Immunogenicity of Therapeutic Proteins, in: W. Wang, C.J. Roberts (Eds.), Aggreg. Ther. Proteins, John Wiley & Sons, Inc., Hoboken, NJ, USA, 2010. doi:10.1002/9780470769829.

[13] M.C. Manning, D.K. Chou, B.M. Murphy, R.W. Payne, D.S. Katayama, Stability of protein pharmaceuticals: an update., Pharm. Res. 27 (2010) 544–75. doi:10.1007/s11095-009-0045-6.

[14] S.P. Hertel, G. Winter, W. Friess, Protein stability in pulmonary drug delivery via nebulization., Adv. Drug Deliv. Rev. 93 (2015) 79–94. doi:10.1016/j.addr.2014.10.003.

[15] J.F. Carpenter, M.J. Pikal, B.S. Chang, T.W. Randolph, Rational design of stable lyophilized protein formulations: some practical advice., Pharm. Res. 14 (1997) 969–75. doi:10.1023/A:1012180707283.

[16] T. Arakawa, S.J. Prestrelski, W.C. Kenney, J.F. Carpenter, Factors affecting short-term and long-term stabilities of proteins., Adv. Drug Deliv. Rev. 46 (2001) 307–26. doi:10.1016/S0169-409X(00)00144-7.

[17] L.L. Chang, M.J. Pikal, Mechanisms of protein stabilization in the solid state., J. Pharm. Sci. 98 (2009) 2886–908. doi:10.1002/jps.21825.

[18] H.-C. Mahler, G. Borchert, H.L. Luessen, Protein Pharmaceuticals: Formulation, Analytics and Delivery, 1st ed., Editio Cantor Verlag für Medizin und Naturwissenschaften GmbH, Aulendorf, Germany, 2010.

[19] M.J. Pikal, K.M. Dellerman, M.L. Roy, R.M. Riggin, The effects of formulation variables on the stability of freeze-dried human growth hormone., Pharm. Res. 8 (1991) 427–36.

[20] N. Radmanovic, T. Serno, S. Joerg, O. Germershaus, Understanding the freezing of biopharmaceuticals: first-principle modeling of the process and evaluation of its effect on product quality., J. Pharm. Sci. 102 (2013) 2495–507. doi:10.1002/jps.23642.

[21] M.J. Pikal, Freeze drying, in: Encycl. Pharm. Technol. Third Ed., Taylor & Francis Group, LLC, 2002. doi:10.1081/E-EPT3-100001712.

[22] E.Y. Chi, S. Krishnan, T.W. Randolph, J.F. Carpenter, Physical stability of proteins in aqueous solution: mechanism and driving forces in nonnative protein aggregation., Pharm. Res. 20 (2003) 1325–36. doi:10.1023/A:1025771421906.

[23] H.-C. Mahler, R. Müller, W. Frieβ, A. Delille, S. Matheus, Induction and analysis of aggregates in a liquid IgG1-antibody formulation., Eur. J. Pharm. Biopharm. 59 (2005) 407–417. doi:10.1016/j.ejpb.2004.12.004.

[24] B.S. Chang, B.S. Kendrick, J.F. Carpenter, Surface-induced denaturation of proteins during freezing and its inhibition by surfactants., J. Pharm. Sci. 85 (1996) 1325–30. doi:10.1021/js960080y.

[25] W. Wang, Protein aggregation and its inhibition in biopharmaceutics., Int. J. Pharm. 289 (2005) 1–30. doi:10.1016/j.ijpharm.2004.11.014.

[26] W. Wang, Y.J. Wang, D.Q. Wang, Dual effects of Tween 80 on protein stability., Int. J. Pharm. 347 (2008) 31–8. doi:10.1016/j.ijpharm.2007.06.042.

[27] S.N. Timasheff, The control of protein stability and association by weak interactions with water: how do solvents affect these processes?, Annu. Rev. Biophys. Biomol. Struct. 22 (1993) 67–97. doi:10.1146/annurev.bb.22.060193.000435.

[28] B.S. Kendrick, B.S. Chang, T. Arakawa, B. Peterson, T.W. Randolph, M.C. Manning, et al., Preferential exclusion of sucrose from recombinant interleukin-1 receptor antagonist: role in restricted conformational mobility and compaction of native state., Proc. Natl. Acad. Sci. U. S. A. 94 (1997) 11917–22.

[29] J.C. Lee, S.N. Timasheff, The stabilization of proteins by sucrose., J. Biol. Chem. 256 (1981) 7193–201.

[30] J.F. Carpenter, J.H. Crowe, The mechanism of cryoprotection of proteins by solutes., Cryobiology. 25 (1988) 244–55.

[31] J.F. Carpenter, J.H. Crowe, T. Arakawa, Comparison of solute-induced protein stabilization in aqueous solution and in the frozen and dried states., J. Dairy Sci. 73 (1990) 3627–3636. doi:10.3168/jds.S0022-0302(90)79065-0.

[32] S. Ohtake, Y. Kita, T. Arakawa, Interactions of formulation excipients with proteins in solution and in the dried state., Adv. Drug Deliv. Rev. 63 (2011) 1053–73. doi:10.1016/j.addr.2011.06.011.

[33] B. Chen, R. Bautista, K. Yu, G. a Zapata, M.G. Mulkerrin, S.M. Chamow, Influence of histidine on the stability and physical properties of a fully human antibody in aqueous and solid forms., Pharm. Res. 20 (2003) 1952–60. doi:10.1023/B:PHAM.0000008042.15988.c0.

[34] N.K. Jain, I. Roy, Effect of trehalose on protein structure., Protein Sci. 18 (2009) 24–36. doi:10.1002/pro.3.

[35] B. Oesterreich, B. Lorenz, T. Schmitter, R. Kontermann, M. Zenn, B. Zimmermann, et al., Characterization of the biological anti-staphylococcal functionality of hUK-66 IgG1, a humanized monoclonal antibody as substantial component for an immunotherapeutic approach., Hum. Vaccin. Immunother. 10 (2014) 926–37. doi:10.4161/hv.27692.

[36] ExPASy ProtParam tool, Accessed:23-04-2013, Http://web.expasy.org/protparam/. (2013). www.expasy.org.

[37] H.T.S. Britton, R.A. Robinson, CXCVIII.—Universal buffer solutions and the dissociation constant of veronal., J. Chem. Soc. (1931) 1456–1462. doi:10.1039/JR9310001456.

[38] F.H. Niesen, H. Berglund, M. Vedadi, The use of differential scanning fluorimetry to detect ligand interactions that promote protein stability., Nat. Protoc. 2 (2007) 2212–21. doi:10.1038/nprot.2007.321.

[39] M.A.H. Capelle, R. Gurny, T. Arvinte, High throughput screening of protein formulation stability: Practical considerations., Eur. J. Pharm. Biopharm. 65 (2007) 131–148. doi:10.1016/j.ejpb.2006.09.009.

[40] A.W.P. Vermeer, W. Norde, A. van Amerongen, The unfolding/denaturation of immunogammaglobulin of isotype 2b and its F(ab) and F(c) fragments., Biophys. J. 79 (2000) 2150–2154. doi:10.1016/S0006-3495(00)76462-9.

[41] Dionex Corporation, Monitoring Monoclonal Antibody Stability by Cation-Exchange Chromatography, Application Note 128 (http://www.dionex.com/en-us/webdocs/4473-AN128-Monitoring-Monoclonal-Antibody-02Feb07-LPN1052-01.pdf), Sunnyvale, CA, USA. (2009) 1–7.

[42] Dionex Corporation, Monitoring Monoclonal Antibody Heterogeneity by Cation-Exchange Chromatography, Application Note 127 (http://www.dionex.com/en-us/webdocs/4470-AN127-Cation-Exchange-Chromatography-02Feb09-LPN1047-01.pdf), Sunnyvale, CA, USA. (2009) 1–5.

[43] S. Yadav, J. Liu, S.J. Shire, D.S. Kalonia, Specific interactions in high concentration antibody solutions resulting in high viscosity., J. Pharm. Sci. 99 (2010) 1152–68. doi:10.1002/jps.21898.

[44] A. Hawe, W. Friess, Development of HSA-free formulations for a hydrophobic cytokine with improved stability., Eur. J. Pharm. Biopharm. 68 (2008) 169–182. doi:10.1016/j.ejpb.2007.04.018.

[45] A. Hawe, M. Wiggenhorn, M. van de Weert, J.H.O. Garbe, H.-C. Mahler, W. Jiskoot, Forced degradation of therapeutic proteins., J. Pharm. Sci. 101 (2012) 895–913. doi:10.1002/jps.22812.

[46] A. Hawe, M. Sutter, W. Jiskoot, Extrinsic fluorescent dyes as tools for protein characterization., Pharm. Res. 25 (2008) 1487–99. doi:10.1007/s11095-007-9516-9.

[47] R.J. Harris, Processing of C-terminal lysine and arginine residues of proteins isolated from mammalian cell culture., J. Chromatogr. A. 705 (1995) 129–34. doi:http://dx.doi.org/10.1016/0021-9673(94)01255-D.

[48] B. Antes, S. Amon, A. Rizzi, S. Wiederkum, M. Kainer, O. Szolar, et al., Analysis of lysine clipping of a humanized Lewis-Y specific IgG antibody and its relation to Fc-mediated effector function., J. Chromatogr. B. Analyt. Technol. Biomed. Life Sci. 852 (2007) 250–6. doi:10.1016/j.jchromb.2007.01.024.

[49] X. Kang, J.P. Kutzko, M.L. Hayes, D.D. Frey, Monoclonal antibody heterogeneity analysis and deamidation monitoring with high-performance cation-exchange chromatofocusing using simple, two component buffer systems., J. Chromatogr. A. 1283 (2013) 89–97. doi:10.1016/j.chroma.2013.01.101.

[50] M. Weitzhandler, D. Farnan, J. Horvath, J.S. Rohrer, R.W. Slingsby, N. Avdalovic, et al., Protein variant separations by cation-exchange chromatography on tentacle-type polymeric stationary phases., J. Chromatogr. A. 828 (1998) 365–72. doi:10.1016/S0021-9673(98)00521-4.

[51] T. Laursen, B. Hansen, S. Fisker, Pain perception after subcutaneous injections of media containing different buffers., Basic Clin. Pharmacol. Toxicol. 98 (2006) 218–21. doi:10.1111/j.1742-7843.2006.pto_271.x.

[52] M. Gaumet, A. Vargas, R. Gurny, F. Delie, Nanoparticles for drug delivery: the need for precision in reporting particle size parameters., Eur. J. Pharm. Biopharm. 69 (2008) 1–9. doi:10.1016/j.ejpb.2007.08.001.

[53] R. Bischoff, B. Barroso, Liquid Chromatography, in: W. Jiskoot, D.J.A. Crommelin (Eds.), Methods Struct. Anal. Protein Pharamceuticals., American Association of Pharmaceutical Scientists, Airlington, USA, 2005: pp. 277–329.

CHAPTER IV

NEBULIZATION OF THE HUMANIZED MONOCLONAL ANTIBODY UK-66 – PHYSICOCHEMICAL STABILITY AND *IN VIVO* EFFICACY

Unpublished manuscript.

Abstract

To deliver proteins via the lung, generation of an inhalable aerosol is required. However, during the process of nebulization the air-liquid interface is substantially increased exposing biomolecules to intensive interfacial stress. Therefore, the previously developed hUK-66 formulations were studied for their suitability to stabilize the antibody during air-jet nebulization. Considering the large sample volumes required for nebulization, an *in vitro* surrogate method simulating the nebulization stress was developed in order to reduce drug substance consumption. A formulation of hUK-66 comprising sucrose and polysorbate 20 proved to preserve the protein stability during the preliminary study as well as the real nebulization process. Furthermore, it was shown that nebulization had no adverse effect on the chemical stability of the antibody. Finally, the immunotherapeutic efficacy of the hUK-66 formulation administered via inhalation was proven by prolonged survival of mice infected intranasally with *S. aureus*. For this *in vivo* study a special set up to enable aerosol delivery to mice being awake and breathing normally has been developed. An additional advantage of this setup was nose-only exposure which reduced the disadvantages of whole body exposure such as adsorption over the skin and large amount of aerosol needed. Altogether, multiple nebulization and intense recirculation of the protein solution within the reservoir had no major effect on conformational stability of the antibody. Hence, the hUK-66 formulation proofed to be stable during nebulization. Furthermore, its immuno-therapeutic potential in treating *S. aureus* infections effectively when administered pulmonary was demonstrated in this study.

1. Introduction

The market withdrawal of the first inhalable insulin product Exubera® in 2008, after only 2 years of commercial distribution due to low patient's compliance, disappointing sales, and suspicions about favoring lung cancer, led to concerns and hesitation in the research and development of pulmonary delivery of biopharmaceuticals. In the following time, research in this field had been significantly reduced and the few clinical trials on macromolecules for pulmonary delivery were suspended [1].

However, pulmonary delivery of proteins is still attractive for other indications. Biopharmaceuticals normally are administered via the parenteral route since oral delivery is characterized by low drug absorption and results in inactivation due to gastrointestinal enzymes as well as adverse pH conditions in the gastrointestinal tract [2–6]. The advantage of pulmonary over parenteral administration is the non-invasive way of application improving patient comfort by avoiding injection pain [2]. Based on the large surface area of alveoli, the short diffusion path through the thin alveolar epithelium into the blood circulation without first-pass effect, and the elevated blood perfusion of the lung, proteins have a higher systemic absorption rate in the lung compared to other non-invasive routes like sublingual, oral, nasal, or transdermal administration [1,3–5,7,8]. Additionally, inhalation of biopharmaceuticals is a convenient way to treat lung diseases more effectively and safely due to induction of high local concentrations at the desired site of action and reduction of side effects by lowered systemic drug exposure [1,4,5,9].

Therefore, in the last years pulmonary delivery of proteins is regaining attention. Even the systemic delivery of insulin via the lung made a promising comeback by the market launch of Afrezza® by Mannkind Corporation and Sanofi in the United States in February 2015. Learning from the failure of Exubera® and its limitations, the inhaler size was reduced and the bioavailability of rapid acting insulin increased. In clinical studies, no severe safety issues were detected. Furthermore, the Technosphere® technology where insulin is precipitated from solution onto diketopiperazine carrier particles, enabled adequate aerosol particle size distribution as well as rapid absorption and elimination [1,10,11].

Since drug delivery to the lung is always accomplished by inhalation of an aerosol, a formulation suitable for aerosolization is required to deliver proteins to the lung. There are three possibilities to generate the aerosol for drug inhalation: Nebulizers and pressurized metered dose inhalers (pMDIs) for liquid formulations as well as dry powder inhalers (DPIs) for solid formulations [5,8,9]. Every delivery device has its own advantages and drawbacks, which were reviewed in detail by several authors [4–9,12]. Although nebulization has some

limitations such as relatively large volume of drug solution associated with lengthy application per inhalation, its advantages regarding pulmonary protein delivery are convincing. While the dried state needed for DPI is able to stabilize the protein against chemical degradation such as hydrolysis or deamidation, liquid formulations are easier, cheaper, and faster to develop since no further process steps such as drying are required [9,12]. The application of nebulizers is convenient for patients who have problems using MDIs and DPIs (such as children and elderly people) and it is suitable when formulation of the drug into MDI or DPI is difficult. Regarding this study, the most important benefit is the ability to conveniently deliver drugs to mechanically ventilated patients through nebulization unlike the other inhaler types which require some kind of coordination of breathing and aerosol generation [4,8,9]. Therefore, most biopharmaceuticals that are currently developed for inhalation are intended for nebulization [9,12]. The predominant challenge for formulation development therefore is efficient stabilization of proteins during the aerosolization process. Especially the high air-liquid interface generated during nebulization may detrimentally affect protein stability and was already shown to lead to aggregation and loss of activity for several proteins [13–16]. Furthermore, protein stability is endangered by solvent evaporation, recirculation, and multiple atomization of the protein solution within the air-jet nebulizer reservoir [17,18]. Hence, an optimized formulation is required for each individual protein and applied nebulization technique to preserve the activity of biopharmaceuticals.

In this study, the ability of the previously developed hUK-66 formulations (Chapter III: Development of a stable formulation for the humanized monoclonal antibody UK-66) to stabilize the antibody during air-jet nebulization was examined. Considering the limited availability of the antibody and the entailed costs, an *in vitro* surrogate method simulating the nebulization stress was developed in order to reduce drug substance consumption. The best-performing formulation of this pre-study was submitted to nebulization and its protein stabilizing potential was compared to non-formulated hUK-66. To assess the effect of the nebulization process onto the antibody, the residual protein in the nebulizer reservoir after nebulization as well as the generated aerosol were analyzed. For this purpose, an aerosol collection apparatus was developed to transfer the aerosol into a liquid state and enable thereby analysis by standard methods.

Since the main reason for protein destabilization during nebulization is the generation of a large air-liquid interface during atomization of the protein solution into a fine mist, so far only aggregate formation due to unfolding at the interface has been studied [12]. However, also chemical destabilization, e.g. through oxidation, may occur during nebulization [12].

Therefore, the collected aerosol and the mAb solution from the reservoir were analyzed with regards to chemical degradation in this study.

Finally, to assess the activity and efficacy of the aerosolized hUK-66 formulation an *in vivo* nebulization set up was developed. To date, only few *in vivo* studies on mice regarding pulmonary protein delivery have been conducted [19–21]. In some of these studies, a microsprayer was used for intratracheal aerosol delivery enabling direct administration of a controllable amount of protein into the lower respiratory tract of anaesthetized mice. However, narcotics frequently result in respiratory depression causing slow and shallow breathing contrary to natural breathing behavior. Hence, for the efficacy study of hUK-66 we aimed to develop a nose-only exposure system for physiologically breathing mice circumventing the disadvantages of whole body exposure like adsorption via the skin and large amount of aerosol needed.

2. Materials and methods

2.1. Materials

hUK-66, a humanized monoclonal antibody (mAb) of the IgG1 subclass, targeting the immunodominant staphylococcal antigen A (IsaA) on the surface of *Staphylococcus aureus* [22], was provided in a concentration of 2.8 mg/ml or 9.81 mg/ml in 1 x PBS buffer, pH 7.4, by the Institute for Molecular Infection Biology (University of Wurzburg, Germany). L-Histidine (Reagent Plus® ≥ 99% (TLC)), sucrose (BioUltra, for molecular biology, ≥99.5%), D-mannitol (BioXtra, ≥98%), and polysorbate 20 (PS 20) were purchased from Sigma-Aldrich (Steinheim, Germany) and employed as formulation excipients. Sodium fluorescein was purchased from Sigma Aldrich (Steinheim, Germany). Ultrapure water was used throughout the study (Milli-Q Synthesis Ultrapure Water Purification System, EMD Millipore Corporation, Billerica, USA).

2.2. Preparation of hUK-66 formulations

For preparation of the mAb bulk solution, hUK-66 drug substance was dialyzed against 50 mM histidine buffer (pH 6) and concentrated to approximately 13 mg/ml using an Amicon® stirred ultrafiltration cell 8010 (EMD Millipore Corporation, Billerica, MA, USA). The cell was equipped with a 50 kDa ultrafiltration membrane disk filter (25 mm, PALL® Life Sciences Corporation, Ann Arbor, MI, USA).

Stock solutions of 1% PS 20 and 1 M sugar or sugar alcohol in 50 mM histidine, mAb bulk solution, and the formulation buffer itself were combined to obtain formulations containing 8.5 mg/ml hUK-66, 0.04% polysorbate 20 (PS 20), and 270 mM mannitol or sucrose, respectively (**Table 1**). For preparation of the reference formulation, the drug substance was diluted to a final concentration of 8.5 mg/ml hUK-66 in PBS, pH 7.4. The formulations were sterile filtered using sterile syringe filter units under LAF (0.2 µm, PES membrane, 13 mm diameter, Nalge Nunc International Corporation, Rochester, USA).

Table 1: Overview of applied hUK-66 formulations.

Formulation	**PBS**	**Sucrose**			**Mannitol**		
Excipients	PBS (pH 7.4)	Histidine buffer (pH 6)	0.04 % PS 20	270 mM Sucrose	Histidine buffer (pH 6)	0.04 % PS 20	270 mM Mannitol

2.3. Mechanical shaking stress

0.65 ml polypropylene tubes (SafeSeal micro tubes, Sarstedt AG & Co, Nümbrecht, Germany) filled with 320 µl aliquots of the respective formulations were fixed horizontally on a shaking device (Eppendorf Thermomixer, Eppendorf AG, Hamburg, Germany). Filling the tubes to 50% provided sufficient air for the formation of a large, constantly renewing air-water interface during agitation. Shaking was performed at room temperature applying a speed of 1450 rpm for an overall shaking time of 8 h. After the defined shaking stress intervals of 15 min, 1 h, as well as 8 h, triplicates of each formulation were drawn and stored at 2-8°C. Due to limited availability of hUK-66, only single samples were prepared for all initial reference solutions.

2.4. Nebulization of hUK-66

Nebulization of the protein formulations was conducted using a Pari LC Sprint Star fine droplet nebulizer with a red nozzle attachment in combination with a Pari Boy N compressor (both PARI GmbH, Starnberg, Germany) providing an aerosol droplet size of 2.2 µm mass median diameter (MMD) [23]. Considering the minimum fill volume of 2 ml, the reservoir was loaded with 2 to 4 ml hUK-66 formulation or reference sample, respectively. After operating the nebulization device for 10 min, the influence of nebulization on stability of the protein solution in the reservoir was analyzed. For aerosol characterization experiments, fluorescein sodium was supplementary added as internal standard to the hUK-66 formulation at a concentration of 2 µg/ml. The recovery as well as stability in the aerosol was analyzed after 5 min operation.

2.5. Aerosol collection for characterization

Analytical characterization of the aerosol required a conversion into fluid state. Therefore, a reflux condenser system [16,24] was combined with a glass impinger based on the set up used in the European Pharmacopoeia (Ph. Eur. 2.9.18) as well as by Khatri et al. [25] for aerosol collection (**Figure 1**). The reflux condenser (**Figure 1**, a) was cooled to -5°C using a precooled mixture of 50% ethylene glycol and 50% water. A round bottom flask (**Figure 1**, b) and an ensuing washing flask (**Figure 1**, c) were filled with 5 and 10 ml histidine buffer, respectively, representing first and second collection stage. The generated aerosol was drawn through the collection apparatus by an applied vacuum. The aerosol which condensed on the walls of the reflux condenser dropped into the round bottom flask (collection stage 1; **Figure 1**, b). In contrast, aerosol which was not condensed by the reflux condenser either deposited in the histidine buffer filled in collection stage 1 or, depending on droplet size, was

directed through the collection medium in the washing flask (collection stage 2; **Figure 1**, c). After nebulization, the system was rinsed with 5 ml of buffer. The samples drawn from the nebulizer reservoir, collection stage 1, and 2 were analyzed with regard to mAb stability and recovery in comparison to the initial formulation. The formulation nebulized for analysis of mAb stability in the aerosol, contained 2 mg/ml hUK-66 due to limited availability of material. As the collection process included dilution and the protein concentration may have been changed further by degradation, 2 µg/ml fluorescein sodium (FS) was included as internal standard in the formulation for calculation of collection recovery. The recovery of the internal standard fluorescein sodium in the collection stages was determined by measuring the fluorescence intensity of the collected samples placed into a 96 well plate at an excitation wavelength of 490 nm and emission wavelength of 515 nm using a LS 50 B Fluorescence Spectrometer (Perkin Elmer, Waltham, MA, USA). The percentage recovery of the nebulized protein was assessed by SEC.

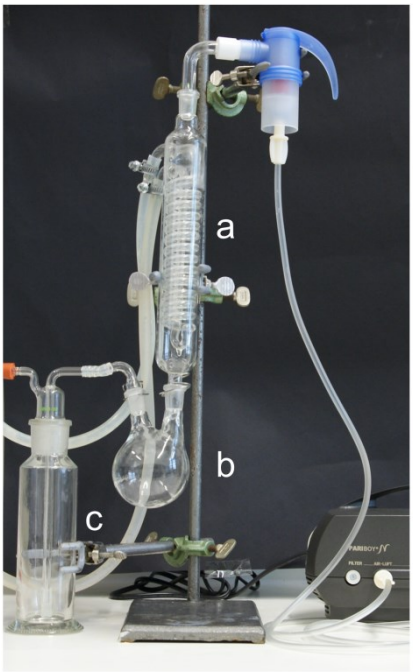

Figure 1: Setup for aerosol collection: Combination of a reflux condenser system and a two-stage impinger consisting of (a) a reflux condenser, (b) a round bottom flask = collection stage 1, and (c) a washing flask = collection stage 2.

2.6. *In vivo* study

2.6.1. Calculation of required mAb formulation concentration

According to literature [26,27], the drug dose delivered to mice can be estimated by the following equation:

$$Dose = \frac{Aerosol\ concentration \cdot Respiratory\ minute\ volume\ \cdot Exposure\ time}{Body\ weight} \quad (1)$$

The respiratory minute volume can be substituted with the tidal volume and the respiratory rate.

$$Respiratory\ minute\ volume = Tidal\ volume\ \cdot Respiratory\ rate \quad (2)$$

Considering the desired dose and exposure time as well as the respiratory characteristics of mice, the required aerosol concentration of the antibody can be calculated by:

$$Aerosol\ concentration\ = \frac{Dose \cdot Body\ weight}{Respiratory\ rate \cdot Tidal\ volume \cdot Exposure\ time} \quad (3)$$

According to this equation, to obtain the desired dose of 5.5 mg/kg after 10 min nebulization, an hUK-66 aerosol concentration of 0.423 µg/ml is required assuming an average body weight of 20 g and a respiratory rate of 163 per minute with a tidal volume of 0.16 ml for an ordinary mouse [26].

$$Aerosol\ concentration = \frac{5.5\,\frac{mg}{kg} \cdot 0.02kg}{163\ min^{-1} \cdot 0.16\ ml \cdot 10\ min} = 0.423\ \mu g/ml \quad (4)$$

Knowing the antibody concentration in the aerosol, the concentration of the whole nebulized solution in the aerosol was required for determination of the initial antibody concentration in the liquid formulation to be nebulized. To estimate the mass of nebulized solution per ml aerosol, the output rate and the flow of the applied nebulizer were required. For this purpose, the output rate was determined gravimetrically by measuring the weight of the nebulizer before and after nebulization of water for 10 min and found to be 0.2 g/min. To assess the volume nebulized per minute, the aerosol was introduced by a tube into a 5 l beaker which was filled with water and fixed upside down into a water bath. The volume of the air which replaced the water during operation for 1 min was determined to be 4 l resulting in a flow of approximately 4 l/min for the applied nebulizer. Incorporating these two nebulizer performance characteristics, the concentration of the nebulized solution in the aerosol can be calculated:

$$\frac{Output\ rate}{Flow} = \frac{0.2\,\frac{g}{min}}{4\,\frac{l}{min}} = 0.05\ \frac{g}{l} = 0.05\ \frac{mg}{ml} = 50\ \frac{\mu g}{ml} \quad (5)$$

Hence, to obtain a mAb mass of 0.42 µg per ml aerosol, the nebulized solution consisted of 0.42 µg mAb in 0.05 mg formulation:

$$hUK\ concentration\ of\ formulation\ for\ nebulization = \frac{0.42\ \mu g\ hUK}{0.05\ mg\ formulation} = 8.46 \frac{\mu g}{mg} = 8.5\ \frac{\mu g}{\mu l} = 8.5\ \frac{mg}{ml} \quad (6)$$

In conclusion, the initial formulation for nebulization required a hUK-66 concentration of 8.5 mg/ml to generate an aerosol concentration which results in a theoretical whole body dose of 5.5 mg/kg.

2.6.2. *In vivo* nebulization setup

Based on the setup used by Rudolph et al [28,29], an acrylic glass cylinder with holes for 10 perpendicularly attached 50 ml tubes was built (**Figure 2**). The ends of the cylinder were conically tapered with apertures for connecting the nebulizer as well as for aerosol outflow at the bottom. A perforated plate at the entrance of the cylindrical tube helped to generate a uniform flow of the aerosol. The mice were placed face first separately into 50 ml polypropylene tubes (Sarstedt AG & Co, Nürnbrecht, Germany) with cut-off tips. These modified tube tips were only big enough for mouth and nose to minimize dermal exposure of the mice to the aerosol [30]. A small whole in the caps of the tubes enabled a flow-through of the aerosol.

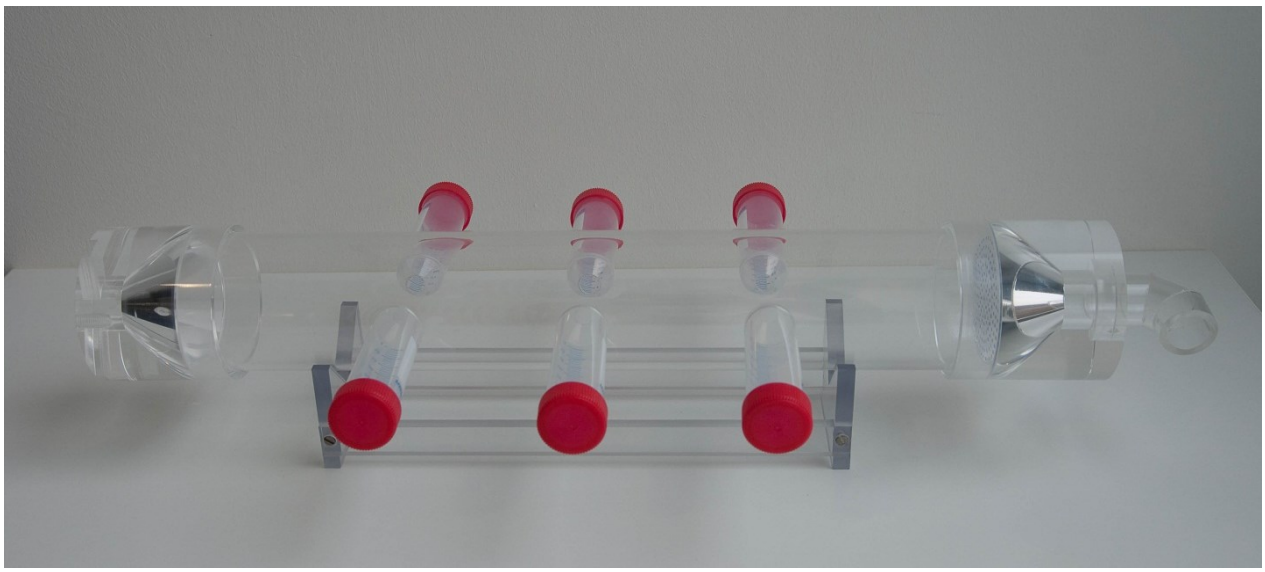

Figure 2: Nebulization array setup for simultaneous treatment of up to 10 mice with therapeutic aerosol. To allow clear identification of all setup details, the two leftmost and rightmost tubes were removed.

2.6.3. *In vivo* animal study of nebulized hUK-66 efficacy

The animal studies were approved by the Ethics Committee of the Lower Franconia authorities. Prior to the experiments, animals were acclimatized for at least 7 days. Female Balb/c mice (average age 6 weeks, weight 17-21 g) (Charles River, Sulzfeld, Germany) were sedated by inhalational anesthesia using isoflurane for subsequent intranasal infection with 20 µl of *Staphylococcus aureus Newman* at a concentration of $1 \cdot 10^{10}$ CFU/ml. Hence, the total infection dose was $2 \cdot 10^{8}$ CFU bacteria per mouse. After an incubation interval of 3 h, infected mice were treated by inhalation of nebulized hUK-66 formulations (n = 20) while control mice received nebulized blank formulations without mAb (n = 20). 2 ml hUK-66 was nebulized within 10 min to obtain a final dose of 5.5 mg/ kg. The mice were kept for another 10 min within the nebulization box to ensure inhalation of the entire nebulized mAb dose. The animals were kept in ventilated cages supplied with filtered air and food as well as water available ad libitum in a 12 h light/12 h dark cycle. Survival rate and body weight of infected mice after treatment with nebulized hUK-66 was monitored over 3 days.

2.7. Analytical methods

2.7.1. Concentration and turbidity measurements using UV-Vis spectroscopy

UV-visible absorbance spectroscopy was performed using a Genesys 10s UV-Vis spectrophotometer (Thermo Fisher Scientific Corporation, Waltham, USA). Volumes of 200-400 µl of each sample were analyzed in a 0.5 ml disposable cuvette (UVette®, Eppendorf AG, Hamburg, Germany) with a path length of 10 mm. UV-visible absorbance spectra were recorded from 200 to 800 nm using intervals of 1 nm. To determine the antibody concentration, an extinction coefficient of 1.475 $ml \cdot mg^{-1} \cdot cm^{-1}$ for absorption at 280 nm was used which was calculated based on the amino acid sequence using ExPASy [31]. Turbidity of the undiluted samples was assessed by measuring the optical density at 350 nm since protein absorption is negligible at this wavelength [32].

2.7.2. Dynamic light scattering (DLS)

Particle size distributions of the undiluted protein samples were measured using a Delsa™ Nano HC Particle Analyzer (Beckman Coulter®, Inc., Fullerton, CA, USA) at 25°C. Every measurement consisted of three individual runs comprising 200 accumulations each. 60 µl of the different samples were analyzed in a glass micro-cuvette (Beckman Coulter®, Inc., Fullerton, CA, USA).

2.7.3. High performance size exclusion chromatography (SEC)

For analyzing the stability and purity of the protein samples by SEC, the samples were diluted to a final concentration of approximately 1 mg/ml and centrifuged at 4400 x g for 30 min at 5°C (Eppendorf Centrifuge 5804 R, Rotor A-4-44, Eppendorf AG, Hamburg, Germany). The supernatants were transferred into 1.5 ml vials with 100 µl glass vial inserts and analyzed using a VWR Hitachi LaChromUltra™ HPLC system equipped with a diode array detector and a 7.8 mm x 300 mm TSK-Gel® G3000SWXL column as well as a TSK-Gel® SWXL Guard column (Tosoh Bioscience, Stuttgart, Germany). A 150 mM potassium phosphate buffer, pH 6.5, was used as mobile phase. 20 µl of each sample was injected and separated at a flow rate of 0.4 ml/min for 40 min at room temperature. The chromatographic data were recorded at 210 nm using a UV-Vis diode array detector and evaluated using the Agilent EZChrom Elite software (Agilent Technologies, Inc., Pleasanton, CA, USA).

2.7.4. Cation exchange chromatography (CEX)

mAb samples were analyzed regarding charge heterogeneity using a VWR Hitachi LaChromUltra™ HPLC system equipped with a diode array detector and a 4 mm x 250 mm PROPAC® WCX-10 analytical column as well as a 4 x 50 mm PROPAC® WCX-10G guard column (Dionex® Corporation / Thermo Fisher Scientific, Inc., Sunnyvale, CA, USA). 10 µl of each sample were run for 52 min at a flow rate of 1.0 ml/min at room temperature. A gradient of mobile phases A (20 mM sodium acetate, pH 5.6) and B (20 mM sodium acetate, 240 mM sodium chloride, pH 5.6) was used. The percentage of B was increasing from 20% (0 min) to 40% (2 min) to 80% (52 min). The column was regenerated after each run by 100% mobile phase B for 4.9 min and re-equilibrated using 80% A and 20% B for another 20 min prior to analysis of the next sample [33]. The data were recorded at 280 nm and 214 nm, respectively, using a UV-Vis diode array detector and evaluated using the Agilent EZChrom Elite software (Agilent Technologies, Inc., Pleasanton, CA, USA).

2.7.5. Statistical analysis

For analysis of the statistical significance of the survival data, the Gehan-Breslow-Wilcoxon test was applied using GraphPad Prism, Version 6.0 (GraphPad Software, Inc., La Jolla, CA, USA).

Data of the individual samples were analyzed for statistically significant differences in size, polydispersity indices, turbidity, monomer, aggregates, or degradation product content over incubation time by one-way analysis of variance (ANOVA) using multiple comparisons versus control by the Holm−Sidak method for comparison of multiple groups. Overall, a significance level of 0.05 was applied (OriginPro 9, OriginLab Corporation, Northampton, MA, USA).

3. Results and discussion

3.1. Aerosol formulation screening using surrogate interfacial stress method

Previous studies concerning formulation development for hUK-66 revealed chemical and physical stability of the antibody during quiescent refrigerated storage in presence of certain stabilizing excipients (Chapter III: Development of a stable formulation for the humanized monoclonal antibody UK-66). To evaluate if these formulations were also capable of stabilizing the antibody against the interfacial stress occurring during nebulization, a surrogate method was applied, which aimed at simulating the nebulization stress and reducing drug substance consumption. Hertel et al. demonstrated that agitation of protein samples at elevated temperatures leads to similar degradation levels as nebulization [34]. In the study of Hertel et al., shaking at 30°C for 10 min in half-filled micro tubes resulted in the best correlation to nebulization stress occurring during vibrating mesh nebulization. However, the jet nebulizer used in the present study does not result in increased reservoir temperatures up to 30-35°C in contrast to the vibrating mesh nebulizer used by Hertel et al. Instead, prolonging the shaking time at a temperature of 25°C resulted in good correlation to aggregation induced by nebulization in the high-throughput study of Hertel et al., as well. Therefore, in our study two hUK-66 formulation candidates as well as hUK-66 in PBS (reference formulation) were agitated for 15 min, 1 h, and 8 h at 25°C in half-filled micro tubes. Formulation candidates contained 0.04% PS 20 and 270 mM sugar or sugar alcohol (mannitol or sucrose, respectively) in 50 mM histidine buffer, pH 6.

For protein aggregation evaluation, solution turbidity was used as indicator being able to reveal both soluble and insoluble aggregation with good sensitivity in contrast to SEC [32,34]. Agitation of the protein formulations at room temperature resulted in an increasing albeit not significant trend in turbidity of the hUK-66 reference formulation over shaking time (**Figure 3**). This might indicate a propensity to aggregation of the protein in PBS. Similar effects have been previously reported for several other therapeutic proteins [34,35]. In contrast, both hUK-66 formulations exhibited constant turbidity levels throughout the mechanical stressing. Potentially, this can be primarily attributed to the presence of PS 20, known as stabilizer against surface induced aggregation [35].

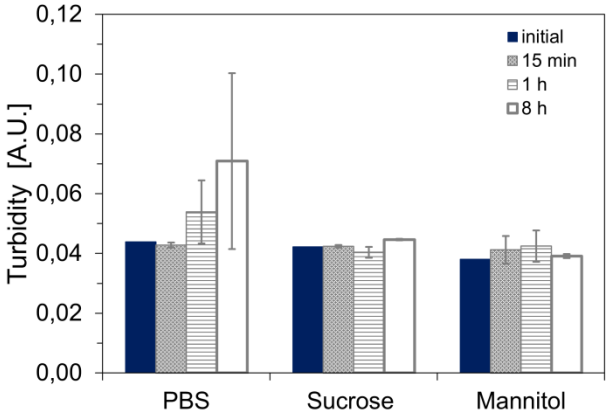

Figure 3: Influence of surrogate stress on turbidity of hUK-66 formulation candidates (sucrose, mannitol) in comparison to the reference formulation (PBS) over agitation time analyzed by UV-Vis absorption measurements at λ = 350 nm. (n=3; ±S.D. except initial samples).

DLS results confirmed the observations regarding aggregation propensity of the PBS formulation of hUK-66 made by turbidity analysis. Analyzed polydispersity indices (PdIs) were below 0.15 for all formulations, demonstrating a quite monodisperse particle size distribution. However, an increasing albeit not statistically significant trend of PdI values and hydrodynamic diameters was observed for hUK-66 in PBS over agitation time while hUK-66 in presence of excipients presented constant results (**Figure 4**).

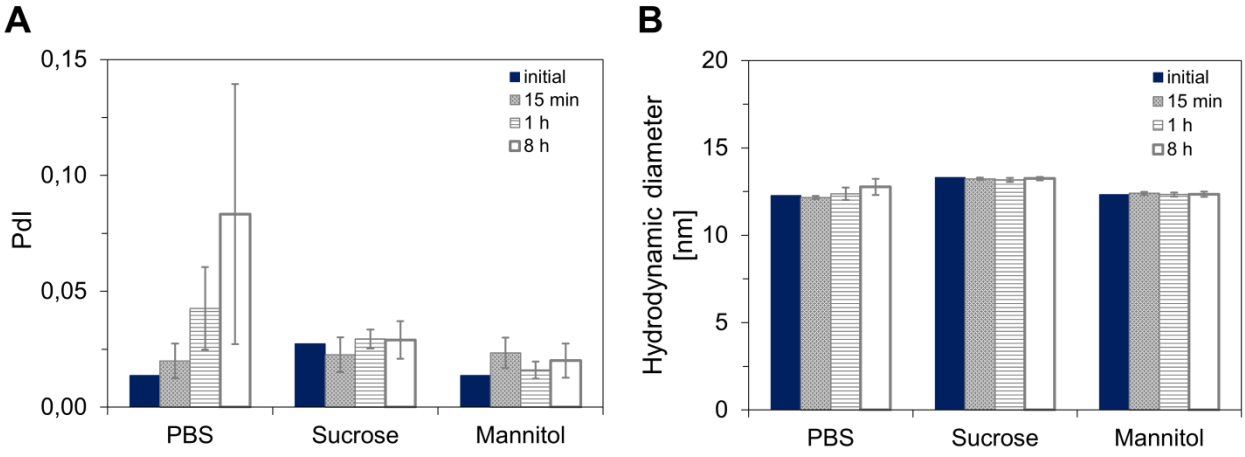

Figure 4: Effect of exposing hUK-66 formulations to mechanically increased air-water interface on homogeneity of particle size distribution within the samples (polydispersity index; PdI) (A) and hydrodynamic diameter of the protein in the respective formulations (B) analyzed by DLS.

Figure 5 depicts the effects of the surrogate interfacial stress method on stability of hUK-66 regarding monomer content, aggregation, and degradation of the different formulations analyzed by SEC as a function of agitation time. The presence of PS 20 and additional sucrose

or mannitol proved to stabilize the antibody against aggregation and degradation due to mechanical stress. In contrast, PBS alone resulted in a slight decreasing trend of monomer content during agitation accompanied by an increasing trend of aggregates and degradation products. However, it has to be noted that even the non-formulated mAb did not aggregate to a large extent as the amount of remaining monomer of 96% stayed very close to the initially measured monomer content of 96.6%. Significance of the trend to aggregation and degradation of the reference formulation could not be analyzed since only single initial samples were prepared due to limited availability of hUK-66.

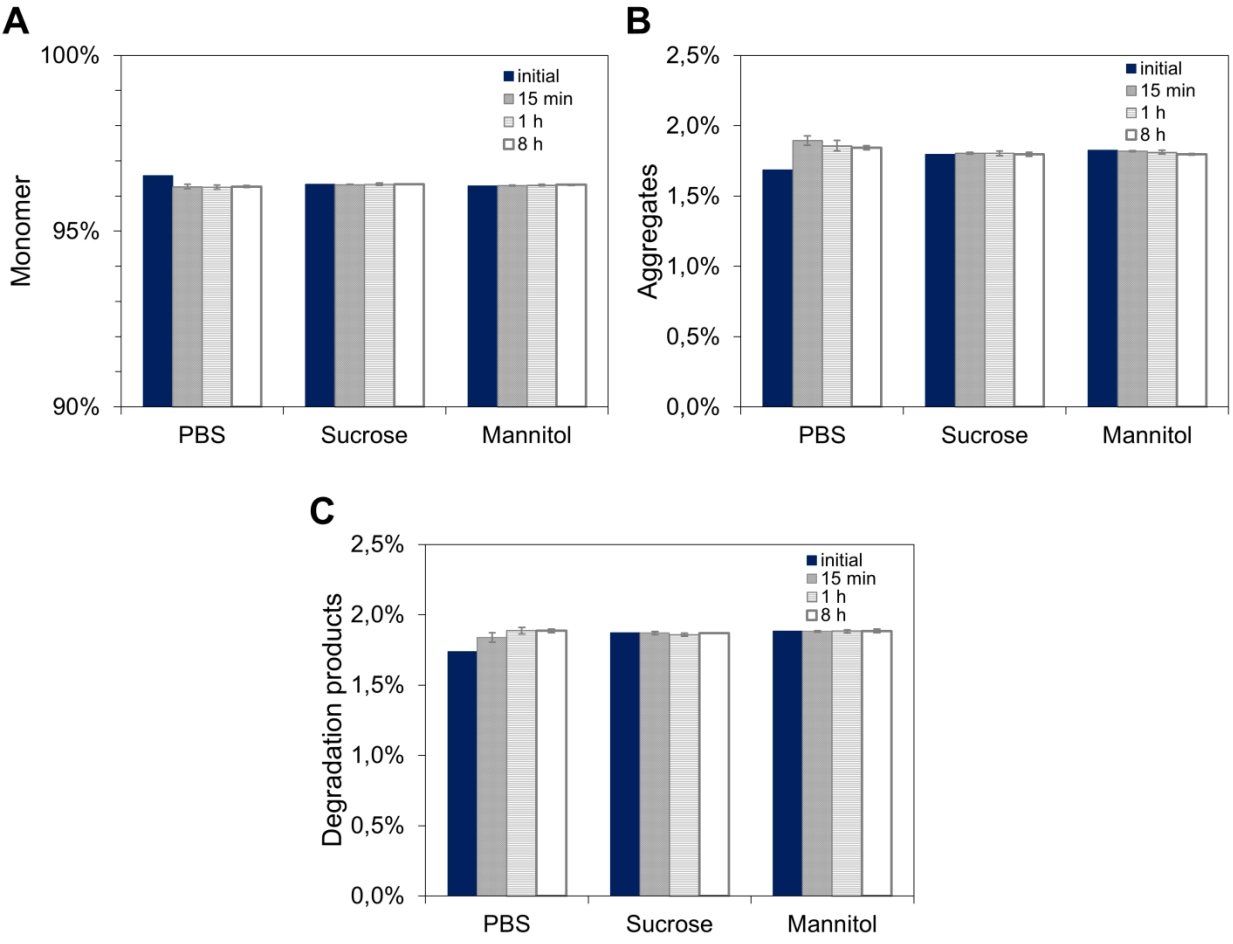

Figure 5: Effect of surrogate interfacial stress on monomer (A), aggregates (B), and degradation product content (C) in different hUK-66 formulations during agitation stress time as assessed by SEC.

Since hUK-66 had shown to be prone to deamidation in aqueous conditions in previous studies (Chapter III: Development of a stable formulation for the humanized monoclonal antibody UK-66), the propensity for chemical degradation during agitation was analyzed using CEX. For neither the reference formulation (PBS) nor the candidate formulations, an increasing tendency of acidic variants due to agitation was observed (**Figure 6**). Hence, this study revealed that the mechanical agitation stress did not lead to chemical degradation of this

antibody. Therefore, the increasing trend in degradation products detected by SEC was not attributable to formation of acidic variants as detected by CEX.

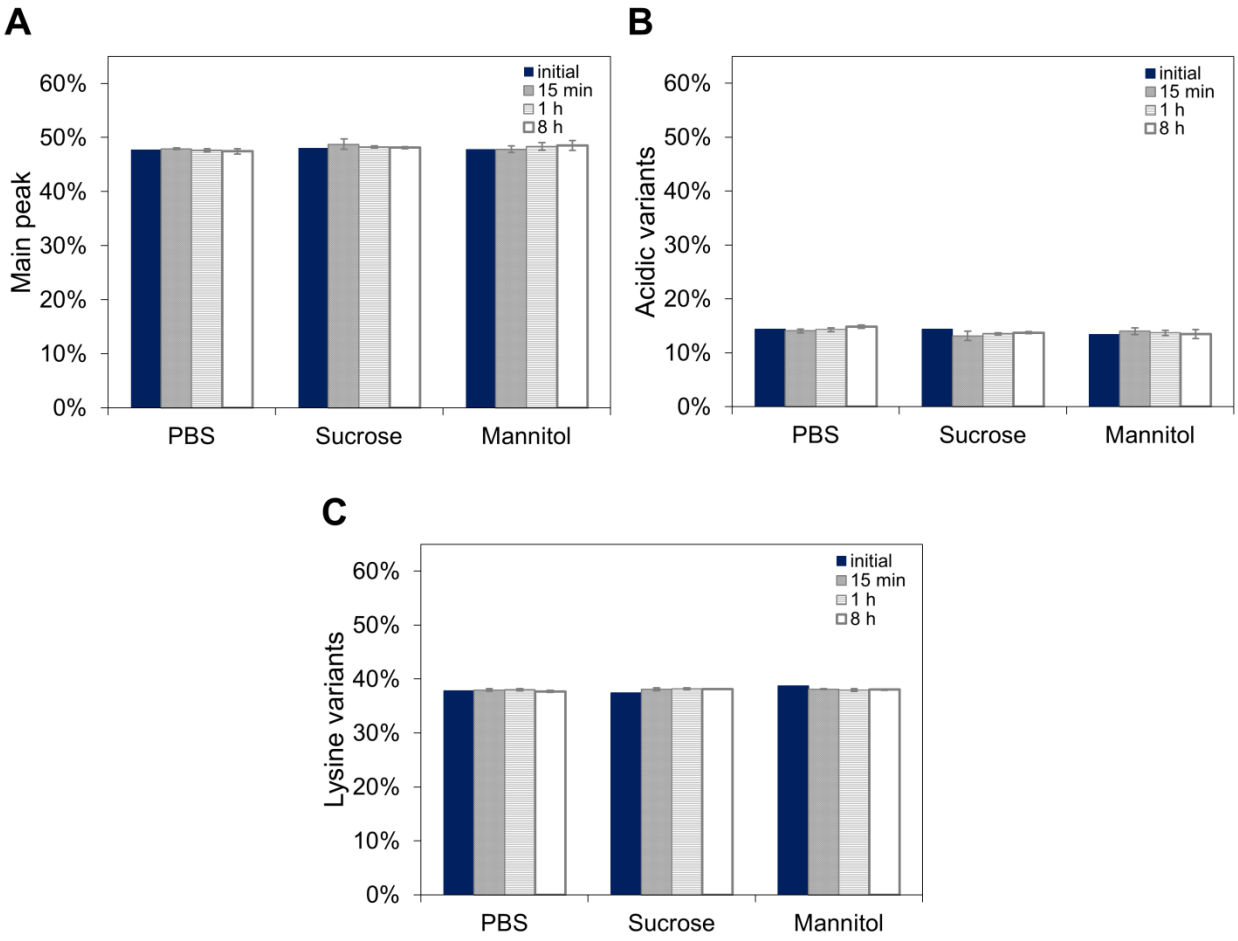

Figure 6: Analysis of chemical degradation of the main peak (A) into acidic (B) and basic (C) variants in different hUK-66 formulations due to surrogate interfacial stress over agitation time using CEX.

From the accelerated stress testing it was concluded that interfacial stress occurring during nebulization may lead to aggregation of non-formulated hUK-66, albeit to a minor extent, underlining the necessity of proper formulation. Both candidate formulations were capable of protecting the antibody against aggregation. This can be accredited to the congruent presence of the surfactant PS 20, a well-known stabilizer against surface induced aggregation [36]. The sugar sucrose and the sugar alcohol mannitol did not differ in their stabilizing potential for hUK-66 during agitation. Since sucrose proved to be the superior stabilizer of the native protein conformation during lyophilization and long-term storage (Chapter III: Development of a stable formulation for the humanized monoclonal antibody UK-66), sucrose was chosen as the most promising formulation for nebulization studies. Furthermore, this formulation fulfilled the requirements for inhalable drug formulations since its pH value of pH 6 is kept within the ideal range for pulmonary delivery of pH 5 to 8 [9].

3.2. Impact of nebulization on stability of hUK-66

After determination of a qualified formulation for nebulization of hUK-66 based on interfacial stress testing, the influence of the actual nebulization process on stability of the antibody was assessed to verify and evaluate the stabilizing potential of the developed formulation. After nebulization of the chosen formulation candidate (sucrose) using a jet nebulizer, protein samples were collected from the nebulizer reservoir as well as from the aerosol collection apparatus and analyzed regarding monomer content, aggregation, and chemical degradation.

3.2.1. Characterization of mAb solution in the reservoir of the air-jet nebulizer

Although the decreasing temperature of the solution in the reservoir of an air-jet nebulizer due to solvent evaporation over nebulization time might appear to be favorable, protein stability is endangered by solvent evaporation, recirculation, and multiple atomization of the protein solution within the nebulizer reservoir [17,18]. Only aerosol droplets of adequate size are escaping the nebulizer while larger droplets are retained by baffles and are redirected into the fluid reservoir [18]. Before leaving the nebulizer as aerosol, a protein molecule undergoes the process of nebulization on average up to 15 times amplifying the risk to unfold and aggregate due to exposure to a large air-liquid interface [6]. Therefore, the effect of nebulization process on hUK-66 formulation was assessed by comparing samples from the nebulizer reservoir after nebulization with initial hUK-66 formulations.

Since turbidity analysis is said to be more sensitive than HPLC for early detection of aggregate formation [32], the optical density at 350 nm of the protein solutions from the reservoir was assessed revealing relatively low turbidity levels of 50 to 65 mAU and hence no indication for strong formation of insoluble aggregates for all samples (**Figure 7A**). Analyzing concentration changes, an increase of the protein concentration within the reservoir by on average 10% was observed, a common effect of air-jet nebulization (**Figure 7B**) [9]. The simultaneously increased amount of excipients per volume of the hUK-66 formulation caused by the solvent evaporation might have influenced the optical characteristics and hence the turbidity. This would explain the higher turbidity values after nebulization of the formulation in contrast to those of the reference without additional excipients.

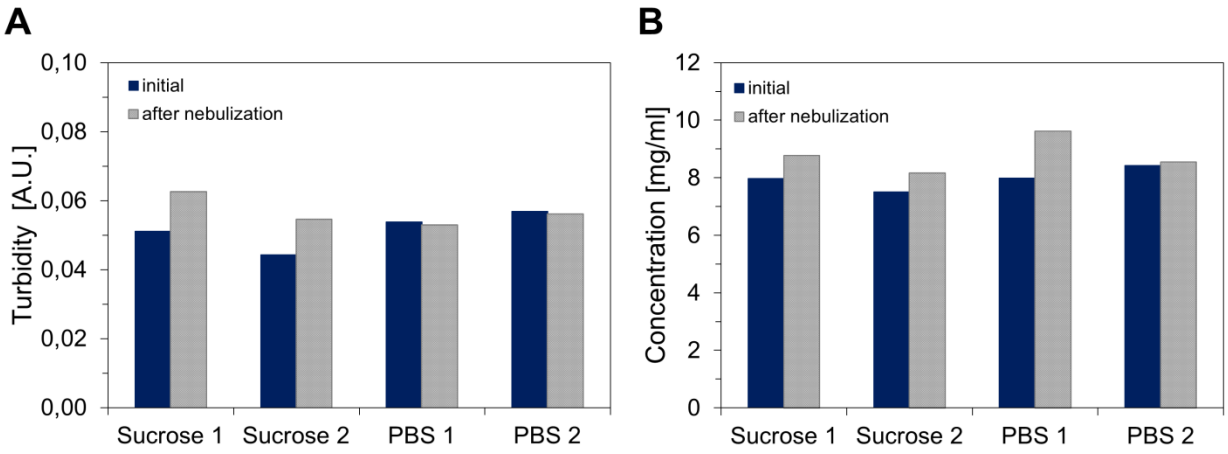

Figure 7: Effect of nebulization process on turbidity (A) and concentration (B) of hUK-66 formulation in the reservoir (sucrose 1 and 2) in comparison to the reference (PBS 1 and 2) analyzed by UV absorption measurements at 350 nm or 280 nm, respectively. Since nebulization of hUK-66 formulation (sucrose) and reference (PBS) were only performed twice due to limited availability of hUK-66, measurement results of every single nebulization were plotted.

DLS measurements resulted for all samples in PdI values below 0.1 with hydrodynamic diameters of 13 to 14 nm indicating a monomodal particle size distribution and no formation of oligomers or large aggregates (**Figure 8**). However, a direct comparison of hUK-66 samples before and after nebulization suggested a slight increase of turbidity, size, and PdI of the analyzed formulation within the reservoir while no trend was observed for non-formulated hUK-66. Although PBS exhibited already higher initial PdI values than the formulation samples, the increase in PdI and mean size, which indicated aggregation propensity, compromised the results of the surrogate stress formulation screening.

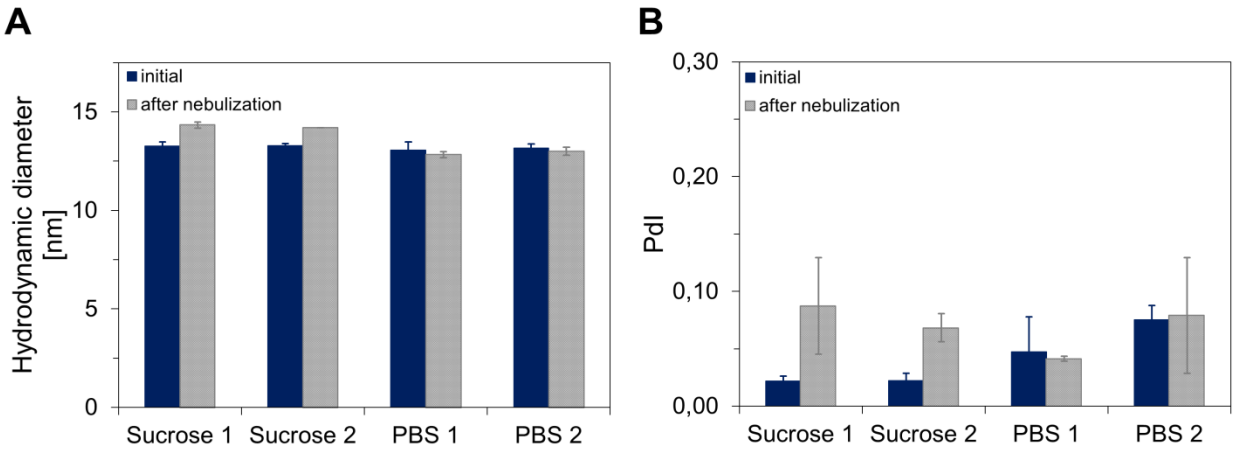

Figure 8: Hydrodynamic diameter (A) and PdI values (B) of different hUK-66 formulations within the reservoir before (dark blue bars) and after (grey bars) nebulization as assessed by DLS. Standard deviations of the inherent 3 runs of one DLS measurement per sample were plotted.

SEC analysis showed neither a loss of monomer nor a formation of soluble aggregates or degradation products for the two hUK-66 formulation samples in the reservoir after nebulization for 10 minutes (**Figure 9A, C, and E**). As demonstrated by the CEX results, exposure to interfacial stress caused by recirculation in the reservoir had no adverse effect on the chemical stability of the antibody (**Figure 9B, D, and F**).

Altogether, the enormous stress created by multiple nebulization and intense recirculation of the protein solution within the reservoir did not result in pronounced aggregation or degradation of the antibody, neither for the developed hUK-66 formulation nor for the hUK-66 PBS reference. This demonstrated a high general stability of the antibody hUK-66. Hence, the majority of the protein was leaving the nebulizer in a stable folded natural state. However, for the chosen formulation it could not be absolutely excluded that some by recirculation unfolded or even aggregated protein molecules were nebulized in a repeated aerosolization step during the nebulization process.

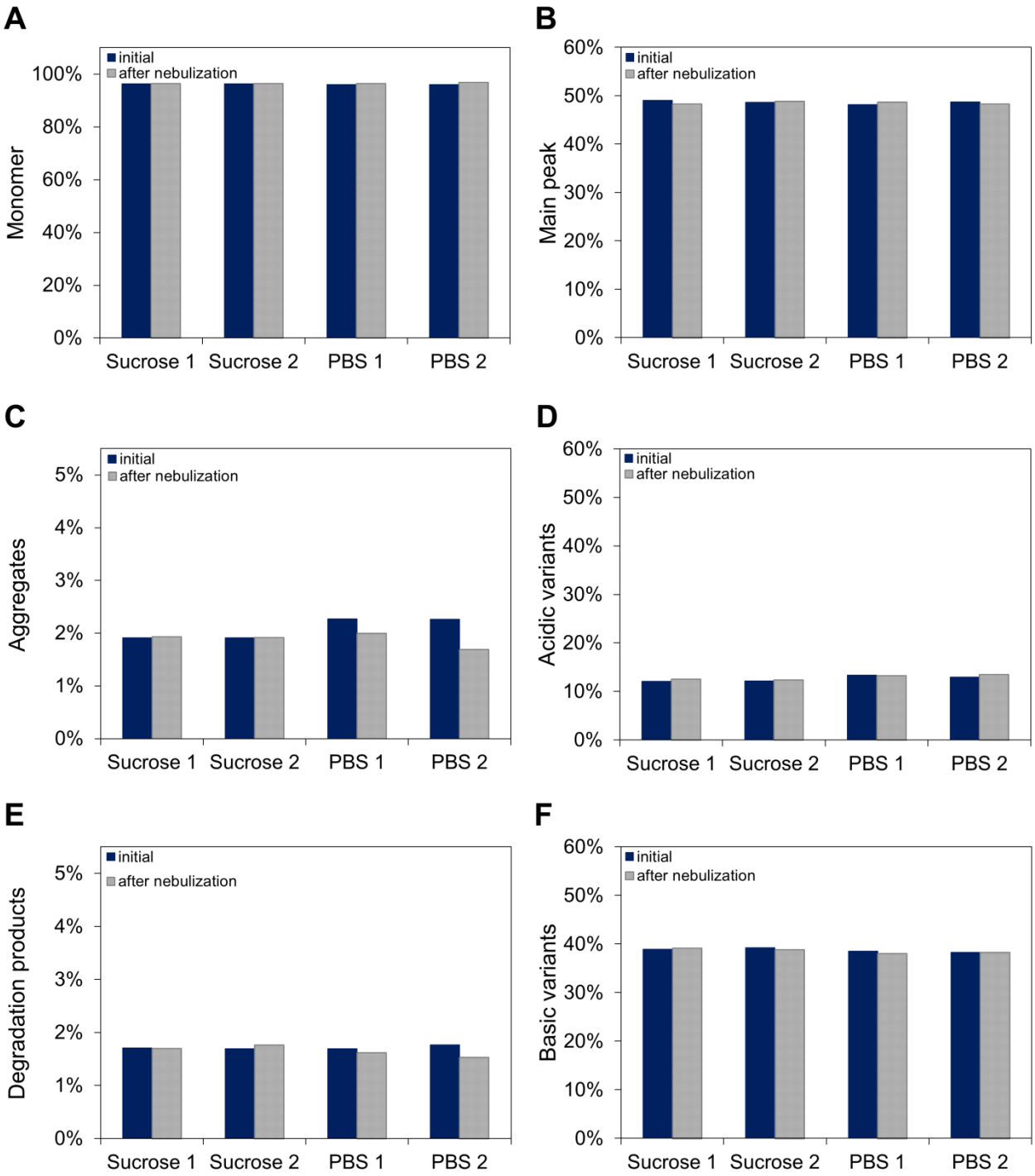

Figure 9: Effect of recirculation of protein solution in nebulizer reservoir during nebulization process on physical and chemical stability of hUK-66 formulation (sucrose 1 and 2) and reference (PBS 1 and 2) regarding monomer as well as main peak content (A and B) and formation of aggregates (C), degradation products (E), acidic variants (D), as well as basic variants (F) as analyzed by SEC (A, C, E) and CEX (B, D,F).

3.2.2. Characterization of nebulized mAb aerosol

In order to evaluate the influence of the actual nebulization process on stability of nebulized protein, the aerosol was collected. After nebulization, a combination of a two stage impinger and a reflux condenser was applied for collection of the aerosol to enable characterization of the liquid using established analytical methods.

Since protein concentration might be affected by degradation, efficiency of aerosol collection using this setup was assessed using an independent internal standard (fluorescein sodium, FS). 40% of the initially nebulized hUK-66 formulation containing FS were collected by the combined impinger-reflux condenser set up. 88% of this collected aerosol were recovered in the second collection stage. However, collection efficiencies for collection by a two stage impinger or a reflux condensation system were reported to be above 90% [16,37]. This indicates an enormous loss of aerosol. Since only 12% were collected in the first collection stage, some protein might still be adsorbed to the glassware and rinsing with 5 ml buffer probably did not result in complete collection of all protein condensed in the reflux condenser.

Nevertheless, analysis of the collected nebulized hUK-66 formulation using dynamic light scattering revealed a slight increase in PdI values after nebulization (**Figure 10**). These results indicate the presence of particles of various sizes within the sample after nebulization. The hUK-66 formulation sample drawn from the reservoir after nebulization showed a high PdI of 0.4 and a large mean hydrodynamic diameter. Regarding DLS analysis, it is well known that the presence of few single very large particulates distorts light scattering measurements and hence can bias the results gained for mean hydrodynamic diameter (cumulant diameter) [38]. From the intensity size distribution it can be seen that the main peak remained constant (contin diameter for polydisperse samples). However, regarding the collected aerosol samples even the main peak size of the contin results was elevated compared to the non-nebulized hUK-66 formulation. Considering the concurrently increased PdI values, the results indicate a presence of some oligomers and larger aggregates since DLS can only resolve particle populations that differ in size by at least factor 3 [39,40].

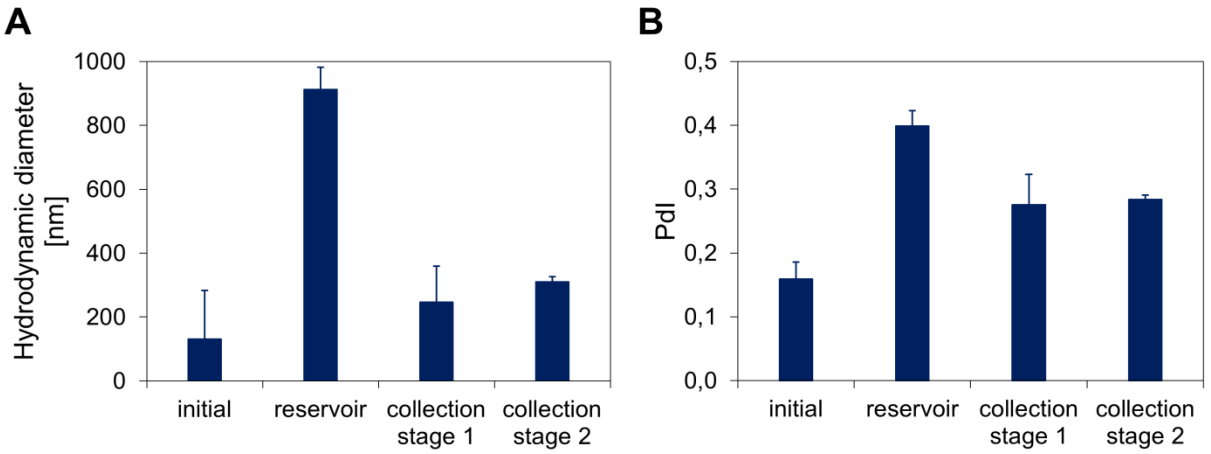

Figure 10: Comparison of hydrodynamic diameter (A) and PdI values (B) of hUK-66 formulation samples before nebulization (initial) and after nebulization collected from the reservoir or collection stage 1 and 2 as assessed by DLS.

Since SEC analysis required centrifugation of the samples to remove insoluble aggregates and particulates, only soluble aggregates were detectable. Whereas the mAb within the reservoir maintained a constant percentage of monomer, aggregates, and degradation products compared to the non-nebulized initial sample, no soluble aggregates were detected in the collected mAb aerosol (**Figure 11**). This might be attributed to the small percentage of aggregates and the strong dilution of the accumulated nebulized mAb within the collection stages. Therefore, contained aggregates potentially were not detectable using SEC due to their low concentration.

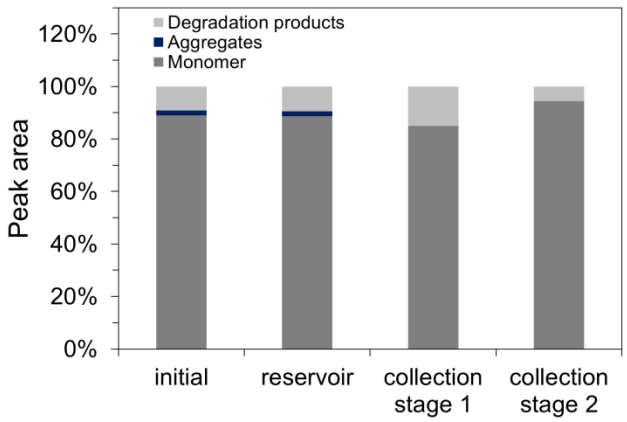

Figure 11: Monomer recovery (light grey), aggregate formation (dark blue), and degradation (mid grey) of hUK-66 formulation after nebulization (reservoir, collection stages 1, and 2) compared to initial sample.

Looking at the SEC chromatograms of the hUK-66 formulation before and after nebulization, not only the strong dilution of the nebulized antibody gathered in the collection stages is apparent but also the up-concentration of mAb within the reservoir due to nebulization with constant aggregate and degradation product levels (**Figure 12**).

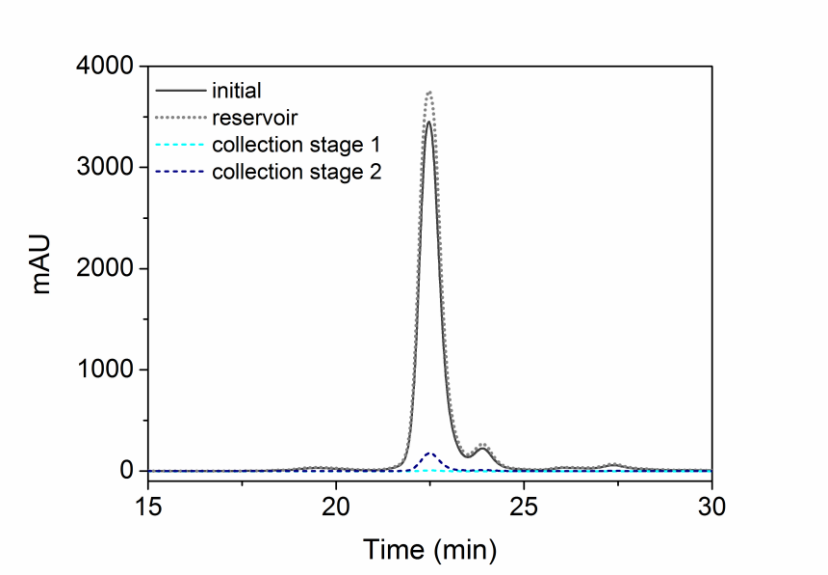

Figure 12: Overlay of SEC chromatographs of hUK-66 formulation before nebulization (black) and after nebulization from the reservoir (grey) as well as collection stage 1 (light blue) and 2 (dark blue).

However, the collection procedure might have distorted the stability of hUK-66 since the mAb is subjected to surface stress during collection by adsorption and condensation to the glass surface of the reflux condenser in the upper stage and by bubbling of the aerosol through the medium in the lower collection stage 2. Comparing different collection methods, Hertel showed that protein was degraded after collection using impinger or condenser even without being nebulized before [41]. In addition, particulates from the collection apparatus or the medium might bias the results since sterility could not be guaranteed during aerosol collection. Therefore, it can be concluded that the formulation containing sucrose and PS 20 was able to preserve hUK-66 stability after nebulization to an acceptable degree considering that polydispersity was only slightly increased after nebulization.

3.3. hUK-66 *in vivo* efficacy study

3.3.1. Evaluation of nebulization setup providing good inhalation conditions

So far, *in vivo* pulmonary delivery of proteins to rodents is mainly done by anesthesia followed by instillation or intratracheal aerosolization [20,21,26] since in these cases the delivered dose is well controlled and directly deposited in the lower respiratory tract. Particularly the instillation process is easy and quick to perform, few equipment is required, and only small amounts of sample are needed [42,43]. However, instillation leads to inhomogeneous pulmonary distribution with low reproducibility whereas aerosol can distribute uniformly even into the peripheral alveolar region [41,42,44]. To introduce therapeutic drugs to the lung, the physiological way of passive inhalation by normally breathing non-anesthetized mammals is preferred since it represents a more realistic scenario for the therapy of humans even though the anatomy of the respiratory tract of rodents and humans is very different [26]. Passive inhalation can be accomplished by the use of a whole body exposure chamber. Nevertheless, this is impaired by potential drug absorption across the skin as well as the gastrointestinal tract and the large space required to saturate with aerosol [26]. A more efficient way is nose-only aerosol exposure where the contact of the aerosol with the animal is mostly concentrated to the snout. Hacha et al. showed effective pulmonary delivery by air-jet nebulization of anti-IL 13 mAb Fab' fragments to mice using the nose-only *inExpose*™ system (SCIREQ Scientific Respiratory Equipment Inc, Montreal, Canada) [19]. To save acquisition costs and leave space for individual optimization, in this study an *in vivo* array nebulization set up for pulmonary delivery of therapeutic biopharmaceutics was constructed based on the setup used by Rudolph et al. [28,29]. It allowed easy and equal inhalation of the generated aerosol by up to 10 mice simultaneously.

Since narcotics lead to respiratory depression causing slow and shallow breathing contrary to natural breathing behavior, the animals were placed in the constructed cylindrical array setup for nebulization without anesthesia. Dermal exposure of the mice to the aerosol [30] was minimized by using tubes with cut-off tips big enough for mouth and nose of the mice but tight enough to prevent leaving the tube (**Figure 13**). The nebulization array box was arranged horizontally since a more homogenous flow and distribution of the aerosol was observed compared to the vertical setup used by Rudolph et al [28].

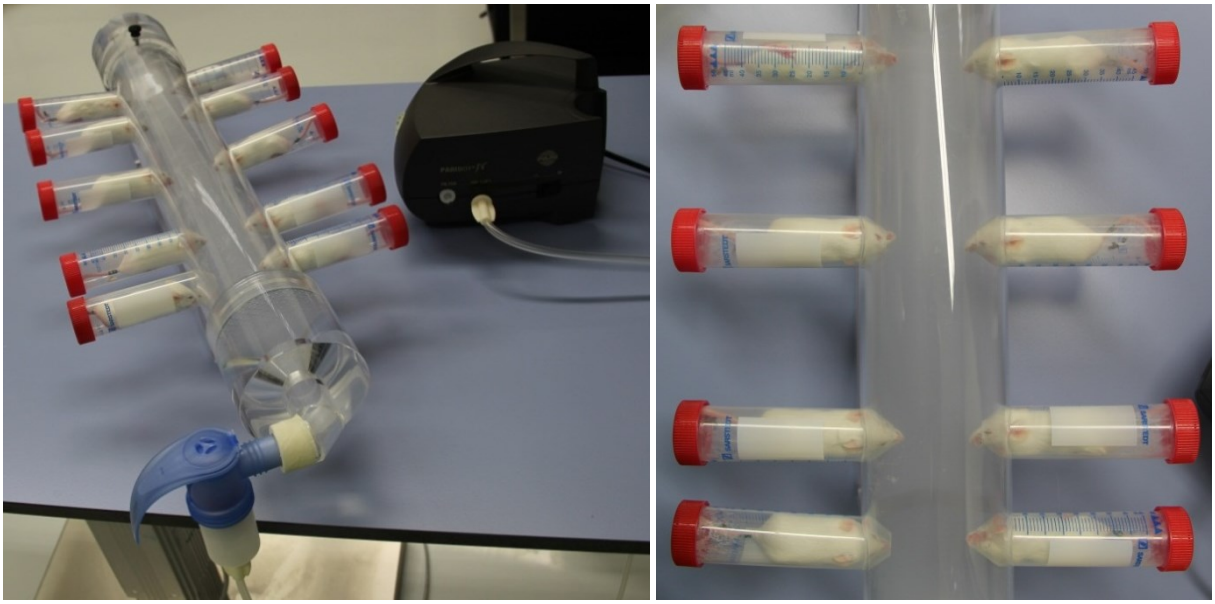

Figure 13: Set up for *in vivo* nebulization. A homogenous aerosol flow is presented to the animals while exposure is mainly concentrated to noses and beaks of the mice.

3.3.2. Survival of infected mice after treatment with nebulized hUK-66

The way to *in vivo* efficacy studies was paved by the evaluation of the hUK-66 formulation containing sucrose and PS 20 which proved to preserve hUK-66 stability during nebulization (chapter IV.3.2.) and hence promised the delivery of bioactive antibody in an aerosolized state. Additionally, the development of the nose-only array nebulization set up enabled optimal experimental conditions to analyze the effect of nebulization of hUK-66 to mice infected with *S. aureus*. This antibody targets the immunodominant staphylococcal antigen A (IsaA) on the surface of *Staphylococcus aureus* [22] and facilitates the fight against staphylococcal infections by the immune system. Its "parent" murine antibody UK-66P already proved to activate phagocytes and promote bacteria killing *in vivo* in an intravenous infection and therapy setup [45]. The further developed humanized version hUK-66 demonstrated similar binding specificity as well as biological activity to that of UK-66P in *in vitro* experiments and induced significant killing activity in blood sample tests [22]. Since infection with *S. aureus* is one of the main causes of nosocomial pneumonia and mechanically ventilated patients are particularly susceptible to pulmonary infections [46,47], in this study hUK-66 was evaluated for its therapeutic efficacy when delivered pulmonary to mice via nebulization. 3 h after intranasal infection with *S. aureus*, 10 mice at a time received a dose of 5.5 mg/kg hUK-66 by passive inhalation for 10 minutes. Their survival after 3 days was compared to a control group which inhaled a placebo formulation without mAb under the same conditions. This experiment was repeated once with identical parameters and the results

are shown in **Figure 14**. Nebulized hUK-66 provided a significant survival benefit compared to the control (P = 0.004; Gehan-Breslow-Wilcoxon test). At the study endpoint after 3 days, 65% of the animals treated with pulmonary delivered hUK-66 survived the *S. aureus* infection whereas only one out of four animals from the control group was still alive. Hence, hUK-66 demonstrated its immunotherapeutic potential in treating *S. aureus* infections effectively when administered pulmonary.

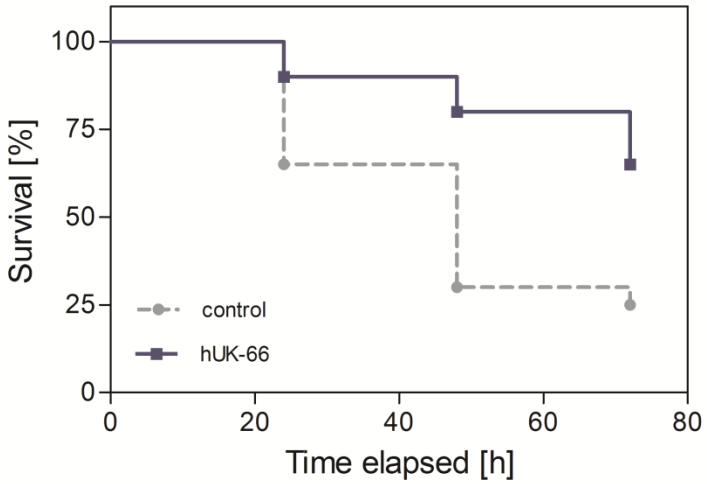

Figure 14: Survival of mice infected with *S. aureus Newman* (infection dose $2 \cdot 10^8$ CFU) after therapy with nebulized hUK-66 compared to an untreated control group (n = 20, data from two independent studies on different days, 10 mice for verum group and control group each).

4. Summary and conclusion

To deliver proteins via the lung, generation of an inhalable aerosol is required. However, during the process of nebulization the protein solution is dissipating into multiple small droplets magnifying the air-liquid interface tremendously and exposing the biomolecules to an intensive interfacial stress. The goal of this study was to stabilize the antibody hUK-66 against this destructive influence by developing a suitable formulation. Since a large sample volume is needed for nebulization in general, a surrogate method to simulate air-jet nebulization stress was applied for evaluation of a suitable formulation in order to save drug substance. A formulation in histidine buffer at pH 6 comprising the excipients polysorbate 20, a well-known stabilizer against surface induced aggregation, and sucrose prevented aggregation of hUK-66 during vigorous shaking over up to 8 h and hence provided a promising basis for successful stabilization during nebulization. To assess the influence of the actual nebulization process on protein stability in this formulation, the remaining protein in the nebulizer reservoir was easily accessible for analysis whereas for the collection of the aerosol a special apparatus was needed. The combination of stage impinger and reflux condenser revealed some disadvantages during aerosol collection. It probably induced protein degradation through adsorption and condensation to the glass surface and bubbling of the aerosol through the medium. Condensation of the aerosol directly into 2 ml polypropylene tubes as shown in recent studies by Hertel et al. [48] appears to be more appropriate. Nevertheless, the analyzed formulation of hUK-66 proved to preserve the protein stability adequately during nebulization. Furthermore, in this study it was shown that nebulization had no adverse effect on the chemical stability of an antibody which had not been analyzed yet [12]. Altogether, multiple nebulization and intense recirculation of the protein solution within the reservoir had no major effect on conformation stability of the antibody. Finally, the immunotherapeutic efficacy of the nebulized antibody hUK-66 to prolong survival of mice infected intranasally with *S. aureus* was proven. For this *in vivo* study a special nose-only exposure set up to enable aerosol delivery to mice being awake and breathing normally was developed successfully.

Hence, the stability of hUK-66 in an optimized formulation during nebulization as well as its immunotherapeutic potential in treating *S. aureus* infections effectively when administered pulmonary were demonstrated in this study.

References

[1] S.-J. Koussoroplis, R. Vanbever, Peptides and Proteins: Pulmonary Absorption, in: Encycl. Pharm. Sci. Technol. Vol. IV, 4th ed., Taylor & Francis Group, LLC, 2013: pp. 2607–2618. doi:10.1081/E-EPT4-120050324.

[2] B.L. Laube, The expanding role of aerosols in systemic drug delivery, gene therapy, and vaccination., Respir. Care. 50 (2005) 1161–76.

[3] Y.Y. Albasarah, S. Somavarapu, K.M.G. Taylor, Stabilizing protein formulations during air-jet nebulization., Int. J. Pharm. 402 (2010) 140–5. doi:10.1016/j.ijpharm.2010.09.042.

[4] G. Pilcer, K. Amighi, Formulation strategy and use of excipients in pulmonary drug delivery., Int. J. Pharm. 392 (2010) 1–19. doi:10.1016/j.ijpharm.2010.03.017.

[5] F. Depreter, G. Pilcer, K. Amighi, Inhaled proteins: challenges and perspectives., Int. J. Pharm. 447 (2013) 251–80. doi:10.1016/j.ijpharm.2013.02.031.

[6] R. Siekmeier, G. Scheuch, Systemic treatment by inhalation of macromolecules--principles, problems, and examples., J. Physiol. Pharmacol. 59 Suppl 6 (2008) 53–79.

[7] R.U. Agu, M.I. Ugwoke, M. Armand, R. Kinget, N. Verbeke, The lung as a route for systemic delivery of therapeutic proteins and peptides., Respir. Res. 2 (2001) 198–209. doi:10.1186/rr58.

[8] S.A. Shoyele, A. Slowey, Prospects of formulating proteins/peptides as aerosols for pulmonary drug delivery., Int. J. Pharm. 314 (2006) 1–8. doi:10.1016/j.ijpharm.2006.02.014.

[9] S.P. Hertel, G. Winter, W. Friess, Protein stability in pulmonary drug delivery via nebulization., Adv. Drug Deliv. Rev. 93 (2015) 79–94. doi:10.1016/j.addr.2014.10.003.

[10] D.B.S. Brashier, A. Khadka, T. Anantharamu, A.K. Sharma, A.K. Gupta, S. Sharma, et al., Inhaled insulin: A “puff” than a “shot” before meals., J. Pharmacol. Pharmacother. 6 (2015) 126–9. doi:10.4103/0976-500X.162013.

[11] B. Hughes, 2009 FDA drug approvals., Nat. Rev. Drug Discov. 9 (2010) 89–92. doi:10.1038/nrd3101.

[12] R. Respaud, L. Vecellio, P. Diot, N. Heuzé-Vourc’h, Nebulization as a delivery method for mAbs in respiratory diseases., Expert Opin. Drug Deliv. 12 (2015) 1027–39. doi:10.1517/17425247.2015.999039.

[13] H. Steckel, F. Eskandar, K. Witthohn, Effect of cryoprotectants on the stability and aerosol performance of nebulized aviscumine, a 57-kDa protein., Eur. J. Pharm. Biopharm. 56 (2003) 11–21. doi:10.1016/S0939-6411(03)00044-4.

[14] R.W. Niven, Protein nebulization II. Stabilization of G-CSF to air-jet nebulization and the role of protectants., Int. J. Pharm. 127 (1996) 191–201. doi:10.1016/0378-5173(95)04209-1.

[15] R.W. Niven, A.Y. Ip, S.D. Mittelman, C. Farrar, T. Arakawa, S.J. Prestrelski, Protein nebulization: I. Stability of lactate dehydrogenase and recombinant granulocyte-colony stimulating factor to air-jet nebulization., Int. J. Pharm. 109 (1994) 17–26. doi:10.1016/0378-5173(94)90117-1.

[16] A.Y. Ip, T. Arakawa, H. Silvers, C.M. Ransone, R.W. Niven, Stability of recombinant consensus interferon to air-jet and ultrasonic nebulization., J. Pharm. Sci. 84 (1995) 1210–4. doi:10.1002/jps.2600841013.

[17] I. Fängmark, J. Carpin, Protein nebulization, J. Aerosol Sci. 27 (1996) S231–S232. doi:10.1016/0021-8502(96)00188-7.

[18] O.N.M. McCallion, K.M.G. Taylor, P.A. Bridges, M. Thomas, A.J. Taylor, Jet nebulisers for pulmonary drug delivery, Int. J. Pharm. 130 (1996) 1–11. doi:10.1016/0378-5173(95)04233-4.

[19] J. Hacha, K. Tomlinson, L. Maertens, G. Paulissen, N. Rocks, J.-M. Foidart, et al., Nebulized anti-IL-13 monoclonal antibody Fab' fragment reduces allergen-induced asthma., Am. J. Respir. Cell Mol. Biol. 47 (2012) 709–17. doi:10.1165/rcmb.2012-0031OC.

[20] A. Maillet, L. Guilleminault, E. Lemarié, S. Lerondel, N. Azzopardi, J. Montharu, et al., The airways, a novel route for delivering monoclonal antibodies to treat lung tumors., Pharm. Res. 28 (2011) 2147–56. doi:10.1007/s11095-011-0442-5.

[21] J. Hill, J.E. Eyles, S.J. Elvin, G.D. Healey, R.A. Lukaszewski, R.W. Titball, Administration of antibody to the lung protects mice against pneumonic plague., Infect. Immun. 74 (2006) 3068–70. doi:10.1128/IAI.74.5.3068-3070.2006.

[22] B. Oesterreich, B. Lorenz, T. Schmitter, R. Kontermann, M. Zenn, B. Zimmermann, et al., Characterization of the biological anti-staphylococcal functionality of hUK-66 IgG1, a humanized monoclonal antibody as substantial component for an immunotherapeutic approach., Hum. Vaccin. Immunother. 10 (2014) 926–37. doi:10.4161/hv.27692.

[23] PARI GmbH, Starnberg, Germany, (2016). http://www.pari.com/de-de/produkte/untere-atemwege/pari-boy-sx/ (accessed March 18, 2016).

[24] H. Steckel, F. Eskandar, K. Witthohn, The effect of formulation variables on the stability of nebulized aviscumine., Int. J. Pharm. 257 (2003) 181–94. doi:10.1016/S0378-5173(03)00126-1.

[25] L. Khatri, K.M. Taylor, D.Q. Craig, K. Palin, An assessment of jet and ultrasonic nebulisers for the delivery of lactate dehydrogenase solutions., Int. J. Pharm. 227 (2001) 121–31. doi:10.1016/S0378-5173(01)00790-6.

[26] C.A. Fernandes, R. Vanbever, Preclinical models for pulmonary drug delivery., Expert Opin. Drug Deliv. 6 (2009) 1231–45. doi:10.1517/17425240903241788.

[27] D.J. Alexander, C.J. Collins, D.W. Coombs, I.S. Gilkison, C.J. Hardy, G. Healey, et al., Association of Inhalation Toxicologists (AIT) working party recommendation for standard delivered dose calculation and expression in non-clinical aerosol inhalation toxicology studies with pharmaceuticals., Inhal. Toxicol. 20 (2008) 1179–89. doi:10.1080/08958370802207318.

[28] C. Rudolph, A. Ortiz, U. Schillinger, J. Jauernig, C. Plank, J. Rosenecker, Methodological optimization of polyethylenimine (PEI)-based gene delivery to the lungs of mice via aerosol application., J. Gene Med. 7 (2005) 59–66. doi:10.1002/jgm.646.

[29] A. Ortiz Arandes, Präklinische Optimierung des nicht-viralen Gentransfers in die Lunge mittels Aerosolapplikation, Dissertation.Ludwig-Maximilians-Universität München, 2009.

[30] M.S. Werley, P. McDonald, P. Lilly, D. Kirkpatrick, J. Wallery, P. Byron, et al., Non-clinical safety and pharmacokinetic evaluations of propylene glycol aerosol in Sprague-Dawley rats and Beagle dogs., Toxicology. 287 (2011) 76–90. doi:10.1016/j.tox.2011.05.015.

[31] ExPASy ProtParam tool, Accessed:23-04-2013, Http://web.expasy.org/protparam/. (2013). www.expasy.org.

[32] W. Wang, Protein aggregation and its inhibition in biopharmaceutics., Int. J. Pharm. 289 (2005) 1–30. doi:10.1016/j.ijpharm.2004.11.014.

[33] Dionex Corporation, Monitoring Monoclonal Antibody Stability by Cation-Exchange Chromatography, Application Note 128 (http://www.dionex.com/en-us/webdocs/4473-AN128-Monitoring-Monoclonal-Antibody-02Feb07-LPN1052-01.pdf), Sunnyvale, CA, USA. (2009) 1–7.

[34] S. Hertel, T. Pohl, W. Friess, G. Winter, Prediction of protein degradation during vibrating mesh nebulization via a high throughput screening method., Eur. J. Pharm. Biopharm. 87 (2014) 386–394. doi:10.1016/j.ejpb.2014.03.020.

[35] H.-C. Mahler, R. Müller, W. Frieβ, A. Delille, S. Matheus, Induction and analysis of aggregates in a liquid IgG1-antibody formulation., Eur. J. Pharm. Biopharm. 59 (2005) 407–417. doi:10.1016/j.ejpb.2004.12.004.

[36] M.C. Manning, D.K. Chou, B.M. Murphy, R.W. Payne, D.S. Katayama, Stability of protein pharmaceuticals: an update., Pharm. Res. 27 (2010) 544–75. doi:10.1007/s11095-009-0045-6.

[37] S.P. Hertel, W. Friess, G. Winter, Comparison of Aerosol Collection Methods for Liquid Protein Formulations, Respir. Drug Deliv. Eur. 2011. 2 (2011) 345–350.

[38] D. Mahl, J. Diendorf, W. Meyer-Zaika, M. Epple, Possibilities and limitations of different analytical methods for the size determination of a bimodal dispersion of metallic nanoparticles., Colloids Surfaces A Physicochem. Eng. Asp. 377 (2011) 386–392. doi:10.1016/j.colsurfa.2011.01.031.

[39] V. Filipe, A. Hawe, W. Jiskoot, Critical evaluation of Nanoparticle Tracking Analysis (NTA) by NanoSight for the measurement of nanoparticles and protein aggregates., Pharm. Res. 27 (2010) 796–810. doi:10.1007/s11095-010-0073-2.

[40] H. Mahler, W. Friess, U. Grauschopf, S. Kiese, Protein aggregation: pathways, induction factors and analysis., J. Pharm. Sci. 98 (2009) 2909–34. doi:10.1002/jps.21566.

[41] S.P. Hertel, Pulmonary Delivery of Pharmaceutical Proteins by Means of Vibrating Mesh Nebulization, Dissertation. Ludwig-Maximilians-Universität Munich, Germany, 2014.

[42] P. Vogel, V.R. Rivera, M.L. Pitt, M.A. Poli, Comparison of the pulmonary distribution and efficacy of antibodies given to mice by intratracheal instillation or aerosol inhalation., Lab. Anim. Sci. 46 (1996) 516–23.

[43] M. Osier, R.B. Baggs, G. Oberdörster, Intratracheal instillation versus intratracheal inhalation: influence of cytokines on inflammatory response., Environ. Health Perspect. 105 Suppl (1997) 1265–71.

[44] M. Sakagami, In vivo, in vitro and ex vivo models to assess pulmonary absorption and disposition of inhaled therapeutics for systemic delivery., Adv. Drug Deliv. Rev. 58 (2006) 1030–60. doi:10.1016/j.addr.2006.07.012.

[45] U. Lorenz, B. Lorenz, T. Schmitter, K. Streker, C. Erck, J. Wehland, et al., Functional antibodies targeting IsaA of Staphylococcus aureus augment host immune response and open new perspectives for antibacterial therapy., Antimicrob. Agents Chemother. 55 (2011) 165–73. doi:10.1128/AAC.01144-10.

[46] G.E. Stein, E.M. Wells, The importance of tissue penetration in achieving successful antimicrobial treatment of nosocomial pneumonia and complicated skin and soft-tissue infections caused by methicillin-resistant Staphylococcus aureus: vancomycin and linezolid., Curr. Med. Res. Opin. 26 (2010) 571–88. doi:10.1185/03007990903512057.

[47] G.L. Bassi, M. Ferrer, J.D. Marti, T. Comaru, A. Torres, Ventilator-associated pneumonia., Semin. Respir. Crit. Care Med. 35 (2014) 469–81. doi:10.1055/s-0034-1384752.

[48] S. Hertel, T. Pohl, W. Friess, G. Winter, That's cool! – Nebulization of thermolabile proteins with a cooled vibrating mesh nebulizer., Eur. J. Pharm. Biopharm. 87 (2014) 357–365. doi:10.1016/j.ejpb.2014.03.001.

CHAPTER V

SURFACE FUNCTIONALIZATION ALLOWING REPETITIVE USE OF OPTICAL SENSORS FOR REAL-TIME DETECTION OF ANTIBODY-BACTERIA INTERACTION

This chapter was published in the Journal of Biophotonics in a slightly modified version and appears in this thesis with permission from the publisher WILEY. The chapter was modified from the published version by integrating supplementary information into the body text.

M. Kutscher, M. Rosenberger, B. Schmauss, L. Meinel, U. Lorenz, K. Ohlsen, R. Hellmann, and O. Germershaus (2015), Surface functionalization allowing repetitive use of optical sensors for real-time detection of antibody-bacteria interaction. J. Biophoton. doi: 10.1002/jbio.201500178

Abstract

In this study, sensor surface functionalization allowing the repetitive use of a sensing device was evaluated for antibody-based detection of living bacteria using an optical planar Bragg grating sensor. To achieve regenerable immobilization of bacteria specific antibodies, the heterobifunctional cross-linker N-succinimidyl 3-(2-pyridyldithio) propionate (SPDP) was linked to an aminosilanized sensor surface and subsequently reduced to expose sulfhydryl groups enabling the covalent conjugation of SPDP-activated antibodies via disulfide bonds. The immobilization of a capture antibody specific for *Staphylococcus aureus* on the sensor surface as well as specific binding of *S. aureus* could be monitored, highlighting the applicability of optical sensors for the specific detection of large biological structures. Reusability of bacteria saturated sensors was successfully demonstrated by cleaving the antibody along with bound bacteria through reduction of disulfide bonds and subsequent re-functionalization with activated antibody, resulting in comparable sensitivity towards *S. aureus*.

1. Introduction

Detection methods for pathogens, microorganism, and other biological specimens are in great demand in the field of life sciences and clinical diagnostics, in particular in the context of infectious diseases. Especially for ubiquitous and often persistent pathogens such as *Staphylococcus aureus*, immediate detection and identification is crucial for the proper choice of medical treatment allowing to avoid systemic spreading and persistence of the infection as well as development of antibiotic resistance [1]. Biosensors promise to improve pathogen detection, providing a wide field of application and permitting sensitive, specific, and rapid analysis of diverse specimens [2–4]. Specifically, label-free optical biosensors such as planar Bragg grating sensors (PBGs), among others, emerged as alternatives to traditional clinical analysis methods, allowing to reduce costs, improve handling and avoid labeling [5–9].

Highly selective detection of pathogens may be achieved by immobilizing target-specific antibodies on the surface of the sensing region of PBGs [3]. Binding of complementary antigens to the antibody-modified sensor surface changes the refractive index in proximity of the sensing grating and leads to a detectable spectral shift of the reflected Bragg wavelength [9].

Several authors have evaluated antibody modified sensors for the detection of biological entities including bacteria [2–5,7,10–13]. However, in most studies antibodies were covalently attached to the sensor surface, permitting only single use or requiring laborious and/or harsh cleaning procedures prior to subsequent analysis. In contrast, reusable sensors would not only reduce installation time, costs, and preparatory work but would also minimize waste and consumption of resources. Towards this end, antibody conjugation through interaction of the Fc part of antibodies with protein A or G would represent a straightforward approach, allowing regeneration of the sensor through cleavage of protein A/G-antibody interaction, e.g. by incubation in acidic guanidine solution [3–5,14,15]. But, both costs and high molecular weight of the linker molecules represent significant drawbacks of this strategy. To alleviate these disadvantages and to improve sensor reusability, we developed antibody modified PBGs using low molecular weight cleavable linkers and tested their sensing capabilities towards different bacterial strains. This paper describes the synthetic strategy used for conjugation of antibodies to the sensor surface by cleavable linkers, provides evidence for successful linker and antibody conjugation based on sensor response, and presents the results of an initial proof-of-concept study employing antibody modified PBGs for repetitive specific detection of *S. aureus*.

2. Materials and methods

2.1. Materials

All applied chemicals were at least of analytical grade unless stated otherwise. The cross-linker N-succinimidyl 3-(2-pyridyldithio) propionate (SPDP) was sourced from Thermo Fisher Scientific Inc. (Rockford, IL, USA). DMSO (Dimethyl sulfoxid, 99.9%, Bio Reagent), APTES ((3-Aminopropyl) triethoxysilane) as well as DTT (DL-Dithiothreitol, ≥98% (TLC), ≥99.0% (titration)) were obtained from Sigma-Aldrich Chemie GmbH (Steinheim, Germany). UK-66, a monoclonal antibody (mAb) targeting the immunodominant staphylococcal antigen A (IsaA), was provided by the Institute for Molecular Infection Biology (University of Wurzburg, Germany), where also the bacterial strains *Staphylococcus aureus* Newman wildtype and *Escherichia coli* 536 were cultivated [16]. The cell densities were adjusted to $3 \cdot 10^{10}$ CFU/ml in 3 ml PBS before use.

2.2. Planar Bragg grating sensor

The sensors are based on a periodic refractive index perturbation in an optical waveguide which reflects a particular wavelength. The spectral position of the reflected Bragg wavelength (λ_B) is determined by the period of the refractive index perturbation Λ and the effective refractive index n_{eff}. In this study, a PBGs was used which was fabricated with the direct writing technique [17,18]. Initially, the integrated waveguide and the Bragg gratings had been isolated from the environment by a silica layer. To allow interaction of the evanescent field with the surrounding medium, which is essential for the detection of changes of the refractive index, the cladding layer above the sensing grating was partially removed by hydrofluoric etching. Subsequently, the sensor surface was coated with a high refractive index titanium dioxide layer. Since the covering layer above the other grating remained unchanged, preventing the evanescent field of this buried grating to interact with the environment, its reflected Bragg wavelength could be used as a reference signal to detect temperature fluctuations during measurements. By connecting a single mode (SM) fiber to the PBGs using UV curable glue, both gratings could be simultaneously monitored during the experiments. A detailed description of the fabrication process of the PBGs can be found elsewhere [19–22]. **Figure 1** illustrates the structure of the planar sensor chip, including a cross-section indicating the interaction of the evanescent field with a surrounding medium.

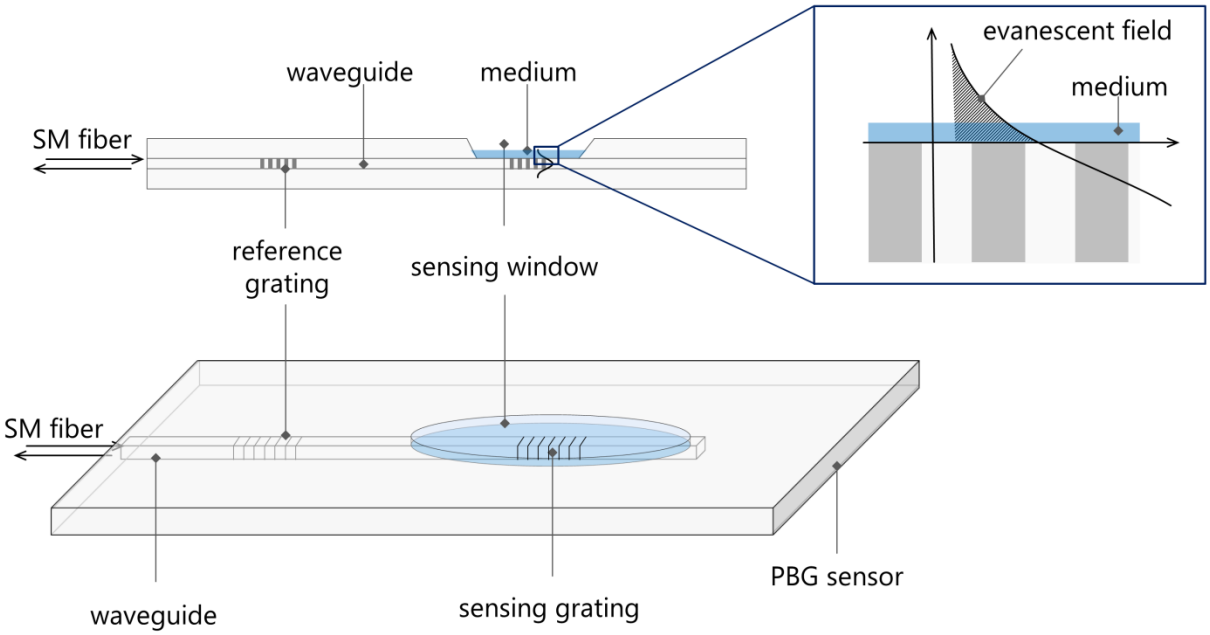

Figure 1: Illustration of the composition and the operation principle of a silica based optical planar Bragg grating sensor.

A Bragg meter, consisting of a tunable laser diode, emitting a wavelength spectrum in the telecommunication range around 1550 ± 40 nm, a circulator, and a photodiode were used for the interrogation of the planar Bragg grating sensors. The sensing system exhibited a sampling rate of 2 Hz and a resolution of 1 pm. Prior to each experiment, the sensor was equilibrated at the respective starting conditions until a stable baseline was observed for at least 5 minutes.

2.3. Modification of the sensor surface with *S. aureus* specific antibody

To prepare the sensor surface for subsequent conjugation steps, the PBGs were first functionalized by aminosilanization. After cleaning the sensor surface with PBS and acetone, the PBGs were immersed in 3 ml 2% (V/V) APTES in acetone for approximately 60 min and rinsed with acetone to remove excess APTES solution. The formed aminosilane layer was cured at 60°C for 105 min. For immobilization of the monoclonal antibody on the sensor surface, the heterobifunctional cross-linker SPDP was used (**Figure 2**) [23–25]. Both, mAb and sensor surface were separately modified with SPDP (**Figure 2**, **Ia and Ib**). SPDP solution was freshly prepared (5.2 mg/ml in DMSO) and mixed with mAb solution (10 mg/ml in PBS, pH 7.4) at a molar ratio of approximately 12.5:1. The mixture was allowed to react at room temperature for 30 min and the modified mAb was purified from reaction byproducts and

excess SPDP by gel filtration into PBS containing 10 mM EDTA (PBS-EDTA) using Illustra NAP-25 columns (GE healthcare, Buckinghamshire, UK).

The sensor was incubated in a 1:21 mixture of SPDP (10 mM in DMSO) and PBS-EDTA, pH 7.4, for 30 min at room temperature and subsequently immersed in PBS-EDTA to remove reaction byproducts and excess SPDP. The SPDP-modified sensor surface was incubated in 50 mM DTT for 45 min to generate free sulfhydryl groups (**Figure 2, II**) and immersed in PBS-EDTA to remove excess DDT as well as reaction byproducts. Finally, the sulfhydryl-activated sensor surface was incubated with SPDP-activated mAb solution for at least 18 h at 4°C (**Figure 2, III**) and non-conjugated mAb was removed by immersion in PBS-EDTA. The mAb modified sensor was stored in PBS-EDTA until use. The process of the mAb conjugation onto the sensor surface was monitored by recording the sensor response during each functionalization step. Prior to each modification, the sensor was equilibrated in PBS-EDTA until a stable baseline signal was obtained. The binding of the single reagents onto the sensor surface was analyzed by observation of absolute Bragg wavelength shift.

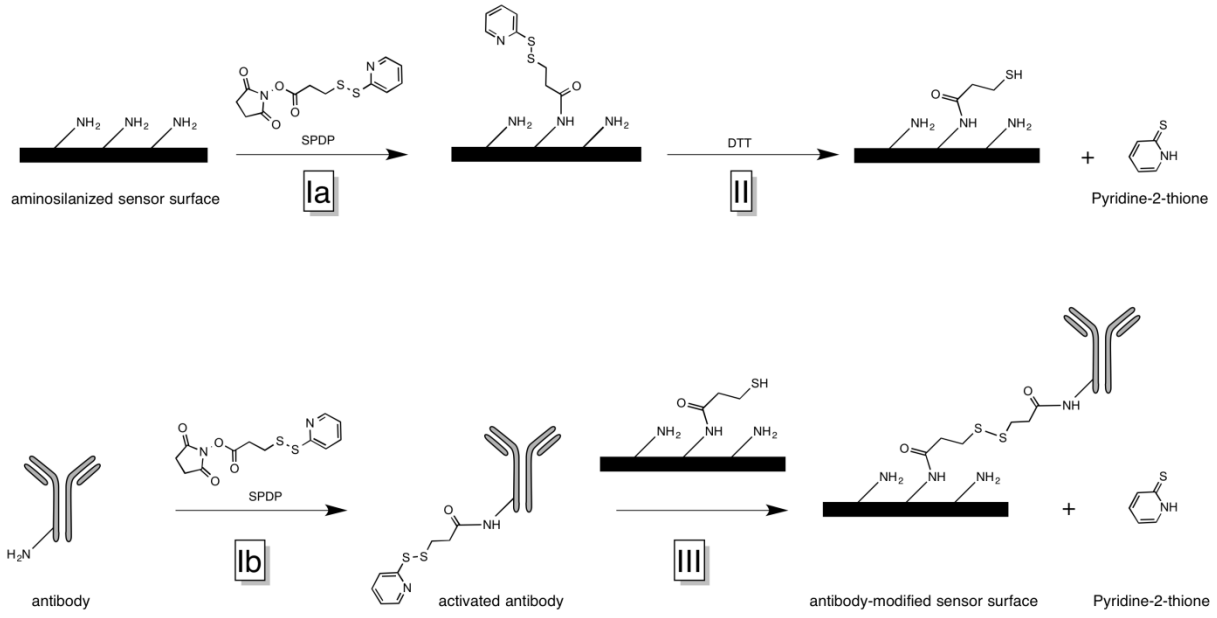

Figure 2: Schematic illustration of the strategy for coupling anti-IsaA antibodies to the functionalized sensor surface using SPDP as a cross-linker.

2.4. Real-time detection of antibody-bacteria interaction

To evaluate the response of antibody modified sensors in the presence of *S. aureus* or *E. coli,* absolute wavelengths shifts were recorded. After equilibration in PBS-EDTA, an antibody-functionalized sensor was exposed to an *E. coli* cell suspension ($3 \cdot 10^{10}$ CFU/ml) for 5 min and subsequently re-immersed into PBS-EDTA. After equilibration of the monitored signal, the same sensor was incubated in a *S. aureus* bacteria suspension ($3 \cdot 10^{10}$ CFU/ml) for 90 min to analyze the selective binding of *S. aureus* to the mAb-modified sensor surface. Subsequently, the sensor was rinsed with PBS-EDTA to remove any unbound bacteria. A second mAb-modified sensor was immersed directly in *S. aureus* bacteria suspension ($3 \cdot 10^{10}$ CFU/ml) for 60 min to investigate the absolute wavelength shift caused by the binding of *S. aureus* without the influence of unspecifically adsorbed *E. coli*. As a control for unspecific binding to the aminosilanized sensor surface, the response of a sensor without attached antibody toward both bacteria strains was investigated. The control sensor was initially exposed to *E. coli* for 20 min and afterwards regenerated using 5 M NaCl for 10 min before incubation with *S. aureus* for 60 min (both at $3 \cdot 10^{10}$ CFU/ml).

2.5. Regeneration of the sensor

For practical application of the sensing device, reusability of the SPDP-modified sensor is a crucial requirement and was investigated in detail. The bacteria saturated sensor was incubated in 50 mM DTT for 30 min (**Figure 3**) while the shift of the sensor signal was recorded [26]. After regeneration of sulfhydryl groups, the sensor was incubated with SPDP-modified mAb overnight (about 20 h) at 4°C to re-functionalize the sensor surface with fresh mAb (**Figure 3**). To demonstrate the functionality of the regenerated sensor, the response to the *S. aureus* bacteria suspension ($3 \cdot 10^{10}$ bacteria/ml) was analyzed.

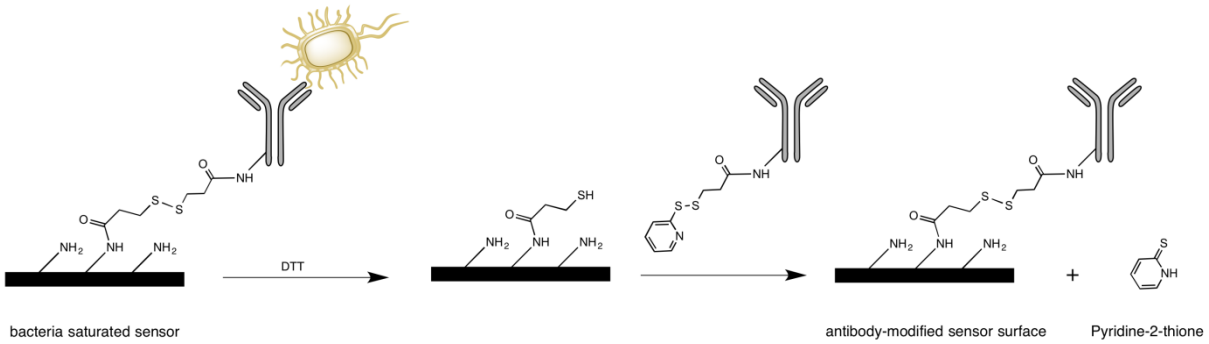

Figure 3: Schematic illustration of the sensor regeneration with DTT induced cleavage of the disulfide bond between the sensor surface and bacteria-saturated antibodies as well as renewed immobilization of activated mAb onto the sensor surface.

3. Results and discussion

3.1. Sensor functionalization

The sensor surface was functionalized by formation of a self-assembled aminosilane monolayer using APTES [27,28] enabling subsequent reaction with SPDP (**Figure 2, Ia**). SPDP is a heterobifunctional cross-linker featuring an amine-reactive part represented by the N-hydroxysuccinimide (NHS) ester as well as a sulfhydryl-reactive part represented by a 2-pyridyldithio group [29–31]. In this study, SPDP was used to cross-link primary amines of the antibody to the aminated sensor surface. For this, both, amino groups of the antibody and of the sensor surface were modified separately with SPDP (**Figure 2, Ia and Ib**). The binding of SPDP altered the refractive index on the sensor surface resulting in a positive shift of the reflected Bragg wavelength by approximately 800 pm over 50 min (**Figure 4A**). Concurrently, the reference peak wavelength remained constant indicating a constant temperature during the binding process. Subsequently, the sensor surface was treated with DTT to generate free sulfhydryl groups by releasing pyridine-2-thione (**Figure 2, II**). Cleaving of pyridine-2-thione caused a reduction of the refractive index, resulting in a negative wavelength shift of 40 pm over 25 min (**Figure 4B**). Finally, a SPDP-modified antibody, which specifically recognizes the IsaA epitope on *S. aureus*, was covalently attached to free sulfhydryl groups on the sensor surface forming disulfide bonds (**Figure 2, III**). The immobilization of antibodies could be monitored in real-time through a steady and significant shift of the reflected Bragg wavelength of 300 pm over 50 min (**Figure 4C**).

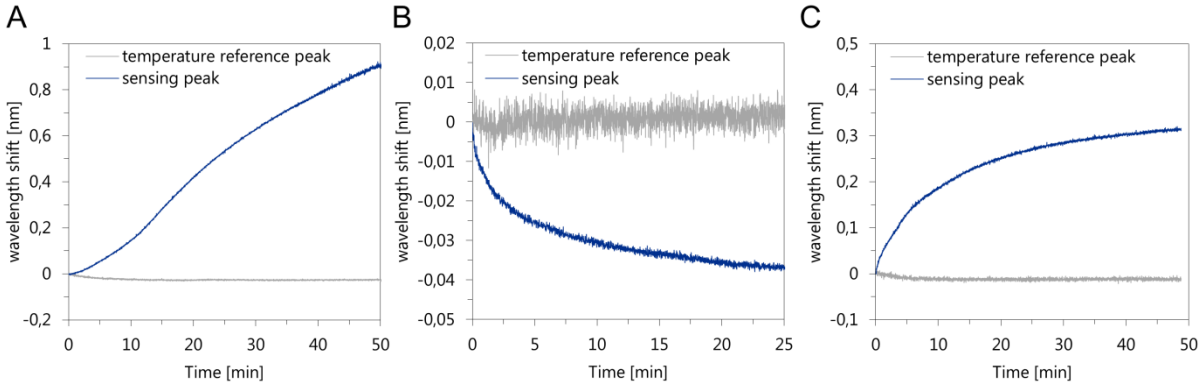

Figure 4: Monitoring of sensor surface functionalization: (A) binding of SPDP to the aminosilanized sensor surface, (B) cleavage of disulfide bonds using DTT exposing sulfhydryl-groups, and (C) conjugation of SPDP modified antibody onto the surface.

3.2. Specific detection of *S. aureus*

The antibody-functionalized sensors were exposed to different bacteria suspensions in PBS to test their ability to specifically detect *S. aureus*. The real-time response of the sensor during incubation with *S. aureus* is shown in **Figure 5A**. The immediate and steady shift of the reflected Bragg wavelength of over 110 pm during 55 min was associated with the binding interaction between *S. aureus*, containing the surface antigen IsaA, and the anti-IsaA antibody immobilized on the sensor surface [16]. In contrast, immersing anti-IsaA antibody-functionalized sensor in an *E. coli* suspension of the same concentration resulted in a constant sensor signal (**Figure 5B**). From the shift of the temperature reference peak when transferring the sensor from PBS to the bacteria suspension, it was apparent that the temperature of the bacteria suspensions was higher than pure PBS but decreased slightly during incubation. Taking into account the negative wavelength shift of 5 pm induced by the temperature fluctuations, a slight positive net shift of the sensing signal in the presence of *E. coli* resulted. However, when returning the sensor into PBS solution, an instantaneous minimal negative shift of the sensing signal was observed indicating desorption of unspecifically bound *E. coli*.

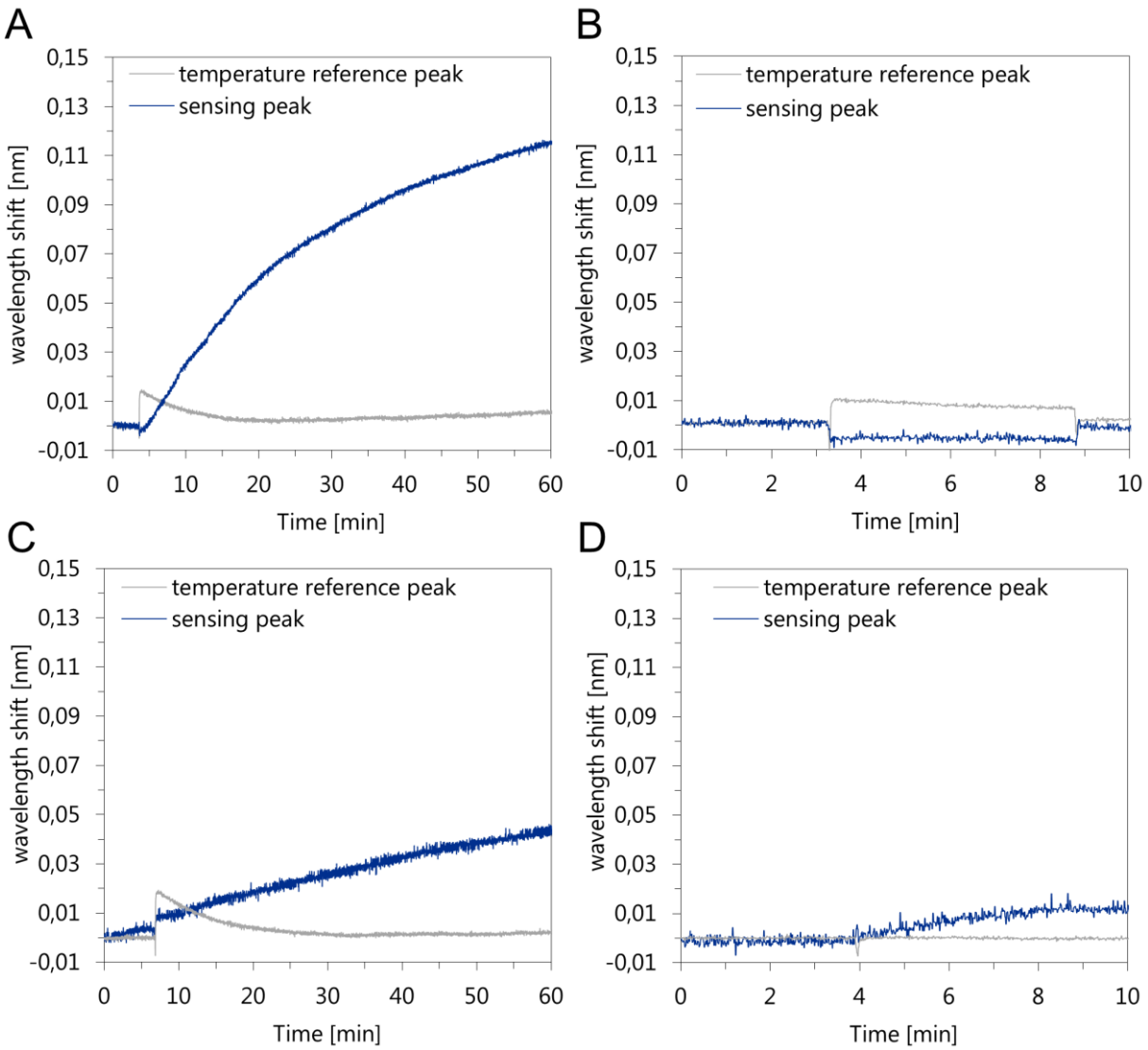

Figure 5: Bragg wavelength shifts of a mAb modified sensor resulting from exposure to (A) *S. aureus*, (B) *E. coli* and of an aminosilanized sensor to (C) *S. aureus* and (D) *E. coli*.

In summary, incubation of mAb-modified sensors with *E. coli* led to minimal, unspecific and reversible adsorption of bacteria to the sensor surface. When the same sensor was subsequently exposed to *S. aureus,* a significant shift of the reflected wavelength was observed, indicating specific binding of *S. aureus* to the antibody-modified sensor surface even after exposure to *E. coli* (**Figure 6**).

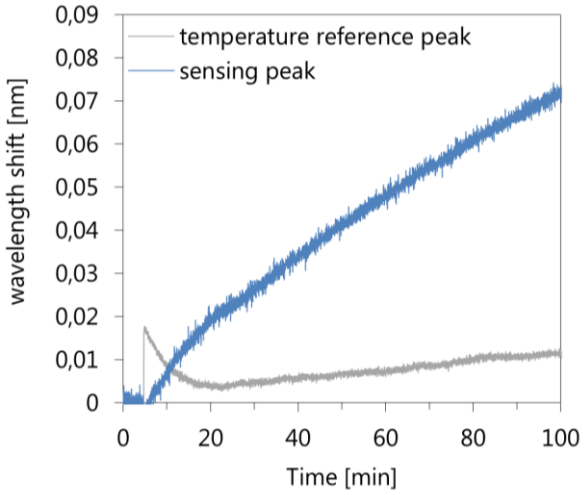

Figure 6: Sensor response to incubation with *S. aureus* following incubation with *E. coli*.

To demonstrate that the immobilization of anti-IsaA antibody on the sensor surface was a necessary prerequisite for specific detection of *S. aureus*, both, *E. coli* and *S. aureus* suspensions were introduced to an aminosilane coated sensor without conjugated antibody (**Figure 5C and 5D**). A slow increase of the reflected wavelength of approximately 40 pm over 60 min was observed in the case of *S. aureus* suspension (**Figure 5C**), while immersion in *E. coli* suspension resulted in a shift of approximately 13 pm in the first 5 minutes and remained constant thereafter (**Figure 5D**). The positive Bragg wavelength shift observed for both bacteria suspensions may be explained by attractive electrostatic interaction between negatively charged surface of bacteria and the positively charged aminosilanized sensor surface [28,32]. It is interesting to note that *E. coli* was shown to exhibit a lower adsorption rate to positively charged surfaces than *S. aureus* in the study by Gottenbos et al., potentially explaining the less distinct amplitude shift of the sensor signal in the case of *E. coli* [32]. Furthermore, *E. coli* showed faster desorption than *S. aureus* in the same study [32]. Hence, the constant sensor signal observed after only 5 minutes may be interpreted as a result of the balance between adsorption and desorption of *E.coli* on the aminosilanized sensor surface. These control experiments suggest that wavelength shifts observed for antibody-modified sensors were not due to unspecific adsorption of bacteria to the sensor surface but resulted from specific antibody-antigen interaction with *S. aureus*.

We would like to emphasize that the sensitivity of modified PBGs described herein is not yet up to par with alternative optical sensing principles and requires further optimization. A similar PBG was described by Bhatta et al., where mAbs were immobilized via interaction with protein A/G and used for the detection of *E. coli* and other biological agents [3]. In this report, *E. coli* were successfully detected at $4.6 \cdot 10^8$ CFU/ml, suggesting higher sensitivity of

this sensor. However, the intention of the study of Bhatta et al. and ours was to show the feasibility of bacteria detection with mAb-modified PBGs and both studies did not determine the limit of quantification or limit of detection of sensors. Further improvement of the sensitivity of mAb-modified PBGs for bacteria detection might be achieved through optimization of several sensor-related parameters in future studies. The oriented immobilization of mAbs on the sensor surface was shown to be conducive for sensitivity since random conjugation may result in steric hindrance and hence loss of binding capacity [12,33,34]. Among other strategies, oriented antibody immobilization may be achieved through oxidation of carbohydrates in the Fc part and subsequent reductive amination [35]. Antibody surface density is another critical parameter closely related to mAb orientation. It has been shown that an optimum mAb density exists, above which steric hindrance results in reduced sensitivity. On the other hand, too low mAb density limits sensitivity due to sub-optimal binding capacity [36,37]. Sensitivity improvements could also be achieved through direct conjugation of Fab' fragments, allowing to reduce molecular weight of mAbs while achieving oriented conjugation via disulfide bridges between the Fab fragment and SPDP-modified sensor surface [38,39].

It should also be noted that antibody selection critically affects performance and reliability of the sensing principle. On the one hand, high selectivity for the target microorganism is required and on the other hand different strains of target bacteria should be detected with comparable efficiency. Lastly, mutation of surface features of the target microorganism may reduce detection efficiency. *S. aureus* specific anti-IsaA antibody used herein to our current knowledge fulfills these requirements. It has been shown that the targeted IsaA antigen is involved in the cell wall metabolism of *S. aureus*, and is regarded as standard housekeeping protein, resulting in lower likelihood of mutation compared to virulence associated antigens [40,41]. Furthermore, IsaA is found conserved in all sequenced *S. aureus* strains and efficient binding of anti-IsaA antibody to major clinical lineages was shown [16,42].

3.3. Regeneration of the sensor

Finally, the feasibility of PBGs regeneration after cleavage of bacteria-saturated antibody was studied. The disulfide-containing cross-linker between the antibody and the sensor could be cleaved by incubation with DTT resulting in an instantaneous distinct shift of the reflected wavelength by approximately 250 pm over 30 min (**Figure 7A**). DTT exhibited a higher refractive index compared to PBS-ETDA leading to a steep increase of the wavelength shift after immersion into DTT solution and a comparable decrease during the transition back to PBS-EDTA (**Figure 7A**). For regeneration of the *S. aureus* specific sensor, SPDP-modified antibody was conjugated to the sensor surface via free sulfhydryl groups as described above, resulting in a positive shift of the sensor signal by approximately 350 pm over 30 min (**Figure 7B**). The functionality of the regenerated sensor was verified by real-time monitoring of capture of *S. aureus*. Incubation of the regenerated sensor with *S. aureus* suspension resulted in a positive reflected wavelength shift of approximately 120 pm within 60 min confirming comparable binding of *S. aureus* before and after sensor regeneration (**Figure 7C**).

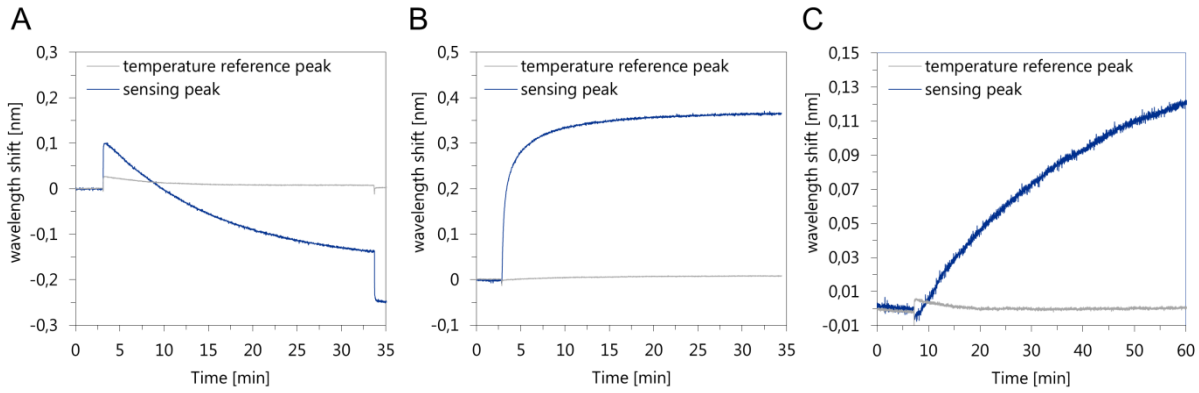

Figure 7: Regeneration of a bacteria saturated sensor by (A) cleaving of the disulfide bond between the cross-linker and the antibody along with bound bacteria using DTT, (B) coupling of fresh activated antibody to the sensor surface, and (C) detection of S. aureus using the regenerated planar Bragg grating sensor.

4. Conclusion

Anti-IsaA antibody modification of aminosilanized PBGs can be used to specifically and selectively detect *S. aureus*. Furthermore, the individual steps during antibody conjugation to the sensor surface are associated with distinct changes of the sensor signal, allowing real-time monitoring of surface modifications. The disulfide-containing cross-linker employed herein allows cleavage of bacteria-saturated antibodies from the sensor surface and simple regeneration of the sensor through incubation with SPDP-activated antibody, resulting in similar sensitivity towards *S. aureus* after regeneration.

These results confirm the applicability of established bioconjugation techniques in the context of bacteria-specific PBGs, allowing for straightforward, inexpensive sensor surface modification. Compared to alternative conjugation strategies based on avidin-streptavidin or protein A/G interaction, the conjugation technique employed herein not only reduces costs and improves sensor ruggedness but also allows regeneration of the sensor and reduces cross-linker molecular weight, potentially promoting broad application and future sensitivity improvements, respectively. While proof-of-concept has been confirmed, the low sensitivity of the current sensor limits its applicability. We anticipate that the combination of established methods for sensitivity enhancement of optical sensors with the inexpensive, regenerable surface functionalization established herein will ultimately lead to reusable antibody-based sensors with high sensitivity.

References

[1] J. García-Lara, M. Masalha, S.J. Foster, Staphylococcus aureus: the search for novel targets., Drug Discov. Today. 10 (2005) 643–51. doi:10.1016/S1359-6446(05)03432-X.

[2] B. Byrne, E. Stack, N. Gilmartin, R. O'Kennedy, Antibody-based sensors: principles, problems and potential for detection of pathogens and associated toxins., Sensors. 9 (2009) 4407–4445. doi:10.3390/s90604407.

[3] D. Bhatta, E. Stadden, E. Hashem, I.J.G. Sparrow, G.D. Emmerson, Multi-purpose optical biosensors for real-time detection of bacteria, viruses and toxins., Sensors Actuators B Chem. 149 (2010) 233–238. doi:10.1016/j.snb.2010.05.040.

[4] D. Bhatta, A.A. Michel, M. Marti Villalba, G.D. Emmerson, I.J.G. Sparrow, E.A. Perkins, et al., Optical microchip array biosensor for multiplexed detection of bio-hazardous agents., Biosens. Bioelectron. 30 (2011) 78–86. doi:10.1016/j.bios.2011.08.031.

[5] D. Bhatta, E. Stadden, E. Hashem, I.J.G. Sparrow, G.D. Emmerson, Label-free monitoring of antibody-antigen interactions using optical microchip biosensors., J. Immunol. Methods. 362 (2010) 121–6. doi:10.1016/j.jim.2010.09.015.

[6] X. Fan, I.M. White, S.I. Shopova, H. Zhu, J.D. Suter, Y. Sun, Sensitive optical biosensors for unlabeled targets: a review., Anal. Chim. Acta. 620 (2008) 8–26. doi:10.1016/j.aca.2008.05.022.

[7] M.N. Velasco-Garcia, Optical biosensors for probing at the cellular level: a review of recent progress and future prospects., Semin. Cell Dev. Biol. 20 (2009) 27–33. doi:10.1016/j.semcdb.2009.01.013.

[8] V.M.N. Passaro, F. Dell'Olio, B. Casamassima, F. De Leonardis, Guided-wave optical biosensors., Sensors. 7 (2007) 508–536. doi:10.3390/s7040508.

[9] R.M. Parker, J.C. Gates, D.J. Wales, P.G.R. Smith, M.C. Grossel, An investigation into dispersion upon switching between solvents within a microfluidic system using a chemically resistant integrated optical refractive index sensor., Lab Chip. 13 (2013) 377–85. doi:10.1039/c2lc41124e.

[10] D. Bhatta, M.M. Villalba, C.L. Johnson, G.D. Emmerson, N.P. Ferris, D.P. King, et al., Rapid detection of foot-and-mouth disease virus with optical microchip sensors., Procedia Chem. 6 (2012) 2–10. doi:10.1016/j.proche.2012.10.124.

[11] B. Lu, J. Xie, C. Lu, C. Wu, Y. Wei, Oriented immobilization of Fab' fragments on silica surfaces., Anal. Chem. 67 (1995) 83–87. doi:10.1021/ac00097a014.

[12] P. Peluso, D.S. Wilson, D. Do, H. Tran, M. Venkatasubbaiah, D. Quincy, et al., Optimizing antibody immobilization strategies for the construction of protein microarrays., Anal. Biochem. 312 (2003) 113–124. doi:10.1016/S0003-2697(02)00442-6.

[13] A. Subramanian, J. Irudayaraj, T. Ryan, Mono and dithiol surfaces on surface plasmon resonance biosensors for detection of Staphylococcus aureus., Sensors Actuators B Chem. 114 (2006) 192–198. doi:10.1016/j.snb.2005.04.030.

[14] F. Baldini, A.N. Chester, J. Homola, S. Martellucci, Optical Chemical Sensors, Vol. 224, Springer Netherlands, 2006. doi:10.1007/1-4020-4611-1.

[15] P.M. Fratamico, T.P. Strobaugh, M.B. Medina, A.G. Gehring, Detection of Escherichia coli O157: H7 using a surface plasmon resonance biosensor., Biotechnol. Tech. 12 (1998) 571–576. doi:10.1023/A:1008872002336.

[16] U. Lorenz, B. Lorenz, T. Schmitter, K. Streker, C. Erck, J. Wehland, et al., Functional antibodies targeting IsaA of Staphylococcus aureus augment host immune response and open new perspectives for antibacterial therapy., Antimicrob. Agents Chemother. 55 (2011) 165–73. doi:10.1128/AAC.01144-10.

[17] G.D. Emmerson, C.B.E. Gawith, S.P. Watts, V. Albanis, R.B. Williams, S.G. McMeekin, et al., Photosensitivity locking technique applied to UV written planar Bragg gratings., Electron. Lett. 39 (2003) 517. doi:10.1049/el:20030379.

[18] G.D. Emmerson, S.P. Watts, C.B.E. Gawith, V. Albanis, M. Ibsen, R.B. Williams, et al., Fabrication of directly UV-written channel waveguides with simultaneously defined integral Bragg gratings., Electron. Lett. 38 (2002) 1531. doi:10.1049/el:20021056.

[19] I.J.G. Sparrow, P.G.R. Smith, G.D. Emmerson, S.P. Watts, C. Riziotis, Planar Bragg Grating Sensors—Fabrication and Applications: A Review, J. Sensors. 2009 (2009) 1–12. doi:10.1155/2009/607647.

[20] M. Girschikofsky, M. Rosenberger, S. Belle, M. Brutschy, S.R. Waldvogel, R. Hellmann, Highly sensitive detection of naphthalene in solvent vapor using a functionalized PBG refractive index sensor., Sensors. 12 (2012) 2018–2025. doi:10.3390/s120202018.

[21] M. Girschikofsky, M. Rosenberger, S. Belle, M. Brutschy, S.R. Waldvogel, R. Hellmann, Optical planar Bragg grating sensor for real-time detection of benzene, toluene and xylene in solvent vapour., Sensors Actuators B Chem. 171-172 (2012) 338–342. doi:10.1016/j.snb.2012.04.046.

[22] S. Scheurich, S. Belle, R. Hellmann, S. So, I.J.G. Sparrow, G. Emmerson, Application of a silica-on-silicon planar optical waveguide Bragg grating sensor for organic liquid compound detection., in: F. Baldini, J. Homola, R.A. Lieberman (Eds.), Proc. SPIE 7356, Opt. Sensors, 2009: p. 73561B–73561B–8. doi:10.1117/12.820484.

[23] Thermo Fisher Scientific Inc, Tech Tip #1: Attach a protein onto glass, silica, or quartz surface using a cleavable crosslinker (https://tools.thermofisher.com/content/sfs/brochures/TR0001-Attach-to-glass-cleavable.pdf), 2008.

[24] O. Germershaus, M. Neu, M. Behe, T. Kissel, HER2 targeted polyplexes: the effect of polyplex composition and conjugation chemistry on in vitro and in vivo characteristics., Bioconjug. Chem. 19 (2008) 244–53. doi:10.1021/bc700311n.

[25] O. Germershaus, T. Merdan, U. Bakowsky, M. Behe, T. Kissel, Trastuzumab-polyethylenimine-polyethylene glycol conjugates for targeting Her2-expressing tumors., Bioconjug. Chem. 17 (2006) 1190–9. doi:10.1021/bc0601119.

[26] Thermo Fisher Scientific Inc, Instructions - SPDP Crosslinkers, (https://tools.thermofisher.com/content/sfs/manuals/MAN0011212_SPDP_CrsLnk_UG.pdf), 2011.

[27] R.M. Parker, D.J. Wales, J.C. Gates, J.G. Frey, P.G.R. Smith, M.C. Grossel, Monolayer detection of ion binding at a crown ether-functionalised supramolecular surface via an integrated optical Bragg grating., Analyst. 139 (2014) 2774–82. doi:10.1039/c4an00283k.

[28] E. Metwalli, D. Haines, O. Becker, S. Conzone, C.G. Pantano, Surface characterizations of mono-, di-, and tri-aminosilane treated glass substrates., J. Colloid Interface Sci. 298 (2006) 825–31. doi:10.1016/j.jcis.2006.03.045.

[29] S.K. Bhatia, L.C. Shriver-Lake, K.J. Prior, J.H. Georger, J.M. Calvert, R. Bredehorst, et al., Use of thiol-terminal silanes and heterobifunctional crosslinkers for immobilization of antibodies on silica surfaces., Anal. Biochem. 178 (1989) 408–13.

[30] B. Johnsson, S. Löfås, G. Lindquist, A. Edström, R.M. Müller Hillgren, A. Hansson, Comparison of methods for immobilization to carboxymethyl dextran sensor surfaces by analysis of the specific activity of monoclonal antibodies., J. Mol. Recognit. 8 (1995) 125–31. doi:10.1002/jmr.300080122.

[31] M.C. Parker, N. Patel, M.C. Davies, C.J. Roberts, S.J. Tendler, P.M. Williams, A novel organic solvent-based coupling method for the preparation of covalently immobilized proteins on gold., Protein Sci. 5 (1996) 2329–32. doi:10.1002/pro.5560051119.

[32] B. Gottenbos, D.W. Grijpma, H.C. van der Mei, J. Feijen, H.J. Busscher, Antimicrobial effects of positively charged surfaces on adhering Gram-positive and Gram-negative bacteria., J. Antimicrob. Chemother. 48 (2001) 7–13. doi:10.1093/jac/48.1.7.

[33] A.K. Trilling, J. Beekwilder, H. Zuilhof, Antibody orientation on biosensor surfaces: a minireview., Analyst. 138 (2013) 1619–27. doi:10.1039/c2an36787d.

[34] A. Makaraviciute, A. Ramanaviciene, Site-directed antibody immobilization techniques for immunosensors., Biosens. Bioelectron. 50 (2013) 460–71. doi:10.1016/j.bios.2013.06.060.

[35] G.T. Hermanson, Bioconjugate Techniques, Elsevier Inc, Academic press Inc, 2013.

[36] E.-S. Kim, C.-K. Shim, J.W. Lee, J.W. Park, K.Y. Choi, Synergistic effect of orientation and lateral spacing of protein G on an on-chip immunoassay., Analyst. 137 (2012) 2421–30. doi:10.1039/c2an16137k.

[37] T.M. Spitznagel, D.S. Clark, Surface-density and orientation effects on immobilized antibodies and antibody fragments., Biotechnology. (N. Y). 11 (1993) 825–9. doi:10.1038/nbt0793-825.

[38] K.L. Brogan, K.N. Wolfe, P.A. Jones, M.H. Schoenfisch, Direct oriented immobilization of F(ab′) antibody fragments on gold., Anal. Chim. Acta. 496 (2003) 73–80. doi:10.1016/S0003-2670(03)00991-7.

[39] K. Bonroy, F. Frederix, G. Reekmans, E. Dewolf, R. De Palma, G. Borghs, et al., Comparison of random and oriented immobilisation of antibody fragments on mixed self-assembled monolayers., J. Immunol. Methods. 312 (2006) 167–81. doi:10.1016/j.jim.2006.03.007.

[40] M.R. Stapleton, M.J. Horsburgh, E.J. Hayhurst, L. Wright, I.-M. Jonsson, A. Tarkowski, et al., Characterization of IsaA and SceD, two putative lytic transglycosylases of Staphylococcus aureus., J. Bacteriol. 189 (2007) 7316–25. doi:10.1128/JB.00734-07.

[41] U. Lorenz, K. Ohlsen, H. Karch, M. Hecker, A. Thiede, J. Hacker, Human antibody response during sepsis against targets expressed by methicillin resistant Staphylococcus aureus., FEMS Immunol. Med. Microbiol. 29 (2000) 145–53. doi:10.1111/j.1574-695X.2000.tb01517.x.

[42] F.C. Tenover, L.K. McDougal, R. V Goering, G. Killgore, S.J. Projan, J.B. Patel, et al., Characterization of a strain of community-associated methicillin-resistant Staphylococcus aureus widely disseminated in the United States., J. Clin. Microbiol. 44 (2006) 108–18. doi:10.1128/JCM.44.1.108-118.2006.

CONCLUSION AND OUTLOOK

The emergence of bacterial resistance against conventional antibiotics is an increasing challenge in treatment of infectious diseases. This is also affecting the standard antibiotic therapy of MRSA pneumonia by vancomycin and linezolid. High clinical failure rates were reported for the systemic use of vancomycin [1]. This is presumably caused by its poor lung penetration [2,3] and the increasing systemic concentration of antibiotic that is required to treat MRSA due to resistance development [1,2]. Thus, higher vancomycin dosages are required which are, however, associated with enhanced incidence of nephrotoxicity [4]. Linezolid is associated with drug interaction issues causing adverse events and increased risk for development of resistance as well [3,5]. Therefore, the demand for new antimicrobial drugs or therapeutic options is high but the development of novel antibiotics is diminishing distinctly. A promising approach for the screening of new antibiotic entities is represented by the novel isolation chip technology which enables high-throughput cultivation of previously undescribed microbial soil organism [6–8]. Application of this method recently resulted in the discovery of teixobactin establishing a new class of lipid II binding antibiotics with activity against MRSA [7–9]. However, teixobactin's efficacy in treatment of MRSA pneumonia in clinical trials is yet to be evaluated. Nevertheless, further application of this cultivation method for screening of even more new antibiotics seems highly promising. The cephalosporines ceftaroline and ceftobiprole exhibit *in vitro* activity against MRSA and have already been approved for pneumonia therapy [10]. Therefore, large well-planed clinical trials studying the efficacy in treating MRSA pneumonia for both cephalosporins could help to improve the antibiotic treatment spectrum for pulmonary MRSA infections. However, development of new antibiotics alone cannot handle the serious problem of escalating antibiotic resistance. Instead, innovative and efficient delivery strategies for the available drugs as well as new therapeutic strategies are required. Local delivery of aerosolized drugs to the site of infection by inhalation enables increased local drug levels, shorter application times, reduced systemic side effects, improved clinical efficacy, and decreased resistance development especially when combined with systemic antimicrobial therapy [11–14]. Whereas for cystic fibrosis nebulization of antibiotics is already commonly applied [13,15–17], in treatment of pneumonia only off-label use of aerosolized antibiotics is reported [17]. Therefore, large clinical trials specifically analyzing the outcome of MRSA pneumonia therapy after inhalation of antibiotics are required to document an important progress in pneumonia therapy. However, not all antibiotics are easily transferable into a suitable

formulation for nebulization. To overcome this issue and to further improve drug delivery efficiency, antibiotics can be encapsulated into nanometer sized drug delivery systems [18]. Nanoparticle complexes (nanoplexes) prepared by self-assembly of a drug and an oppositely charged polyelectrolyte allow higher drug loading than ordinary nanoparticles, increased bioavailability, and enhanced solubility of poorly water-soluble drugs [18].

In chapter II of this thesis, we used isothermal titration calorimetry (ITC) along with supplemental analytical methods as a versatile screening tool for optimal preparation conditions for nanoplex formation of ciprofloxacin and dextran sulfate regarding salt type and ionic strength [19]. This analytical set up might find useful application in further studies to enable preparation of nanoplexes for MRSA therapy. Particularly linezolid seems to be a rational candidate for nanoplex formation owing to its poor water-solubility [20,21]. Similar to ciprofloxacin, linezolid is reported to be positively charged at low pH values [21] probably enabling self-assembly with a negatively charged polyelectrolyte to overcome its solubility issues. However, detailed studies are required to assess the nanoplex formation conditions and the potential therapeutical benefit of linezolid nanoplexes. Since nanoplexes enable liquid formulations of poorly water-soluble antibiotics, they should be analyzed for their suitability to be nebulized regarding aerosol characteristics and drug stability in subsequent studies.

A further possibility to increase therapeutic outcome of local antibiotic therapy by liposomal encapsulation has been discussed by reviewing latest achievements in local antibiotic drug delivery in chapter I of this thesis. Liposomal drug delivery systems are worth to be examined closely for MRSA pneumonia therapy by inhalation since they can facilitate sustained drug release, decreased dosing frequency, as well as improved mucus penetration [22]. Furthermore, nebulized liposomal drug delivery systems have already shown to increase vancomycin concentration in the lung compared to aerosolized vancomycin solution providing an encouraging basis for further investigations [23]. Additionally, expansion of the studies to lipid-polymer hybrid nanoparticles can be included in subsequent research to improve physical robustness of the drug delivery system [24,25].

Immunotherapeutic therapy using antibodies specifically directed against the infection triggering pathogen is another approach to combat MRSA pneumonia which has been discussed in this thesis [26,27]. A lyophilized formulation for hUK-66, an antibody directed against bacterial cell surface components of *S. aureus* with immunogenic characteristics, was developed to stabilize this protein against typical stresses occurring during production or shelf life and to enable efficacious drug application. To treat lung diseases by antibodies, nebulization is a promising way to yield high drug concentrations at the site of action since

penetration from blood circulation into lung tissue is impaired by the high molecular size of these macromolecules [28].

In chapter IV the developed formulation was also shown to be capable of protecting stability of hUK-66 during nebulization using an air-jet nebulizer. Most importantly, it proved to prolong survival of mice infected with *S. aureus* after application via inhalation in an *in vivo* study. Despite these notable results, there is still room for improvement in protein stabilization. Therefore, it would be interesting to supplement this study by using vibrating mesh nebulizers since these nebulizers proved to preserve protein stability better than air-jet nebulizers. Advantages of mesh nebulizers over air-jet nebulizers are the avoidance of multiple aerosolization and recirculation of protein molecules within the nebulizer, portability, faster nebulization rate, higher lung deposition, minimal residual volume, and minimized solvent evaporation [29–31]. The possible inherent heating of the mesh device jeopardizing protein stability can be controlled by active cooling of the device [30]. Furthermore, potential for optimization of the *in vivo* studies might be provided by repeated application of the nebulized antibody in treatment of pneumonia. Earlier preliminary studies of multiple hUK-66 application via inhalation failed due to numerous debilitating narcoses of the animals. In this thesis, a special setup was successfully developed overcoming the drawbacks of narcosis. Application of this setup enables mostly nose only nebulization to awake and normally breathing mice. Hence, a new foundation for a resume of *in vivo* studies evaluating multiple mAb nebulizations has been established. This potentially paves the way for further improvements in therapy of pneumonia by nebulized antibodies.

Especially the combination of several approaches seems to be effective for treatment of infectious diseases caused by multi-drug resistant bacteria and hence might present a rational subject for future investigations. The guideline for therapy of nosocomial pneumonia by the American Thoracic Society already considers the use of aerosolized antibiotics adjunctive to systemic treatment as reasonable but calls for further research in the use of aerosolized antibiotics [32]. A recent study which combined systemic and local treatment of VAP caused by several multi-drug resistant pathogens revealed highly promising results encouraging future clinical trials for the evaluation of the combination of systemic and aerosolized antibiotics in treatment of MRSA pneumonia [33]. In addition, combining antibiotics with immunotherapeutic antibodies can be of great interest for MRSA pneumonia therapy. This has been demonstrated by the use of antibody-vancomycin conjugates targeting intracellular bacteria which resulted in more efficient treatment of bacteria in mice than plain vancomycin [34]. Moreover, for treating lung infections and reducing the risk of antibiotic resistance

development, systemic antibiotics might be applied along with local administration of hUK-66. In addition, the alternating use of nebulized antibiotics and antibodies would be also conceivable. Finally, a combined application of several antibodies with different effector functions such as activation of the host immune system, opsonization, antimicrobial activity, and toxin neutralization presents a promising scenario to combat MRSA [35]. A first step in this direction could be provided by concomitant therapy using hUK-66, which opsonizes *S. aureus* and hence activates bacterial killing by the immune system, in addition to an anti-alpha-hemolysin mAb, which neutralizes toxins generated by *S. aureus* [36]. Furthermore, antibodies targeting other immunodominant structures or virulence factors are developed to reduce the bacterial burden during infection. Further development of these antibodies for combined application with hUK-66 might be promising.

Besides the application of effective drugs, an important aspect for efficient and rapid therapy of pneumonia is the immediate detection and identification of the infection triggering pathogens to enable proper selection of medical treatment. In chapter V of this thesis, selective detection of *S. aureus* could be achieved by immobilizing target-specific hUK-66 antibodies on the surface of an optical planar Bragg grating sensor. Furthermore, a sensor surface functionalization has been evaluated allowing the repetitive use of this sensing device for antibody-based detection of living bacteria to improve sensor reusability and reduce installation time, costs, as well as preparatory work [37]. However, the sensitivity of the modified PBGs described herein is not yet competitive compared to alternative optical sensing principles and requires further optimization. This might be achieved by oriented antibody immobilization through oxidation of carbohydrates in the Fc part and subsequent reductive amination [38] since random conjugation may result in steric hindrance and hence loss of binding capacity [39–41]. Sensitivity might also be improved through direct conjugation of Fab' fragments, which allows the reduction of mAbs' molecular weight while oriented conjugation could be achieved via disulfide bridges between the Fab fragment and SPDP-modified sensor surface [42,43]. In addition, the transfer of this reusable surface functionalization technique to other optical sensing principles might be an opportunity to enhance detection limits. Potential optical sensors are fiber-based devices such as, e.g., fiber Bragg gratings, nanofiber loops, or fiber-optic couplers [44]. A different approach to improve *S. aureus* detection by optical biosensors could be the development of planar polymer sensor chips functionalized with the capture antibody hUK-66 providing the benefit of being disposable and low-cost to avoid cross-sensitivity and to reduce preparatory work. Suitable materials could be polymethylmethacrylate (PMMA) and cyclic olefin copolymers (COP)

which have already proven to be applicable for the production of optical fiber biosensors [45–47]. A potential starting point for antibody immobilization onto these polymers might be represented by an anthraquinone-linker [48–50].

In conclusion, the current state of the art in therapy of pneumonia caused by MRSA has been reviewed and inherent problems and challenges have been discussed in this thesis. Furthermore, potential solutions for the increasing issue of antibiotic resistance have been assessed such as drug delivery systems, local drug delivery by nebulization and immunotherapeutic approaches. Additionally, a reusable detection method for fast identification of infection triggering pathogens has been evaluated. Hence, this thesis paves the way for further studies regarding MRSA pneumonia therapy by local drug delivery of antibiotics, immunotherapeutic drugs or combinations of both.

References

[1] G.E. Stein, E.M. Wells, The importance of tissue penetration in achieving successful antimicrobial treatment of nosocomial pneumonia and complicated skin and soft-tissue infections caused by methicillin-resistant Staphylococcus aureus: vancomycin and linezolid., Curr. Med. Res. Opin. 26 (2010) 571–88. doi:10.1185/03007990903512057.

[2] A.S. Pumerantz, PEGylated liposomal vancomycin: a glimmer of hope for improving treatment outcomes in MRSA pneumonia., Recent Pat. Antiinfect. Drug Discov. 7 (2012) 205–12. doi:10.2174/157489112803521904.

[3] M. Segarra-Newnham, T.J. Church, Pharmacotherapy for methicillin-resistant Staphylococcus aureus nosocomial pneumonia., Ann. Pharmacother. 46 (2012) 1678–87. doi:10.1345/aph.1R370.

[4] T.P. Lodise, B. Lomaestro, J. Graves, G.L. Drusano, Larger vancomycin doses (at least four grams per day) are associated with an increased incidence of nephrotoxicity., Antimicrob. Agents Chemother. 52 (2008) 1330–6. doi:10.1128/AAC.01602-07.

[5] A.C. Kalil, M. Klompas, G. Haynatzki, M.E. Rupp, Treatment of hospital-acquired pneumonia with linezolid or vancomycin: a systematic review and meta-analysis., BMJ Open. 3 (2013) e003912. doi:10.1136/bmjopen-2013-003912.

[6] D. Nichols, N. Cahoon, E.M. Trakhtenberg, L. Pham, A. Mehta, A. Belanger, et al., Use of ichip for high-throughput in situ cultivation of "uncultivable" microbial species., Appl. Environ. Microbiol. 76 (2010) 2445–50. doi:10.1128/AEM.01754-09.

[7] G. Wright, Antibiotics: An irresistible newcomer., Nature. 517 (2015) 442–4. doi:10.1038/nature14193.

[8] A. Kali, Teixobactin: a novel antibiotic in treatment of gram positive bacterial infections., J. Clin. Diagn. Res. 9 (2015) DL01. doi:10.7860/JCDR/2015/13033.5720.

[9] L.L. Ling, T. Schneider, A.J. Peoples, A.L. Spoering, I. Engels, B.P. Conlon, et al., A new antibiotic kills pathogens without detectable resistance., Nature. 517 (2015) 455–9. doi:10.1038/nature14098.

[10] N.E. Holmes, S.Y.C. Tong, J.S. Davis, S.J. van Hal, Treatment of methicillin-resistant Staphylococcus aureus: vancomycin and beyond., Semin. Respir. Crit. Care Med. 36 (2015) 17–30. doi:10.1055/s-0034-1397040.

[11] M.H. Kollef, C.W. Hamilton, A.B. Montgomery, Aerosolized antibiotics: do they add to the treatment of pneumonia?, Curr. Opin. Infect. Dis. 26 (2013) 538–44. doi:10.1097/QCO.0000000000000004.

[12] J. Garnacho-Montero, Y. Corcia-Palomo, R. Amaya-Villar, L. Martin-Villen, How to treat VAP due to MDR pathogens in ICU patients., BMC Infect. Dis. 14 (2014) 135. doi:10.1186/1471-2334-14-135.

[13] J.K. Hagerman, K.E. Hancock, M.E. Klepser, Aerosolised antibiotics: a critical appraisal of their use., Expert Opin. Drug Deliv. 3 (2006) 71–86. doi:10.1517/17425247.3.1.71.

[14] F.G. Zampieri, A.P. Nassar, D. Gusmao-Flores, L.U. Taniguchi, A. Torres, O.T. Ranzani, Nebulized antibiotics for ventilator-associated pneumonia: a systematic review and meta-analysis., Crit. Care. 19 (2015) 150. doi:10.1186/s13054-015-0868-y.

[15] T. Abu-Salah, R. Dhand, Inhaled antibiotic therapy for ventilator-associated tracheobronchitis and ventilator-associated pneumonia: an update., Adv. Ther. 28 (2011) 728–47. doi:10.1007/s12325-011-0051-z.

[16] P.A. Flume, D.R. VanDevanter, Clinical applications of pulmonary delivery of antibiotics., Adv. Drug Deliv. Rev. 85 (2015) 1–6. doi:10.1016/j.addr.2014.10.009.

[17] L.B. Palmer, Aerosolized antibiotics in the intensive care unit., Clin. Chest Med. 32 (2011) 559–74. doi:10.1016/j.ccm.2011.05.012.

[18] W.S. Cheow, K. Hadinoto, Green amorphous nanoplex as a new supersaturating drug delivery system., Langmuir. 28 (2012) 6265–75. doi:10.1021/la204782x.

[19] M. Kutscher, W.S. Cheow, V. Werner, U. Lorenz, K. Ohlsen, L. Meinel, et al., Influence of salt type and ionic strength on self-assembly of dextran sulfate-ciprofloxacin nanoplexes., Int. J. Pharm. 486 (2015) 21–9. doi:10.1016/j.ijpharm.2015.03.022.

[20] M. Takhi, C. Murugan, M. Munikumar, K.M. Bhaskarreddy, G. Singh, K. Sreenivas, et al., Synthesis and antibacterial activity of novel oxazolidinones bearing N-hydroxyacetamidine substituent., Bioorg. Med. Chem. Lett. 16 (2006) 2391–5. doi:10.1016/j.bmcl.2006.01.109.

[21] L. Chen, B. De Borba, J. Rohrer, Determination of Morpholine in Linezolid by Ion Chromatography (https://www.thermoscientific.com/content/dam/tfs/ATG/CMD/CMD%20Documents/AN-1062-Determination-of-Morpholine-in-Linezolid-by-IC-AN-70702.pdf), Appl. Note Thermo Fish. Sci. Sunnyvale, CA, USA. 1062 (2013) 1–7.

[22] Q.T. Zhou, S.S.Y. Leung, P. Tang, T. Parumasivam, Z.H. Loh, H.-K. Chan, Inhaled formulations and pulmonary drug delivery systems for respiratory infections., Adv. Drug Deliv. Rev. 85 (2015) 83–99. doi:10.1016/j.addr.2014.10.022.

[23] M.J. de Jesús Valle, J.G. González, F.G. López, A.S. Navarro, Pulmonary disposition of vancomycin nebulized as lipid vesicles in rats., J. Antibiot. (Tokyo). 66 (2013) 447–51. doi:10.1038/ja.2013.32.

[24] W.S. Cheow, K. Hadinoto, Lipid-polymer hybrid nanoparticles with rhamnolipid-triggered release capabilities as anti-biofilm drug delivery vehicles., Particuology. 10 (2012) 327–333. doi:10.1016/j.partic.2011.08.007.

[25] K. Hadinoto, A. Sundaresan, W.S. Cheow, Lipid–polymer hybrid nanoparticles as a new generation therapeutic delivery platform: A review., Eur. J. Pharm. Biopharm. 85 (2013) 427–443. doi:10.1016/j.ejpb.2013.07.002.

[26] K. Ohlsen, U. Lorenz, Immunotherapeutic strategies to combat staphylococcal infections., Int. J. Med. Microbiol. 300 (2010) 402–10. doi:10.1016/j.ijmm.2010.04.015.

[27] U. Lorenz, B. Lorenz, T. Schmitter, K. Streker, C. Erck, J. Wehland, et al., Functional antibodies targeting IsaA of Staphylococcus aureus augment host immune response and open new perspectives for antibacterial therapy., Antimicrob. Agents Chemother. 55 (2011) 165–73. doi:10.1128/AAC.01144-10.

[28] R. Respaud, L. Vecellio, P. Diot, N. Heuzé-Vourc'h, Nebulization as a delivery method for mAbs in respiratory diseases., Expert Opin. Drug Deliv. 12 (2015) 1027–39. doi:10.1517/17425247.2015.999039.

[29] S.P. Hertel, G. Winter, W. Friess, Protein stability in pulmonary drug delivery via nebulization., Adv. Drug Deliv. Rev. 93 (2015) 79–94. doi:10.1016/j.addr.2014.10.003.

[30] S. Hertel, T. Pohl, W. Frieß, G. Winter, That's cool! - Nebulization of thermolabile proteins with a cooled vibrating mesh nebulizer., Eur. J. Pharm. Biopharm. (2014). doi:10.1016/j.ejpb.2014.03.001.

[31] A. Maillet, N. Congy-Jolivet, S. Le Guellec, L. Vecellio, S. Hamard, Y. Courty, et al., Aerodynamical, immunological and pharmacological properties of the anticancer antibody cetuximab following nebulization., Pharm. Res. 25 (2008) 1318–26. doi:10.1007/s11095-007-9481-3.

[32] American Thoracic Society, Infectious Diseases Society of America, Guidelines for the management of adults with hospital-acquired, ventilator-associated, and healthcare-associated pneumonia., Am. J. Respir. Crit. Care Med. 171 (2005) 388–416. doi:10.1164/rccm.200405-644ST.

[33] L.B. Palmer, G.C. Smaldone, Reduction of bacterial resistance with inhaled antibiotics in the intensive care unit., Am. J. Respir. Crit. Care Med. 189 (2014) 1225–33. doi:10.1164/rccm.201312-2161OC.

[34] S.M. Lehar, T. Pillow, M. Xu, L. Staben, K.K. Kajihara, R. Vandlen, et al., Novel antibody-antibiotic conjugate eliminates intracellular S. aureus., Nature. 527 (2015) 323–8. doi:10.1038/nature16057.

[35] M. Otto, Basis of virulence in community-associated methicillin-resistant Staphylococcus aureus., Annu. Rev. Microbiol. 64 (2010) 143–62. doi:10.1146/annurev.micro.112408.134309.

[36] B.E. Ragle, J. Bubeck Wardenburg, Anti-alpha-hemolysin monoclonal antibodies mediate protection against Staphylococcus aureus pneumonia., Infect. Immun. 77 (2009) 2712–8. doi:10.1128/IAI.00115-09.

[37] M. Kutscher, M. Rosenberger, B. Schmauss, L. Meinel, U. Lorenz, K. Ohlsen, et al., Surface functionalization allowing repetitive use of optical sensors for real-time detection of antibody-bacteria interaction., J. Biophotonics. 8 (2015). doi:10.1002/jbio.201500178.

[38] G.T. Hermanson, Bioconjugate Techniques, Elsevier Inc, Academic press Inc, 2013.

[39] P. Peluso, D.S. Wilson, D. Do, H. Tran, M. Venkatasubbaiah, D. Quincy, et al., Optimizing antibody immobilization strategies for the construction of protein microarrays., Anal. Biochem. 312 (2003) 113–24. doi:10.1016/S0003-2697(02)00442-6.

[40] A. Makaraviciute, A. Ramanaviciene, Site-directed antibody immobilization techniques for immunosensors., Biosens. Bioelectron. 50 (2013) 460–71. doi:10.1016/j.bios.2013.06.060.

[41] A.K. Trilling, J. Beekwilder, H. Zuilhof, Antibody orientation on biosensor surfaces: a minireview., Analyst. 138 (2013) 1619–27. doi:10.1039/c2an36787d.

[42] K.L. Brogan, K.N. Wolfe, P.A. Jones, M.H. Schoenfisch, Direct oriented immobilization of F(ab′) antibody fragments on gold., Anal. Chim. Acta. 496 (2003) 73–80. doi:10.1016/S0003-2670(03)00991-7.

[43] K. Bonroy, F. Frederix, G. Reekmans, E. Dewolf, R. De Palma, G. Borghs, et al., Comparison of random and oriented immobilisation of antibody fragments on mixed self-assembled monolayers., J. Immunol. Methods. 312 (2006) 167–81. doi:10.1016/j.jim.2006.03.007.

[44] X. Fan, I.M. White, S.I. Shopova, H. Zhu, J.D. Suter, Y. Sun, Sensitive optical biosensors for unlabeled targets: a review., Anal. Chim. Acta. 620 (2008) 8–26. doi:10.1016/j.aca.2008.05.022.

[45] G. Emiliyanov, P. Høiby, L. Pedersen, O. Bang, Selective serial multi-antibody biosensing with TOPAS microstructured polymer optical fibers., Sensors. 13 (2013) 3242–3251. doi:10.3390/s130303242.

[46] G. Emiliyanov, J.B. Jensen, O. Bang, P.E. Hoiby, L.H. Pedersen, E.M. Kjaer, et al., Localized biosensing with Topas microstructured polymer optical fiber., Opt. Lett. 32 (2007) 460–2. doi:10.1364/OPN.18.12.000019.

[47] C. Markos, W. Yuan, K. Vlachos, G.E. Town, O. Bang, Label-free biosensing with high sensitivity in dual-core microstructured polymer optical fibers., Opt. Express. 19 (2011) 7790–8. doi:10.1364/OE.19.007790.

[48] L. Bruun, C. Koch, B. Pedersen, M.H. Jakobsen, J. Aamand, A quantitative enzyme-linked immunoassay for the detection of 2, 6-dichlorobenzamide (BAM), a degradation product of the herbicide dichlobenil., J. Immunol. Methods. 240 (2000) 133–42. doi:10.1016/S0022-1759(00)00190-3.

[49] E.S. Jauho, U. Boas, C. Wiuff, K. Wredstrøm, B. Pedersen, L.O. Andresen, et al., New technology for regiospecific covalent coupling of polysaccharide antigens in ELISA for serological detection., J. Immunol. Methods. 242 (2000) 133–43. doi:10.1016/S0022-1759(00)00248-9.

[50] www.exiqon.com/aq-link-technology, Acessed: 21-12-2015, http://www.exiqon.com/aq-link-technology.

LIST OF ABBREVIATIONS

BAL	Bronchioalveolar lavage
BSA	Bovine serum albumin
CAP	Community-acquired pneumonia
CEX	Cation exchange chromatography
CFU	Colony-forming unit
CIP	Ciprofloxacin
DLS	Dynamic light scattering
DS	Dextran sulfate
E. coli	*Escherichia coli*
ELF	Epithelial lining fluid
FcRN	Neonatal Fc receptor
FS	Fluorescein sodium
HAP	Hospital-acquired pneumonia
HPLC	High performance liquid chromatography
IsaA	Immunodominant staphylococcal antigen A
ITC	Isothermal titration calorimetry
LAF	Laminar air flow
mAb	Monoclonal antibody
MIC	Minimum inhibitory concentration
MRSA	Methicillin- resistant *Staphylococcus aureus*
PBG	Planar Bragg grating
PBS	Phosphate buffered saline
PS 20	Polysorbate 20
PdI	Polydispersity index
pI	Isoelectric point
S. aureus	*Staphylococcus aureus*
S.D.	Standard deviation
SEC	Size exclusion chromatography
UV	Ultraviolet
VAP	Ventilator-associated pneumonia
VIP	Vasoactive intestinal peptides

ACKNOWLEDGEMENTS

First and foremost, I want to express my gratitude to Prof. Dr. Dr. Lorenz Meinel for the possibility to join his research group, for his commitment to enable outstanding equipment conditions at his chair and the possibility to present parts of my work at the annual CRS Germany Local Chapter meetings. Thank you for your professional and dedicated scientific input as well as for motivating me to pursue my parallel studies of pharmacy and granting me spare time to prepare myself for the second state examination of pharmacy.

I deeply thank Prof. Dr. Oliver Germershaus for his dedicated guidance of my work, his constant support, and for giving me the opportunity to work in the laboratory of Prof. Kunn Hadinoto in Singapore as well as to attend the 2nd Galenus Workshop on Pulmonary Drug Delivery in Dublin. I am very grateful for all your valuable and honest scientific and personal advice. Especially, I want to thank you for always finding some spare time despite the long distance, your young family, and the takeover of your new chair.

Many thanks go to Dr. Knut Ohlsen from the Institute for Molecular Infection Biology at the University of Würzburg for the initiation of this interesting project, for the financial support, for provision of materials, and for being part of my thesis committee. This thank is extended to Dr. Udo Lorenz from the Department of General, Visceral, Vascular and Paediatric Surgery, University Clinic of Würzburg. Thank you both for the numerous interesting scientific discussions and your support.

Additionally, I want to acknowledge the essential help of Babett Österreich, Martina Selle, Tobias Hertlein, and Annika Parg from the Institute for Molecular Infection Biology at the University of Würzburg by preparing bacteria samples and conducting the animal studies.

Furthermore, I am very grateful to Prof. Kunn Hadinoto and Wean Sin Cheow from the Nanyang Technological University of Singapore for their fruitful scientific collaboration and for inviting me to their lab in Singapore where I could experience a very pleasant and productive time.

I also want to thank all my PhD colleagues and the whole team for the good time we spent together in Würzburg. Dr. Sascha Zügner, Christine Schneider, and Doris Moret were always supportive when I had questions regarding organization and student supervision. I wish to address special thanks to Isabel Schulz, Gabriel Jones, and Sebastian Puhl who became close friends. Moreover, I would like to thank Vera Kohl, Nina Hecht, Eva Heusler, Joel Wurzel,

and the other members of the team for the nice atmosphere and the enjoyable time we spent together inside and outside of the university.

I would like to thank Georg Walter, Matthias Völker, and Karl Vollmuth for their help regarding technical problems of all kind and regarding the manufacturing of the customized mouse box for my animal studies.

Gilyos GmbH is kindly acknowledged for the possibility to use their freeze drying equipment during my work as well as the Division of Electron Microscopy at the Biocenter of the University of Würzburg for using their scanning electron microscope. I thank Prof. Dr. Petra Högger who supplied the Pari Boy N compressor for my nebulization experiments.

Furthermore, I want to acknowledge the financial support of the Federal Ministry of Education and Research (BMBF) in the frame of Grants No. 0315565 (GO-Bio 3) and 01DP12030 for funding my work as well as my research stay in Singapore. Additionally, I thank the University of Würzburg Graduate Schools for their financial support in the frame of the DAAD PROMOS program for attending the 2nd Galenus Workshop on Pulmonary Drug Delivery in Dublin, Ireland.

I want to thank my family, especially my grandparents, and all my close friends for their important continuous encouragement during the whole time.

Of course, I deeply thank my parents for their constant support and encouragement in all those years and for simply being my family. Thank you for all you made possible and for always believing in me.

Finally, I want to thank Manuel for his fruitful scientific collaboration and proof-reading of this thesis. But most of all, thank you for your support, never ending encouragement, your patience and for being always there for me.

PUBLICATIONS AND PRESENTATIONS

PUBLICATIONS

M. Kutscher, M. Rosenberger, B. Schmauss, L. Meinel, U. Lorenz, K. Ohlsen, R. Hellmann, and O. Germershaus, Surface functionalization allowing repetitive use of optical sensors for real-time detection of antibody-bacteria interaction., J. Biophotonics. 8 (2015). doi:10.1002/jbio.201500178.

M. Kutscher, W.S. Cheow, V. Werner, U. Lorenz, K. Ohlsen, L. Meinel, K. Hadinoto, and O. Germershaus, Influence of salt type and ionic strength on self-assembly of dextran sulfate-ciprofloxacin nanoplexes., Int. J. Pharm. 486 (2015) 21–29. doi:10.1016/j.ijpharm.2015.03.022

O. Germershaus, V. Werner, M. Kutscher, and L. Meinel, Deciphering the mechanism of protein interaction with silk fibroin for drug delivery systems, Biomaterials. (2014) 1-8. doi:10.1016/j.biomaterials.2013.12.083.

CONFERENCES

Controlled Release Society Germany Local Chapter Meeting 2014, Kiel

M. Kutscher, K. Hadinoto, L. Meinel, O. Germershaus, Impact of salt on self-assembly of polyelectrolyte-drug nanoplexes

(poster presentation).

2nd Galenus Workshop on Pulmonary Drug Delivery, Dublin, Ireland, 2013

(participation only)

Controlled Release Society Germany Local Chapter Meeting 2013, Ludwigshafen

M. Kutscher, L. Meinel, O. Germershaus, Spray-dried alginate microspheres as controlled release system for pulmonary protein delivery

(poster presentation).

Controlled Release Society Germany Local Chapter Meeting 2012, Würzburg,

(participation only)

DOCUMENTATION OF AUTORSHIP

This section contains a list of the individual contribution for each author to the publications reprinted in this thesis. Unpublished manuscripts are handled, accordingly.

M1	**Marika Kutscher, Knut Ohlsen, Lorenz Meinel, Oliver Germershaus;** Local Drug Delivery Options for Treatment of Nosocomial Pneumonia due to Methicillin Resistant Staphylococcus Aureus by Antibiotics and Therapeutic Antibodies. Unpublished manuscript.				
Author		**1**	**2**	**3**	**4**
Study design/concept development		x	x	x	x
Manuscript planning		x		x	x
Manuscript writing		x			
Correction of manuscript			x	x	x
Supervision of Marika Kutscher				x	x

P1	**Marika Kutscher, Wean Sin Cheow, Vera Werner, Udo Lorenz, Knut Ohlsen, Lorenz Meinel, Kunn Hadinoto, Oliver Germershaus (2015);** Influence of Salt Type and Ionic Strength on Self-Assembly of Dextran Sulfate-Ciprofloxacin Nanoplexes. International Journal of Pharmaceutics, 486(1), 21-29.								
Author		**1**	**2**	**3**	**4**	**5**	**6**	**7**	**8**
Preparation of polyelectrolyte-drug nanoplexes		x	x	x					
Determination of CIP complexation efficiency (CE)		x		x					
Static light scattering (SLS)		x		x					
Dynamic light scattering (DLS)		x							
Electrophoretic light scattering (ELS)		x							
Scanning electron microscopy (SEM)		x							
Isothermal titration calorimetry		x		x					
Release study		x	x						
Statistical analysis		x							x
Study design/concept development		x	x			x	x	x	x
Data analysis and interpretation		x	x						x
Manuscript planning		x							x
Manuscript writing		x							
Correction of manuscript			x	x	x	x	x	x	x
Supervision of Marika Kutscher							x		x

M2	**Marika Kutscher, Knut Ohlsen, Lorenz Meinel, Oliver Germershaus;** Development of a Stable Formulation for the Humanized Monoclonal Antibody UK-66. Unpublished manuscript.			
Author	**1**	**2**	**3**	**4**
Sample preparation for formulation screening	x			
Short-term storage stability of minimally formulated drug substance	x	x		
pH screening under accelerated and stressed storage conditions	x			
Formulation screening for liquid and lyophilized dosage forms under long-term storage conditions	x			
UV-Vis spectroscopy	x			
Electrophoretic mobility assay	x			
Dynamic scanning fluorimetry (DSF)	x			x
pH measurement	x			
Dynamic light scattering (DLS)	x			
Size exclusion chromatography (SEC)	x			
Cation exchange chromatography (CEX)	x			
Study design/concept development	x	x	x	x
Data analysis and interpretation	x	x		x
Manuscript planning	x		x	x
Manuscript writing	x			
Correction of manuscript		x	x	x
Supervision of Marika Kutscher			x	x

M3	**Marika Kutscher, Knut Ohlsen, Lorenz Meinel, Oliver Germershaus;** Nebulization of the Humanized Monoclonal Antibody UK-66 – Physicochemical Stability and In-Vivo Efficacy. Unpublished manuscript.			
Author	**1**	**2**	**3**	**4**
Preparation of hUK-66 formulations	x			
Mechanical shaking stress	x			
Nebulization of hUK-66	x			
Aerosol collection for characterization	x			
Calculation of required mAb formulation concentration	x			x
In vivo nebulization setup	x			x
In vivo animal study of nebulized hUK-66 efficacy	x	x		
Concentration and turbidity measurements using UV-Vis spectroscopy	x			
Dynamic light scattering (DLS)	x			
Size exclusion chromatography (SEC)	x			
Cation exchange chromatography (CEX)	x			
Statistical analysis	x			x
Study design/concept development	x	x	x	x
Data analysis and interpretation	x	x		x
Manuscript planning	x		x	x
Manuscript writing	x			
Correction of manuscript		x	x	x
Supervision of Marika Kutscher			x	x

P2	**Marika Kutscher, Manuel Rosenberger, Bernhard Schmauss, Lorenz Meinel, Udo Lorenz, Knut Ohlsen, Ralf Hellmann, Oliver Germershaus (2015);** Surface functionalization allowing repetitive use of optical sensors for real-time detection of antibody-bacteria interaction. Journal of Biophotonics.

Author	**1**	**2**	**3**	**4**	**5**	**6**	**7**	**8**
Modification of the sensor surface with *S. aureus* specific antibody	x	x						
Real-time detection of antibody-bacteria interaction	x	x						
Regeneration of the sensor	x	x						
Study design/concept development	x	x					x	x
Data analysis and interpretation	x	x						x
Manuscript planning	x	x						x
Manuscript writing	x	x[1]						
Correction of manuscript			x	x	x	x	x	x
Supervision of Marika Kutscher				x				x

x[1] M. Rosenberger wrote the paragraph 2.2.“Planar Bragg grating sensor” of the materials and methods section.

Erklärung zu den Eigenanteilen des Doktoranden sowie der weiteren Doktoranden als Koautoren an Publikationen und Zweitpublikationsrechten bei einer kumulativen Dissertation.

Für alle in dieser kumulativen Dissertation verwendeten Manuskripte liegen die notwendigen Genehmigungen der Verlage (‚reprint permission') für die Zweitpublikation vor, außer das betreffende Kapitel ist noch gar nicht publiziert. Dieser Umstand wird einerseits durch die genaue Angabe der Literaturstelle der Erstpublikation auf der ersten Seite des betreffenden Kapitels deutlich gemacht oder die bisherige Nichtveröffentlichung durch den Vermerk „unpublished" oder „nicht veröffentlicht" gekennzeichnet.

Die Mitautoren der in dieser kumulativen Dissertation verwendeten Manuskripte sind sowohl über die Nutzung als auch über die oben angegebenen Eigenanteile informiert und stimmen dem zu.

Die Beiträge der Mitautoren an den Publikationen sind in den vorausgehenden Tabellen aufgeführt.

Prof. Dr. Dr. Lorenz Meinel Unterschrift

Marika Kutscher Unterschrift